The Role of Developmental Regulatory Factors YAP1 and FOXM1 and Associated Molecular Signaling in the Induction of Cardiomyocyte Hypertrophy and Fibrosis in Rodent Diabetic Cardiomyopathy Model

Thesis submitted for the Degree of

Doctor of Philosophy (Science)

In Life Science and Biotechnology

By

ARUNIMA MONDAL

Department of Life Science and Bio-technology

Jadavpur University

2024

CERTIFICATE FROM THE SUPERVISOR

This is to certify that the thesis submitted by **ARUNIMA MONDAL** entitled "**The Role of Developmental Regulatory Factors YAP1 and FOXM1 and Associated Molecular Signaling in the Induction of Cardiomyocyte Hypertrophy and Fibrosis in Rodent Diabetic Cardiomyopathy Model**", who got her name registered on 01.10.2018 for the award of Ph.D. (Science) degree of Jadavpur University, is absolutely based on her own research work under the supervision of **Dr. ARUNIMA SENGUPTA**, Assistant Professor, Department of Life science and Biotechnology, Jadavpur University, Kolkata- 700032, India. This thesis or any part of it has not been submitted anywhere for any degree/diploma or any other academic award previously.

Dr. Arunima Sengupta,   12|3|24

Assistant Professor,

Department of Life science and Biotechnology,

Jadavpur University,

Kolkata

Dr. Arunima Sengupta
UGC – Assistant Professor
Dept. of Life science and Bio-technology
JADAVPUR UNIVERSITY, KOLKATA

* Established on and from 24th December, 1955 vide Notification No.10986-Edn/IU-42/55 dated 6th December, 1955 under JadavpurUniversity Act, 1955 (West Bengal Act XXIII of 1955) followed by Jadavpur University Act,1981 (West Bengal Act XXIV of 1981)

দূরভাষ:২৪১৪-৬৭১০   Website:www.jadavpur.edu   Phone : 2414-6710

DECLARATION

I hereby declare that the work reported in this thesis entitled "**The Role of Developmental Regulatory Factors YAP1 and FOXM1 and Associated Molecular Signaling in the Induction of Cardiomyocyte Hypertrophy and Fibrosis in Rodent Diabetic Cardiomyopathy Model**" is entirely original and was performed by me under the supervision of Dr. ARUNIMA SENGUPTA, Assistant Professor, Department of Life Science and Bio-technology, Jadavpur University, Kolkata- 700032. India.

Furthermore, I declare that the contents of this thesis have not been submitted for the award of any degree, diploma, fellowship, associateship or any other similar title of any University or Institution.

Date: 12/03/24

Arunima Mondal

ARUNIMA MONDAL

Department of Life science and Biotechnology

Jadavpur University

Kolkata- 700032, India

PREFACE

The thesis aims to unravel the complex molecular mechanism associated with the pathophysiology of diabetic cardiomyopathy entitled **"The Role of Developmental Regulatory Factors YAP1 and FOXM1 and Associated Molecular Signaling in the Induction of Cardiomyocyte Hypertrophy and Fibrosis in Rodent Diabetic Cardiomyopathy Model"**.

The thesis contains 5 major chapters. **Chapter 1** elaborate the **background and introduction** study on Diabetic cardiomyopathy and associated cellular signaling with reference to the critical role of the developmental regulatory molecules under study. **Chapter 2** addresses the **aims and objectives** of the research work. **Chapter 3** deals with the **materials and methods** used to conduct the aforementioned research investigations. **Chapter 4** describes the **results and discussion** of our study following **Chapter 5** with the **conclusion** of the overall research work.

The results and discussion chapter further elaborates the overall research work in 3 subchapters. **Chapter 4.A** reports the role of YAP1-FOXM1 in hyperglycemia mediated cardiomyocyte hypertrophy and fibrosis induction. **Chapter 4.B** explains the findings on YAP1 mediated RAS signaling dysregulation in promoting hyperglycemia induced cardiomyocyte EMT and fibrotic response. And **Chapter 4.C** reports the study on hyperglycemia induced YAP1 overexpression in orchestrating β-catenin / TGF-β signaling mediated cardiac fibrosis.

In the course of the scientific study, I am thankful to all other scientists who have worked tirelessly in this field which have and have inspired me to work further.

Arunima Mondal

(Arunima Mondal)

Department of Life science and Bio-technology,

Jadavpur University,

Kolkata-700032

Dedicated to,

my parents without whom the journey to this day would not have been possible.

Thesis Title: The Role of Developmental Regulatory Factors YAP1 and FOXM1 and Associated Molecular Signaling in the Induction of Cardiomyocyte Hypertrophy and Fibrosis in Rodent Diabetic Cardiomyopathy Model

ABSTRACT

Cardiovascular diseases (CVDs) are currently the leading cause of increasing morbidity and mortality worldwide. Among the different types of CVDs, cardiomyocyte hypertrophy deteriorates the functional ability of heart leading to increased risk of heart failure. At the tissue level, cardiac hypertrophy is characterized by thickening of ventricular wall, increased myocardial fibrosis and impaired cardiac contractility. The underlying cause of cardiomyocyte hypertrophy often involves genetics, hypertension, coronary artery disease, inflammation, oxidative stress etc. Metabolic disease such as diabetes is currently a major health burden which is also associated with the development of various cardiac diseases. While different medications are being used against diabetic cardiomyopathy, the role of specific molecular players in the disease pathogenesis seek further research in-depth that may help in identification of novel therapeutic targets in future. This study primarily aims to understand the transcriptional regulation of FOXM1 upon high glucose stress in cardiac cells both *in vitro* and *in vivo*. *yap1* and *foxm1*, two important genes expressed during early developmental period, were found to be upregulated in hyperglycemic condition. Inhibition of these molecules in the high glucose condition with specific inhibitors resulted in significant amelioration of cardiomyocyte hypertrophy and fibrosis. YAP1 has been observed to upregulate AKT activation followed by subsequent GSK3β inhibition that in turn upregulates FOXM1 expression leading to exacerbated hypertrophy. In the hyperglycemic cells, activated YAP1 also modulated renin angiotensin system (RAS) through upregulation of angiotensin converting enzyme (ACE) and downregulating its homolog molecule angiotensin converting enzyme2 (ACE2). Moreover, YAP1-dependent increased expression of ACE and ACE2 has been observed to be mediated through *β-catenin* overexpression in cardiomyocyte and cardiac fibroblast *in vitro*. Activated ACE induced epithelial to mesenchymal transition (EMT) - mediated pro-fibrotic remodeling *via* upregulated TGF-β-SMAD2/3 pathway. In nutshell, the study demonstrates the role of YAP1 in cardiomyocyte hypertrophy and fibrosis by FOXM1 and ACE respectively in high glucose stress condition.

ACKNOWLEDGEMENTS

CONTENTS

SUMMARY

Cardiac diseases are the most common complications that affect majority of diabetic patients. Hypertrophy of cardiomyocyte and fibrosis of heart muscle often lead to structural and functional abnormalities leading to risks of heart failure in diabetic individuals. YAP1 and FOXM1 are recently being investigated for their role in hypertrophic and fibrotic disorders. However, the precise role of YAP1 and FOXM1 and its mode of interactions with other molecules in the induction of high glucose mediated cardiomyopathies are still not clear. In this study we have observed high glucose mediated upregulation of FOXM1 induces hypertrophy and increased fibrotic response of cardiomyocyte. As the underlying mechanism, we have further observed that improper glucose metabolism activates YAP1, a key organ size regulatory molecule that further activates AKT-GSK3β signalling in cardiomyocyte. YAP1 and AKT manipulation resulting in altered expression of FOXM1 points to a possible interaction of YAP1 and FOXM1 in the cardiomyocyte. Modulation of YAP1, AKT and FOXM1 decreases the overexpression of hypertrophic and fibrotic markers in hyperglycemia treated cardiomyocyte. Further, in our study we have observed, high glucose mediated activation of renin angiotensin system, specifically Angiotensin-II plays a critical role in mediating cardiac hypertrophy and fibrosis. Recent researches have reported ACE2 in amelioration of Ang-II mediated diabetes related cardiomyopathies. However, the precise mode of action of ACE-ACE2 signaling in diabetic cardiomyopathy is still not well understood. In this study, we have observed YAP1 to also regulate the differential expression of ACE and ACE2 in hyperglycemic stress to induce cardiac fibrotic remodeling. High glucose mediated YAP1 overexpression in cardiomyocyte and cardiac fibroblast upregulates β-catenin expression that further promotes ACE activity along with reduced ACE2 expression. This leads to increased cardiac fibroblast activation with increased EMT like process in cardiac cells. Increased YAP1-βcatenin activity has been observed to upregulate pro-fibrotic TGF-β signaling in both cardiomyocyte and cardiac fibroblast. Inhibition of either YAP1 or β-catenin in the hyperglycemic cells shifts the expression of RAS pathway towards increased ACE2 expression which accompanied reduced EMT and fibrotic marker expression proving beneficial in the diabetic cardiomyopathy. Altogether our study suggests that hyerglycemic stress in adult cardiac cells mediate YAP1 activation, thus inducing expression of key signaling molecules such as FOXM1, β-catenin, ACE thereby promoting cardiac hypertrophy and fibrosis.

LIST OF FIGURES

LIST OF TABLES

Page No.

LIST OF PUBLICATIONS

- Mondal, A., Das, S., Samanta, J., & Chakraborty, S. (2022). YAP1 induces hyperglycemic stress-mediated cardiac hypertrophy and fibrosis in an AKT-FOXM1 dependent signaling pathway. *Archives of Biochemistry and Biophysics*, *722*, 109198.

- Samanta, J., Mondal, A., Saha, S., Chakraborty, S., & Sengupta, A. (2020). Oleic acid protects from arsenic-induced cardiac hypertrophy via AMPK/FoxO/NFATc3 pathway. *Cardiovascular toxicology*, *20*, 261-280.

- Samanta, J., Mondal, A., Das, S., Chakraborty, S., & Sengupta, A. (2021). Induction of cardiomyocyte calcification is dependent on FoxO1/NFATc3/Runx2 signaling. *In Vitro Cellular & Developmental Biology-Animal*, 1-14.

- Das, S., Mondal, A., Dey, C., Chakraborty, S., Bhowmik, R., Karmakar, S., & Sengupta, A. (2023). ER stress induces upregulation of transcription factor Tbx20 and downstream Bmp2 signaling to promote cardiomyocyte survival. *Journal of Biological Chemistry*, *299*(4).

- Das, S., Mondal, A., Samanta, J., Chakraborty, S., & Sengupta, A. (2021). Unfolded protein response during cardiovascular disorders: a tilt towards pro-survival and cellular homeostasis. *Molecular and Cellular Biochemistry*, *476*, 4061-4080.

- Kumari, L., Ehsan, I., Mondal, A., Al Hoque, A., Mukherjee, B., Choudhury, P., ... & Ghosh, P. (2023). Cetuximab-conjugated PLGA nanoparticles as a prospective targeting therapeutics for non-small cell lung cancer. *Journal of Drug Targeting*, *31*(5), 521-536.

LIST OF ABBREVIATIONS

DCM: Diabetic cardiomyopathy

HG: High Glucose

NG: Normal Glucose

AngII: Angiotensin II

APS: Ammonium Persulfate

bp: Base pair

cDNA: Complementary Deoxyribonucleic acid

Col-1: *Collagen-1*

Col-3: *Collagen-3*

CVF: Collagen Volume Fraction

DMEM: Dulbecco's Modified Eagle Medium

DMSO: Dimethyl Sulphoxide

DNA: Deoxyribonucleic acid

DTT: Dithiothreitol

ECM: Extracellular matrix

EDTA: Ethylene-Diamine-Tetra-Acetic acid

H&E: Hematoxylin and eosin

H2O2: Hydrogen peroxide

hrs: Hours

IF: Immunofluorescence

KCl: Potassium Chloride

KH2PO4: Potassium dihydrogenphosphate

M: Molar

mg: Millligram

mins: Minutes

ml: Millilitre

mM: Millimolar

mRNA: Messenger Ribonucleic acid

N: Normal

Na2HPO4: Disodium hydrogen orthophosphate

Na3VO4: Sodium Orthovanadate

NaCl: Sodium Chloride

NaF: Sodium fluoride

ng: Nanograms

NP-40: Nonidet P-40 (4-Nonylphenyl-polyethylene glycol)

PBS: Phosphate Buffered Saline

PMSF: Phenylmethylsulfonyl fluoride

qRT-PCR: Quantitative Real time Reverse Transcription-Polymerase Chain Reaction

RAAS: Renin-Angiotensin-Aldosterone System

RAS: Renin-Angiotensin System

RNA: Ribonucleic acid

rpm: Revolutions per minute

RT-PCR: Reverse Transcription-Polymerase Chain Reaction

SDS: Sodium Dodecylsulfate

SDS-PAGE: Sodium Dodecyl Sulfate-Poly-Acrylamide Gel Electrophoresis

SMAD: Suppressor of Mothers Against Decapentaplegic

TEMED: *N,N,N',N'*-Tetramethylethane-1,2-diamine

TGF-ß: Transforming Growth Factor beta

Tm: Melting temperature

Tris: Tris (hydroxymethyl) aminomethane

ß-mhc: *Beta myosin heavy chain*

µm: Micrometre

µM: micromolar

CHAPTER 1

BACKGROUND
&
INTRODUCTION

1.1 Heart and structure of cardiac tissue

The heart is a hollow, muscular organ of the body that pumps blood throughout the body as the main unit of the circulatory system. In mammalian system the heart through its repeated beating action maintains a continuous flow of blood through an intricate network of vessels carrying oxygen and nutrients to the tissues and carries back metabolic by-products to the heart for refilling at the lungs. The circulatory system is grouped into systemic circulation where the heart pumps blood through the aorta to the body and the pulmonary circulation pumps blood to the lungs. The coronary circulation involves circulation of blood to the muscle of the heart.
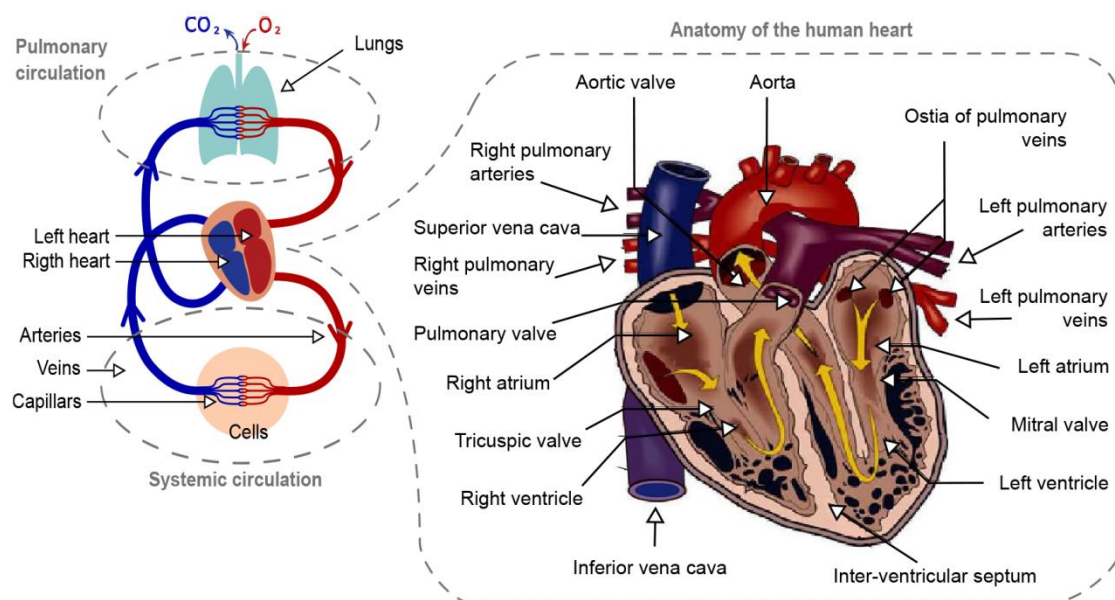
Figure 1. Circulatory system in human body and structure of human heart (Acevedo 2014)

The heart consists of four chambers, two upper chambers known as atria and two lower chambers known as ventricles. The right atria receive deoxygenated blood from the body through caval veins and left atria receive oxygenated blood from the lungs through pulmonary veins. The right ventricle receives deoxygenated blood from the right atria through right atrio-ventricular orifice and sends it to the lungs for reoxygenation. The right atrio-ventricular orifice is guarded by the tricuspid valves that prevent the flow back of blood to the atria. The oxygen rich blood from the left atria passes to the left ventricle through left atrio-ventricular orifice guarded by bicuspid or mitral valves. The left ventricle pumps out the oxygenated blood to the whole body through the major artery, aorta. The aortic orifice is

guarded by three semilunar aortic valves to stop blood from coming back to the ventricle(Hall and Hall 2020).

The cardiac wall is made up of three layers:

1. Endocardium: the innermost layer of heart wall made of simple squamous epithelium cells

2. Myocardium: The middle and thickest layer is the myocardium, made largely of cardiac muscle cells i.e. cardiomyocyte, built upon a framework of collagenous fibres, with the blood vessels that supply the myocardium and the nerve fibres that help regulate the heart. It is the contraction of the myocardium that pumps blood through the heart and into the major arteries. The muscle of the left ventricle is much thicker and better developed than that of the right ventricle in order to generate a greater amount of pressure required to pump blood into the long systemic circuit("19.1 Heart Anatomy - Anatomy and Physiology | OpenStax" n.d.).

3. Epicardium: Outermost layer of heart made of a mesothelium overlying some elastin-rich loose connective tissue.
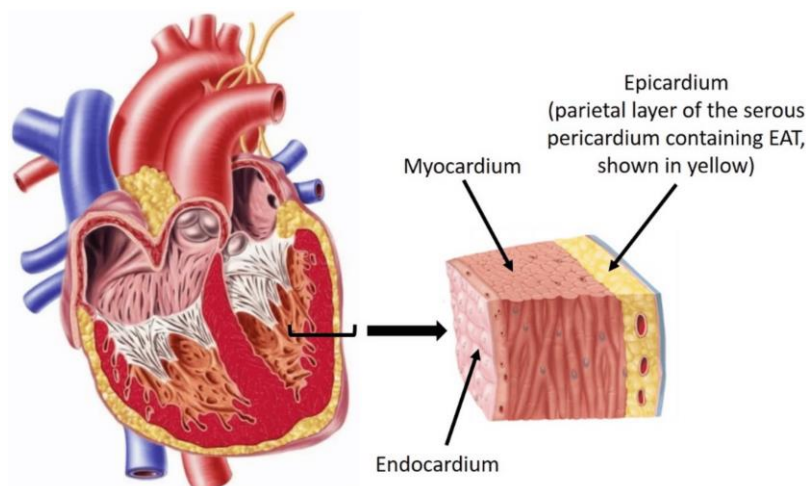
Figure 2. Anatomical structure of heart(Krishnan et al. 2022)

1.2 Types of cells present in heart

The mammalian heart consists of four major cell types; cardiac fibroblasts (CFs), cardiac muscle cells or cardiomyocyte, smooth muscle cells (SMCs), and endothelial cells (ECs). CFs produces the extracellular matrix (ECM) scaffold of the heart and is thought to constitute more than half of all heart cells. Cardiomyocyte are estimated to provide about 30% of the

total cell number but account for over 70% of the total cardiac mass because of their large volume. In contrast, SMCs, which support the vascular system, and ECs, which form the interior lining of the heart, blood vessels, and cardiac valves, are generally believed to be much less abundant(Xin, Olson, and Bassel-Duby 2013).

Cardiomyocyte are the main contractile units of heart that function to pump blood in and out of heart to supply the entire body.
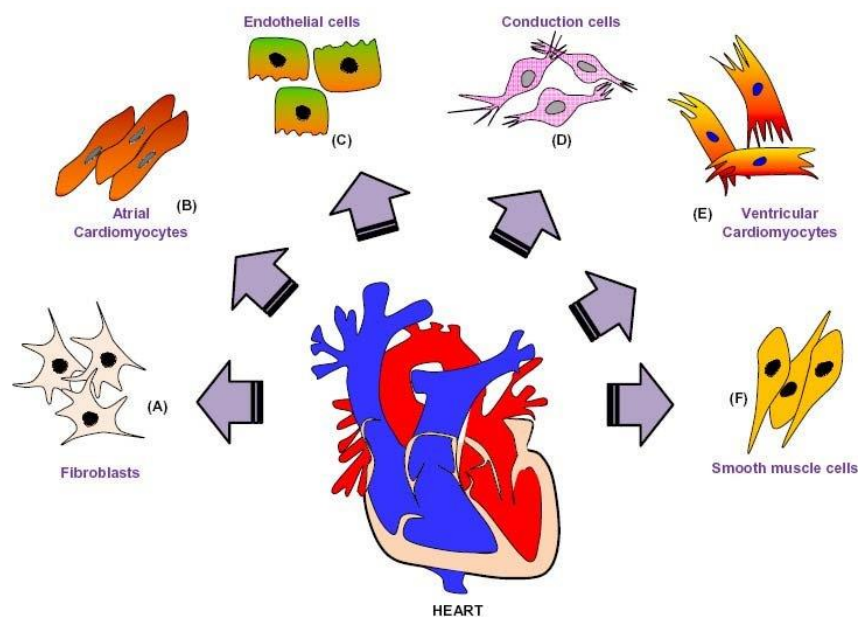
Figure 3. Types of cell present in heart(Nandi and Mishra 2015)

1.3 Disease of cardiac muscle

Cardiovascular diseases are one of the leading causes of high mortality and morbidity rate globally. An estimated 17.9 million people died from CVDs in 2019, representing 32% of all global deaths. Of these deaths, 85% were due to heart attack and stroke(World Health Organization 2016). Among these, cardiomyopathies are characterized by a group of disease of cardiac muscle that results in abnormal thickening (hypertrophic cardiomyopathy) and stiffening (restrictive cardiomyopathy) of cardiac muscle, thinning of muscle (dilated cardiomyopathy) among other abnormalities. Disorders of cardiac muscles result in reduced pumping ability of the heart eventually leading to heart failure(Vučković et al. 2022).

Cardiomyopathy can be genetic (Hypertrophic cardiomyopathy) or acquired as results of exposure to other diseases such as coronary artery disease, inflammation of cardiac muscle or metabolic disorders such as diabetes("Cardiomyopathy | Cdc.Gov" n.d.).
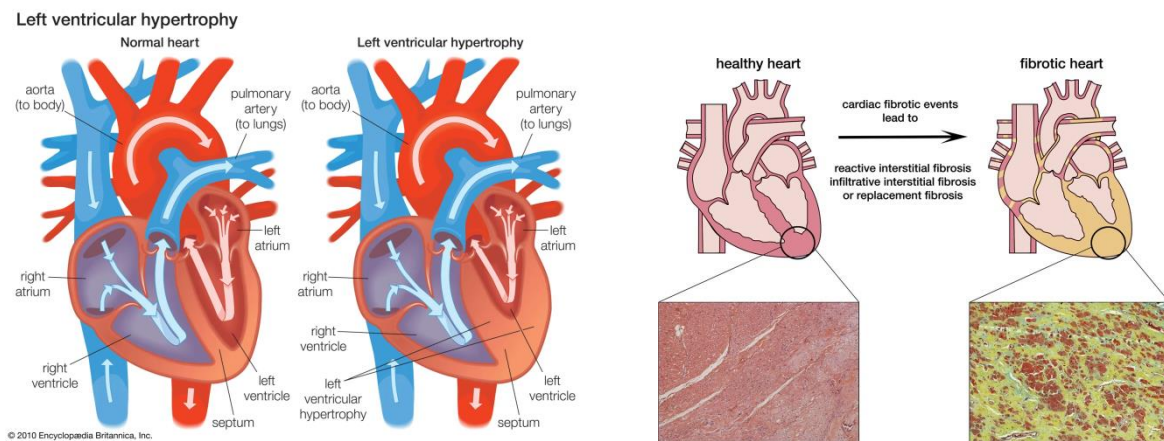
Figure 4A. cardiac hypertrophy("Cardiovascular Disease - Ventricular Dysfunction, Heart Failure, Treatment | Britannica" n.d.) **B. fibrosis**(Hinderer and Schenke-Layland 2019)

1.4 Cardiomyocyte hypertrophy and fibrosis

Cardiac hypertrophy is one of the leading causes of heart attack related deaths. It is characterized by increased size of cardiomyocyte and often accompanied by fibrotic remodelling of tissue. Injury or stress condition in the cardiac tissue leads to increased incidence of cardiomyocyte apoptosis or cell death. To meet the required demand the remaining cell responds by increasing the size of the cell or by increased fibroblast activity as cardiomyocyte are mostly terminally differentiated cells. However, these changes are maladaptive in nature with loss of contractile capacity of the existing hypertrophic cardiomyocyte. The exaggerated wound healing response by fibroblast can lead to ECM stiffness, myocardial scarring; eventually resulting in increased chances of heart failure.

At the molecular level, cellular hypertrophy and fibrosis is associated with fetal gene reactivation and irregular molecular signalling leading to the pathological condition. Understanding these molecular signatures is the key step towards therapeutics development and reducing disease progression.

1.5 Diabetes: Effect of metabolic disorders on cardiovascular system

Diabetes mellitus is currently one of the global health issues leading to high mortality and morbidity rate. In the current modern lifestyle, high fat food consumption, sedentary lifestyle contributes to increased incidence of diabetes in the population(Phang et al. 2023). Diabetes is an endocrine disorder associated with disease characterized by body cells' inability to uptake glucose from food sources resulting in high levels of glucose in the blood. There are two major forms of diabetes, type1 and type2. Type 1 Diabetes mellitus is an autoimmune

disease where the insulin producing β-cells are destroyed. Insulin is the hormone that promotes glucose absorption in the cells. In type 2 diabetes mellitus, high blood sugar results from insulin resistance of cells and inefficient insulin production by pancreatic β-cells.

The prolonged exposure of body cells to this high blood sugar leads to various pathological stress to other organs including lung, kidney and especially heart. Cardiomyopathies are the most common consequences of diabetes.

Diabetic cardiomyopathy is represented as the disorders of cardiac muscles in individuals with diabetes mellitus, in the absence of other cardiac complications such as coronary artery disease, valve disorders or hypertension. Cardiomyocyte hypertrophy and interstitial fibrosis are the most common cardiomyopathy leading to structural and functional damage to cardiac tissue(Jia, Hill, and Sowers 2018).

Understanding how the high glucose stress acts to shift the molecular balance at the cellular level leading to such pathogenesis is the main objective of our study.
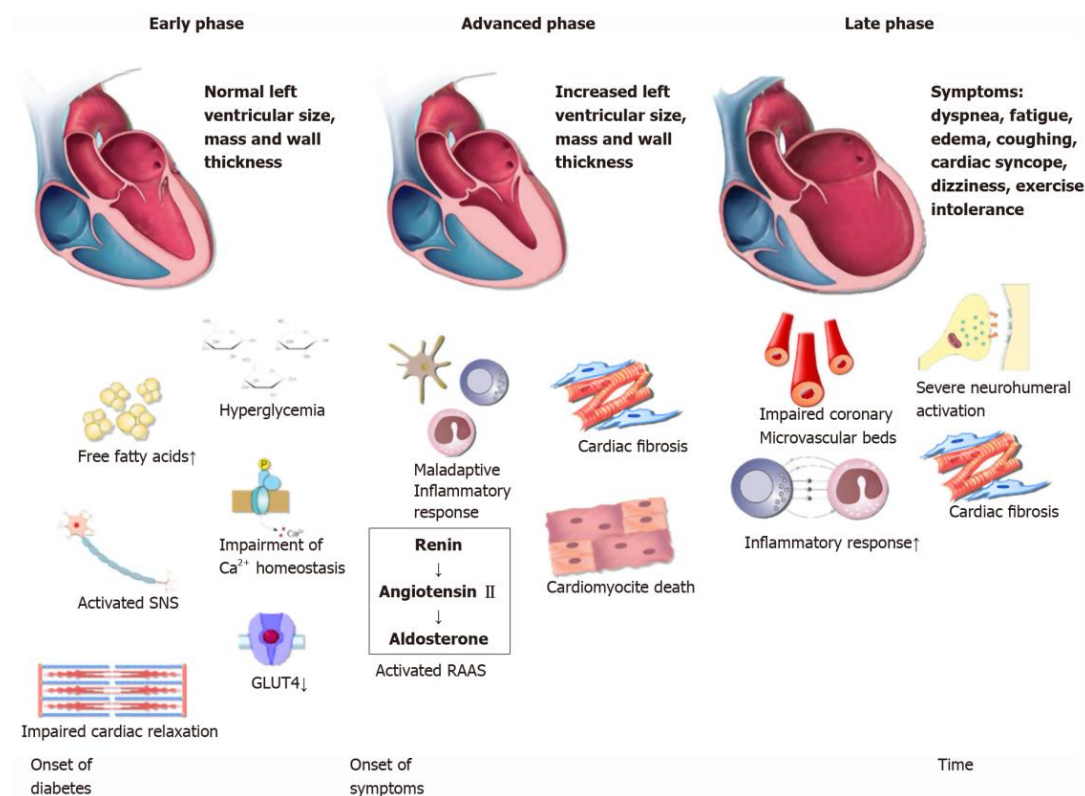
Figure 5. Diabetic cardiomyopathy (Kumric et al. 2021)

1.6 Hippo-YAP signalling in myocardial pathophysiology

Hippo pathway is known to be a master regulator of organ size and development regulator. In the mammalian system, it comprises of four main molecules namely the mammalian STE20-like protein kinase 1/2 (MST1/2), the large tumor suppressor homologue 1/2 (LATS1/2), yes associated protein (YAP), and transcriptional coactivator with PDZ-binding motif (WWTR1, also known as TAZ). Hippo regulation works by negative YAP regulation via two modes, 'ON' or 'OFF' to regulate the expression of genes governing the size and development of organs. In the 'ON' state, MST1/2 is phosphorylated which activates LATS1/2 kinases. Phosphorylated LATS1/2 further goes onto phosphorylates YAP/TAZ. Once phosphorylated, YAP/TAZ is either retained in the cytoplasm and/or subjected to proteasomal degradation, inhibiting their transcriptional activity. During the 'OFF' stage, the non-phosphorylated YAP1 remains active and thus translocates to the nucleus to induce the transcription of vital genes associated with cell proliferation, differentiation, growth and apoptosis. Thus, mutation in the hippo regulatory genes, results in overactive YAP1 leading to tissue overgrowth, known as hippopotamus like phenotype thus acquiring the name(J. Xie et al. 2022; Juan and Hong 2016).
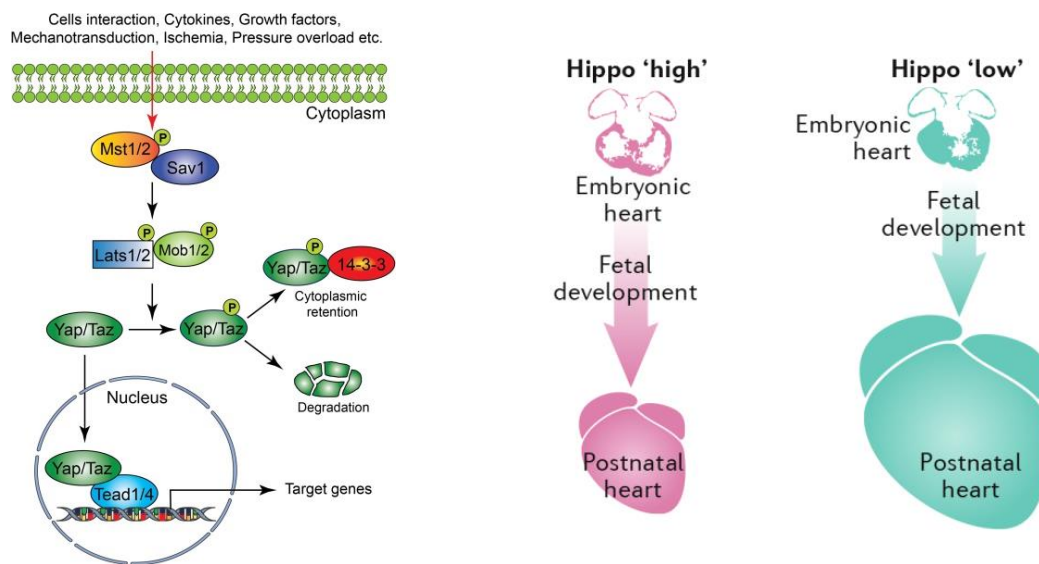
Figure 6. Hippo signaling pathway and its effect on cardiac growth and development(Mia and Singh 2022; Jun Wang et al. 2018)

In recent research, Hippo-YAP signalling has been extensively studied because of its crucial role in cancer development and progression(Zanconato, Cordenonsi, and Piccolo 2016; Abylkassov and Xie 2016). YAP1 has also been reported to be involved in hypertrophy and

fibrotic disease induction in several organs such as lung, liver, kidney among others(N. Zhang et al. 2010; Mia and Singh 2022; Wong et al. 2016).

Hippo signalling has been reported in several studies to play a critical role in the development of heart as well as its regeneration potential in the developed heart post injury. However, not without the probable risk factor of inducing pathogenesis in the adult tissue as part of fetal gene reactivation, sustained YAP1 activity have also been speculated to promote pathological remodelling in the heart(Zheng, Chen, and Zhang 2022).

While various reports already suggested the different role of YAP1 in cardiac development and disease induction, very few reports were made on the precise role of YAP1 in the cardiomyocyte hypertrophy and fibrosis induction especially in the context of diabetes or hyperglycemic stress. In our studies, we have reported the role of YAP1 in the hyperglycemia induced cardiomyocyte hypertrophy and fibrosis and its probable mechanism of action.

1.7 Role of FOXM1 transcription factor in cardiomyocyte hypertrophy and fibrosis

FOXM1 i.e. Forkhead Box Family M1 is a Forkhead family protein known for its key role as transcription factor in promoting cell proliferation and metastasis(Liao et al. 2018; Gartel 2017). FOXM1 protein has a conserved DNA binding domain and has been shown to regulate expression of various G2/M-specific cell cycle regulatory genes, such as Plk1, cyclin B2, Nek2 and CENPF promoting cell cycle progression, proliferation; thus imparting a crucial role in organogenesis(Laoukili et al. 2005). FOXM1 overexpression has been extensively reported to be associated with various forms of cancer progression(Gartel 2017; Myatt and Lam 2007). Found to express mostly in embryonic cells such as in the mesenchymal and epithelial cells of the liver, lung, renal cortex and regenerating tissues, FOXM1 also plays a critical role in early cardiac growth and development(Y. Li et al. 2019; Bolte et al. 2011; Sengupta et al. 2012). But, the expression of FOXM1 declines to a basal level in the adult fully grown tissue. FOXM1 expression is reported to be reactivated in adult cells during injury or repair(Y. Li et al. 2019). In the pathologically stressed organ FOXM1 overexpression has recently been reported to be a cause of structural and functional anomaly induction. In recent reports activated FOXM1 has been suggested to induce lung and kidney fibrosis(Balli et al. 2013; Y. Li et al. 2019; Y. Wang et al. 2020). While very few papers were available at the time of our publication regarding the role of FOXM1 in cardiac pathogenesis,

a detailed understanding of the FOXM1 signaling in cardiac biology was even more in need of exploring(Mondal et al. 2022). In our study we have observed, high level of FOXM1 expression in both diabetic cardiomyopathy mouse model and in vitro hyperglycemia stress induced H9c2 cardiomyocyte cells that associated with hypertrophic enlargement of cells and increased fibrosis induction(Mondal et al. 2022). In vitro inhibition of FOXM1 in the hyperglycemic cells resulted in amelioration of cardiomyocyte hypertrophy and fibrosis defining the precise role of FOXM1 in diabetic cardiomyopathy induction. Further, our experimental analysis regarding YAP1 modulation also led us to figure out the YAP1 mediated signalling regulation of FOXM1.

1.8 YAP-FOXM1 and AKT-GSK3β signalling

The PI3K-AKT pathway is an important cell signalling pathway that regulates cell cycle, proliferation and survival(Fresno Vara et al. 2004; Porta, Paglino, and Mosca 2014). PI3K-AKT signalling plays a central role in cancer biology, by controlling the expression of various cell cycle regulatory genes such as CREB, p27 among others(Porta, Paglino, and Mosca 2014; Peltier, O'Neill, and Schaffer 2007; Y. Xie et al. 2019). PI3K upon pro proliferating signal is activated that goes on to phosphorylate and activate AKT that further leads to cell survival and proliferation(Y. Xie et al. 2019).

Moreover, PI3K/AKT, MAPK and AMPK pathways are essential regulatory signaling systems for proper metabolic control and their disruption often leads to impaired glucose homeostasis and associated pathological outcomes(Schultze et al. 2012).

While AKT acts to promote cellular growth and survival during stress condition, there are several molecular factors that act to restrain the activity of AKT downstream to keep the proliferative capacity of P13K-AKT signalling in check(Y. Xie et al. 2019). One of the most common mediators of this activity is Glycogen synthase Kinase 3-beta (GSK3β) molecule(Y. Xie et al. 2019). Apart from the crucial role of PI3K-AKT in the progression of cancer, PI3k and AKT has also been reported to be associated with skeletal muscle atrophy and fibrotic disorders of several organs like lung and kidney(Jincheng Wang et al. 2022; Y. Zhang et al. 2021; Yoshida and Delafontaine 2020). However, very few studies were known to elucidate the role of PI3K-AKT signalling in diabetic cardiomyopathy induction. In our study our aim was to explore the probable role PI3K-AKT plays in cardiomyocyte hypertrophy and fibrosis induction.

Based on literature reports, YAP1 and AKT interaction through PI3K(Lin et al. 2015), our initial experiment also showed AKT activity to be dependent on YAP1 promoting cardiomyocyte pathogenesis. In HG with high YAP1 activity, AKT phosphorylation was observed to be significantly high. Also, in normal glucose maintained cells, YAP1 activation resulted in significantly upregulated AKT activity along with cardiomyocyte hypertrophy and fibrosis induction. Inhibition of YAP1 with verteporfin inhibitor significantly reduced the phosphorylation and activation of AKT leading to improved cardiomyocyte pathological phenotypes. Further probing into molecular mechanism revealed, this action was mediated through a negative regulation of GSK3β that is believed to restrict the FOXM1 activity in cardiac cells. The FOXM1-GSK3β association was previously reported by another study and our observations in cardiomyocyte further confirmed this association in the signaling cascade(Sinha et al. 2020).

1.9   YAP and RAS signalling in cardiac cells

Renin angiotensin system is an important hormone regulated system in the body that acts to maintain fluid balance, ionic homeostasis and blood pressure in the body. There are three major components in the group, Renin, Angiotensin and aldosterone.
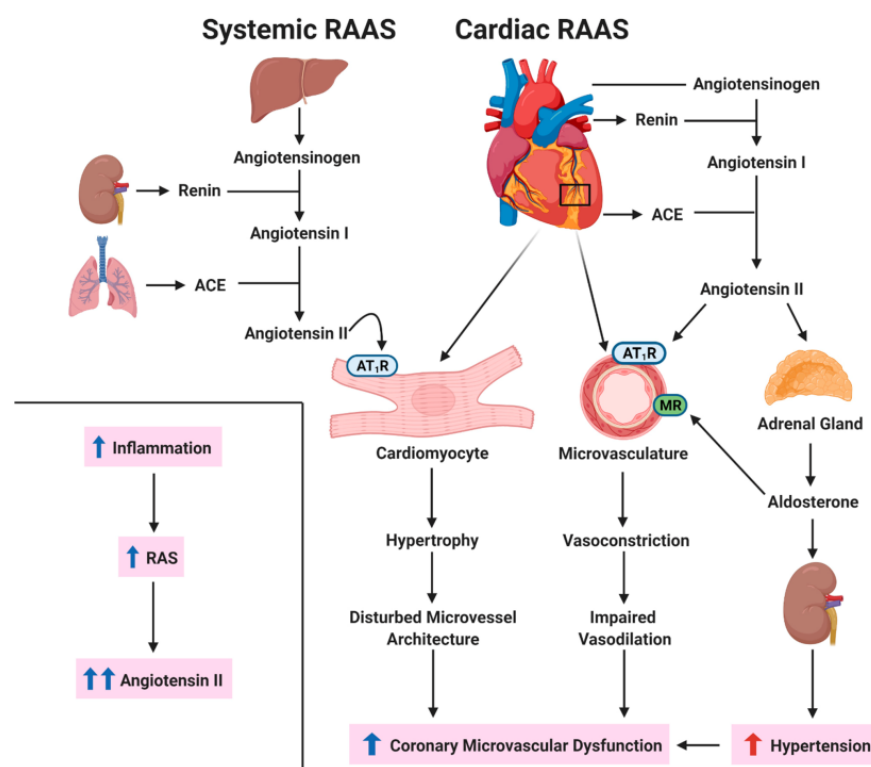
Figure 7. RAS system(Najjar et al. 2021)

When blood flow is reduced in kidney, the juxtaglomerular cells in the kidney releases renin in the circulation that converts precursor angiotensinogen secreted from liver to another precursor hormone Angiotensin-I. Angiotensin-I is then finally converted to the functional hormone Angiotensin-II by the action of Angiotensin Converting Enzyme (ACE)(Kumar N , Abbas V 2005; Patel et al. 2017). Angiotensin-II causes vasoconstriction, increases blood pressure, releases aldosterone from the adrenal cortex that promotes sodium retention and maintains the electrolyte balance. Angiotensin-II also increases the extracellular fluid volume resulting in increased blood pressure(Patel et al. 2017). Thus, Renin-Angiotensin system controls a well maintained balance between the functioning of the heart and the filtering organ kidney(Patel et al. 2017). However, dysfunctioning of the system often has severe consequences not only on the heart and kidney but affecting almost all other organs.

Angiotensin-II pathway is by far the most crucial signaling in cardiovascular pathology. Overactive Ang-II mediates blood vessel constriction, impaired blood flow and hypertension leading to high risk of heart failure as well as atherosclerosis, arterial aneurism among others(Patel et al. 2017). Increase in circulating level of Ang-II or its receptor in cell, AT1R results in cardiac hypertrophy and fibrosis induction. Moreover, Ang-II has a significant role in alterations of cardiac energy metabolism, shifting the balance towards fatty acid β-oxidation from carbohydrate metabolism resulting in energy deficit and eventually pathological cardiac remodelling(Mori et al. 2013). In the diabetic individual, RAS has been shown to be severely activated with high levels of tissue Ang-II leading to diabetic nephropathy. RAS activation in diabetes mellitus along with hypertension has been shown to be associated with cardiovascular complication(Ribeiro-Oliveira et al. 2008). As ACE is the main mediator in generating the functional Ang-II from precursor hormones, clinically, various ACE blockers, such as Benazepril, captopril etc. are used to treat hypertensive heart disorders. Rather recently ACE2, a new homolog molecule has surfaced as the body system's own coping mechanism for ACE activity. ACE2 acts on Ang-II to convert it into another bioactive peptide Angiotensin 1-7 (Ang 1-7)(Mori et al. 2013). Ang 1-7 is a vasodilator, anti-inflammatory and anti-oxidant compound that confers a protective effect on the cardiovascular system. Also ACE2, converts the precursor Angiotensin-I hormone into another beneficial peptide Angiotensin 1-9 that is also known to be anti-hypertrophic and anti-inflammatory in nature(Jackman et al. 2002). Moreover, by acting on Ang-II, ACE2 reduces the circulating level of Ang-II thus directly benefiting the cardiovascular as well as other overactive RAS affected organs. It is of interest to understand more of ACE2 regulation

as it can be more effective in reducing Ang-II load as well as delivering its cardioprotective role compared to the classical ACE blocker drugs. Further, ACE2 upregulation may directly alleviate the cardiac remodelling in metabolic disorders. In the following study, apart from the YAP-FOXM1 signaling axis in cardiomyocyte hypertrophy, we have also looked into the YAP mediated RAS regulation in diabetic cardiac fibrotic disorders.

Initially, we have observed a steady upregulation of ACE and downregulated ACE2 expression in the HG treated cardiac fibroblast and cardiomyocyte cells. This regulation was later observed to have a synchronized effect with the expression of YAP1 in cardiac cells. While verteporfin mediated YAP inhibition resulted in reduced ACE expression and ACE2 upregulation, on the other hand YAP1 activation resulted in significantly high ACE level in the cells with reduced ACE2 expression concomitant with pathological remodelling. ACE-ACE2 expression level was also observed to be associated with cardiac β-catenin expression. In the cardiac cells, along with fibrosis induction, ACE and ACE2 were also noted to influence EMT-like process through TGF-β signaling. So, based on our molecular manipulation, we were able to understand that YAP-RAS signaling may promote cardiac fibrosis through EMT-like process and ACE2 in the cardiovascular system, is sufficient to ameliorate cardiac fibrotic remodelling.

1.10 YAP mediates EMT like process in fibrosis induction in cardiac cells

In the first part of our study, our main focus was to understand the role of YAP1 cardiac hypertrophy induction. Further, we extended our objective to see the precise role YAP1 might play in regulating hyperglycemia induced cardiac fibrotic remodelling. In this regard we initially observed in hyperglycemic stress, there is an upregulated EMT-like process in the cardiac cells associated with increased fibrosis.

Cardiac fibrosis is an important process in post- myocardial infarction heart. It is a critical process in tissue repair and wound healing during myocardial infarction. TGF-β plays a central role in this reparative fibrosis process(wu et al. 2021). However, during prolonged stress condition, persistent overexpression of TGF-β induces pathological fibrotic remodelling in various organs including heart(Meng, Nikolic-Paterson, and Lan 2016; wu et al. 2021). The pro-fibrotic activity of TGFβ has been known to be associated with induction of various fibrogenic gene expression and EMT-like process. TGF-β1 and its downstream signaling molecule p-SMAD2/3 promotes fibroblast to myofibroblast transition, excessive

ECM deposition, and inhibition of ECM degradation aggravating fibrotic remodelling of tissue(Meng, Nikolic-Paterson, and Lan 2016). In our study, we have found that YAP1 overexpression in the HG treated cardiac cells promotes overactive fibrotic response via TGF-β1-p-SMAD2/3 signaling through an exaggerated EMT-like process.
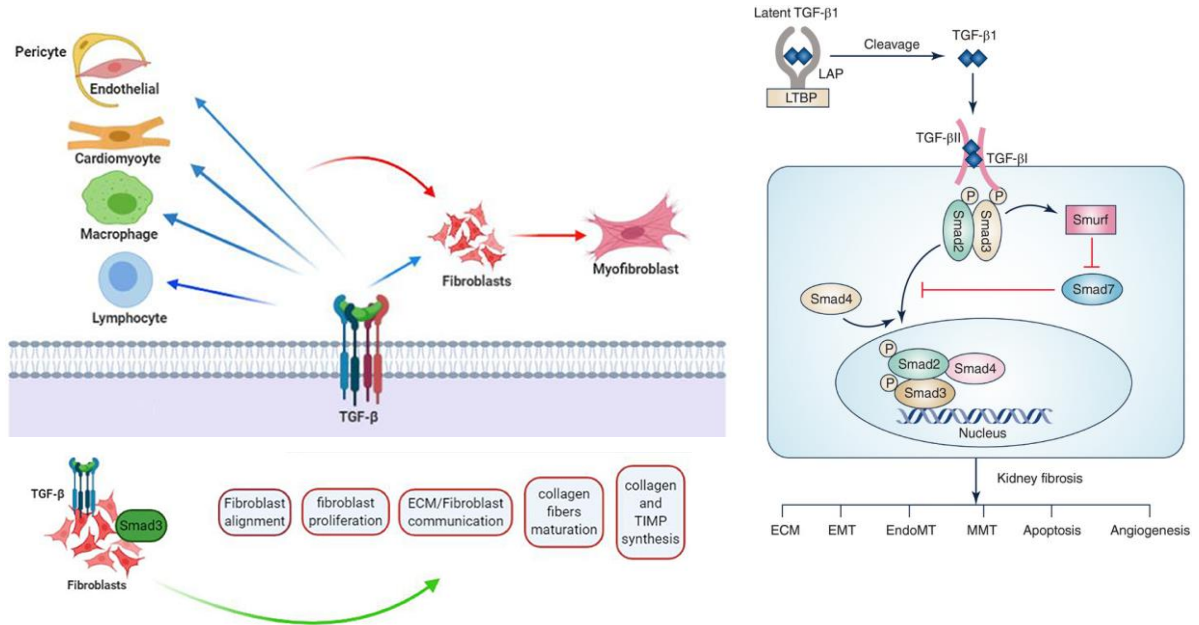
Figure 8. EMT TGF fibrosis(Saadat et al. 2021; Tang et al. 2018)

In the cardiac fibroblast cells and H9c2 cells, YAP1 inhibition in the hyperglycemic stress resulted in reduced TGF-β1 expression, lower ECM expression of fibrosis marker COL1, FN and reduced EMT activity. Thus, confirming the pro-fibrotic role of YAP1 in diabetic cardiomyopathy.

1.11 Role of YAP-βcatenin in cardiac fibrosis induction

Wnt/β-catenin pathway is one of the major cardiac development regulatory pathways. During embryogenesis, Wnt signaling in cardiac progenitor cells regulates cell specification, differentiation and proliferation(D. Li, Sun, and Zhong 2022; Chakraborty, Sengupta, and Yutzey 2013b). Hence, β-catenin signaling draws particular interest in the cardiac regeneration field. But the role of β-catenin yet remains controversial regarding it's proliferative as well as regenerative potential and pathological remodelling induction. This could be attributed to the fact that, in adult tissue, unchecked β-catenin level may go over to its regenerative activity, to induce pathological response. Hence, it is essential to better understand the different aspects of β-catenin signaling in order to draw a therapeutic implication in future.

In our study we have observed β-catenin overexpression in the hyperglycemic cardiomyocyte, associated with increased fibrotic marker expression and EMT. Inhibition of β-catenin by XAV-939 treatment result in an improvement in the cardiac fibrotic response in the HG treated cardiomyocytes(Fig. 27 and 28). Along with this, reduced EMT-like process was observed in the HG cells treated with XAV-939 with TGFβ downregulation. While β-catenin inhibition had no effect on the expression of YAP1, but YAP1 modulation had simultaneous effect on the expression of β-catenin. This result led us to believe that YAP1 may act upstream to β-catenin in cardiac cells. In this study, we further observed, β-catenin inhibition depleted ACE level in the hyperglycemic cardiac cells while ACE2 expression was increased significantly contributing to improved pathological cardiac phenotype. Therefore, our study observed, a YAP1-β-catenin mediated RAS signaling regulation in cardiac cells in the induction of EMT-mediated fibrosis in hyperglycemia induced cardiomyopathy.

1.12 TGFβ as the major mediator of cardiac fibrosis

As was discussed earlier, TGF-β is a well-known mediator in wound healing and tissue repair process. In cardiac stress or injury, TGF-β expression is upregulated to initiate a reparative process by promoting ECM production. This however, like inflammatory processes, can be detrimental if overactive or sustained over a prolonged period of stress inducing environment. In case of metabolic syndromes, the consistent high sugar level provides just the stress to induce TGF-β overexpression in cardiac cells that was observed in our experimental analysis. In both HG treated CF cells as well as H9c2 cardiomyocyte overexpression of TGF-β was observed along with increased level of its downstream effector p-SMAD2/3. The resultant increased expression of fibrotic molecule COL1 and FN could be alleviated with TGF-β inhibition in the hyperglycemic condition. TGF-β inhibition resulted in rescue of an EMT-like process, indicating its role in EMT-like process mediated fibrosis. In the follow up experiments, we observed both YAP and β-catenin, overexpression leads to increased TGF-β expression while TGF-β manipulation had little effect on the expression of YAP, β-catenin or RAS molecule ACE/ACE2. Although ACE2 upregulation significantly eliminated TGF-β regulated pro-fibrotic remodelling. In, conclusion, YAP1 may regulate various signaling molecule like FOXM1, β-catenin, TGF-β, ACE, ACE2 among others in the hyperglycemia stressed cardiac cells, to promote pathological remodelling such as cardiomyocyte hypertrophy and fibrosis. In future, more study may reveal further interactions between these molecules leading to better understanding of the signaling network and more precise mode of regulation of the molecules in cardiac development and pathophysiology.

CHAPTER 2

AIMS
&
OBJECTIVES

Currently, Diabetes has become a global epidemic disease and diabetic patients often are at severe risk of developing heart disease. Often accompanied by hypertension, diabetic individuals tend to develop cardiac hypertrophy and fibrosis with severely impacted ventricular function leading to increased incidence of heart failure.

Till date β-blockers remain the most common drugs prescribed to diabetic individuals with hypertension and heart disease. Anti-hypertensive drugs reduce oxidative stress, inflammation, improve endothelial function, increase bradykinin level, and prevent hypertrophic and fibrotic remodelling in the heart to some degree("Arterial Hypertension: Benefits and Limitations of Treatment." n.d.). **However, these drugs in diabetic patients often lower the heart rate, thus, masking the key sign of lowered blood glucose level. It may potentially increase obesity, which can lead to possibility of a coronary heart condition, arrhythmia or heart disease**("Beta Blockers and Diabetes | Orlando | UCF Health" n.d.). **Thus, the treatment of diabetic cardiomyopathy may still require development of more targeted drugs.**

In this context, ACE inhibitors are also currently in use to treat hypertension and in many cases preferred over β-blockers, in diabetic patients, albeit the potential side effects of hypotension, hyperkalemia. Developing a drug that can mimic the natural antagonist of ACE may be a better therapeutic option in combating diabetic cardiac remodelling. Also it is essential to develop a therapeutic option that can specifically target the cardiac pathological conditions like hypertrophy and fibrosis, rather than just anti-hypertensive medications with some degree of beneficial regulations.

RATIONALE: Hyperglycemia has been known to be a leading cause of cardiac hypertrophy and fibrosis. Hence there is an increasing drive to understand the disease pathogenesis in recent times. The main focus of this study is to understand how the hyperglycemic stress in cardiac cells acts at the molecular level to induce pathological remodeling. Growth regulatory molecules like YAP1 FOXM1, GSK3β, β-catenin have been extensively reported in various organs to play a critical role in the disease progression. However little information was available at the time of this study regarding the effect of YAP1, FOXM1, β-catenin expression in cardiac hypertrophy and fibrosis induction especially in the context of hyperglycemia stress. Here, in this study we aim to not only understand the role of the molecules in the disease induction under hyperglycemic stress but also understand the detailed mechanism of action.

HYPOTHESIS:

Therefore the overall hypothesis of our study is:

Hypothesis1: Hyperglycemia mediated YAP1 overexpression induces cardiac hypertrophy and fibrosis in an AKT-FOXM1 dependent signaling pathway

Hypothesis2: Hyperglycemia mediated dysregulation of ACE-ACE2 activity by YAP promotes EMT-mediated cardiac fibrosis

AIMS:

Aim1: To determine if diabetes or hyperglycemic stress results in pathological remodeling of cardiac tissue and cells leading to hypertrophy of cardiomyocyte and fibrosis

- Generating in vivo model of diabetes in mice
- Analysis of Hypertrophy and fibrosis markers
- Analysis of markers of hypertrophy and fibrosis in vitro model of high glucose treatment in H9c2 cardiomyocyte and adult mice primary fibroblast cultured cells.
- Analysis of the expression of important cardiac growth regulatory molecules such as YAP1, FOXM1, β-catenin and others in the high glucose treated cells

Aim2: To investigate the precise role of hyperglycemia induced YAP1, FOXM1 in the induction of cardiomyocyte hypertrophy and fibrosis.

- Manipulation of YAP1, FOXM1, AKT and associated molecules to understand the molecular pathway of action in disease induction
- Activation inhibition study to access any significant rescue of the pathological phenotype

Aim3: Determining the role of YAP1 and RAS signaling in hyperglycemia mediated EMT and cardiac fibrotic remodeling.

- Analysis of EMT and fibrotic markers in both cardiac fibroblast and cardiomyocyte in detailed co labelling staining in cardiac tissue.
- Molecular manipulation of YAP1, β-catenin and ACE/ACE2 to understand their role in disease induction and pathway of actin in cardiac cells.
- To perform any molecular manipulation that may help in alleviating the pathological condition

OBJECTIVES:

Hence, the main objective of our study is to identify the molecular mechanisms of hypertrophy and fibrosis in diabetic cardiomyopathy. Specifically, the study aims to understand the molecular regulation of YAP1 in the induction of other putative pro-hypertrophic and pro fibrotic genes in cardiac cells such as, FOXM1, ACE, β-catenin among others. The specific objectives of the study are as follows:

1. **To study the role of YAP1 and FOXM1 in the pathogenesis of hyperglycemia induced cardiomyocyte hypertrophy and fibrosis.**

2. **Molecular manipulation of YAP1 and FOXM1 to determine their signaling interaction and outcome in pathological cardiac remodeling.**

3. **To study the interaction of YAP1 and RAS signaling molecule ACE-ACE2 in cardiac fibrotic remodelling.**

4. **To determine the precise molecular regulation of YAP1 in cardiac fibrotic remodelling involving β-catenin, TGFβ-smad2/3 pro fibrotic molecules.**

CHAPTER 3

MATERIALS
&
METHODS

3.1 Animal Studies

All animals used in the experimental studies were maintained at the animal facility as per the CPCSEA guidelines. Animals were provided with standard chow feed and water ad libitum. The mice were kept under standard conditions of 12-hr light and 12-hr dark cycle with 50% relative humidity and a temperature of 25 ± 20C. Animals were acclimatized for a week before starting the experiments. All the experimental procedures were approved by the Institutional Ethical Committee, Presidency University (Registration PU/IAEC/SC/39), registered under "Committee for the purpose of Control and Supervision of Experiments on Laboratory Animals (CPCSEA)", Ministry of Environment and forests, Govt. of India.

Generation of Diabetic animal model:

Diabetes was induced *in vivo* by injecting adult male Swiss Albino mice (8 weeks old) with alloxan at a dose of 150 mg/kg body weight intra-peritoneally (Du et al. 2016). The animals were starved overnight prior to injection. The control animals were injected with equal volume of 0.9% saline solution as vehicle. Mice with blood glucose >200 mg/dl maintained upto 2 weeks were taken for experimental analysis (C. Li et al. 2019). Blood glucose was periodically measured using Accu-chekR glucometer (Roche).

3.2 Heart weight body weight ratio

Heart weight (HW) and body weight (BW) of each animal was taken prior to sacrifice. HW to BW Ratio was calculated in mg/g (milligram/gram) unit to assess cardiac hypertrophy.

3.3 Immunohistological analyses

Heart tissues from experimental animals were washed in PBS and fixed in 4% paraformaldehyde overnight. Tissues were embedded in paraffin blocks and sectioned at 5μm. For histological staining, sections were deparaffinized, rehydrated and subjected to subsequent staining procedures(Samanta et al. 2019).

3.3.1 Wheat Germ Agglutinin (WGA) staining: Cardiomyocyte size determination

Animal tissue sections were stained with FITC conjugated wheat germ agglutinin (WGA, #L4895, SIGMA) and nuclei were counterstained with DAPI (#D9542, SIGMA). The protocol is as follows:

1. The slide is placed in xylene for 10 mins, 2 times.

2. Next, the tissue is placed in a series of graded ethanol: 100% ethanol for 3 mins, 2 times, 90% ethanol for 2 mins, 70% ethanol for 2 mins, 50% ethanol for 2 mins, 30% ethanol for 2 mins, and finally kept in distilled water for 2 mins.

3. Antigen retrieval in the citrate buffer may be done if required.

4. The tissue is then incubated in a blocking solution containing 2% Bovine serum albumin (BSA) + PBS+0.1% Triton-x 100 for 1 hr at room temperature.

5. Next, the section is incubated in WGA solution at a recommended dilution of 1:100 of stock solution in PBS for 1hr. (WGA stock concentration is 1mg/ml dissolved in PBS) in the dark.

6. After draining the WGA solution, DAPI (nuclear stain) dissolved in PBS (1.2µl in 1.5ml) was added on the tissue and incubated for another 15 mins at room temperature in the dark.

7. Wash with 1x PBS, 3 times.

8. Mount the tissue with cell mounting media.

Images were taken by Leica DFC7000T at 40x magnification across different fields. Cell size was measured using ImageJ (NIH) software.

3.3.2 Masson's Trichrome Staining: Fibrosis detection

Tissue samples were stained with Masson's Trichrome reagent for assessment of collagen deposition. The amount of collagen was quantified as percent fibrotic tissue area with respect to the total tissue area using ImageJ (NIH) software. The staining protocol was followed as mentioned.

1. The slide is deparaffinized by placing it on a 60°C hot plate.

2. The slide is then placed in xylene for 7 mins.

3. Next, the tissue is rehydrated following alcohol down-gradation in 100% ethanol for 2 mins, 2 times, 90% ethanol for 2 mins, 70% ethanol for 2 mins and 50% ethanol for 2 mins and finally in distilled water for 2 mins.

4. Next, the slide is placed in Bouin's solution, for mordanting. The Bouin's solution with the slides is microwaved for 5 mins and allowed to cool down for 15 mins.

5. The slide is then washed in running tap water for 5 mins to remove the excess picric acid from Bouin's solution.

6. The tissue is then stained with Weigert's iron haematoxylin for 10 mins.

7. Slides are rinsed in running tap water for 5 mins for bluing and rinsed with distilled water.

8. The slide is then placed in Biebrich scarlet solution for 3 mins and rinsed in distilled water.

9. Freshly prepared phosphotungstic acid solution is added to the tissue for 10 mins and discarded.

10. The slide is then transferred directly to aniline blue solution and kept overnight.

11. Next day, the slide is rinsed well with distilled water to remove the excess stain of aniline blue.

12. Next, the slide is placed in 1% acetic acid solution for 1 min and rinsed in distilled water.

13. The tissue is then dehydrated by alcohol upgradation in 50% ethanol for 2 mins, 70% ethanol for 2 mins, 90% ethanol for 2 mins and then 100% ethanol for 2 mins twice.

14. Finally the slide is cleared in xylene for 2 mins, 2 times.

15. The slide is air dried and mounted with DPX.

3.3.3 Immunostaining of cardiac tissue by DAB staining method

For detection of the protein expression in the tissue the tissues were stained with YAP1 (1:200; #14074 Cell Signaling), FOXM1 (1:100; #sc-502 Santa Cruz Biotechnology), α-SMA (1:640, #19245 Cell signaling), periostin (1:500; #ab14041, Abcam) antibodies. The tissues were then incubated in secondary antibody (goat anti-rabbit IgG H and L –HRP secondary antibody #ab97051, Abcam) following which the antibodies were developed using DAB Substrate Kit (ab64238).

1. The slides with tissue sections are dried on a 60°C hot plate.

2. The slides are deparaffinized in xylene for 7 mins, 3 times.

3. The slides are gradually rehydrated in a series of graded ethanol: 100% ethanol for 2 mins, two times, 90% ethanol for 2 mins, 70% ethanol for 2 mins, 50% ethanol for 2 mins. Then washed in distilled water for 2 mins.

4. Antigen retrieval is done in the citrate buffer. The slides are placed in citrate buffer containing coplin jar and microwaved until the boils, and kept for further 2-3 mins after boiling. The slides are let to cool down.

5. The slides are washed in distilled water for 2 mins twice and with PBS.

6. The tissues are incubated in 0.3% hydrogen peroxide in PBS for 15 mins to quench endogenous peroxidase.

7. The slides are washed with PBS for 2 mins twice.

8. The slides are then washed in 0.1% Triton-x 100 + PBS for 5 mins, 2 times.

9. The tissues are then incubated in a blocking solution (2% BSA, 0.1% Triton-X 100, PBS) for 1 hr at room temperature to block any nonspecific background staining.

10. The slides are then drained and incubated in primary antibody diluted in fresh blocking solution overnight in a humid chamber.

12. Next day, the slides are rinsed in PBS+ 0.1% Triton-X 100 for 5 mins, 2 times

13. HRP conjugated secondary antibody is applied to the slides diluted in blocking buffer to the concentration recommended by the manufacturer and incubated at room temperature for 1 hr.

14. The slides are rinsed in PBS for 5 mins, 3 times.

15. Next, DAB substrate was applied to the tissues at recommended concentration. Incubation is done upto 30 mins as required.

16. Next, a solution of 0.5% copper sulphate + 0.9% sodium chloride in distilled water is added to the tissues for 1-10 mins as required.

17. The tissues are washed in PBS, 4 times.

18. The tissues are then counterstained with haematoxylin and bluing under tap water is done for 5 mins.

19. The tissue section is then dehydrated in 50%, 70%, 90% ethanol each for 2 mins and finally in 100% ethanol for 2 mins, 2 times.

20. The slides are then placed in xylene for 2 mins, 2 times.

21. The slides are then mounted in DPX.

3.3.4 Immunofluorescence studies in tissue sections

1. For, immunofluorescence study, the deparaffinised, rehydrated tissue sections were placed in blocking solution (2% BSA with 0.1% Tween20) for 1 hr at room temperature (RT) and subsequently incubated overnight in following primary antibodies at 4 °C as per recommended concentrations: COL1 (1μg/mL, #PA5-95137, Invitrogen), Fibronectin (1:200, #ab2413, Abcam), E-cadherin (1:200, #PA5-85088, Invitrogen), N-cadherin (3μg/mL, ##33-3900, Invitrogen), YAP1 (1:200; #14074 Cell Signaling Technology), β-catenin (1:100, #8480, Cell Signaling Technology), TGF-β1 (2 μg/ml, #ab 64715, Abcam), ACE (1:50; sc-23908, santa cruz), ACE2 (2μg/mL, # ab15348, Abcam). Next day, the tissues were washed and incubated with fluorescence tagged secondary antibodies: Goat AntiRabbit IgG H&L (Alexa Fluor 488) (1:1000, #ab150077; Abcam), Goat Antimouse IgG H&L (TexasRed) (1:1000, #ab6787; Abcam) for 1 hr at RT. For co-labelling staining, the sections were again placed in blocking solution for 1hr and incubated with the second primary antibodies: Mf20 (1:200; Developmental Studies Hybridoma Bank, University of Iowa), α-actinin (1:400, # ab137346, Abcam) Vimentin (1:1000, #ab17321, Abcam), Vimentin (1:1000, # ab20346, Abcam) for overnight at 4°C.

2. Next day, slides were incubated with corresponding secondary antibodies as before

3. Finally nucleus was counterstained by placing sections in DAPI (#D9542, Sigma) solution for 15 mins.

4. Slides were washed and mounted with cell mounting media and imaged at Leica microscope.

3.4 RNA isolation from heart tissue

For in vivo RNA expression analysis, heart tissues were taken from adult rat ventricle and processed in the following protocol.

1. The harvested tissues are minced thoroughly.

2. 500 µl of Trizol is added to the chopped tissues, homogenized finely.

3. Then 100µl chloroform is added and thoroughly mixed with hands and incubated for 2-3 mins.

4. The samples are centrifuged at 12,000 g or 12 rcf for 15 mins at 4°C.

5. The top aqueous layer containing RNA is transferred carefully and taken in a fresh tube.

6. The RNA is then precipitated using 250 µl chilled isopropanol and kept at -80°C overnight.

7. Next day, the samples are centrifuged at 12,000 g for 10 mins, at 40C.

8. The supernatant is removed and the RNA pellet is washed with 200 µl of 75% chilled ethanol.

9. The samples are then centrifuged at 7500 g (7.4 rcf) at 4°C for 5 mins.

10. The ethanol is removed and the pellets are air dried by keeping the tubes in an inverted position for maximum 30 mins at room temperature.

11. The RNA pellet is finally resuspended with 20-50 µl DEPC water.

12. The samples are incubated at 60°C for 5 mins for better dissolution of RNA, and then tapped to mix and short spin was performed.

13. The RNA is then used for cDNA preparation or can be stored at -80°C for long term use.

Determination of the RNA concentration

The concentration of RNA samples were determined using Qubit 4.0 fluorometer. The Qubit 4.0 machine measures the concentration of RNA directly as per manufacturer's protocol in µg/µl.

3.5 Preparation of cDNA from RNA samples

For reverse transcription of cDNA from RNA, RNA is taken at an amount of 1 µg. 4 µl of reaction buffer mix is added to it as per manufacturer's protocol. 1 µl of reverse transcriptase enzyme is added and the total volume is adjusted with nuclease free water up to 20 µl (170-8891, BIORAD). The entire mixture is shortly vortexed and set up according to manufacturer's instructions in a thermal cycler according to the following program. The cDNA is stored at -20°C.

STEP 1	STEP 2	STEP 3	STEP 4
25°C	42°C	85°C	4°C
5 mins	30 mins	5 mins	∞

3.6 Real Time-Polymerase Chain Reaction (Real Time-PCR)

For real time PCR process 1 µl each of cDNA samples are taken at and mixed with 5 µl of EvaGreen Supermix (172-5201AP, BIORAD). Forward and reverse primers are added to a final concentration of 0.4 picomole. Primers are obtained from IDT and the final volume is adjusted to 10 µl with nuclease free water. The reaction is set at three technical and three independent biological replicates. The real time PCR is run using either BIORAD CFX manager software or Applied Biosystems Real time PCR machine. The resulting Cq values that are obtained are further taken for fold change analysis. The various mouse primers that were used are as follows.

TABLE 1. MOUSE PRIMER LIST

Primer		Sequence	Amplicon size (bp)	Annealing temperature (°C)
yap1(M)	Forward	5'-ACCCTCGTTTTGCCATGAAC-3'	172	56.5
	Reverse	5'-TTCAACCGCAGTCTCTCCTT-3'		
foxm1 (M)	Forward	5'-AAGGCAAAGACAGGAGAGCT-3'	188	55.7
	Reverse	5'- AGGGCTCCTCAACCTTAACC-3'		
bnp (M)	Forward	5'-AAGTCCTAGCCAGTCTCCAGA-3'	91	56.2
	Reverse	5'-GAGCTGTCTCTGGGCCATTTC-3'		
beta-mhc (M)	Forward	5'-ACGGATGCCATACAGAGGAC-3'	340	56.1
	Reverse	5'-CCTCATAGGCGTTCTTGAGC-3'		
col1 (M)	Forward	5'-CACCCTCAAGAGCCTGAGTC-3'	269	58
	Reverse	5'-GCTTCTTTTCCTTGGGGTTC-3'		
col3(M)	Forward	5'-ACGTGGTAGTCCTGGTGGTC-3'	287	60
	Reverse	5'-GACCTCGTGCTCCAGTTAGC-3'		
serca2 (M)	Forward	5'-GGGCGAGCCATCTACAACAA-3'	150	60
	Reverse	5'-TGTCACCAGATTGACCCAGAGT-3'		
beta-actin (M)	Forward	5'-CCTCTATGCCAACACAGTGC-3'	206	56
	Reverse	5'-CCTGCTTGCTGATCCACATC-3'		

3.7 Western blot

To analyse protein expression in different in vivo samples, the harvested cardiac tissues were taken and the protein was isolated according to the following protocol.

3.7.1 Protein isolation from cardiac tissue

1. The cardiac tissue is cleaned in PBS and minced finely with a tissue cutter blade.

2. Minced tissue is taken in 200 μl RIPA lysis buffer containing protease and phosphatase inhibitors (GX-2811AR, Puregene and GX-1211AR, Puregene) at recommended concentrations and homogenized properly by keeping on ice.

3. Then it is kept on ice for few mins.

4. The homogenized sample is then centrifuged at 10,000 rpm, for 10 mins at 4°C.

5. The supernatant containing the protein lysate is then carefully collected and quantified or stored at -80°C for further use.

3.7.2 Determination of protein concentration using Bradford method:

1. 1-2 μl of protein sample was taken in 199-198 μl of diluent (ddH2o) (total diluent and protein sample volume is to be 200 μl.

2. 1 ml of Bradford reagent (ML-106, #Himedia) was added to each sample.

3. The tubes were briefly vortexed and incubated at room temperature for 10 mins.

4. The absorbance was measured at 595 nm.

5. Protein concentration was calculated following the equation provided by the manufacturer.

After determining the concentration, the total protein lysates were subjected to SDS-PAGE separation, and transferred to the PVDF membrane. Finally the membrane bound protein was immune probed with the specific antibody as per requirement.

3.7.3 Protein separation by SDS-PAGE

1. SDS-PAGE gel is cast with the BIORAD resolver, stacker, TEMED and 10% APS as per the manufacturer's protocol.

2. Required amount of protein (10-100μg according to the abundance of target proteins) is taken and mixed with equal volume of Laemmli sample buffer mixed with beta-mercaptoethanol (Laemmli buffer to β-mercaptoethanol ratio is 19:1). The microcentrifuge tubes containing the sample mixtures are then placed on boiling water for 5 mins and then snap chilled on ice for 5 mins. The sample was then loaded in each well of the gel. Equal amount of each protein sample is loaded along with molecular weight markers.

3. The gel apparatus is filled with a 1x running buffer.

4. The gel electrophoresis is run at 100 volts until all the proteins separate properly.

3.7.4 Protein transfer from gel to membrane

1. The PVDF membrane is activated with 100% methanol for about 1 min. and then soaked in the transfer buffer. The filter papers and mesh is also kept soaked in transfer buffer at 4°C until transfer.

2. The resolved gel is carefully taken out from the glass plates and placed in transfer buffer.

3. The transfer unit is prepared by sandwiching the gel and membrane between mesh and filter paper in the following order: from black colour back side of the transfer cassette at the base: mesh, filter paper, gel, PVDF membrane, filter paper, and mesh. Filter paper is cut at the top corner to mark the first lane. The cassette is pressed firmly to remove any bubbles inside for proper transfer of protein from gel to membrane.

4. The cassettes are then placed in the transfer apparatus with transfer buffer, cool pack and placed on a magnetic stirrer.

5. Transfer is done at 100 volts for about 1-1.5 hours.

3.7.5 Immunoblotting

1. After transfer, the membrane is taken and washed in 1X TBST (PBS+ 0.2% Tween 20).

2. The membrane is then incubated in blocking buffer (5% BSA in TBST for phospho-proteins or 5% non-fat dry milk in TBST for other proteins) for 1 hour with gentle shaking at room temperature.

3. Following blocking, the membrane is incubated overnight in primary antibody diluted with blocking buffer according to manufacturer's instructions at 4°C with gentle shaking.

4. Next day, the blot is washed with TBST; for 5 mins, 3 times.

5. The blot is then incubated with a secondary antibody diluted in blocking buffer according to recommended concentration with gentle shaking at room temperature for 1 hour.

6. The blot is then washed in TBST for, 3x5 mins with gentle shaking.

7. The blot is washed finally with TBS.

3.7.6 Developing of the blot

1. The membrane is then wiped with tissue paper to remove TBST. A mixture of peroxide solution: luminol enhancer solution (in the ratio of 1:1) is prepared in the dark and added to the blot (#1610182, BIORAD western blot).

2. The blot is then visualized in a chemidoc or developed using X-Ray film. For X-Ray film developing, the film is placed over the membrane with a signal and then the bands are developed by placing them in developer solution. Finally the film is dipped in fixer solution and washed in water and dried before imaging.

3. The protein expression was quantified by measuring the band intensity using Image J software and statistically analysed.

The following antibodies were used in the western blot studies: p-YAP (1:1000; #13008 Cell Signaling), YAP (1:1000 WB; 1:50 IP; #14074 Cell Signaling), Anti-O-Linked N-Acetylglucosamine antibody [RL2] (1:1000; ab2739, Abcam), FOXM1(1:500 #sc-502, Santa Cruz), p-AKT (1:1000; #9271 Cell Signaling), AKT (1:1000; #9272 Cell Signaling), p-GSK3β (1:1000; #9322 Cell Signaling) GSK3β (1:1000; #9315 Cell Signaling). β-catenin (1:1000, #8480, Cell Signaling), TGF-β1 (1 μg/ml, #ab64715, Abcam), ACE (1:500; #sc-23908, santa cruz), ACE2 (2μg/mL, #ab15348, Abcam), p-SMAD2/3 (1:1000, #8828, Cell Signaling Technology), SMAD2/3 (1:1000, #8685, Cell Signaling Technology). Membrane was further incubated in anti-rabbit IgG, HRP-linked Antibody (1:1000 dilution, catalog no.: 7074S; Cell Signaling Technology), antimouse IgG, HRP-linked Antibody (1:1000 dilution, catalog no.: 7076S; Cell Signaling Technology) GAPDH antibody (1:2000; #BB-AB0060 BioBharatiLifeScience Pvt.Ltd.) was used as loading control.

3.8 Cell culture and treatments

3.8.1 H9c2 rat cardiomyoblast culture

H9c2 rat cardiomyoblast cell line was initially obtained from Dr. Santanu Chakraborty's lab, Department of Life Sciences, Presidency University and also from NCCS, Pune. The cell line was maintained as follows.

1. The H9c2 cells were maintained in containing Dulbecco's modified Eagle's medium (DMEM) media (#12800-017, Gibco) supplemented with 10% Fetal Bovine Serum (FBS), RM1112, Himedia and 2% penicillin-streptomycin cocktail of antibiotic (#15140122, Gibco).

2. The cells were maintained in an incubator with 5% carbon dioxide at 37°C.

3. When the cells were confluent, the cells were washed with sterile PBS and trypsinized with 2ml 0.25% trypsin-EDTA (#25200072, Invitrogen). The dislodged cells were neutralized with 8 ml complete media and then passaged in fresh culture plates.

4. For experiments, the cells were seeded in culture plates from the mother plates that were maintained as per requirement of experiments. For, RNA and protein samples, cells were directly seeded to the plates and for immunostaining cells were seeded over coverslips placed in the culture plates.

3.8.2 Fibroblast Culture

To establish primary cardiac fibroblast cell culture, male adult Wistar rats were sacrificed and hearts collected. Following PBS wash, the hearts were digested with collagenase type 2 (80 units/ml DMEM; Sigma #C6885). The solution was then centrifuged to pellet down cells. The supernatant was discarded and pellet was suspended in fresh DMEM media containing 10% FBS and pen strep and plated for cells to attach for at least 3 hours in incubator maintained at 5% CO2, and 37°C condition. The cells were then passaged as usual and subjected to treatments as per requirement(Tarbit et al. 2021).

3.9 In vitro hyperglycemia model establishment

For, molecular modulation, in vitro model of hyperglycemia, was generated by treating H9c2 or fibroblast cells first with no glucose media overnight. Then the cells were treated with 5mM glucose containing DMEM media as normal glucose (NG) maintained cells and 25mM glucose containing DMEM media as high glucose (HG) maintained cells. Cells were kept in

the respective media for at least 48 hours. For molecular manipulation assays, cells were pre-treated with the required molecular activator or inhibitors following HG treatment. Control cells are kept untreated in NG for the said durations.

The following activator and inhibitors were used in the study of signalling mechanism in H9c2 cells:

1. Verteporfin (SML0534, Sigma) was used for YAP inhibition at a dose of 1 μM, for 24 hr

2. Thiostrepton (ab143458, Abcam) was used to inhibit FOXM1 at a dose of 1 μM, 24 h.

3. LY294002 (L9908, SIGMA) was used for AKT inhibition at a dose of 10 μM, 2 h

4. FOXM1 recombinant protein (H00002305-P0, Abnova) was used for FOXM1 activation at a dose of 0.1 nanogram protein per ml DMEM for overnight.

5. Resorcinolnapthalein (13082, CAYMAN) was used for ACE2 activation at a dose of 20 μM for 24 h.

Following activators and inhibitors were used for signalling mechanism study in rat cardiac fibroblast:

1. Verteporfin (SML0534, Sigma) was used for YAP inhibition at a dose of 1 μM, for 24 hr

2. XAV-939 (ab120897, Abcam) was used to inhibit β-catenin at a dose of 5 μM for 7 h.

3. SB431542 (ab120163, Abcam) used for TGF-β inhibition at 10 μM dose for 30 min.

3.10 Phalloidin staining to detect cardiomyocyte hypertrophy

The H9c2 cardiomyocytes were stained with phalloidin to detect the cell size upon different experimental treatments. The protocol of phalloidin staining is as follows.

1. The cells are washed with 1x PBS for 5 mins.

2. The cells are then fixed with 4% PFA in PBS for 10 mins with gentle shaking at room temperature.

3. The cells are then thoroughly washed with PBS for 5 mins x3 times.

4. The cells are then either stored in PBS at 4°C or directly taken for staining.

5. The cells are then permeabilized with 0.2% Triton-X 100+PBS for 10 mins with gentle shaking at room temperature.

6. Following permeabilization, the cells are incubated in a blocking reagent (2% BSA+PBS+0.1% Triton-X 100) for 30 mins- 1 hr at room temperature with gentle shaking.

7. The cells are now incubated with Alexa fluor 488 tagged phalloidin (A12379, Thermo Fisher) diluted in PBS at a ratio of 1:400 - 1:500 for 2 to 2.5 hrs at 4°C with gentle shaking.

8. Finally, the cells are counterstained with DAPI nuclear stain (Genetix) in PBS (1:200) for 30 mins with gentle shaking.

9. The cells are then washed with PBS for 5 mins x3times.

10. The cells are mounted with cell mounting media and imaging was done using a fluorescent microscope. The cell size was measured using Image J software.

3.11 Immunofluorescence staining of cells

The H9c2 cells were stained with primary antibody by immunofluorescence staining. The IF protocol is as follows:

1. The H9c2 cells are washed with PBS for 5mins.

2. The cells are then fixed with 4% PFA dissolved in PBS for 10 mins, at room temperature.

3. After fixation, the cells are thoroughly washed with PBS for 5mins, 3 times and either stored in PBS at 4°C or taken directly for immunostaining.

4. The cells are permeabilized with 0.2% Triton-X 100+PBS for 10 mins with gentle shaking at room temperature.

5. Then the cells are washed once with PBS and incubated in blocking reagent (2% BSA+PBS+0.1% Triton-X 100) for 30 mins - 1 hr at room temperature with gentle shaking.

7. The cells are then incubated with primary antibody (ab52857, Abcam or ab39670, Abcam ChIP grade) diluted in blocking reagent at recommended dilution, overnight at 4°C with gentle shaking.

9. Following day, the cells are washed with PBS, 5 mins x3 times.

10. The cells are then incubated with secondary antibody that is goat anti-rabbit IgG H and L (Alexa Fluor 488) secondary antibody (1:1000 dilution, ab150077, Abcam), Goat Antimouse IgG H&L (TexasRed) (1:1000 dilution, ab6787; Abcam) diluted in PBS or in blocking buffer at recommended dilution for 2-2.5 hrs at room temperature with gentle shaking.

12. The cells are then washed in PBS, for 5 mins x3 times.

13. The nuclei are then counterstained with DAPI (1:200) in PBS for 30 mins at room temperature with gentle shaking.

14. The cells are then washed with PBS for 5 mins x3 times.

15. The cells are finally mounted with cell mounting media and images are taken in a fluorescence microscope.

The quantitative analyses were performed by counting total number of immunopositive cells and total cells across different fields and calculated as percent positive cells.

3.12 DAB staining of cells

For antibody supporting IHC staining the following protocol was followed:

1. The cells are washed with PBS for 5 mins.

2. Then the cells are fixed in 4% PFA in PBS for 10 mins at room temperature with gentle shaking.

3. The cells are again thoroughly washed with PBS, 3 times for 5 mins each.

4. Following fixation, the cells may be stored in PBS or taken directly for DAB staining.

5. The cells are permeabilized with 0.2% Triton-x 100+PBS for 5 mins at room temperature.

6. The cells are then incubated in 0.3% hydrogen peroxide in PBS for 15 mins to quench the endogenous peroxidase in the cells.

6. The cells are then again permeabilized with 0.2% Triton-x 100+PBS for 5 mins at room temperature.

7. The cells are then incubated with blocking reagent (2%BSA+0.1% Triton-x 100+PBS) for 30 mins-1 hr at room temperature with gentle shaking.

8. The cells are then incubated with the required primary antibody diluted in blocking buffer at recommended dilution overnight at 4°C with gentle shaking.

9. Next day, the primary antibody cells are washed with PBS for 5 mins, 3 times.

10. The cells are then incubated in a secondary antibody that is goat anti-rabbit IgG H and L(HRP) (ab97051, Abcam) at recommended dilution in blocking buffer for 1 hr (or more if required) at room temperature with gentle shaking.

11. The cells are washed with PBS for 5 mins, 3 times.

12. Next, 1 drop (30 µl) of DAB chromogen is mixed with 50 drops (1.5 ml) of DAB substrate and added to the cells and kept for 15-30 mins until the colour is developed.

13. A few drops of 0.5% copper sulphate and 0.9% sodium chloride solution in distilled water are added to the cells to enhance the colour of the DAB stain for a few seconds as per requirement.

14. The cells are then washed with PBS several times.

15. Cell nuclei are counterstained with haematoxylin keeping for about 80 secs or more as per requirement.

16. Bluing of the nucleus is done under tap water for 5 mins.

17. Finally the cells are dehydrated with ethanol upgradation in the following order: 50%, 70%, 90% and 100 % ethanol for 2 mins each and air dried.

18. The cells are then mounted with cell mounting media and imaging was done under a bright field microscope.

3.13 RNA isolation from H9c2 cardiomyocyte

1. The cells are washed with PBS for 5 mins.

2. 500 µl (or more as per requirement) of Trizol is added to 60 mm culture plates and the cells are scraped and taken in Eppendorf tubes.

3. The trizol containing cells are pipetted up and down several times to homogenize the cells.

4. The tubes are kept at room temperature for about 5 mins.

5. Steps 3 to 13 of section 3.4 (RNA isolation from cardiac tissue) are followed.

RNA concentration is measured and cDNA is synthesized according to the protocol mentioned in section 3.4 and 3.5 respectively. Next, Real Time-PCR is done with the in vitro cDNA samples according to the process mentioned in the section 3.6. The primer sequences used in the PCR are listed below:

TABLE 2. RAT PRIMER LIST

Primer		Sequence	Amplicon size (bp)	Annealing temperature (°C)
yap1(R)	Forward	5'-CGCTGAGTTCCGAAATCCTG-3'	234	56.1
	Reverse	5'-AGAGCAGAGCAACAGTGGAT-3'		
foxm1 (R)	Forward	5'-ACCAATATCCAGTGGCTTGG-3'	210	54
	Reverse	5'-GCTGTTGATCGCGAACTGTA-3'		
bnp(R)	Forward	5'- AGTCCTAGCCAGTCTCCAGA -3'	172	60
	Reverse	5'-GTCTCCTGGATCCGGAAG-3'		
beta-mhc(R)	Forward	5'-CCAGTCCCGAGGTGTACTTT-3'	195	60
	Reverse	5'-TCCTCCTTCATGTTGGCCAT-3'		
col1(R)	Forward	5'- ATCCTGCCGATGTCGCTAT-3'	207	60
	Reverse	5'- CCACAAGCGTGCTGTAGGT-3'		
col3(R)	Forward	5'- CTGGTCCTGTTGGTCCATCT-3'	131	60
	Reverse	5'- ACCTTTGTCACCTCGTGGAC-3'		
tgf-β1(R)	Forward	5′-CTGAACCAAGGAGACGGAATAC-3′	247	53
	Reverse	5′-CTCTGTGGAGCTGAAGCAATAG-3′		
ctgf (R)	Forward	5'-CTGTTCTAAGACCTGTGGGATG-3'	120	60
	Reverse	5'-TCCTCTAGGTCAGCTTCACA-3'		
mmp2 (R)	Forward	5'-AGCTCCCGGAAAAGATTGAT-3'	180	60
	Reverse	5'-TCCAGTTAA AGG CAG CGT CT-3'		
mmp9 (R)	Forward	5'-CCACCGAGCTATCCACTCAT-3'	160	58
	Reverse	5'-GGT CCG GTT TCA GCA TGT TT-3'		
β-catenin (R)	Forward	5'-ACAGCACCTTCAGCACTCT-3'	167	56.1
	Reverse	5'-AAGTTCTTGGCTATTACGACA-3'		
ace (R)	Forward	5'-ATTGCTTTGGGTGTGGAAGA-3'	102	60
	Reverse	5'-TTGAGCTTGGCGATCTTGTT-3'		
ace2 (R)	Forward	5'-TGCACAAAGGTCACAATGGA-3'	111	60
	Reverse	5'-ATTGGCTCCGTTTCTTAGCA-3'		

3.14 Protein isolation from H9c2 cells

1. The cells are washed with PBS for 5 mins.

2. 500 μl – 1mL PBS are added to the plates and cells are then scraped with a cell scraper. The PBS containing cells are collected in test tubes.

3. The tubes are centrifuged at 3000RPM for 5minutes, to pellet down the cells. The supernatant is discarded.

4. Next, 200-300 μl of RIPA lysis buffer containing protease and phosphatase inhibitors (GX-2811AR, Puregene and GX-1211AR, Puregene) according to manufacturer's recommended dilution, are added to the cells.

3. The tubes are vortexed thoroughly several times following 2-3 times, freezing thawing at -20°C.

6. The samples are then centrifuged at 14,000 rpm for 20 mins at 4°C.

7. The supernatant which is the protein lysate is collected carefully and stored at -80°C for long term usage.

Following concentration measurement, by Bradford reagent (protocol as mentioned earlier in section 3.7.2) the proteins are subjected to SDS-PAGE and Western Blot analyses as mentioned in the section 3.7. All the antibodies used are mentioned in section 3.7.6.

3.15 Sirius Red staining in H9c2 cardiomyocyte to detect fibrotic depositions

Collagen deposition can be identified by Sirius red staining. For collagen amount estimation, H9c2 cells were seeded in a 96 well plate and treated as per experimental condition. The cells were then washed in PBS and fixed in methanol for 10 minutes at 4°. Then 200μl of 0.1% Sirius red solution made in saturated picric acid was added to each well and incubated for 1 hr at room temperature. The cells were then washed with acidified water (5ml acetic acid to 1ml distilled water) for three times, until the water ran clear. Finally, the dye bound stain was eluted with 200μl 0.1N NaOH solution for 1 hr at room temperature and the collagen content was estimated from the standard curve. The standard curve was obtained from known concentration of collagen1 stained with picrosirius red and absorbance measured at 570nm.

For imaging H9c2 cells seeded on coverslips were stained in similar manner, washed with acidified water and then dehydrated with 100% ethanol 3times and mounted on slides(Kohli et al. 2013; Trackman, Saxena, and Bais 2017).

3.16 MTT Assay for drug dosage determination

1. The cells for MTT assay are seeded in well plates as per requirement.

2. Post treatment, the DMEM media is discarded and cells are washed with PBS x2 times.

3. 800 µl of MTT working solution is added to each well and incubated at 37°C for 3 hrs.

4. The solution was discarded and the purple colour formazan dye precipitate was dissolved with 400-500 µl of extraction buffer.

5. Finally the O.D of the solution is measured at 570 nm.

MTT stock solution:

5mg/ml MTT reagent dissolved in 1X PBS. Solution is filtered through a 0.45 micron filter and stored at 4°C. MTT working solution is prepared by 1:10 dilution of the stock in 1X PBS.

3.17 Statistical analysis

Statistical significance was calculated by Student's unpaired two-tailed T test between the control and treated group. For experiments with more than two groups, statistical analyses were performed by ANOVA analyses by Graphpad Prism software. Statistical analysis is represented as mean ± standard error of mean (SEM).

The level of significance in each case was considered as $p<0.05$. In our graphical representations of data, * indicates $p<0.05$ between control and treated group, ** means $p<0.01$, ***, $p<0.0001$ between control and treated group, # indicates $p<0.05$, ## indicates $p<0.01$, ### $p<0.0001$ between 2 treated groups.

Buffer recipes:

1. 1X PBS (1L)

8g NaCl; 0.2g KCl; 1.44g NaH_2PO_4; 0.24g K_2HPO_4

Dissolved in dH2o, pH is adjusted to 7.4 and final volume is adjusted to 1L.

2. 10mM citrate buffer

1.92gm citric acid is added to 500 ml water, then pH is adjusted to 6.0 with 1N NaOH and 0.5ml Tween 20 is added. Finally the volume is adjusted with water up to 1 litre. The citrate buffer is store at 4°C.

3. Weigert's haematoxylin

Stock solution A: Haematoxylin powder: 0.25 gm; 95% alcohol: 25 ml

Stock solution B: 29% ferric chloride 1ml, distilled water; HCl: 0.25 ml

Stock solutions are stable for 1 year.

25 ml of solution A and solution B are mixed well to make a fresh working solution each time.

4. Biebrich scarlet solution

0.45 g Biebrich scarlet; 0.05 g Acid Fuchsin; 49.5 ml dH2O; 0.5 ml glacial acetic acid

Stable for 6 months

5. Phosphotungstic acid

1.25 gm phopshotungstic acid in 50 ml dH2O. (Stable for 6 months, prepare fresh each time if possible)

6. Aniline Blue

1.24 gm aniline blue powder in 49.5 ml dh20. ; 0.5 ml glacial acetic acid

(Stable for 6 months)

7. Copper sulphate solution

0.5% CuSo4; 0.9% NaCl in dH2o

8. 1x Running buffer (1 L)

25mM Tris; 190 mM glycine; 0.1% SDS

Volume adjusted to 1L, stored at 4°C, adjusted to room temperature prior to use

9. 1x Transfer buffer

2mM Tris; 190mM glycine; 20% methanol

Final volume adjusted to 1 L. Buffer stored at -20°C.

10. 1x TBS and TBST (1 L)

Tris- 3g; NaCl- 8.7g

Volume adjusted to 1 L with dH2o.

For TBST preparation, 0.1% Tween 20 is added to the required volume of TBS.

For, western blot blocking buffer preparation, either 5% non-fat dry milk or 5% BSA is added to the required volume of TBST.

11. MTT Extraction buffer (20 ml)

16 ml absolute isopropanol; 4ml Triton-X 100; 66.8 μl 12N HCl

Solution is vortex mixed and stored at room temperature.

CHAPTER 4

RESULTS
&
DISCUSSION

CHAPTER 4.A

The role of YAP1-FOXM1 in hyperglycemia mediated cardiomyocyte hypertrophy and fibrosis induction

4.A.1 Chapter overview:

Diabetic cardiomyopathy is currently one of the leading causes of morbidity around the world. Poorly regulated blood sugar, often leads to increased cellular apoptosis, hypertrophy and fibrotic remodelling in the cardiac cells. As cardiomyocyte cells cease to divide in adult tissues, it has poor ability to respond to any tissue injury, often resulting in cardiomyocyte hypertrophy and fibrosis leading to heart failure. Therefore, it has become a growing research interest in current times, to understand the molecular players in the pathogenesis of high glucose induced cardiomyopathies. Hyperglycemic stress has been observed to mediate an array of fetal gene reactivation. Likewise, various recent studies have reported hyperglycemia to promote the expression of YAP1, a hippo signaling molecule in the cardiac tissue. YAP1 is a critical early organ growth regulatory molecule. Also, hyperglycemia is observed to upregulate the expression of another key cardiac developmental molecule FOXM1 in the adult tissue. Both YAP1 and FOXM1 have been known to have a baseline expression in the postnatal cardiac cells, and their activation following injury or stress has been shown to have pathological implication in various organs. However, limited information is known till date regarding YAP1-FOXM1 interaction in the cardiac cells, in hyperglycemia mediated cardiac hypertrophy and fibrosis induction.

In this section our study has demonstrated that high glucose mediated YAP1 overexpression increases the cardiac AKT activation resulting in GSK3-β inhibition. GSK3-β negatively regulates FOXM1 in the adult cardiac cells. Activated YAP1 thereby nullifies the inhibitory regulation of FOXM1, resulting in FOXM1 accumulation that goes on to trigger further pro-hypertrophic and fibrotic gene transcription and activation.

4.A.2 Hyperglycemia induces cardiac hypertrophy and fibrosis in adult mice and impairs cardiac function.

To analyse the effect of high glucose stress on cardiomyocyte, mice under experiment were injected with alloxan to mimic type II diabetic condition. From the initial time-point experiment (Fig. 9A), we observed a significant increase of blood glucose level in day1 (382 ± 17.58 mg/dl) after injecting the mice with alloxan at a dose of 150 mg/kg body weight compared to the day 0 (126 ± 9.04 mg/dl) group. The data also shows the blood glucose level stays at significantly higher level up to 2 weeks (1 week: 340 ± 19.53 mg/dl; 2 week: 208.5 ± 12.93 mg/dl) compared to the day 0 group. The mice with high blood glucose level kept for 2 weeks were used as diabetic cardiomyopathy (DCM) group. The DCM group showed significant increase in heart weight to body weight ratio (5.78 ± 0.21 mg/g) compared to the

control group (4.66 ± 0.06 mg/g) (Fig. 9B). The PFA fixed tissue sections stained with WGA antibody showed significant enlargement of the cardiac cells in the DCM group (2.6 ± 0.22-fold) compared to the control group (Fig. 9D' and 9D) indicating induction of cardiac hypertrophy in hyperglycemic stress condition. Massons' trichrome staining showed significantly increased collagen deposition in the DCM group (4.37 ± 0.24 fold) compared to the control heart tissue sections (Fig. 9E' and 9E) which confirmed increased fibrotic response in cardiac tissue under hyperglycemia stress.
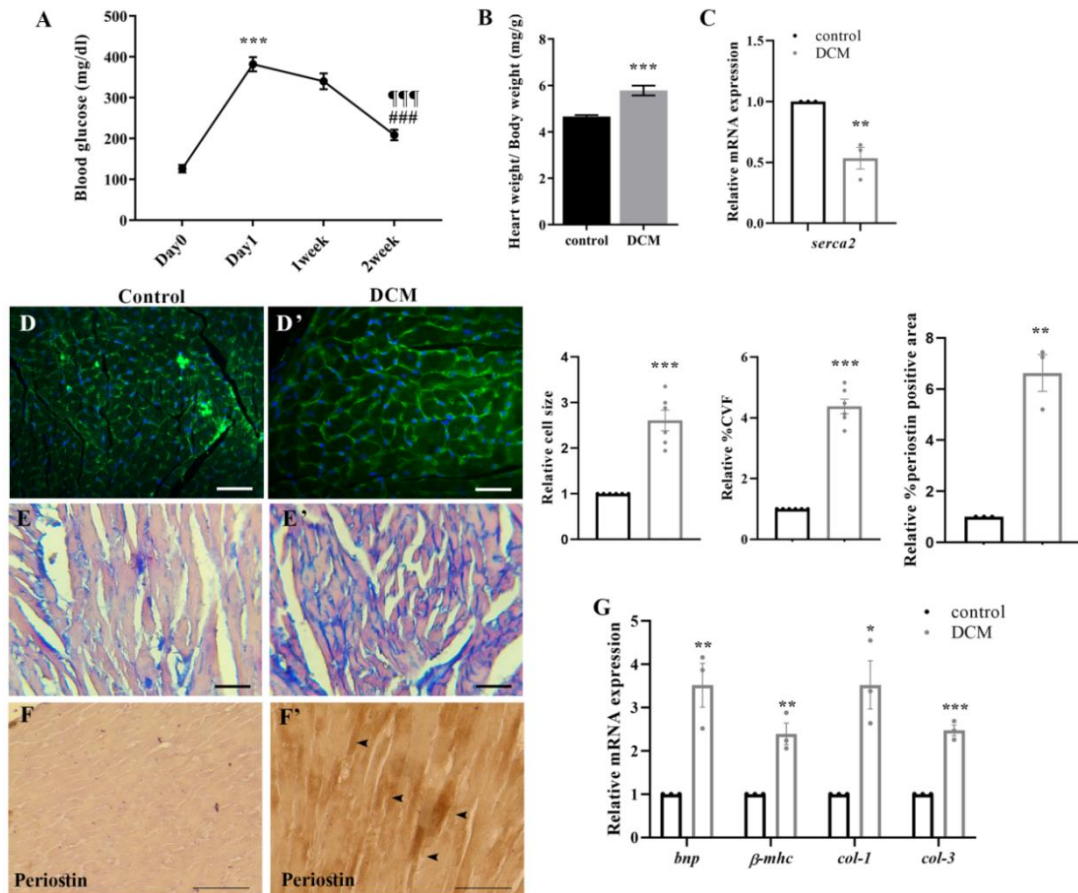
Figure 9. High glucose stress induces cardiac hypertrophy and fibrosis in the adult heart. A. The fasting blood glucose level of adult mice after alloxan injection Statistical significance was calculated by one way ANOVA. ***, p<0.0001 with respect to day0; ###, p<0.0001 with respect to 1 week; ¶¶¶, p<0.0001 with respect to day1. **B.** Graphical representation of the heart weight to body weight ratio (mg/g). **C.** *serca2* expression in heart showing cardiac function in the experimental model animal group. **D-D'.** WGA staining shows cellular hypertrophy in high glucose stress to control condition. The graph represents mean cell size of control and DCM tissue quantified using ImageJ software (NIH). **E-E'.** Masson's trichrome staining shows increased collagen deposition in the DCM mice heart indicating cardiac fibrosis in the diabetic animal. The corresponding graph represents relative collagen deposition as par cent collagen volume fraction (CVF) quantified using ImageJ (NIH) software. **F-F'.** Periostin immunostaining showed increased expression in the DCM than in the control group. **G.** m-RNA expression level of hypertrophy marker *bnp*, *β-mhc* and fibrosis marker *col-1*, *col-3* done by real time PCR can be seen to be significantly upregulated in the DCM group compared to the control group. Statistical significance of B-F was performed using Student's t-test. . ***, p<0.0001 (n=6). Scale bar represents 20μm.

To further confirm the occurrence of cardiac hypertrophy and fibrosis due to high glucose (HG) stress, we looked into the mRNA expression of the key marker genes. We observed a significant increase in hypertrophy marker *bnp* (3.51 ± 0.5-fold) and *β-mhc* (2.39 ± 0.24-fold) expression and an increased expression of fibrosis marker *col1* (3.52 ± 0.55-fold) and *col3* (2.47 ± 0.12-fold) in the DCM group compared to the control animals (Fig. 9C). Moreover, periostin expression is markedly increased in the diabetic cardiac tissue (6.63 ± 0.71-fold, Fig. 9F') as compared to the control tissue (Fig. 9F) suggesting increased fibrosis in the tissue. These results correlate with our previous findings as shown in Fig. 9D, 9E and 9F indicating hyperglycemia mediated hypertrophy and fibrosis induction in our diabetic cardiomyopathy animal model. In the DCM animal model reduced expression of *serca2* gene (0.53 ± 0.08-fold) (Fig. 9C) was observed that along with elevated *bnp* levels further indicated impaired contractile function in the DCM animals.

4.A.3 High glucose promotes hypertrophy and fibrosis in H9c2 cardiomyocyte cells.

Next to investigate the molecular mechanism of induction of cardiac hypertrophy and fibrosis in hyperglycemic condition further we have investigated the findings in the in vitro model of hyperglycemia. In this experiment when H9c2 cells were treated with high glucose medium (25mM glucose) for 48 h we observed high expression of *bnp* (2.43 ± 0.48-fold) *β-mhc* (3.56 ± 0.55-fold) along with *col1* (2.5 ± 0.40-fold), *col3* (4.34 ± 0.5-fold) over control cells (Fig. 10D) that indicated cardiomyocyte hypertrophy and fibrosis induction as it was observed in the diabetic cardiomyopathy model in vivo. We also confirmed cellular hypertrophy under high glucose condition from phalloidin stained cells where increase in cell size (3.46 ± 0.28-fold, Fig. 10A') was seen in the cells treated with high glucose media compared to the cells treated with normal glucose (NG) (Fig. 10A). In the immunostaining experiment we also observed a significant increase in the myofibroblast marker α-SMA expression in the high glucose group (21.36 ± 2.44 %, Fig. 10B') compared to the control group (4.56 ± 0.57 %, Fig. 10B) and increased fibrosis marker periostin expression in the high glucose group (20.97 ± 1.93 %, Fig. 10C') to the control group (6.94 ± 0.97 %, Fig. 10C) that further confirms the observation that high glucose induces fibrotic responses in the cardiac cells.
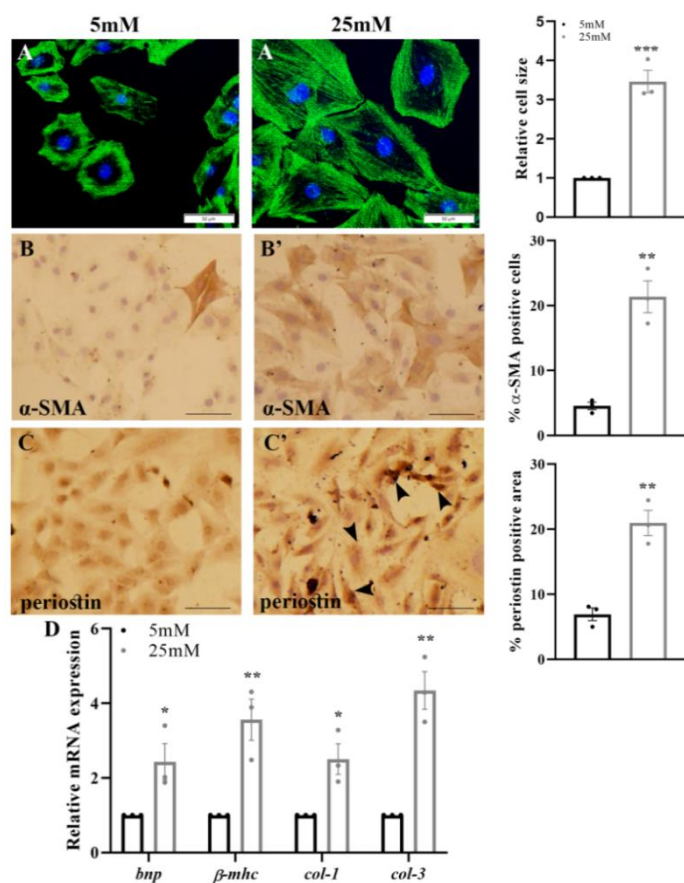
Figure 10. Hyperglycemia induces hypertrophy and fibrosis along with YAP1, FOXM1 in H9c2 cells. A-A'. Phalloidin staining images showing enlarged cell size in the high glucose treated cells compared to the normal glucose treated cells. B-B'. Immunostaining with α-SMA antibody showing higher number positive cells in cells treated with HG to that of NG treated cells. C-C'. Periostin immunostaining images showing increased expression indicative of fibrosis in the HG treated cells compared to the NG treated cells. Scale bar represents 50μm. D. Real time PCR data showing increased expression of hypertrophy marker bnp, β-mhc and fibrosis marker col-1, col-3 in the HG treated H9c2 cells compared to the NG treated cells.

4.A.4 YAP1, FOXM1 overexpression in murine diabetic cardiomyopathy model.

Since altered glycemic condition in different tissues lead to activation of YAP1 and its target genes we wanted to further investigate the effect of high glucose in regulating YAP1 and its downstream effectors in our hyperglycemic model. In the DCM tissue *yap1* showed an increased mRNA expression (2.86 ± 0.6 fold) compared to the control tissue (Fig. 11A). In the immunohistochemistry data of YAP1 antibody in mice tissue sections, an overall increased number of YAP1 positive cells was seen in the hyperglycemic tissue (38.42 ± 5.96 %, Fig. 11D') compared to the control tissue (7.41 ± 1.68 %, Fig. 11D). Western blot data shows in diabetic cardiac tissue, significantly increased expression of YAP1 (3.51 ± 0.29-fold, Fig. 11B) to the control group at total protein level along with increased activity evident from the reduced expression of inhibitory p-YAP1/YAP1 (0.13 ± 0.02-fold, Fig. 11B) compared to the control group. Moreover, immunoprecipitation experiment showed high level of O-GlcNAcylation of YAP1 in the DCM animals (2.07 ± 0.38-fold) compared to the control animal (Fig. 11C). As YAP1 is known to be majorly activated following O-GlcNAcylation, therefore, our data confirms the initial observation that high glucose induces

YAP1 overexpression and activity in the cardiac tissue and its downstream transcriptional effectors resulting in increased hypertrophic and fibrotic response.
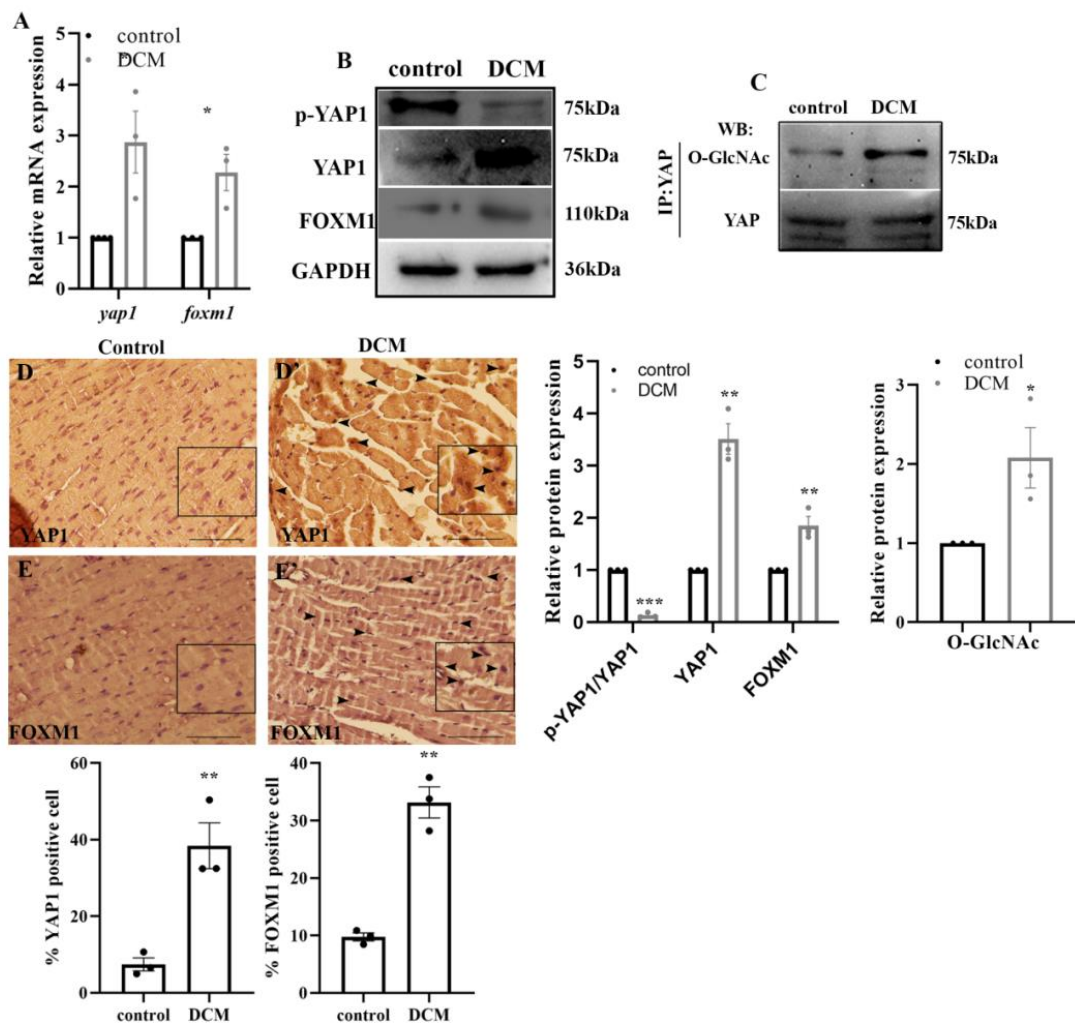
Figure 11. High glucose induces YAP1, FOXM1 overexpression along with increased expression of hypertrophy and fibrosis markers. A. m-RNA expression of *yap1* and *foxm1* by real time PCR shows up regulated expression in the DCM group compared to the control group. **B.** Western blots images show increased YAP1, FOXM1 expression in the HG group. **C.** Expression of O-GlcNAc of YAP in IP experiments. Immunoprecipitation was performed with YAP antibody and expression of O-GlcNAc was observed by western blotting with O-GlcNAc antibody. **D-D'.** Immunostaining with YAP1 antibody shows overexpression of YAP1 in the diabetic heart tissues compared to the control tissue **E-E'.** FOXM1 antibody staining shows increased expression in the DCM group compared to the control tissue. Statistical significance was calculated by students' t t-test. ***, $p<0.0001$; **, $p<0.01$; *, $p< 0.05$; between DCM and control group, n=3. Scale bar represents 20μm.

Likewise, we have also observed that the expression level of FOXM1 was significantly increased in diabetic cardiac tissues as compared to control tissues both at the mRNA level (2.27 ± 0.35-fold, Fig. 11A) and protein level (1.85 ± 0.17-fold, Fig. 11B) as detected by real time RT-PCR assay and western blot analyses respectively. Immunostaining with FOXM1

antibody shows an overall increased number of FOXM1 positive cells (33.17 ± 2.7 %, Fig. 11E') in the diabetic tissue over the control tissue (9.75 ± 0.7 %, Fig.10E). Thus, like YAP1 we also observed an increased expression of FOXM1 transcription factor in the diabetic animals compared to the control animals which may suggest that the increased level of expression of FOXM1 in adult cardiac cells may play a crucial pathological role in the adult cardiac cells. Next we have used H9c2 cardiomyocyte cells to dissect out the molecular hierarchy of the YAP1/FOXM1 mediated signaling pathway in inducing hypertrophy and fibrosis in diabetic cardiomyopathy.

4.A.5 Induction of hyperglycemic condition in H9c2 cells in vitro similarly results in increased expression of YAP1 and FOXM1

In the high glucose treated cells we observed significant upregulation of yap1 mRNA expression (3.96 ± 0.98 fold, Fig. 12A), along with higher expression of foxm1 m-RNA (4.21 ± 0.51 fold, Fig. 12A) over normal glucose treated cells. We observed significantly increased expression of YAP1 in the high glucose condition (1.93 ± 0.07-fold, Fig. 12B) compared to control group. We have also found significant reduction in the activity of YAP1 from p-YAP1/YAP1 expression (0.31 ± 0.07-fold, Fig. 12B) compared to the control as seen in western blot experiments. Increased activity of YAP1 was also evident from the higher YAP-O-GlcNacylation (1.88 ± 0.21-fold, Fig. 12C) observed in the high glucose treated H9c2 cells as compared to the NG treated cells. Significantly increased expression of cellular FOXM1 protein in the hyperglycemic cells (1.58 ± 0.12-fold, Fig. 12B) compared to control cells was also seen in the hyperglycemic condition over normal glucose condition. These data correlate with the higher YAP1 and FOXM1 expression seen in diabetic cardiomyopathy in vivo. Immunostaining data performed on high glucose treated and fixed H9c2 cells with YAP1 antibody clearly showed a significantly increased number of positive cells (21.1 ± 2.09 %, Fig. 12D') in the hyperglycemic condition over the normoglycemic cells (6.04 ± 0.73 %, Fig. 12D. A higher number of FOXM1 immnunopositive cells can also be seen in 25mM glucose condition (28.6 ± 4.0 %, Fig. 12E') over normal glucose treated cells (6.95 ± 0.29 %, Fig. 12E), which further confirmed the fact that YAP1, FOXM1 show upregulated expression in the high glucose treated H9c2 cells.
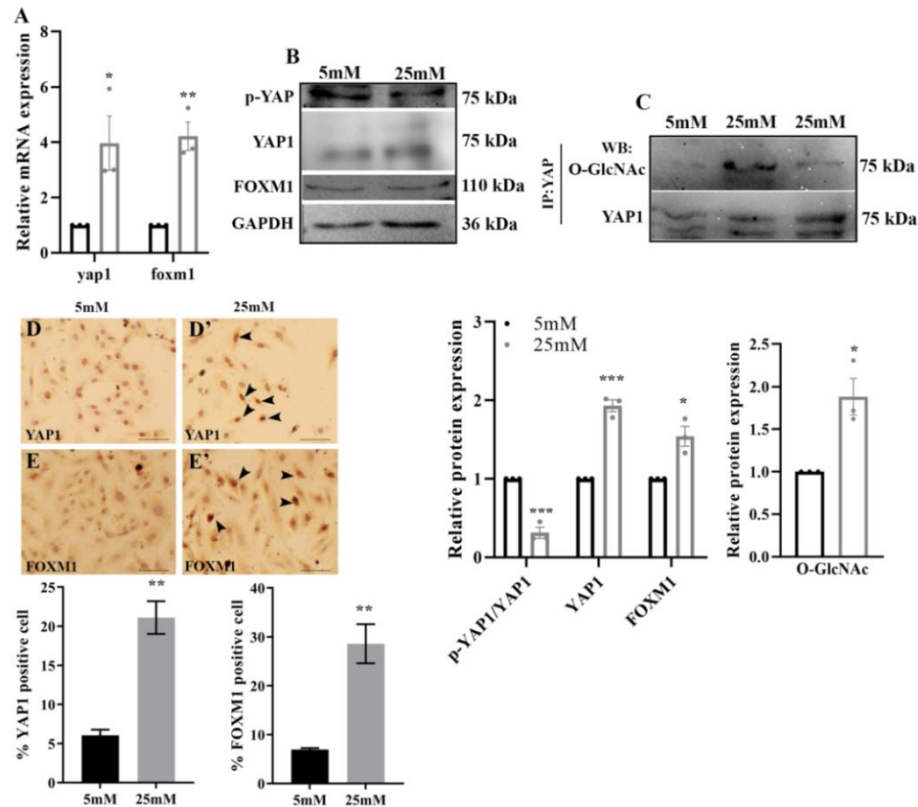
Figure 12. Hyperglycemia induces hypertrophy and fibrosis along with YAP1, FOXM1 in H9c2 cells. A. Real time PCR data of *yap1* and *foxm1* shows upregulated expression in the H9c2 cells treated with high glucose (HG) (25 mM) media compared to the normal glucose (NG) (5 mM) treated cells. **B.** Western blot data showing increased expression of YAP1, FOXM1 in the 25mM group compared to the 5mM group. **C.** Western Blot images of O-GlcNAc in IP experiments. Immunoprecipitation was performed by YAP antibody followed by western blotting with O-GlcNAc antibody. Representative images show one more replicate image of HG treated condition **D-D'.** H9c2 cells with YAP1 antibody staining show increased YAP1 positive cells in HG treated cells compared to NG. **E-E'.** Immunostaining images of FOXM1 antibody showing overexpression in HG treated H9c2 cells compared to NG treated cells. Scale bar represents 50µm. Statistical significance was calculated by students' t test. ns, p: non-significant, *, p< 0.05, **, p<0.01*** , p<0.0001 between the high glucose and the normal glucose group. n=3

4.A.6 AKT-GSK pathway is activated in murine diabetic heart.

In the cardiac tissue YAP1 is known to be associated with AKT-GSK3β signaling that is an important signaling pathway in glucose metabolism. On the other hand, as AKT- GSK3β has recently been reported to regulate FOXM1 expression, we further attempted to investigate the expression of FOXM1 along with AKT and GSK3β to identify the molecular hierarchy of the YAP1/FOXM1 mediated signaling pathway in inducing hypertrophy and fibrosis in diabetic cardiomyopathy.

We have observed a significantly increased level of p-AKT (3.28 ± 0.39-fold, Fig. 13A) over total AKT in the diabetic condition along with simultaneous decrease in the activity of

GSK3β as evident from the increased expression of inhibitory phosphorylated form of GSK3β (2.15 ± 0.23-fold, Fig. 13A) over total GSK3β. These data suggest that high glucose promotes AKT activity and reduces GSK3β activity in the cardiomyocyte. In the adult heart under high glucose stress this abnormally higher expression of YAP1, FOXM1 protein and altered AKT/GSK3β signaling pathway over the basal level indicates the pathological status of diabetic cardiomyopathy.
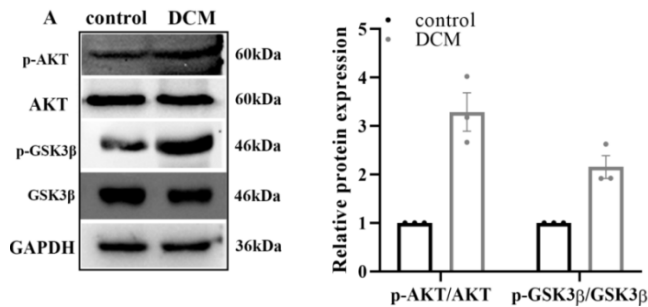
Figure 13. High glucose induces AKT signaling in diabetic heart. **A.** Western blot images show increased expression of ser473 p-AKT/AKT in the DCM group compared to the control group with increased ser9 p-GSK3β/GSK3β in the DCM group was observed compared to the control group.

4.A.7 High glucose upregulates AKT-GSK3β pathway in H9c2 cardiomyocyte

Western blot results from high glucose and normal glucose treated cells also showed significantly upregulated expression of ser473 p-AKT (1.79 ± 0.11 fold, Fig. 14A) to total AKT and increased ser9 inhibitory phosphorylation of GSK3β (2.46 ± 0.26-fold, Fig. 14A) compared to total GSK3β in the cells under hyperglycemic environment indicating increased activity of AKT along with decreased activity of GSK3β in the hyperglycemic cells. These results correlate with our in vivo data (Fig. 11 and Fig. 13) where YAP1, FOXM1 and AKT showed a significantly upregulated expression in the diabetic cardiomyopathy animal group.
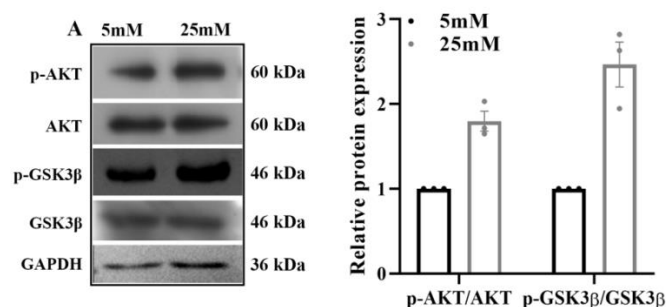
Figure14. Hyperglycemia induces AKT signaling in H9c2 cells. **A.** Western blot images shows expression of ser473 p-AKT/AKT was significantly higher in the HG group compared to the NG group with increased ser9 p-GSK3β/GSK3β in the NG group was observed compared to the control group.

4. A.8 YAP1 down regulation in H9c2 cells resulted in recovery from pathogenic condition

To determine whether YAP1 is indispensable in inducing cardiac hypertrophy and fibrosis, H9C2 cells maintained in presence of high glucose containing media were treated with either

in presence or absence of YAP inhibitor, verteporfin (VP). Inhibition of YAP1 activity by verteporfin in H9C2 cells with 25 mM glucose resulted in reduced expression of YAP1 (6.72 ± 1.43 %, Fig. 15A") compared to 25 mM glucose treated cells without inhibitor (25.19 ± 3.23 %, Fig. 15A'). If YAP1 activity is necessary to induce cardiac hypertrophy and fibrosis then pre-treatment with verteporfin would fail to induce cardiac hypertrophy and fibrosis even in presence of high glucose as compared to cells maintained in absence of verteporfin. Interestingly, a significant reduction in the H9c2 size or hypertrophic condition was observed from phalloidin staining in the cells treated with high glucose with verteporfin (1.93 ± 0.04-fold, 15B") compared to high glucose condition without the inhibitor (3.61 ± 0.41-fold, Fig. 15B). Furthermore, the data also showed a significant decrease in expression of myofibroblast marker α-SMA (3.91 ± 0.96 %, Fig. 15C") compared to high glucose treated cells without verteporfin (20.57 ± 2.29 %, Fig. 15C'). Therefore, the data confirmed the obvious role of YAP1 overexpression in the induction of cardiomyocyte hypertrophy and fibrosis under hyperglycemic stress and would suggest that active YAP1 is necessary to induce cardiac hypertrophy and fibrosis in hyperglycemic condition.
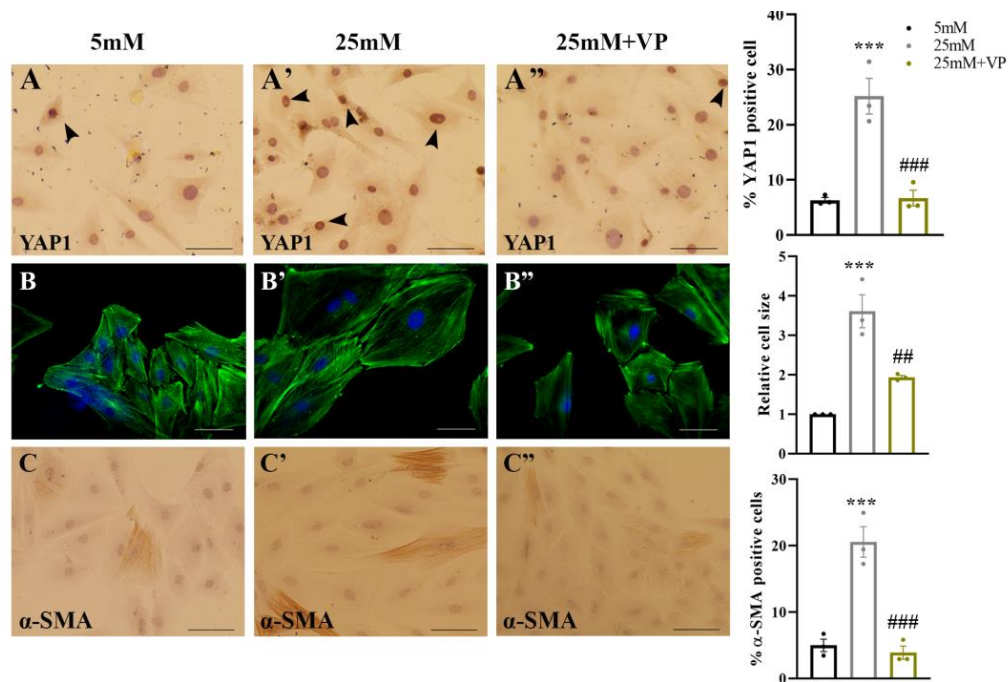
Figure 15. YAP1 inhibition in H9c2 cells reduces the hypertrophy and fibrosis in the H9c2 cells. A-A". Verteporfin (VP) inhibits the expression of YAP1 in the H9c2 cells. **B-B".** Phalloidin staining images showing YAP1 inhibition significantly reduces H9c2 cell size in the HG condition compared to the HG conditioned cells without inhibitor. **C-C".** α-SMA staining images showing reduced expression in the HG treated cells with VP compared to the HG cells without VP. Scale bar represents 50μm. Statistical significance was calculated by one way ANOVA. *, p< 0.05; ***, p<0.0001 between 25 mM and 5 mM group. #, p< 0.05; ##, p<0.01; ### p<0.0001 between 25 mM+ verteporfin and 25 mM group. n=3

4.A.9 YAP1 inhibition in HG cardiomyocyte results in reduced expression of AKT/GSK3β signaling with reduced FOXM1 expression

To Further look into the association between YAP1, FOXM1 and AKT we have next observed the status of these molecules under verteporfin treated condition in the high glucose group. Interestingly, verteporfin treatment in H9c2 cells under hyperglycemic condition in turn resulted in an increased cytoplasmic localization of FOXM1 (69.06 ± 3.32 % cytoplasmic to 4.77 ± 0.30 % nuclear, Fig. 16A") compared to hyperglycemic cells without inhibitor (34.87 ± 2.28 % overall cellular expression, Fig. 16A'). This result indicates that during hyperglycemic stress YAP1 overexpression in the cardiomyocyte promotes FOXM1 expression. YAP1 inhibition with its specific inhibitor causes the cytoplasmic retention of FOXM1 protein in the cardiomyocyte. This data further confirms the proposed association between YAP1 and FOXM1 molecules in the cardiomyocyte.

From western blot analysis, we have also observed a downregulated expression of ser473 p-AKT/AKT (1.13 ± 0.29 fold, Fig. 16B) in the 25mM glucose with verteporfin group compared to 25mM glucose treated cells without inhibitor (3.0 ± 0.72 fold, Fig. 16B) which confirmed reduced activity of AKT in verteporfin treated cells in high glucose condition. Reduced activity of AKT in turn significantly downregulated the inhibitory phosphorylation on GSK3β (0.76 ± 0.09 fold) in the verteporfin treated high glucose group over high glucose group without inhibitor (2.73 ± 0.69 fold, Fig. 16B). The results conferred that in the high glucose treated H9c2 cells YAP1 promotes the activity of AKT and reduces GSK3β activity. Overall, all these data indicate that YAP1 regulates the expression of FOXM1 and AKT/ GSK3β signaling and under high glucose condition promotes cardiomyocyte hypertrophy and fibrosis.
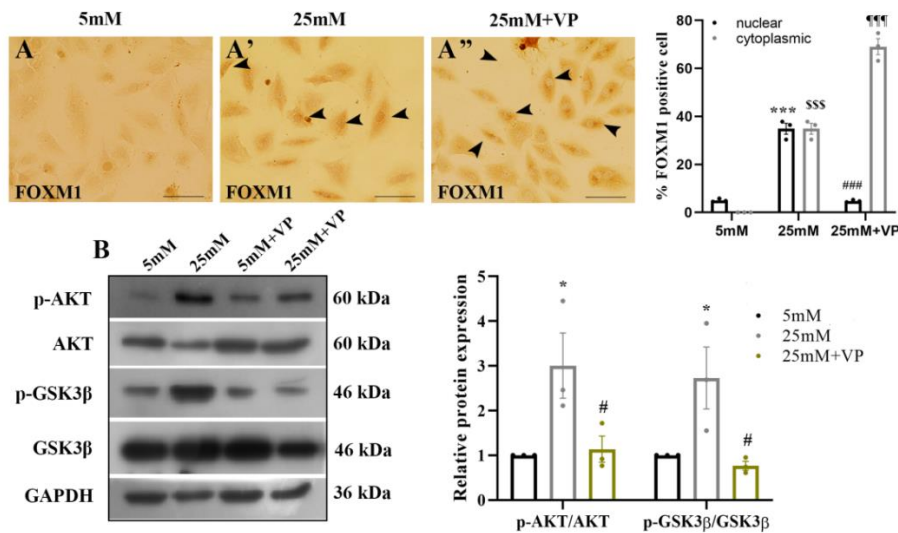
Figure 16. Inhibition of YAP1 in H9c2 cells results in increased cytoplasmic localization of FOXM1 and increased AKT activity. A. FOXM1 immunostaining images showing increased cytoplasmic localization of FOXM1 in the verteporfin treated high glucose cells to that of high glucose treated cells without YAP1 inhibitor. ***, p<0.0001 between 25 mM nuclear and 5 mM nuclear groups; $$$, p<0.0001 between 25mM cytoplasmic and 5mM cytoplasmic groups. ###, p<0.0001 between 25 mM nuclear and 25 mM without VP group; ¶¶¶, p<0.0001 between 25 mM cytoplasmic and 25 mM without VP cytoplasmic group. n=3 **B.** Western blot data shows reduced ser473 p-AKT/AKT and reduced inhibitory ser9 p-GSK/GSK3β expression in the HG treated cells with VP compared to the HG cells without VP. Statistical significance was calculated by one way ANOVA. *, p< 0.05; ***, p<0.0001 between 25 mM and 5 mM group. #, p< 0.05; ##, p<0.01; ### p<0.0001 between 25 mM+ verteporfin and 25 mM group. n=3

4.A.10 FOXM1 inhibition resulted in decreased hypertrophy and fibrogenic condition of H9c2 cardiomyocyte cells

Like in the observations found with verteporfin treated cells, we next attempted to observe the effect of FOXM1 inhibition on the cells using its specific inhibitor thiostrepton (Th). In this experimental group, we observed a significant inhibition of the FOXM1 expression in the thiostrepton treated hyperglycemic cells (5.12 ± 1.4 %, Fig. 17A") compared to hyperglycemic cells without the inhibitor (27.07 ± 3.24 %, Fig. 17A'). This observation was followed by significant reduction in hypertrophy and fibrotic response in H9c2 cells under hyperglycemic condition that was pre-treated with thiostrepton, as was observed from phalloidin and α-SMA staining. In the phalloidin staining, we have observed a significant reduction in cell size (1.9 ± 0.06-fold, 17B") in the high glucose with thiostrepton group compared to control group (3.81 ± 0.37-fold, Fig. 17B') and significantly decreased number of α-SMA positive cells (3.52 ± 0.54 %, Fig. 17C") in the hyperglycemic cells treated with thiostrepton over hyperglycemic cells without FOXM1 inhibitor (21.35 ± 2.44 %, Fig. 17C'). These data so far proved that FOXM1 overexpression in the cardiomyocyte resulted in

increased pathogenesis of hypertrophy and fibrosis which is one of the potential pathways through which hyperglycemia acts to induce cardiac hypertrophy and fibrosis.

However, thiostrepton mediated FOXM1 inhibition interestingly had almost insignificant effect on the YAP1 expression (21.74 ± 0.93 %, Fig. 17D") in the high glucose condition to that of high glucose cells treated with thiostrepton group (17.61 ± 1.15 %, Fig. 17D'). These data indicate that either YAP1 acts upstream to FOXM1 in cardiomyocyte to induce hypertrophy and fibrosis or, YAP1 and FOXM1 act independently to induce hypertrophy and fibrosis in cardiomyocyte treated with high glucose which eventually leads to pathogenesis.
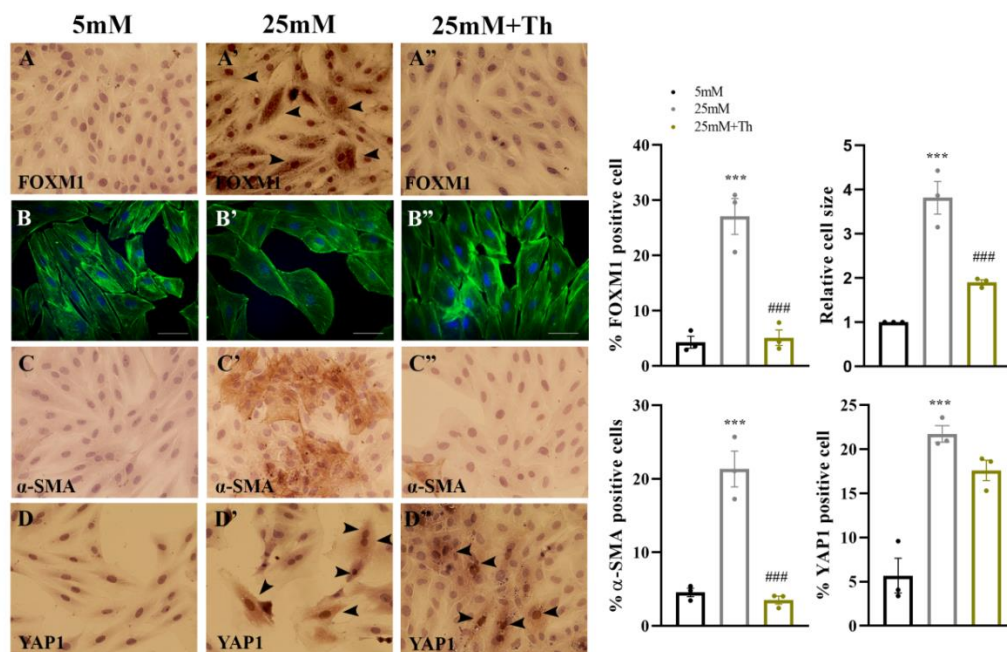
Figure 17. FOXM1 inhibition in H9c2 cells reverse cardiomyocyte hypertrophy and fibrosis. A-A". FOXM1 immunostaining images showing reduced expression in H9c2 cells treated with thiostrepton (Th). **B-B".** Phalloidin staining images of H9c2 cells treated with Th shows reduction in cell size in treated cells. **C-C".** α-SMA immunostainng images show reduced number of cell positive staining in HG treated cells with Th treatment compared to only HG cells. **D-D".** Immunostaining images of YAP1 in H9c2 cells treated with FOXM1 inhibitor Th shows no changes in YAP1 expression in the 25mM with Th compared to the 25mM group without Th. YAP1 shows high expression in both groups. Scale bar represents 50μm. Statistical significance was calculated by one way ANOVA. ***, p<0.0001 between 25 mM and 5 mM group; ###, p<0.0001 between 25 mM+ Th and 25 mM group. n=3

4.A.11 YAP1 up regulation followed by FOXM1 inhibition indicates regulation of FOXM1 activity by YAP1 in the H9c2 cells as their possible pathway of action

In order to investigate whether YAP1 mediated induction of cardiomyocyte hypertrophy and fibrosis is dependent on FOXM1 activity, H9C2 cells under normoglycemic condition were

pre-treated with YAP activator, S1P followed by FOXM1-specific inhibitor, thiostrepton for overnight. If YAP1 mediated induction of cardiomyocyte hypertrophy is FOXM1 dependent then H9C2 cells pre-treated with FOXM1-specific inhibitor thiostrepton would fail to induce cardiac hypertrophy and fibrosis even in presence of YAP activator, S1P. Conversely, if H9c2 cells without the FOXM1 inhibitor but in presence of S1P in normoglycemic condition would still induce cardiac hypertrophy and fibrosis suggesting that YAP1 mediated induction of cardiomyocyte hypertrophy is FOXM1 dependent. Here, our experiment found a significant increase of the cell size in the S1P treated H9c2 cells in normal glucose (5mM) condition (2.99 ± 0.3 fold, Fig. Fig. 18C') compared to cells under normal glucose condition without S1P (Fig. 18C). We also observed significantly higher expression of α-SMA in S1P treated cells in normal glucose condition (24.09 ± 0.96 %, Fig. 18D') compared to normal glucose treated cells without YAP1 activator (2.20 ± 0.09 %, Fig. 18D). Significantly increased periostin expression (21.2 ± 3.85 %, Fig. 18E') was found even in the normoglycemic treated cells with S1P compared to the cells that were maintained without YAP1 activator (3.67 ± 0.38 %, Fig. 18E). FOXM1 expression in the S1P treated group was significantly higher (72.61 ± 3.89 %, Fig. 18B') in contrast to the cells maintained in normal glucose media (3.97 ± 0.25 %, Fig. 18B).

Interestingly, we observed a reversal in cell size to almost normoglycemic condition in the S1P treated cells that were simultaneously treated with thiostrepton (1.51 ± 0.04-fold, Fig. 18C") compared to S1P treated cells without thiostrepton (2.99 ± 0.3-fold, Fig 18C'). A significant decrease in the number of α-SMA positive cells were observed in the S1P and thiostrepton treated group (2.32 ± 0.22 %, Fig. 18D") compared to S1P treated group without thiostrepton (24.09 ± 0.96 %, Fig. 18D). Immunostaining revealed significantly reduced expression of periostin (6.12 ± 1.18 %, 18E") in S1P and thiostrepton treated cells in comparison to S1P treated cells without thiostrepton (21.2 ± 3.85 %, Fig. 18E').

As for the target gene expression, we have observed a diminished FOXM1 expression in the S1P group treated with thiostrepton (5.84 ± 0.62 %, 18B") compared to S1P treated group without thiostrepton (72.61 ± 3.89 %, Fig. 18B'); while FOXM1 inhibition with thiostrepton had no significant effect on YAP1 expression (25.33 ± 4.33 % vs. 27.08 ± 3.1 %, Fig. 18A" and 18A') seen in S1P+thiostrepton group compared to S1P treated group without thiostrepton. This data confirmed that YAP1 activation followed by FOXM1 inhibition

resulted in reduced cardiomyocyte size and fibrosis in vitro suggesting a FOXM1 mediated activity of YAP1 in induction of cardiomyocyte hypertrophy and fibrosis. The data also suggests that FOXM1 acts downstream of YAP1.
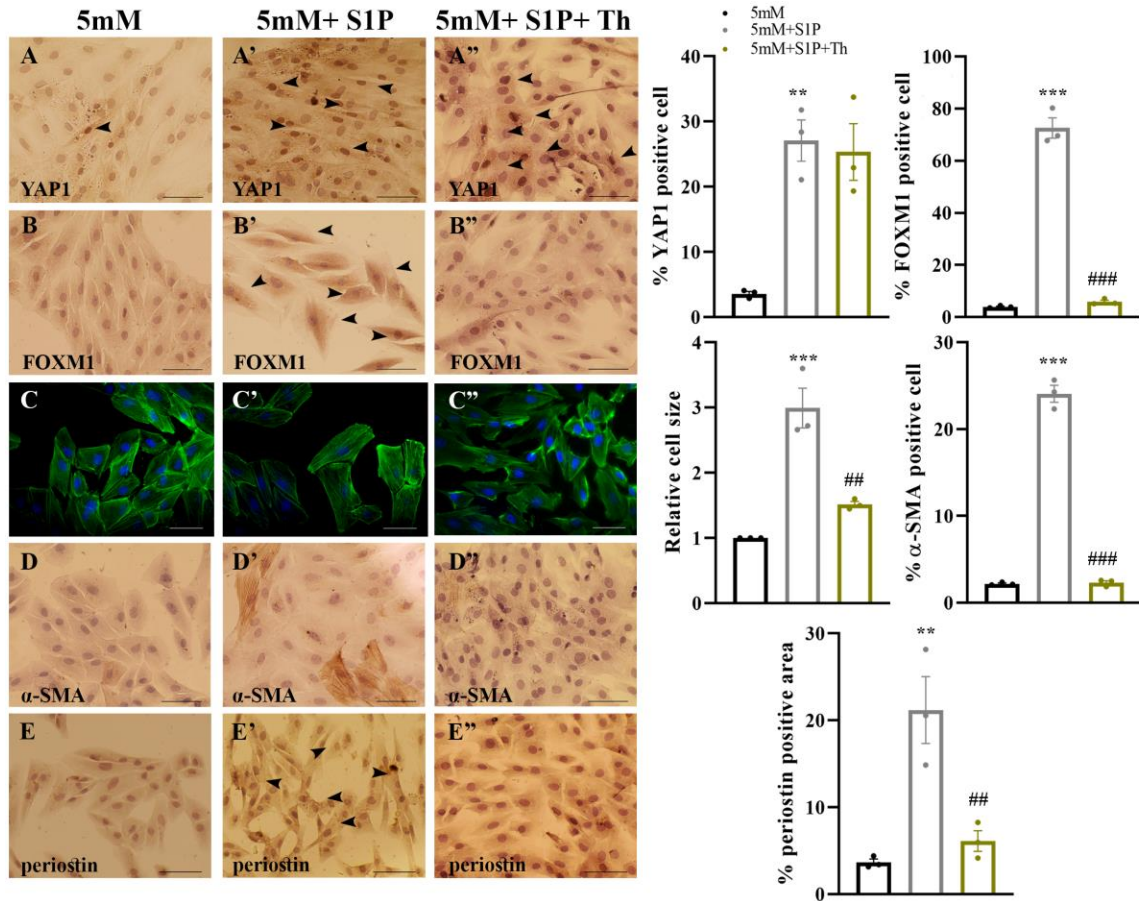
Figure 18. Upregulation of YAP1 with S1P followed by inhibition of FOXM1 with thiostrepton determines FOXM1 is a downstream effector of YAP1 in H9c2 cells. A-A". Immunostaining images of YAP1 shows increased expression in S1P treated cells. Thiostrepton mediated FOXM1 inhibition in the S1P treated group has no effect on YAP1 expression. **B-B".** Immunostaining images of FOXM1 shows upon YAP1 activation there is increased FOXM1 expression in NG H9c2 cells. However, this increase is ameliorated following S1P treatment along with Th. **C-C".** Phalloidin staining shows there is an increase in cell size in the S1P mediated YAP1 activated H9c2 cells. Upon Th treatment in the S1P group, this phenotype was reversed to NG condition. **D-D".** α-SMA immunostaining images show upon S1P treatment there is an increase in the number of α-SMA positive cells which is again reduced to NG condition when cells are treated with S1P along with Th. **E-E".** Periostin marker immunostaining images also show increased positive staining in the S1P group compared to NG group that was also reduced upon Th treatment. Scale bar represents 50μm. Statistical significance was calculated by one way ANOVA. ***, $p<0.0001$; **, $p<0.01$ between 5 mM+S1P group and 5 mM group. ###, $p<0.0001$; ##, $p<0.01$ between 5 mM+S1P+ thiostrepton and 5 mM+ S1P group. n=3

4.A.12 Simultaneous activation of YAP1 and inhibition of AKT shows increased GSK3β activity and inhibition of FOXM1 expression in H9c2 cells

In order to further confirm that YAP1 induced FOXM1 activity in the cardiomyocyte is mediated through AKT-GSK3β signaling, we attempted to modulate the expression of AKT in H9c2 cells with LY294002 (LY). We have observed that LY294002 treatment in the hyperglycemic H9c2 cells significantly reduced the expression of FOXM1 ($5.4 \pm 0.37\%$, Fig. 19A') compared to the high glucose cells without inhibitor ($28.20 \pm 3.29\%$, Fig. 19A). But LY294002 had no significant effect on the expression of YAP1 ($24.96 \pm 0.9\%$, Fig. 19B') in the high glucose with LY294002 group to the high glucose without inhibitor group ($22.20 \pm 0.97\%$, Fig. 19B). These results indicate that AKT-GSK3β may be a downstream effector of YAP1 that furthers regulates FOXM1 expression in a signaling pathway.

However, to confirm our observations earlier we have performed a simultaneous upregulation of YAP1 with S1P along with inhibition of AKT with LY294002 in the normal glucose condition. Firstly in the S1P treated cells with LY294002 treatment under normal glucose condition there was a significantly reduced FOXM1 expression (6.55 ± 0.22 %, Fig. 19D") compared to the S1P treated cells without LY294002 (62.32 ± 4.01 %, Fig. 19D'). Now, at par with our previous report of S1P mediated YAP1 activation (Fig 18), a reduction in the cell size was observed in the S1P with LY294002 treated normoglycemic cells (1.06 ± 0.06-fold, Fig. 19E") compared to the S1P group without inhibitor (2.23 ± 0.06-fold, 19E'). In the α-SMA immunostaining data we have also observed a reduced number of positively stained cells in the S1P with AKT inhibitor group (3.18 ± 0.7 %, Fig. 19F") compared to the S1P treated group without AKT inhibitor (17.78 ± 3.42 %, Fig. 19F). But, as was observed earlier, no significant change was observed in the expression of YAP1 in the S1P treated cells that was simultaneously treated with AKT inhibitor LY294002 (25.65 ± 2.21 %, Fig. Fig. 19C") to that of H9c2 cells treated with only S1P (28.49 ± 1.85 %, Fig. 19C'). This indicates that YAP1 acts upstream of AKT-GSK in the regulatory pathway.

To follow up with our findings in the western blot data, we observed increased p-AKT/AKT in the S1P treated group (2.07 ± 0.32 fold, Fig. 19G) compared to H9c2 cells without the YAP activator S1P. Also a simultaneous increased Ser9-p-GSK3β/ GSK3β was observed in the S1P treated H9c2 cells (2.22 ± 0.31fold, Fig. 19G) compared to the H9c2 cells without S1P that confirms our hypothesis that YAP1 expression increases AKT activity in the cardiomyocyte cells that in turn inhibits GSK3β activity with increased inhibitory Ser9 phosphorylation of GSK3β. With GSK3β inhibition, FOXM1 is stabilized in the cardiomyocyte (Fig. 19D" and 19D') and thus, YAP1 confers its regulatory effect on FOXM1 via AKT/ GSK3β signaling. Further, we observed a reduced p-AKT activity in the S1P mediated YAP1 activated group that has been treated with LY294002 (0.90 ± 0.28 fold, Fig. 19G) compared to the only S1P treated cells without LY294002, along with reduced inhibitory p-GSK3β in the S1P treated cells with LY294002 (0.82 ± 0.36 fold, Fig. 19G) compared to only S1P treated cells. This correlates with our findings that although FOXM1 expression is high in S1P treated cells, with AKT inhibition the FOXM1 expression has been downregulated (Fig. 19D" and 19D'), confirmed now by the regulatory effect of GSK3β.

In the normal glucose treated cells with activated YAP1 expression, on application of AKT inhibitor we observed an improved pathological state of the H9c2 cells similar to verteporfin mediated YAP1 inhibited condition which may suggest YAP1 have some association with AKT/GSK signaling in the exertion of its regulatory effect on FOXM1 as well as hypertrophy and fibrosis induction. But in this experimental group as we have observed that AKT inhibition reduced FOXM1 expression but had an insignificant effect on YAP1. From this observation we can conclude that AKT acts downstream to YAP1 rather than a co-regulation or upstream regulation. This also indicates that in hyperglycemia, YAP1 mediated AKT expression inhibits GSK3β activity that leads to an increased FOXM1 expression in the H9c2 cells.
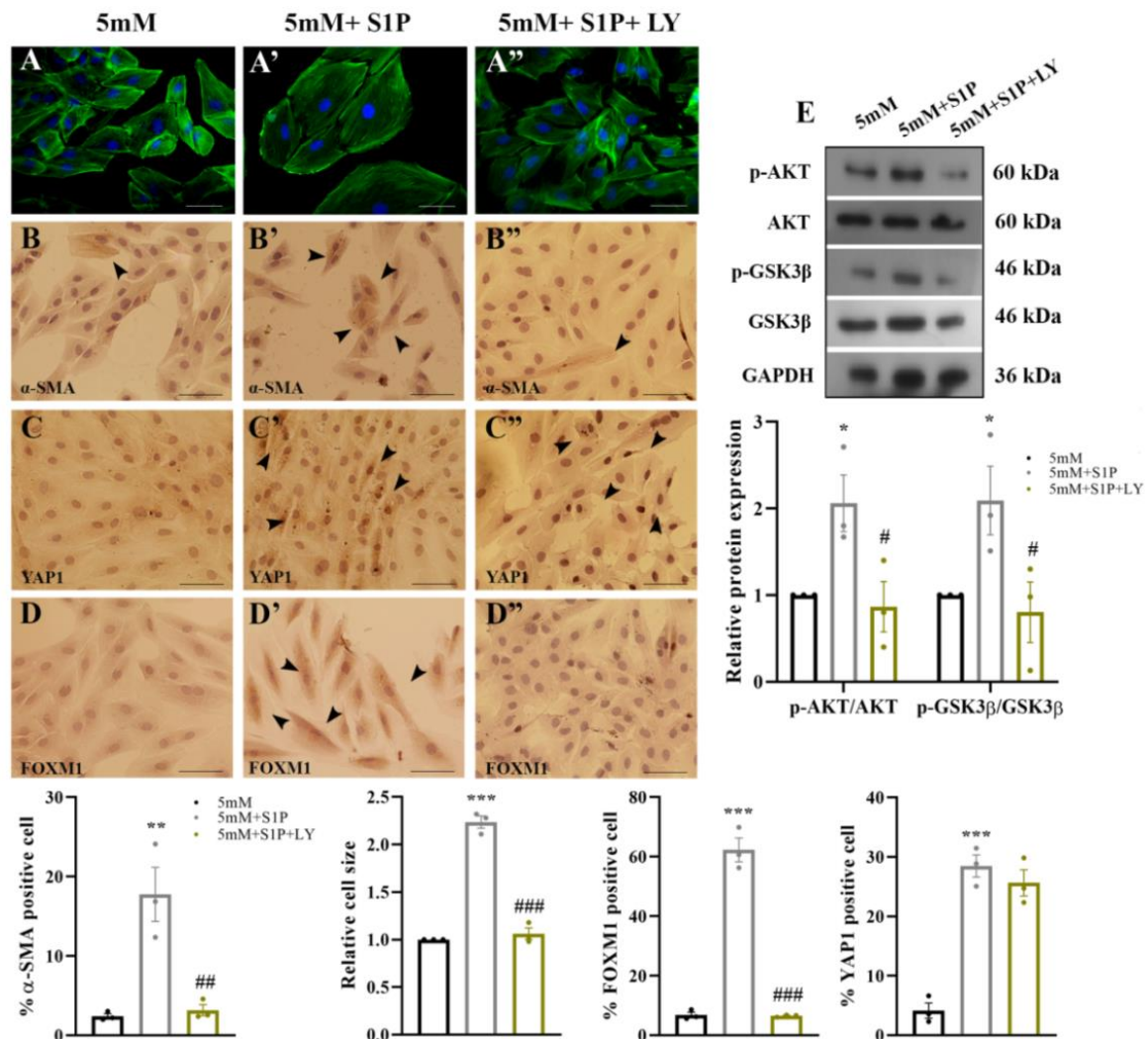
Figure 19. YAP1 upregulation along with AKT inhibition determines YAP1 regulates FOXM1 via AKT-GSK3β signalling pathway. A-A". Phalloidin staining images showing increase in the H9c2 size in S1P treated cells. However, LY294002 treatment attenuated the increase in cell size even when cells were treated with S1P. **B-B".** α-SMA immunostaining images showing increased number of positive cells on S1P treatment. But, when cells were treated with S1P along with LY294002 (LY), the α-SMA staining was significantly reduced. Scale bar represents 50µm. **C-C".** YAP1 immunostaining images show increased expression of YAP1 in S1P treated group. In the S1P with AKT inhibitor LY group, YAP1 had no significant changes in expression compared to only S1P group. **D-D".** FOXM1 immunostaining images showing increased positive cells in the S1P group compared to the control group. However, FOXM1 expression was significantly reduced upon LY treatment even under S1P treated condition. **E.** Western blot images showing increased p-AKT/AKT and inhibitory Ser9 p-GSK3β/GSK3β in the S1P treated H9c2 cell group compared to the control group. This was again downregulated when cells were treated with S1P along with LY. Statistical significance was calculated by one way ANOVA. ***, $p<0.0001$; **, $p<0.01$; *, $p<0.05$ between 5 mM +S1P and 5 mM group. ###, $p<0.0001$; ##, $p<0.01$; #, $p<0.05$ between 5 mM +S1P+ LY294002 and 5 mM+ S1P group. n=3

4.A.13 Overexpression of FOXM1 in normoglycemic condition results in cardiomyocyte hypertrophy and high α-SMA expression indicating a definite role of FOXM1 in the hyperglycemia mediated pathogenesis of cardiac cells

Finally, as very little work has been reported on the role of FOXM1 in the cardiomyopathy induction in the adult heart, to confirm the effect of FOXM1 overexpression on cardiomyocyte we have treated H9c2 cells with FOXM1 recombinant protein and observed overexpression of hypertrophic and fibrotic markers with cell size enlargement and increased number of α-SMA positive cells even under normal glucose condition. Phalloidin staining showed a significant enlargement of overall cell size in the FOXM1 recombinant protein (FOXM1 RP) group (2.33 ± 0.11-folds, Fig. 20B') was seen over control cells (Fig. 20B). In immunostaining experiment, we observed that the cells treated with FOXM1 recombinant protein showed significant increase in the number of α-SMA positive cells (40.54 ± 3.77 %, Fig. 20C') compared to control cells (3.65 ± 0.08 %) (Fig.20C). In the periostin immunostaining data we have also observed significantly increased periostin expression in the FOXM1 RP group (28.49 ± 2.81 %, Fig. 20D') compared to the control group (6.26 ± 1.39 %) (Fig. 20D).

Also, to further support our proposed hypothesis, we have performed a YAP1 inhibition followed by exogenous administration of FOXM1 protein in the H9c2 cells, where it was observed that even if we inhibit YAP1 activity, addition of FOXM1 protein to the medium resulted in an increased hypertrophic and fibrotic response in the H9c2 cells. In the phalloidin staining we observed an (2.4 ± 0.31%, Fig. 20B") increase in cell size in the VP with FOXM1 recombinant protein as compared to control cells (Fig. 20B). in the VP with FOXM1 RP group an increased number of α-SMA positive staining (45.52 ± 1.94%, Fig. 20C") was observed compared to control cells (3.65 ± 0.08%) (Fig. 20C). Also, in the VP with FOXM1 RP treated cells a significantly increased periostin immunostaining (31.51 ± 1.8%, Fig. 20D") was observed compared to control cells (6.26 ± 1.3%, Fig. 20D) These observations suggest that in cardiomyocyte cells, FOXM1 overexpression induces cardiomyocyte hypertrophy and fibrosis leading to cardiac pathogenicity. Therefore, in conclusion, our study has inferred that in the adult diabetic heart increased YAP1-FOXM1 expression via AKT-GSK3β signaling is responsible for the induction of cardiomyocyte hypertrophy and fibrosis.
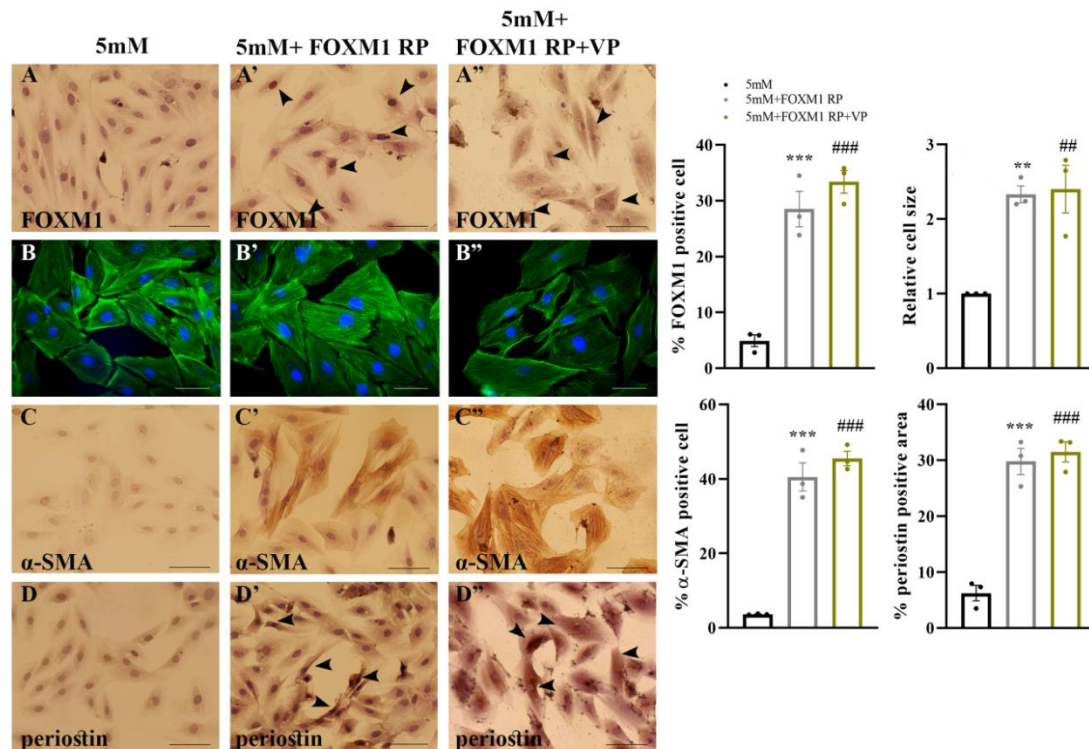
Figure 20. FOXM1 overexpression with recombinant protein promotes cardiomyocyte hypertrophy and fibrosis even in the normoglycemic condition. A-A". FOXM1 immunostaining images show increased expression of FOXM1 in the recombinant FOXM1 protein treated group compared to the control group, even when YAP1 is downregulated with verteporfin treatment. **B-B".** Phalloidin images show enlargement in the H9c2 cell size upon recombinant protein treatment. The enlarged cell size was also observed in the VP treated cells followed by FOXM1 RP treatment. **C-C".** α-SMA immunostaining images show increased number of positive staining in both the FOXM1 RP and VP with FOXM1 RP treated group compared to the control groups. **D-D".** Periostin immunostaining images show FOXM1 RP treatment leads to increased periostin staining compared to the control group. This was also observed in the VP treated group that were simultaneously treated with FOXM1 RP. Scale bar represents 50μm. Statistical significance was calculated by one way ANOVA. ***, $p<0.0001$; **, $p<0.01$ between 5 mM +FOXM1 RP and 5 mM group. ###, $p<0.0001$; ##, $p<0.01$ between 5 mM+FOXM1 RP+ VP and 5 mM+ S1P group. n=3

4.A.14 Chapter Discussion:

Diabetic cardiomyopathy is currently one of the leading health issues worldwide that prompts us to look into the understanding of the disease mechanism at the molecular level. YAP1 and FOXM1 are important cardiac development regulatory molecules that have recently been investigated for their role in pathogenesis (Noguchi, Saito, and Nagase 2018; P. Wang et al. 2014; Penke et al. 2018). In our study we aim to see how the hyperglycemic stress is perceived at the transcriptional level in cardiomyopathy induction and their specific mechanism of action. We have reported that hyperglycemic stress in both in vivo and in vitro conditions largely induces the expression of YAP1 as seen from total YAP1 expression compared to the control group (Fig. 11 and 12). We have also found that hyperglycemia causes increased YAP1 activity as confirmed by reduced p-YAP1/ total YAP1 expression compared to the normoglycemia group. Moreover, increased O-GlcNAcylation of YAP1 was also observed in the high glucose treated condition indicating increased YAP1 activation in hyperglycemic condition (Fig. 11 and 12).

YAP1 is an important effector molecule in the hippo pathway that regulates organ size and growth during development (Zhou et al. 2015; Jun Wang et al. 2018). In recent years several studies reported overexpression of YAP1 to be associated with hypertrophic disorders (P. Wang et al., n.d.; Abe et al. 2019). Also some studies reported high glucose condition like diabetes stimulates YAP1 expression leading to pathogenesis(X et al. 2017). However, little work has been done on the role of YAP1 in cardiomyocyte hypertrophy and fibrosis induction especially under hyperglycemic stress condition. In our study we have observed enlargement of H9c2 cell size and increased expression of fibrotic markers like periostin and α-SMA in the high glucose treated H9c2 cells that confirmed the observation that high glucose induces cardiomyocyte hypertrophy and fibrosis (Fig. 10). Interestingly we observed that inhibition of YAP1 in H9c2 cells with its specific inhibitor verteporfin, there is a significant reduction in the H9c2 size and reduced fibrotic responses in the hyperglycemia stressed cardiomyocyte (Fig. 15). Also, in cells under normoglycemic condition when treated with YAP1 activator S1P, this resulted in increased cellular hypertrophy and fibrosis in the H9c2 cells (Fig. 18 and 19).

FOXM1, an important cardiac development regulatory molecule has been shown in several studies to be associated with hippo-pathway molecule YAP1 (Fan, Cai, and Xu 2015; Weiler et al. 2017; Bolte et al. 2011). Reports suggest FOXM1 is downregulated in different adult

organs and have been shown to express during injury in some organs like liver and lung to facilitate tissue repair and regeneration(Kalin, Ustiyan, and Kalinichenko 2011). However, recent reports have shown FOXM1 overexpression in adult lung tissue to cause fibrosis(Penke et al. 2018). But, no studies so far addressed the role of FOXM1 in cardiac pathogenesis in the diabetic condition. In this study we have observed high expression of FOXM1 in the diabetic tissue as well as hyperglycemia treated cardiomyocyte cells that are consistent with the increased hypertrophy and fibrotic condition observed in the experimental groups (Fig. 11 and 12). In a separate study of treating H9c2 cells externally with FOXM1 recombinant protein to overexpress under normal glucose condition we have observed an increase in the H9c2 cell size and increased fibrosis (Fig. 20). On the contrary, in the high glucose treated H9c2 cells thiostrepton mediated FOXM1 inhibition reduced the hypertrophic and fibrotic condition (Fig. 17). This observation for the first time reported that FOXM1 plays a crucial role in the induction of hyperglycemic stress mediated cardiomyocyte hypertrophy and fibrosis. Also, we have shown that YAP1 inhibition in H9c2 cells in high glucose condition decreased FOXM1 expression and reversed the pathological phenotype (Fig. 16). Interestingly, YAP1 activation in H9c2 cells in normal glucose condition upregulated FOXM1 expression and aggravated hypertrophy and fibrotic condition in cardiomyocytes (Fig. 18). Also, while thiostrepton mediated FOXM1 downregulation resulted in amelioration of cardiomyocyte hypertrophy and fibrosis, inhibition of FOXM1 had little effect on the expression of YAP1 (Fig. 17). This observation shows that there might be an association between YAP1 and FOXM1 in the cardiomyocyte and the effect of overexpression of YAP1 might be mediated through FOXM1 at the transcriptional level. However, to further confirm the molecular hierarchy in this signalling pathway; in a follow up experiment, we demonstrated that activation of YAP1 with simultaneous inhibition of FOXM1 did not result in cardiomyocyte hypertrophy and fibrosis as compared to only YAP1 activated cells where visible cardiomyocyte enlargement and fibrosis were seen (Fig. 18). If FOXM1 have acted independently of YAP1 then inhibition of FOXM1 would not have any effect on YAP1 activation and hence, reduction of hypertrophy and fibrosis of cardiomyocyte. Thus, it confirms the hypothesis in our study that FOXM1 is a downstream effector of YAP1 in the hyperglycemic cardiomyocyte cells.

In our previous experiments we have observed that hyperglycemia resulted in an increased expression of AKT and p-GSKβ expression along with YAP1 and FOXM1 (Fig. 13 and 14). AKT-GSK3β is a well-known signaling mediator in glucose metabolism pathway and reports

have previously shown that this pathway is activated in cardiac cells in response to injury(Chakraborty, Sengupta, and Yutzey 2013b). In recent studies GSK3β has been reported to regulate the expression of FOXM1(Chen et al. 2016). Therefore to understand the detailed regulatory mechanism of FOXM1 under hyperglycemic stress we have further looked into the association of YAP1, AKT and GSK3β . We have found that increased p-AKT activity with increased inhibitory p-GSK3β that was observed in the high glucose conditioned cells were in sync with the expression of YAP1 in the cardiomyocyte. In Fig. 16 we have observed that verteporfin treatment in the high glucose incubated H9c2 cells reduced the p-AKT and inhibitory p-GSK3β protein levels. With reduced GSK3β inhibition the active GSK3β may lead to reduced FOXM1 expression. Furthermore, YAP1 activation with S1P in Fig. 19 clearly showed upregulated AKT activity which in turn increased the inhibitory effect of p-GSK3β , thus aggravating the FOXM1 activity. To confirm the proposed mechanism of AKT mediated FOXM1 activation by YAP1 we have performed a similar experiment of simultaneous overexpression of YAP1 with its activator S1P followed by inhibition of AKT by LY294002. Here we have observed in Fig. 19 that in spite of high YAP1 expression in the S1P treated groups, on LY294002 treatment there is an increased cytoplasmic retention of FOXM1 along with reduced H9c2 cell size and reduced expression of fibrosis markers α-SMA and periostin as compared to the S1P only treated cells (Fig. 19). This data indicates that YAP1 mediated FOXM1 activity is regulated via AKT-GSK3β signaling pathway in the cardiomyocyte cells under hyperglycemic stress condition which ultimately leads to cardiac hypertrophy and fibrosis.

With diabetes being the most serious metabolic disorder that largely affects cardiac function; it is necessary to look into the molecular disturbances in the cardiac cells caused by the hyperglycemic stress. Our data altogether shows that YAP1 and FOXM1 in the cardiac myocyte, in diabetic or hyperglycemic stress is upregulated to a pathological level and works via AKT/GSK3β signaling to induce cardiomyocyte hypertrophy and fibrosis. As currently both FOXM1 and AKT remains one of the widely looked out molecules as drug therapy option in various disease models there remains a need to understand the detailed regulation of these molecules for development of better targeted therapy(AL 2008; Penke et al. 2018). Therefore our reports on the detailed pathway of action of YAP1 and FOXM1 in diabetic cardiomyopathy will help in better combating the disease outcome in future.
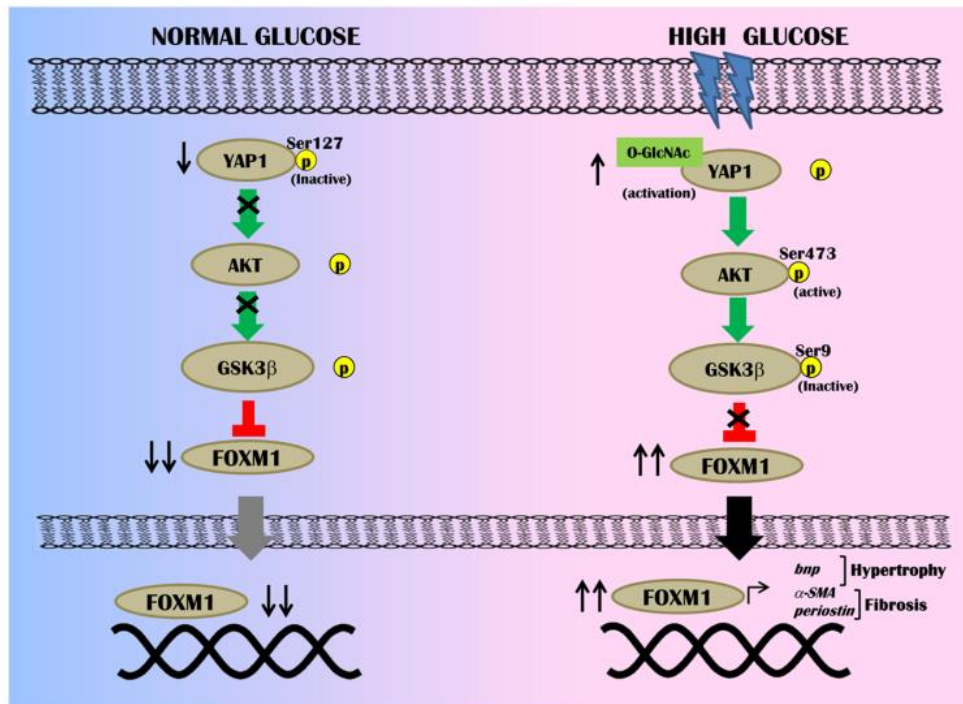
Figure 21. Schematic diagram representing the signaling pathway of YAP1-FOXM1 activity in the induction cardiomyocyte hypertrophy and fibrosis. Under hyperglycemia stress YAP1 is activated in the cardiomyocyte following reduced inactivating phosphorylation on YAP1. High Glucose also increased activating O-GlcNAcylation of YAP1. Elevated YAP1 level further leads to increased AKT phosphorylation, thus promoting AKT activity. Increased AKT mediated inactivation of GSK3β under hyperglycemic stress results in removal of the inhibitory regulation of GSK3β over FOXM1. Upregulated YAP1 therefore leads to aberrant FOXM1 accumulation within the cardiomyocyte. This elevated FOXM1 eventually promotes pathological remodelling of cardiomyocyte leading to cardiomyocyte hypertrophy and fibrosis.

CHAPTER 4.B

YAP1 mediates RAS signaling dysregulation in promoting hyperglycemia induced cardiomyocyte EMT and fibrotic response

4. B.1 Chapter Overview:

Diabetic cardiomyopathy is currently one of the major metabolic disorders worldwide leading to increased rate of heart failure in patients. Hypertrophy of cardiomyocytes and increased collagen deposition which leads to fibrosis in the myocardium are common occurrences in the hyperglycemic stressed heart(Dillmann 2019; Boudina and Abel 2010). Recent research has focused extensively to understand how the hyperglycemic stimulus is perceived at the molecular level in cardiac tissue to induce the pathogenesis of hypertrophy and fibrosis. In our previous study we have reported an altered fetal gene expression such as YAP1, FOXM1 under hyperglycemic stress is one of the major contributing factors in cardiomyocyte hypertrophy induction(Mondal et al. 2022). High glucose in the adult cardiomyocyte resulted in increased YAP1 activation through both downregulating the phosphorylation of YAP1 and increased N acetyl glycosylation of YAP1 further leading to AKT activation and subsequent downregulation of its downstream effector GSK3β. GSK3β is observed to restrict FOXM1 overexpression in the postnatal heart. YAP1 overexpression under hyperglycemia thereby leads to FOXM1 accumulation in the cardiac tissue, promoting pathological hypertrophy of the heart(Mondal et al. 2022). Activated YAP1 in the following study has further been observed to play a direct role in inducing cardiac fibrosis along with an unusual regulation of RAS signalling molecules.

Now, activated Angiotensin-II (Ang-II), the main component of RAS signalling has been well known to induce cardiomyocyte hypertrophy and fibrosis. Angiotensin converting enzyme (ACE) promotes Ang-II production from the precursor Angiotensinogen and hence, the blocking of upregulated ACE is clinically used to treat hypertension and associated cardiac and renal disorders(Ribeiro-Oliveira et al. 2008). Interestingly, ACE blocker such as captopril, enalapril is used as anti-hypertensive drug in diabetic patients albeit with some limitations and side effects(Goyal, Cusick, and Thielemier 2023). Developing drugs that can mimic the natural antagonist of ACE may be a better therapeutic option in combating diabetic cardiac remodelling. In the body system ACE2, a physiological analogue of ACE molecule has recently been in research focus for its perpetual benefit in counteracting the pathological effects of ACE. ACE2, like ACE acts on Angiotensin-I and Angiotensin-II but to rather convert it into corresponding beneficial peptides Angiotensin 1-9 and Angiotensin 1-7 which are vasodilator and cardioprotective in nature(Maruyama and Imanaka-Yoshida 2022; Imai et al. 2010). Although some studies have reported the role of ACE2 molecule, but the extensive

regulation of ACE-ACE2 in the cardiac hypertrophy and fibrosis induction especially in the context of hyperglycemic stress is not well documented. **Here, in our study, we have reported the regulation of differential expression of ACE and ACE2 by YAP1 during hyperglycemic injury to influence the induction of cardiac hypertrophy and fibrosis.**

In addition to YAP1, we have also observed the cardiac growth regulatory molecule β-catenin to be significantly upregulated in both cardiac fibroblast and myocyte. Extensive studies have reported that Wnt/β-catenin signalling is directly responsible in cardiac growth and development(D. Li, Sun, and Zhong 2022; Chakraborty, Sengupta, and Yutzey 2013a). Cardiac-injury induced activation of β-catenin has often shown to promote cardiac pathogenesis over time(Ozhan and Weidinger 2015; Zhao et al. 2019). In our study, hyperglycemia stimulated β-catenin overexpression in the adult cardiac cells was observed to initiate irregular fibrotic response and increased ACE activity. In vitro β-catenin activation was also found to have an inhibitory effect on ACE2 expression, thus further promoting cardiac fibrosis.

Moreover, we have identified TGF-β as one of the downstream effector molecule that might be involved in regulating ACE/ACE2 signaling to induce EMT mediated cardiomyocyte fibrosis upon hyperglycemic injury. TGF-β is a key player in the hypertrophic and fibrotic remodelling of cardiac tissue promoting cardiac fibroblast activation and fibrotic ECM deposition(Khalil et al. 2017). In this study, ACE has been observed to positively affect TGF-β expression, while ACE2 was seen to downregulate TGF-β-SMAD2/3 signaling and alleviate fibrotic condition.

Moreover, activated cardiac fibroblast releasing TGFβ, CTGF, and MMPs has been reported to induce EMT process in the progression of fibrosis(Kalluri and Weinberg 2009). In the hyperglycemic cardiomyocyte we have observed a similar upregulation of TGFβ, CTGF, MMP2 and MMP9 with a concomitant increased EMT and fibrosis. **Altogether, our study reports hyperglycemia mediated cardiac fibroblast activation may promote YAP1-β-catenin expression to further regulate ACE/ACE2 activity to induce EMT mediate cardiac fibrosis.**

4.B.2 Diabetes-induced upregulation of YAP/β-catenin expression results in increased fibrotic response in rodent cardiac tissue

Alloxan mediated diabetes induction resulting in persistent elevated blood glucose in the cardiac tissue resulting in increased cardiac fibrotic remodeling that was earlier reported in our previous study along with compromised cardiac function(Mondal et al. 2022). Here, the status of EMT-mediated cardiac fibrosis was examined *in vivo* in control and diabetic mouse heart by immunofluorescence staining. To determine the fibrotic response and EMT like process, two sets of analyses were performed with colocalization immunostaining of the target molecules with cardiomyocyte marker mf20/α-actinin in one group and fibroblast marker vimentin in another group. Study of EMT markers with cardiomyocyte specific markers mf20/α-actinin revealed significant increased expression of mesenchymal marker N-cadherin (N-cad) in the diabetic tissue (47.48 ± 2.47%, Fig. 22B') compared to the control tissue (12.77 ± 0.76%, Fig. 22B). Conversely, expression of the epithelial marker counterpart E-cadherin (E-cad) was observed to be significantly reduced (17.97 ± 0.48%, Fig. 22A') in the diabetic heart to that of the control heart (37.12 ± 2.48%, Fig. 22A). Colocalization study of the expression of N-cad and E-cad with fibroblast marker vimentin showed similar changes in fibroblast cell population as of myocte cells in the diabetic cardiac tissue (50.78 ± 2.33%, Fig. 22H' and 15.95 ± 0.23%, Fig. 22G' respectively) compared to control cardiac tissue (14.78 ± 0.76%, Fig. 22G; 50.62 ± 3.61%, Fig. 22H respectively). These data indicate that increased EMT activity may lead to the activation of fibroblast to induce cardiac fibrosis under hyperglycemic stress. Comparable EMT-like process was observed in the cardiac myocyte that was speculated to induce fibrotic response in the cardiomyocyte as well resulting in overall structural and functional damage in the cardiac tissue. Similar to increased collagen deposition and periostin expression in the diabetic cardiac tissue reported earlier(Mondal et al. 2022), we have also observed increased expression of TGFβ in the diabetic cardiomyocyte (45.59 ± 2.81%, Fig. 22F') to that of control tissue (10.21 ± 0.83%, Fig. 22F). In the vimentin positive diabetic tissue, TGFβ expression was also upregulated (50.14 ± 4.44%, Fig. 22L') compared to the control tissue (15.26 ± 1.24%, Fig. 22L). Downstream to TGF-β upregulation pro-fibrotic signaling molecule p-SMAD2/3 activity is observed to be increased in the diabetic cardiac tissue (2.74 ± 0.32-fold, Fig. 22M) compared

to control tissue indicating TGF-β-SMAD2/3 pathway may be a potential pathway in the induction of diabetic cardiac fibrosis.

To elucidate the associated molecular regulations we have further observed, increased expression of β-catenin in the diabetic cardiac tissue. Co labelled staining of β-catenin with mf20 shows increased expression (40.88 ± 4.04%, Fig. 22C') in the tissue myocyte following diabetes induction compared to the control tissue (18.63 ± 0.97%, Fig. 22C). β-catenin expression was significantly upregulated in the diabetic cardiac fibroblast (40.34 ± 3.8%, Fig. 22I') compared to control tissue (15.69 ± 2.12%, Fig. 22I). Protein expression data of β-catenin also shows overall upregulated expression of β-catenin in the diabetic cardiac tissue (3.52 ± 0.89-fold, Fig. 22M) to that of control tissue. Along with β-catenin, RAS regulatory molecules were observed to have altered expression in the heart tissue following diabetic stress induction. Significantly increased expression of ACE was observed in the diabetic cardiomyocyte (45.64 ± 3.07%, Fig. 22D') compared to the control tissue (10.59 ± 0.3%, Fig. 22D) leading to hypertrophy and fibrosis induction in cardiac tissue. Significantly increased expression of ACE in the vimentin positive fibroblast cells in the cardiac tissue in diabetic model (38.72 ± 3.87%, Fig. 22J') compared to control tissue (19.66 ± 2.06%, Fig. 22J) was observed. However, ACE2 was observed to have significant reduction in expression in the diabetic cardiac tissue (13.85 ± 1.88%, Fig. 22E') to that of control tissue (51.67 ± 4.87%, Fig. 22E) in the myocytes co-labelled with α-actin. Co-labelling with vimentin also showed ACE2 was downregulated in diabetic cardiac fibroblast (16.7 ± 0.88%, Fig. 22K') compared to control tissue (38.15 ± 1.14%, Fig. 22K). Total protein expression level of ACE was observed to be increased in the diabetic tissue (2.55 ± 0.27-fold, Fig. 22M) while ACE2 expression level was significantly downregulated in the diabetic tissue (0.35 ± 0.01-fold, Fig. 22M). As ACE2 observed to be protective in counterbalancing the effect of ACE in various tissues, the depleted level of ACE2 in diabetic cardiac tissue is assumed to aggravate the pathological phenotype. Altogether these *in vivo* observations suggest that hyperglycemia induced EMT-like process in cardiac tissue may activate pro-fibrotic TGFβ-SMAD2/3 pathway and RAS signaling activation eventually promoting adverse fibrotic remodelling.
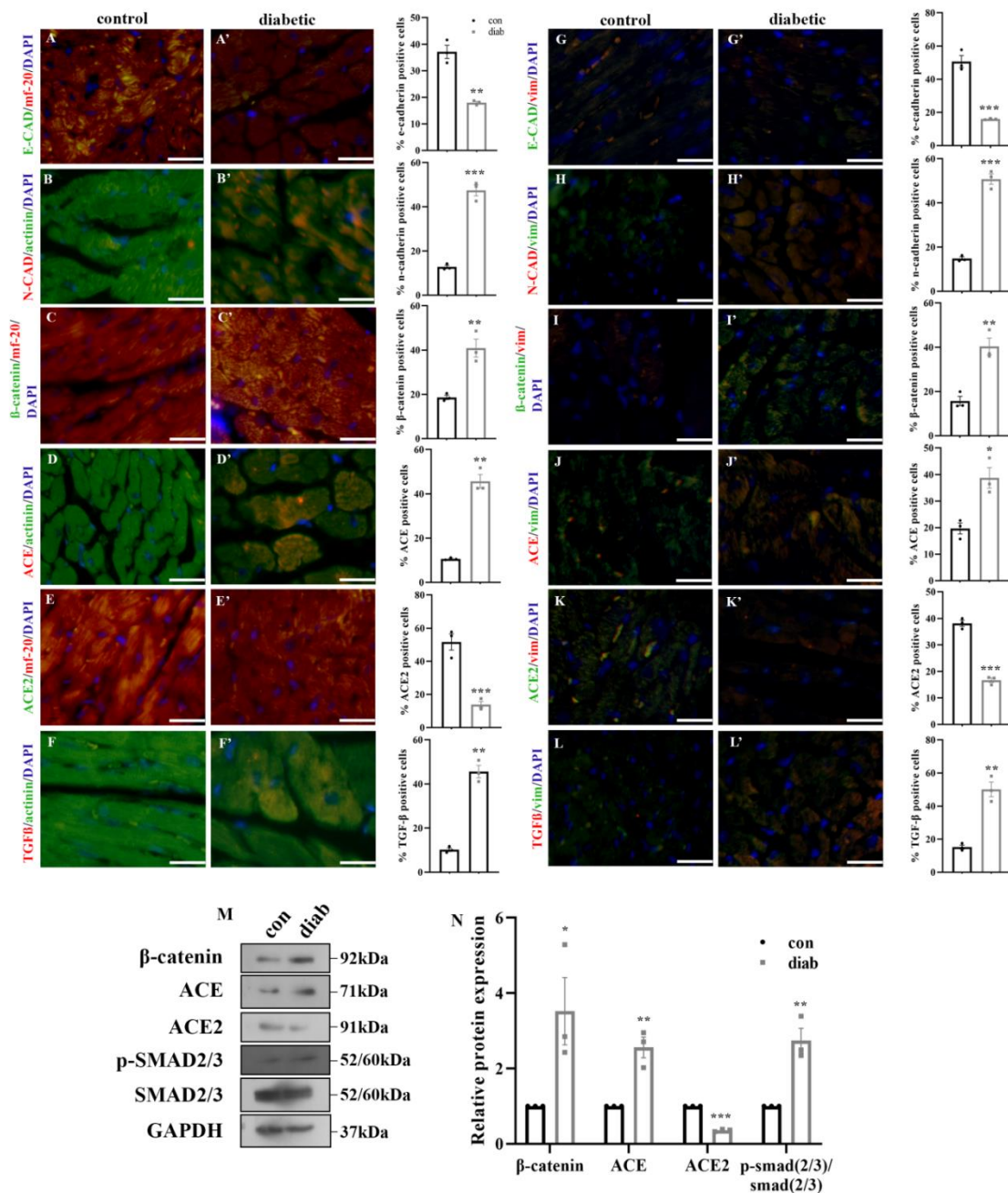
Figure 22. Diabetes mediated upregulated YAP/β-catenin expression results in increased fibrotic response in rodent cardiac tissue. A-A'. Immunofluorescence staining images of E-cad with cardiomyocyte marker mf20 showing significantly reduced expression in the diabetic (diab) tissue compared to control tissue. **B-B'.** N-cad IF images show significantly increased expression in the diab tissue to that of control tissue. **C-C'.** Tissue IF images of β-catenin showing upregulated expression in the diab tissue to that of control tissue. **D-D'.** IF data of ACE showing significantly increased expression in the diab tissue compared to control tissue **E-E'.** ACE2 immunostaining images show significantly reduced level of ACE2 in the diab cardiac tissue compared to control tissue. **F-F'.** IF staining images for TGF-β antibody revealing upregulated expression in the diab tissue compared to control tissue. **G-G'.** IF staining images of E-Cad with vimentin (vim) fibroblast marker show significantly reduced expression of E-cad in the diab tissue compared to control tissue. **H-H'.** N-cad expression images co-labelled with vim indicating increased expression in the diab tissue over control tissue. **I-I'.** immunostaining images of β-catenin show increased expression in the fibroblast cells of diab tissue to that of control tissue. **J-J'.** ACE IF images with vim co-labelling shows increased fibroblast expression of ACE in the diab tissue

compared to control tissue expression. **K-K'.** IF data of ACE2 showing reduced expression in the diabetic cardiac fibroblast tissue compared to control tissue. **L-L'.** TGF-β IF staining images show upregulated expression in the diab fibroblast specific tissue to that of control tissue. **M.** Western blot images of β-catenin, ACE, ACE2 and p-SMAD(2/3)/SMAD(2/3) of diabetic tissue and control Statistical significance was calculated by one way ANOVA. **, $p<0.01$; ***, $p<0.0001$ between diab and con groups. n=3. Scale bar in A-L represents 50μm.

4.B.3 Hyperglycemia induces EMT mediated fibrosis in cardiomyocyte

Primary investigation of the effect of high glucose in induction of fibrosis on cardiac tissue (Fig. 22) prompted us to extend the experimental analysis on the main contractile cells of cardiac tissue that is cardiomyocyte(Litviňuková et al. 2020). Preliminary observations were performed with H9c2 cardiomyocyte cells with HG treatment for 48 hours. Gene expression analyses of pro-fibrotic molecules *tgf-β1* (2.57 ± 0.11-fold) and *ctgf* (2.34 ± 0.33-fold) in H9c2 cells showed a significant increase in the HG treated cells compared to the control cells (Fig. 23G). A significant increase in several other key fibrotic markers such as *col1* and *col3* in high glucose treated H9c2 cells were previously reported in earlier studies by our lab (Mondal et al. 2022). Qualitative analyses for collagen accumulation with picrosirius red (Fig. 23A' and 23A) in H9c2 cells showed increased collagen staining in the HG treated cells compared to control cells. Further, total collagen content was estimated by elution with 0.1N NaOH solution and spectrophotometric analysis showed (2.70 ± 0.3-fold) increased collagen deposition in the HG treated cells (Fig. 23A') to that of NG treated cells (Fig. 23A). Excessive fibrosis within the cellular network was further observed in immunostaining results with COL1 and fibronectin antibody staining. Both COL1 (40.36 ± 1.65 % vs. 10.37 ± 1.16%, Fig. 23B', 23B) and FN had significantly increased expression in the HG treated cells (8.56 ± 1.21-fold, Fig. 23C', 23C) respectively compared to the NG conditioned cells.

In the same experimental condition, we have also observed significant increased expression of *mmp2* (3.10 ± 0.22-fold, Fig. 23G) and *mmp9* (7.9 ± 2.07-fold, Fig. 23G) gene expression respectively along with increased expression of TGF-β1 in the hyperglycemic cells (47.27 ± 0.62%, Fig. 23D') over control cells (15.95 ± 1.81%, Fig. 23D). Also, significantly increased SMAD2/3 activity (1.68 ± 0.13-fold, Fig. 23H) was observed in the HG treated cells. The role of MMP2 and MMP9 in regulating EMT and the active role of TGF-β1 in cardiac fibrosis encouraged us to further probe whether EMT mediated fibrosis could be a potential process of pathophysiology associated with hyperglycemia stress induced cardiac injury.

In the immunostaining results, the epithelial cell marker E-cad expression was found to have a higher expression in the NG acclimatised cells (60.57 ± 1.16%, Fig. 23E) whereas a very low expression of the same was observed in the HG treated cells (22.32 ± 2.57%, Fig. 23E'). On the contrary, the mesenchymal cell marker N-cad had significantly increased expression

in the hyperglycemic H9c2 cells (54.2 ± 2.34%, Fig. 23F') to that of the NG treated cells (19.38 ± 2.15, Fig. 23F). All these results indicate hyperglycemia promotes EMT like process in the H9c2 cells leading to progressive fibrotic changes in cells.
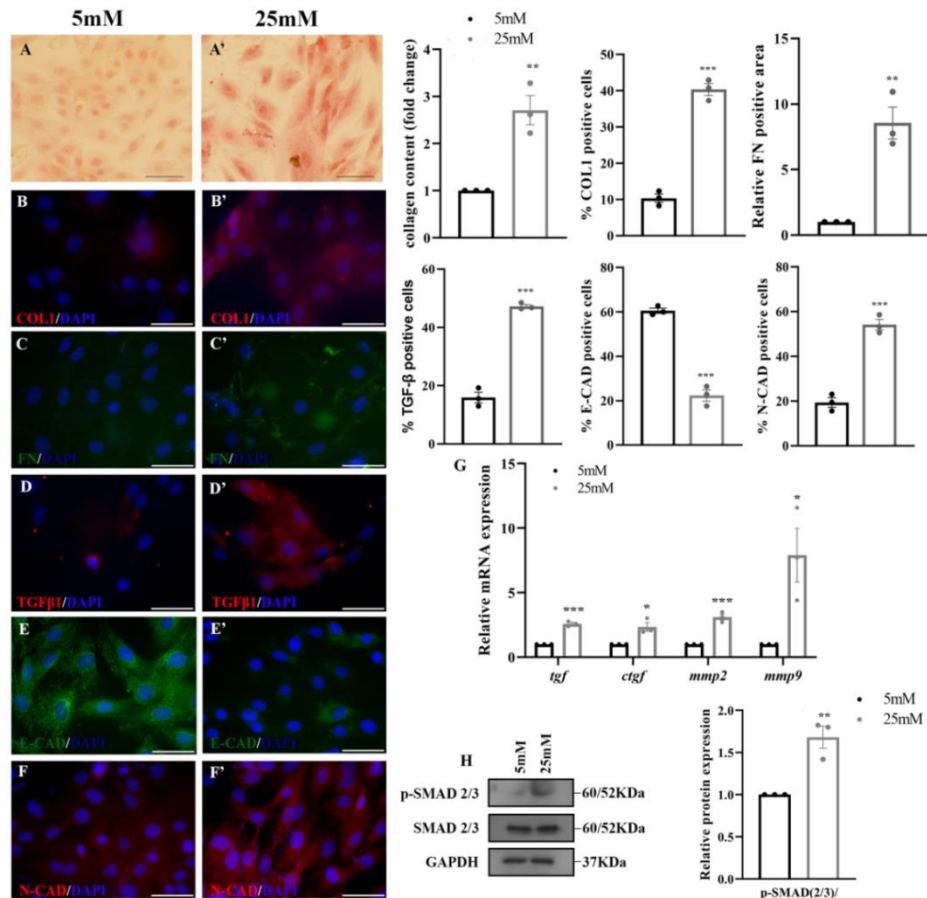
Figure 23. Hyperglycemia induces EMT mediated fibrosis in cardiomyocytes. A-A'. Picrosirius red staining images showing collagen deposition in H9c2 cells. Increased collagen deposition is observed in the HG treated H9c2 cells compared to the NG subjected cells. Scale bar represents 20μM. **B-B'.** Immunofluorescence images of COL1 antibody showing increased expression in the HG treated H9c2 cells compared to the NG treated cells. **C-C'.** FN immunostaining data shows increased expression in the HG treated cells to that of NG treated cells. **D-D'.** Immunostaining of H9c2 cells with TGF-β1 antibody showing increased expression in the HG group compared to NG group. **E-E'.** IF images of E-cad antibody shows reduced expression in the HG treated cells over NG cells. **F-F'.** N-cad immunostaining images showing high expression in the HG group compared to the NG group. **G.** Quantitative Real Time PCR analysis showed significantly increased expression of *tgf*, *ctgf*, *mmp2* and *mmp9* gene in the HG treated cells compared to the NG treated cells. **H.** western blot analysis of p-SMAD2/3 expression showing increased SMAD activity in the HG treated cells compared to the NG treated cells. Statistical significance was calculated by one way ANOVA. *, p< 0.05; ***, p<0.0001; **, p<0.01 between 25 mM and 5 mM groups; n=3.Scale bar in B-D represents 50μM.

4.B.4 Hyperglycemia mediates upregulation of YAP1, β-catenin expression and dysregulated RAS signalling in cardiomyocyte

HG treatment of H9c2 cells resulted in significantly excessive activation of YAP1 (62.90 ± 4.43%, Fig. 24A') to that of NG (20.63 ± 2.66%, Fig. 24A) which was also reported earlier in

our study(Mondal et al. 2022). But in this study we also observed overexpression of β-catenin in the hyperglycemic cells (57.33 ± 2.77%, Fig. 24B') compared to NG treated cells (18.28 ± 2.19%, Fig. 24B) seen from the IF as well as western blot experimental results (2.86 ± 0.43-fold, Fig. 24F). Immunofluorescence staining and immunoblot images also revealed increased ACE expression in the hyperglycemic group (60.63 ± 0.97%, Fig. 24C') compared to the NG group (10.27 ± 1.9%, Fig 24C) (3.02 ±0.48-fold, Fig. 24F) respectively. Also, HG stress resulted in significantly reduced ACE2 immunostaining in the H9c2 cells (17.40 ± 3.56%, Fig. 24D') compared to the NG containing cells (63 ± 2.43%, Fig. 24D). This was also observed in the western blot experimental analysis where ACE2 has significantly downregulated expression (0.54 ± 0.03-fold, Fig. 24F) in the hyperglycemic group to that of normoglycemic group.
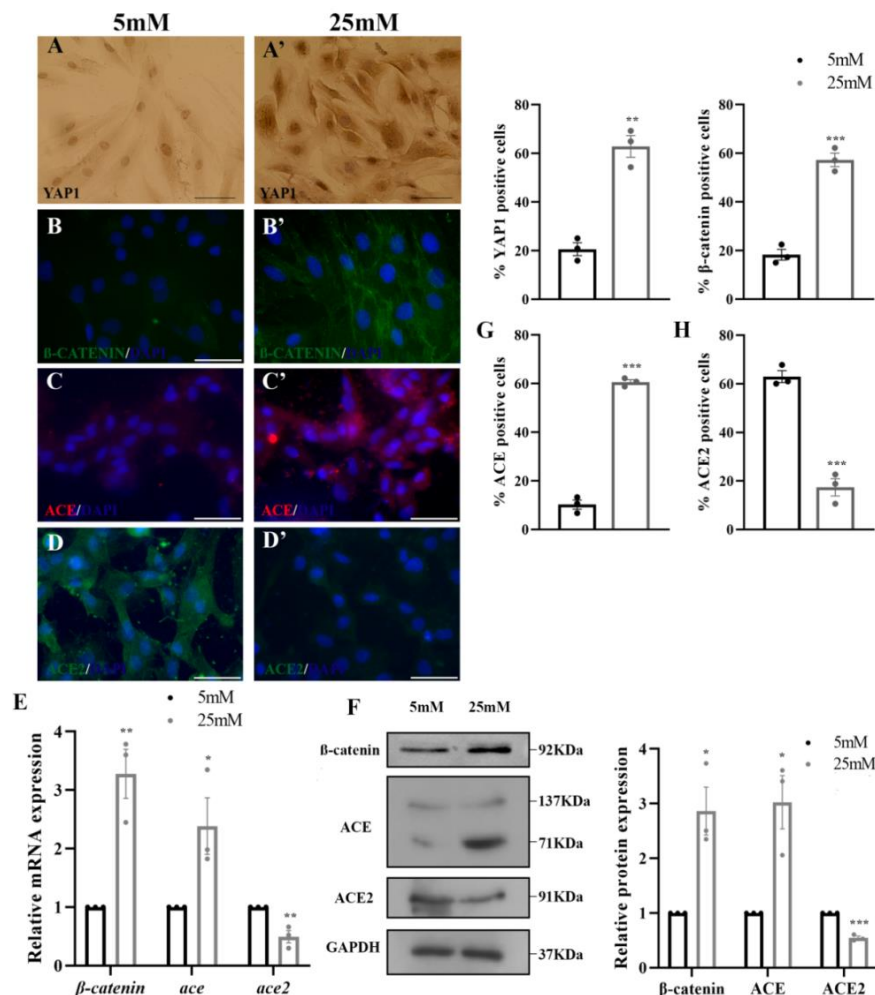
Figure 24. Hyperglycemia mediates upregulation of YAP1, β-catenin expression and dysregulated RAS signalling in cardiomyocyte. A-A'. YAP1 antibody staining in the DAB method showed significantly increased expression in the 25mM glucose treated cells compared to 5mM glucose treated H9c2 cells. Scale bar represents 20μM. **B-B'.** β-catenin IF staining images showing significantly upregulated expression in the HG treated cells to that of NG treated cells. **C-C'.** Immunofluorescence staining images of ACE antibody shows significant increased TGF-β1 expression in the HG H9c2 cells over NG cells. **D-D'.** ACE2 immunostaining data revealed significantly downregulated expression in the HG cells

compared to NG cells. **E.** Quantitative Real time PCR expression analyses showing significantly upregulated expression of *β-catenin*, *ace* and *ace2* in the HG cells compared to NG cells. **F.** Western blot images showing significantly increased expression of β-catenin, ACE and ACE2 in the HG cells to that of NG cells. GAPDH was used for loading control. Statistical significance was calculated by one way ANOVA. *, $p < 0.05$; ***, $p < 0.0001$; **, $p < 0.01$ between 25 mM and 5 mM groups; n=3. Scale bar in B-D represents 50μM.

4.B.5 YAP1 mediated differential expression of ACE-ACE2 is responsible to induce cardiomyocyte fibrosis through TGF-β-SMAD signaling pathway

Next, to determine whether YAP1 plays a critical role in the induction of cardiac fibrosis and EMT during hyperglycemic stress, we have pre-treated H9c2 cells to YAP1 inhibitor, Verteporfin (VP) for 24 hours followed by incubation in HG media. VP mediated YAP1 inhibition in the H9c2 cardiomyocyte cells, resulted in significant amelioration of pathological phenotypes that was observed in the YAP1 upregulated HG stressed cells. Immunofluorescence staining for EMT marker E-cad and N-cad showed significantly recovered expression of E-cad in the YAP1 inhibitor group (56.12 ± 1%, Fig. 25C'') to that of HG without inhibitor group (28.33 ± 1.47%, Fig. 25C'). Conversely, in the N-cad IF images expression was shown to be reduced in HG conditioned cells pre-treated with verteporfin (37.78 ± 1.69%, Fig. 25D'') as opposed to only HG treated cells (59.86 ± 1.99%, Fig. 25D'), indicating hyperglycemia mediated overactive YAP1 results in induced pathological EMT in cardiomyocyte. Moreover, the expression of COL1 (29.06 ± 2.06%, Fig. 25A'' vs. 53.09 ± 1.92%, Fig. 25A') and FN (1.72 ±0.12-fold, Fig. 25B'' vs. 3.84 ± 0.46-fold, Fig. 25B') were again observed to be significantly reduced in the YAP1 inhibited cells as compared to the hyperglycemic cells without VP. Picrosirius red staining for collagen accumulation showed significantly reduced collagen staining in the VP treated cells (1.58 ± 0.14 fold, Fig. 25F'') maintained in HG compared to HG treated cells without VP (2.55 ± 0.34-fold, Fig. 25F'). This confirms YAP1, like in cardiac fibroblast cells also induces exaggerated fibrotic remodeling in the H9c2 cells possibly following too much EMT response in the cells. These data suggest that inhibition of YAP1 may be beneficial in reducing the cardiomyocyte fibrosis in the context of hyperglycemic injury. Along with this, treatment with VP resulted in significant downregulation of TGF-β1 expression in the hyperglycemic H9c2 cells (32.77 ± 1.27%, Fig. 25E'') compared to cells without VP (53.98 ± 1.42%, Fig 25E'), to indicate the fibrotic activity of YAP1 is mediated via TGF-β signalling.
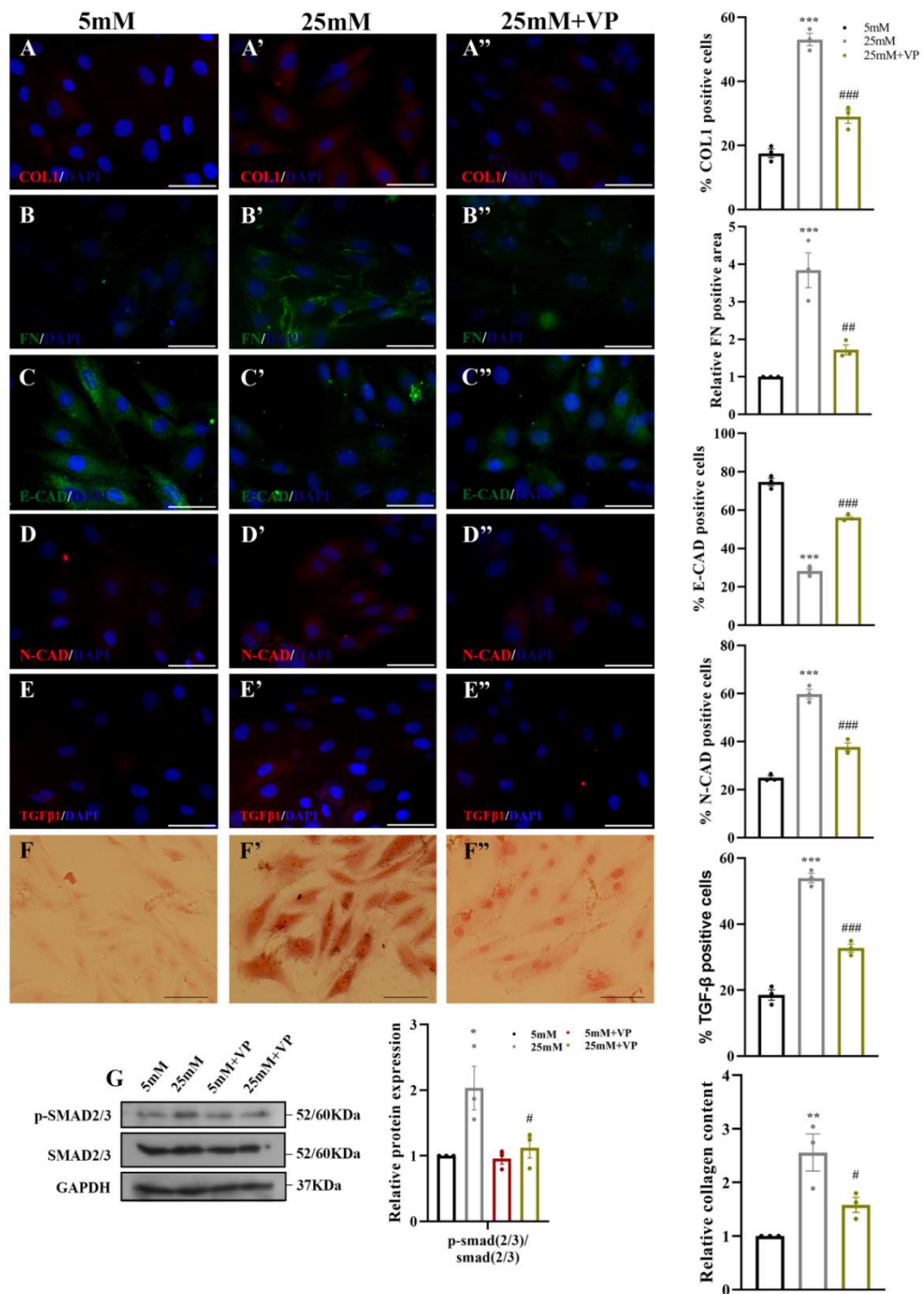
Figure 25. YAP1 mediates fibrotic response in H9c2 cardiomyocyte through TGF-β-SMAD pathway. A-A''. Immunofluorescence data of COL1 antibody showing increased expression in the 25mM glucose treated H9c2 cells compared to 5mM glucose treated cells which is reduced in the 25mM+VP treated cell. **B-B''.** Immunostaining data of FN antibody shows significantly reduced expression in the VP treated H9c2 cells compared to HG cells without VP. **C-C''.** E-cad immunostaining showing significantly increased e-cad positive cells in the VP+25mM glucose treated cells to that of 25mM glucose cells without VP. **D-D''.** N-cad antibody IF staining images showing significantly reduced expression in the VP treated cells to that of HG cells without VP. **E-E''.** TGFβ1 expression in the IF data shows increased expression in the HG treated cells to NG cells. TGF-β1 expression is reduced in the VP treated H9c2 cells compared to HG cells without VP treatment **F-F''.** Picrosirius red staining shows increased collagen deposition in the HG H9c2 cells to NG cells. In the VP treated hyperglycemic cells collagen deposition was observed to be significantly lower

compared to hyperglycemic cells without VP treatment. Scale bar represents 20µM. **G.** Western blot images revealing significantly increased expression of p-SMAD2/3 in the HG treated H9c2 cells which are observed to be significantly downregulated in the VP pre-treated groups. Statistical significance was calculated by one way ANOVA. *, $p < 0.05$; **, $p<0.01$; ***, $p<0.0001$ between 25 mM and 5 mM groups. #, $p< 0.05$; ##, $p<0.01$; ### $p<0.0001$ between 25 mM + VP and 25 mM groups. n=3. Scale bar represents 50µm.

Moreover, both by Western blot and immunostaining analysis we show a significantly higher expression of β-catenin in the hyperglycemic condition which got reduced following VP pre-treatment compared to the untreated group (1.39 ± 0.29-fold vs. 3.01 ± 0.5-fold, Fig. 26D and $31.19 \pm 3.16\%$, Fig. 26A'' vs. $49.23 \pm 3.4\%$, Fig. 26A' respectively). Western blot and IF data against ACE antibody in the experimental groups showed downregulated ACE expression following VP treatment of hyperglycemic cells compared to cells without inhibitor (1.07 ± 0.12-fold vs. 2.39 ± 0.38-fold, Fig. 26D and $39.40 \pm 0.34\%$, Fig. 26B'' vs. $57.56 \pm 1.38\%$, Fig. 26B') respectively. For ACE2 expression, we observed YAP1 inhibition in the HG treated cells resulted in significant stabilization of ACE2 expression in the cells compared to cells without VP treatment ($45.33 \pm 2.22\%$, Fig. 26C'' vs. $23.58 \pm 1.37\%$, Fig. 26C') (0.69 ± 0.05-fold vs. 0.42 ± 0.05-fold, Fig. 26D), that proved YAP1 may have some regulation in the expression of the RAS signalling in promoting cardiac remodeling through ACE and ACE2.
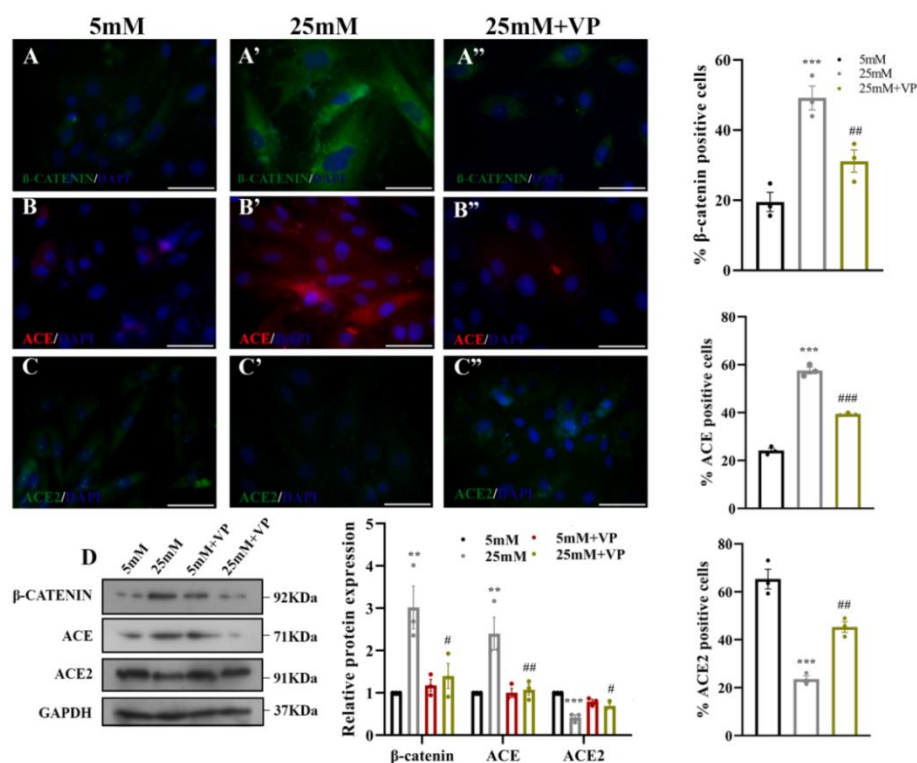
Figure 26. YAP1 induces altered ACE-ACE2 ratio to induce cardiac fibrosis through TGF-β-SMAD pathway. A-A''. β-catenin immunofluorescence images show upregulated expression in the hyperglycemic H9c2 cells compared to normoglycemic cells which was reduced following VP treatment . **B-B''.** IF images of ACE antibody staining showed

significantly increased ACE expression in the HG group to that of NG cells and reduced expression in the VP treated group to that of HG treated cells without VP. **C-C".** Immunostaining data of ACE2 staining in HG treated H9c2 cells showing reduced expression compared to NG cells and VP pre-treated HG cells to that of untreated HG cells. **G.** Western blot images revealing significantly increased expression of β-catenin and ACE in the HG-treated H9c2 cells which are observed to be significantly downregulated in the VP pre-treated groups. ACE2 expression was observed to be significantly downregulated in the 25mM groups which was observed to be significantly upregulated following VP treatment. GAPDH was used as loading control. Statistical significance was calculated by one way ANOVA. **, $p < 0.01$; ***, $p < 0.0001$ between 25 mM and 5 mM groups. #, $p < 0.05$; ##, $p < 0.01$; ### $p < 0.0001$ between 25 mM + VP and 25 mM groups. n=3. Scale bar represents 50μm.

4.B.6 Cardiac β-catenin activation regulates ACE-ACE2 activity to aggravate EMT and fibrosis in cardiac cells

Next, to understand the precise signalling pathway of YAP1, β-catenin and RAS molecule ACE and ACE2 we attempted to modulate the expression of β-catenin with XAV-939 and observe the subsequent expression pattern of the concerned molecules. XAV treatment resulted in reduced β-catenin expression in the high glucose treated H9c2 cells compared to high glucose treated cells without inhibitor in IF experiments and western blot data (26.74 ± 1.97%, Fig. 27B'' vs. 58.94 ± 2.22, Fig. 27B') (1.14 ± 0.12-fold vs. 2.19 ± 0.29-fold, Fig. 27E) respectively. The IF result showed that in the hyperglycemic cells where ACE expression was observed to be significantly higher (58.37 ±0.88%, Fig. 27C''), following XAV treatment it was found to be significantly reduced compared to the HG cells without XAV (29.85 ± 5.59%, Fig. 27C'). The same was observed in western blot data of β-catenin in the experimental groups (1.11 ± 0.88-fold vs. 2.78 ± 0.39-fold, 27E). ACE2 expression in the XAV pre-treated hyperglycemic H9c2 cells was found to be significantly increased compared to the experimental group without XAV treatment in both IF and western blot experiments (52.85 ± 0.99%, Fig. 27D'' vs. 25.32 ± 2.5%, Fig. 27D') (0.81 ± 0.04-fold vs. 0.48 ± 0.01-fold, Fig. 27E) respectively. However, XAV treatment had very little effect on the expression of YAP1 as compared to the HG without XAV cells (35.08 ± 2.19% vs. 36.31 ± 1.25%, Fig. 27A'', 27A'). This result confers that β-catenin regulates the expression of ACE-ACE2 signaling in high glucose stress cardiomyocyte downstream to YAP1.
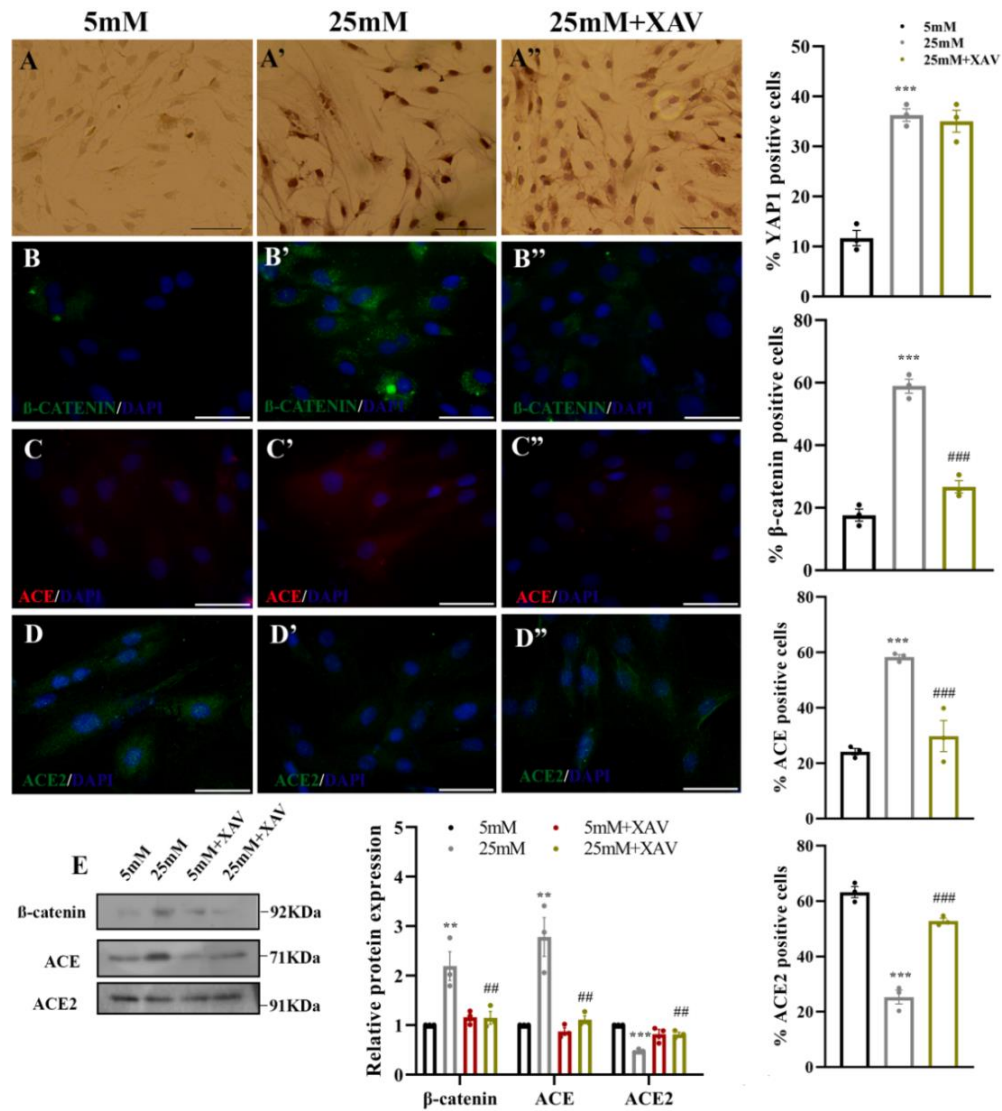
Figure 27. Cardiac β-catenin activation aggravate EMT and fibrosis in cardiac cells. A-A''. COL1 immunostaining results showing HG induced increased COL1 staining compared to NG cells, which is observed to be significantly lower in XAV-939 treated group indicating β-catenin overexpression causes increased fibrotic response in the HG cells. **B-B''.** Immunofluorescence images of FN antibody revealing significantly increased staining in the HG group which is ameliorated following XAV treatment. **C-C''.** EMT marker E-cad was observed to be significantly reduced in the HG treated cells compared to NG treated cells. Significant upregulation of E-cad expression was observed in the XAV-939 pre-treated HG cells to that of untreated HG cells. **D-D''.** N-cad immunostaining data revealed significantly reduced expression in the XAV-939+25mM glucose treated cells to that of 25mM glucose treated cells without XAV-939. **E-E''.** immunostaining images of TGF-β1 antibody shows the upregulated expression of TGF-β1 in the HG H9c2 cells to NG cells is significantly downregulated in the XAV-939 treated cells. **F-F''.** Picrosirius red staining data shows increased collagen staining in the hyperglycemic cells compared to normoglycemic cells which is further ameliorated in the XAV-939 pre-treatment groups. Scale bar represents 20μM. **G.** Western blot data shows significantly increased expression of p-SMAD2/3 in the HG H9c2 compared to the NG cells. GAPDH was used as loading control. Statistical significance was calculated by one way ANOVA. **, $p<0.01$; ***, $p<0.0001$ between 25 mM and 5 mM groups. #, $p< 0.05$; ##, $p<0.01$; ### $p<0.0001$ between 25 mM + XAV-939 and 25 mM groups. n=3. Scale bar represents 50μm.

β-catenin inhibition in the H9c2 cells was observed to have an inhibitory effect on the progression of EMT in the H9c2 cells as well as fibrotic remodeling. E-cad immunostaining showed the epithelial marker to have increased expression (59.81 ± 3.75%, Fig. 28C'') in the XAV treated group compared to the HG cells without XAV treatment (30.58 ± 0.62%, Fig. 28C'), whereas N-cad mesenchymal marker showed reduction in expression in the XAV-939 treated group (37.11 ± 1.67% , Fig. 28D'') to that observed in the HG group without XAV-939 treatment (53.79 ± 1.69%, Fig. 28D'). Finally, in the XAV pre-treated experimental groups, COL1 and FN deposition was observed to be significantly reduced compared to the HG treated cells without XAV (32.12 ± 2.92%, Fig. 28A'' vs. 47.49 ± 3.18%, Fig. 28A') (2.6 ± 0.3-fold, 28B'' vs. 7.24 ± 0.78-fold, Fig. 28B') respectively. Collagen deposition in the ECM estimated from picrosirius red staining, was also observed to be significantly lower (1.53 ± 0.26-fold, Fig. 28F'') following β-catenin inhibition compared to HG cells without β-catenin inhibition (2.93 ± 0.23-fold, Fig. 28F').
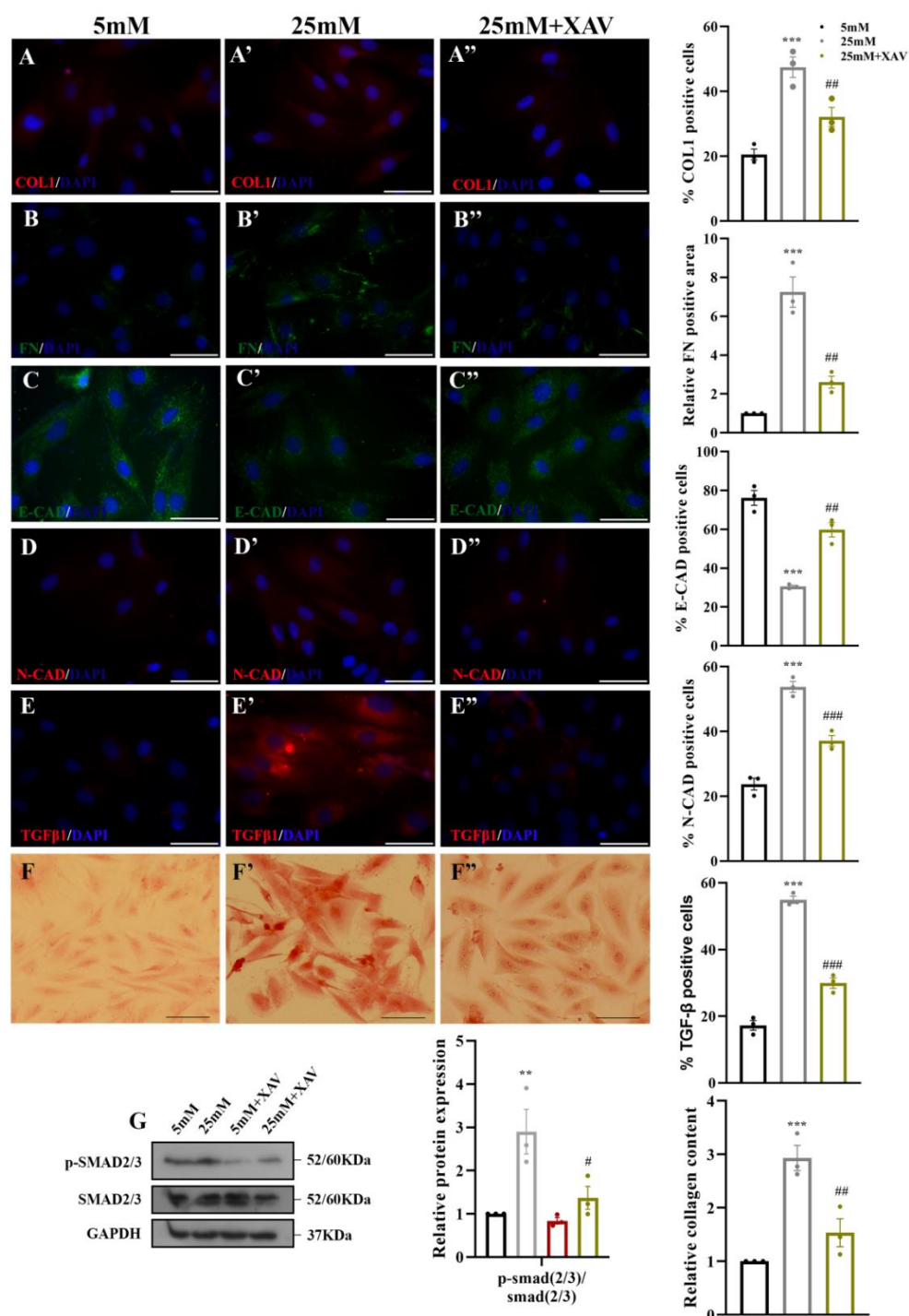
Figure 28. Cardiac β-catenin regulates ACE-ACE2 activity to promote EMT and fibrosis in cardiac cells. A-A". immunostaining images of YAP1 antibody showing increased expression in the HG treated cells compared to NG treated cells. In the XAV-939 treated HG cells there was no significant changes in the expression compared to untreated cells. Scale bar represents 20μM. **B-B".** Immunofluorescence images of β-catenin antibody staining showing increased β-catenin expression in the HG treated H9c2 cells to NG treated cells that is significantly reduced following XAV treatment. **C-C".** IF data of ACE antibody shows increased expression of ACE in the HG treated cells which is reduced following XAV treatment in the HG cells. **D-D".** IF data of ACE2 antibody showing increased expression in the XAV+25mM group compared to 25mM group without XAV indicating the regulation of β-catenin on ACE2 expression. **G.** Western blot data shows significantly increased expression of ACE and β-catenin in the HG H9c2 compared to the NG cells. XAV treatment in the HG cells resulted in reduced expression of ACE, β-catenin and elevated level of ACE2

80

compared to HG cells without XAV. Statistical significance was calculated by one way ANOVA. ***, p<0.0001 between 25 mM and 5 mM groups. ##, p<0.01; ### p<0.0001 between 25 mM + XAV-939 and 25 mM groups. n=3. Scale bar represents 50μm.

4.B.7 Inhibition of TGF-β pathway results in normalization of EMT activity and concomitant reduced fibrotic remodelling

To, Further confirm whether YAP1, β-catenin activity is exerted through TGF-β signaling, we have treated H9c2 cells first with YAP1 activator S1P following TGF-β inhibition with SB431542 . Consistent with the findings in diabetic tissue, immunostaining experiment data showed that YAP1 activation in the NG condition resulted in increased expression of YAP1 (42.59 ± 2.17% vs. 12.51 ± 1.15%, Fig. 29A', 29A), β-catenin (62.75 ± 4.02% vs. 13.72 ± 0.72%, Fig. 29B', 29B) and ACE (57.23 ± 3.29% vs. 19.14 ± 1.54%, Fig 29C', 29C) compared to the cells without YAP1 activation. ACE2 IF images revealed S1P treatment significantly affected ACE2 expression (31.52 ± 0.9%, Fig. 29D') compared to the normoglycemic cells without YAP1 activation (58.53 ± 2.11%, Fig. 29D). Similar observation was seen in the western blot experimental analyses (3.58 ± 0.33-fold β-catenin, 4.02 ± 0.73-fold ACE, 0.29 ± 0.11-fold ACE2, Fig. 29E).

Immunostaining images with YAP1, β-catenin, ACE and ACE2 antibody in the S1P experimental groups further treated with SB431542 showed no significant alterations in their expression levels as compared to cell groups without TGFβ inhibitor (43.04 ± 1.33%, Fig. 29A'' vs. 42.59 ± 2.17%, Fig. 29A' YAP1, 55.98 ± 2.72%, Fig. 29B'' vs. 62.75 ± 4.02%, Fig. 29B' β-catenin, 54.26 ± 1.64%, Fig. 29C'' vs. 57.23 ± 3.29%, Fig. 29C' ACE, and 33.14 ± 1.16, Fig. 29D'' vs. 31.52 ± 0.9%, Fig. 29D' ACE2) indicating both YAP, β-catenin as well as ACE and ACE2 all acts upstream to TGFβ- SMAD pathway to signal the EMT and fibrosis process. Western blot data reflected similar observation in the total protein expression (2.94 ± 0.29-fold vs. 3.58 ± 0.33-fold β-catenin, 3.53 ± 0.6-fold vs. 4.02 ± 0.73-fold ACE, 0.31 ± 0.1-fold vs. 0.29 ± 0.11-fold ACE2 and 0.23 ± 0.03-fold vs. 2.45 ± 0.55-fold p-SMAD, Fig. 29E) in the S1P with SB421543 treated group compared to that of S1P treated cells without SB431542.
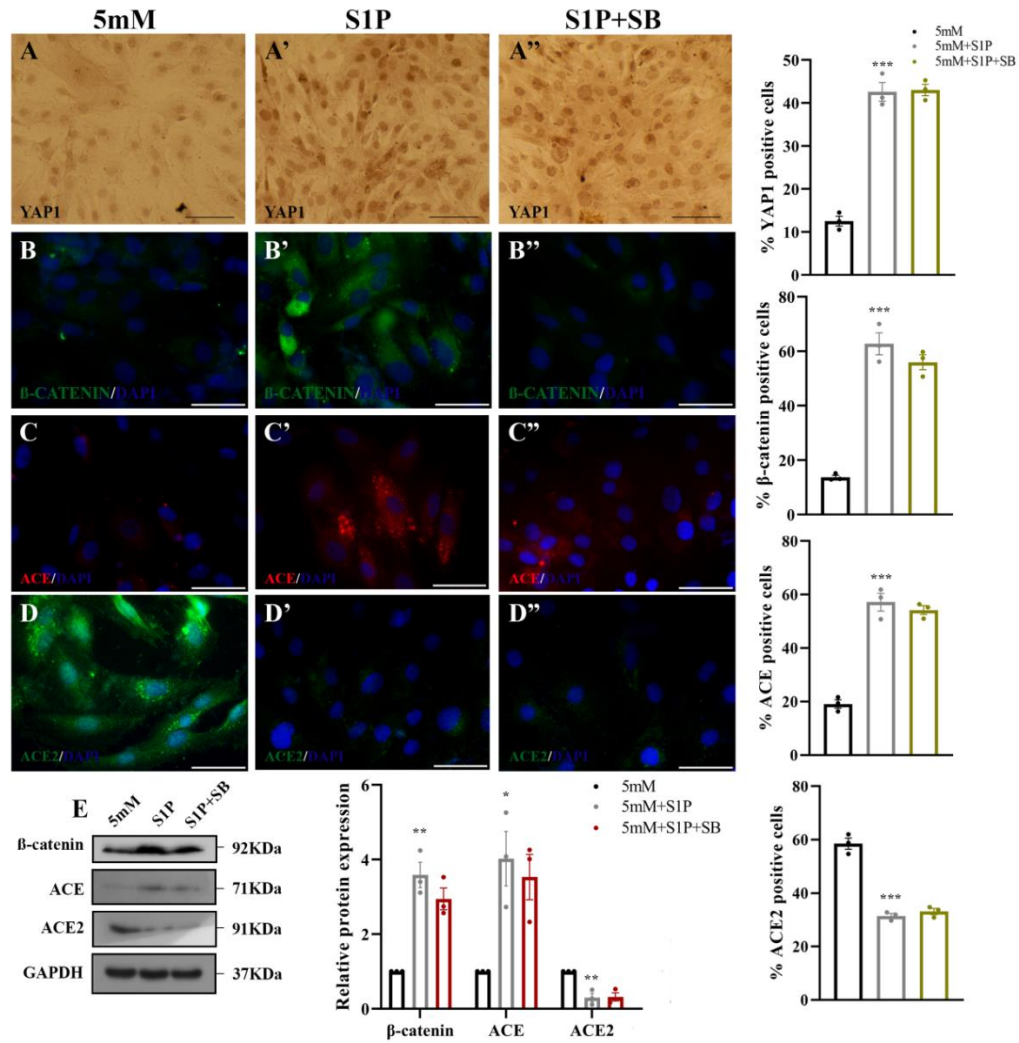
Figure 29. Inhibition of TGF-β pathway results in normalization of EMT activity and concomitant reduced fibrotic remodelling. A-A''. Immunofluorescence images of COL1 antibody shows significantly upregulated expression under S1P treatment, which is observed to be significantly reduced following SB431542 (SB) treatment. **B-B''.** IF data of FN antibody showing significantly upregulated expression in S1P treated NG cell group to that of untreated NG cells. FN staining was observed to be significantly lower in the S1P+SB group to that of S1P treated cells without SB. **C-C''.** In the IF images, E-cad expression was observed to be significantly lower in the S1P treated NG cells compared to NG cells without S1P, which was found to be significantly lower following SB treatment. **D-D''.** N-cad immunostaining results show increased expression in the S1P treated cells compared to NG cells without S1P. In the S1P+SB cells N-cad expression was observed to be significantly reduced compared to S1P treated cells without SB. **E-E''.** TGF-β1 expression was observed to be significantly upregulated following S1P treatment compared to NG cells without S1P treatment. In the SB treated S1P pre-treatment cells, this upregulation was inhibited compared to S1P treated cells without SB. **F-F''.** Picrosirius red staining showed increased collagen deposition in the S1P treated cells compared to NG cells without S1P. Collagen deposition is observed to be significantly reduced following SB treatment compared to the S1P treated cells without SB. Scale bar represents 20μM. **G.** Western blot data shows significant increase in the expression of p-SMAD2/3 in the H9c2 cells which were observed to be significantly reduced following SB431542 mediated TGF-β inhibition. Statistical significance was calculated by one way ANOVA. *, p< 0.05; **, p<0.01; ***, p<0.0001 between 5 mM+S1P and 5 mM groups. ##, p<0.01; ### p<0.0001 between 5 mM + S1P+SB431542 and 5 mM+S1P groups. n=3. Scale bar represents 50μm.

In the S1P treated group, SB431542 mediated TGF-β inhibition promoted E-cad expression (51.44 ± 2%, Fig. 30C'') compared to the group without SB431542 treatment (25.83 ± 1.16%, Fig. 30C'). Likewise, SB431542 treatment resulted in reduced N-cad level (36.37 ± 0.95%, Fig. 30D'') in the S1P group compared to S1P treated cells without TGF-β inhibition (54.61 ± 2.23%, Fig. 30D'). Immunostaining for COL1 antibody in the experimental groups showed while YAP1 activation with S1P resulted in overexpression of the fibrotic marker (56.93 ± 3.02%, Fig. 30A') compared to the NG treated cells (16.62 ± 1.37%, Fig. 30A), this was further ameliorated with SB431542 mediated TGFβ inhibition (34.62 ± 2.19%, Fig. 30A''). FN expression in the immunofluorescence data also showed significantly increased expression in the S1P treated 5mM group (10.26 ± 1.07-fold, Fig. 30B') with reduction in expression in the S1P+SB+5mM group (2.67 ± 0.25-fold, Fig. 30B'') to that observed in the S1P+5mM group (10.26 ± 1.07-fold, Fig. 30B'). Collagen deposition in the picrosirius staining data was observed to be significantly increased in the 5mM+S1P group (2.6 ± 0.46-fold, Fig. 30F') which was reduced in S1P treated cells with SB431542 pre-treatment (1.39 ± 0.09-fold, Fig. 30F'') compared to S1P treated cells without SB431542 (2.6 ± 0.46-fold, Fig. 30F). Thus, indicating TGF-β to be a critical mediator of YAP1-β-catenin-RAS signaling in promoting cardiomyocyte EMT and fibrotic remodelling under hyperglycemic stress.
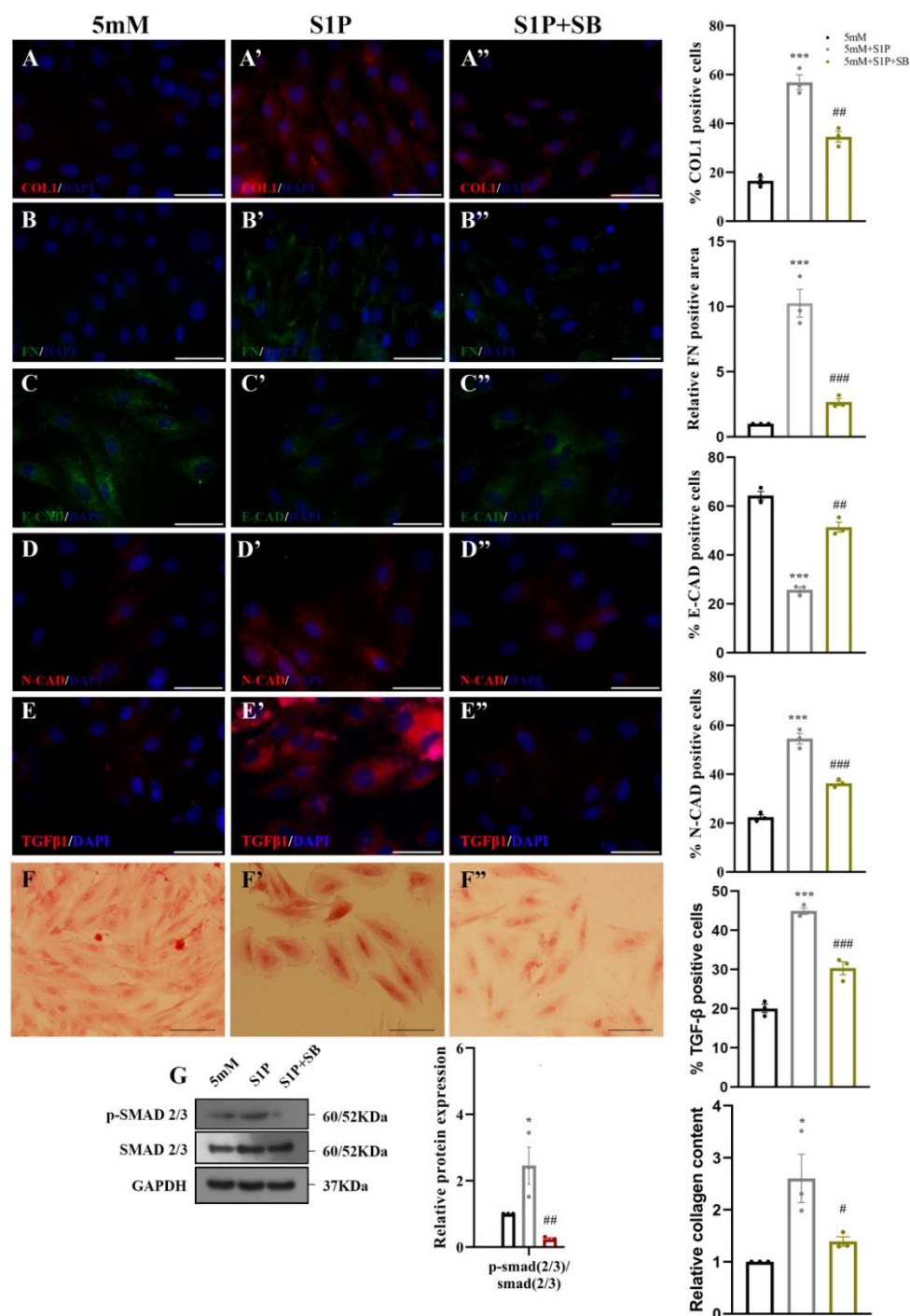
Figure 30. YAP1 regulates TGF-β pathway in hyperglycemic cardiomyopathy through β-catenin-ACE/ACE2 activity. A-A". YAP1 immunostaining images indicating upregulated expression in the S1P treated cells to that of NG group. In the SB treated HG cells there was no significant change observed in the YAP1 expression compared to HG cells without SB treatment. Scale bar represents 20µM. **B-B".** β-catenin IF images showing upregulated expression following S1P treatment to that of untreated NG cells. SB treatment in the S1P treated cells had no significant effect on the β-catenin expression compared to only S1P treated cells **C-C".** IF images of ACE antibody showing upregulated expression in the S1P treated cells compared to cells without S1P. S1P+SB group had no significant changes in the expression of ACE compared to S1P treated cells without SB. **D-D".** ACE2 immunostaining images show significantly reduced expression in the S1P treated NG cells compared to NG cells without S1P. Significantly upregulated expression of ACE2 was observed in S1P+SB cells compared to only S1P treated cells. **G.** Western blot data shows no significant changes

was observed in the expression of β-catenin, ACE and ACE2 expression in the S1P+SB treatment group compared to the S1P treated group. Statistical significance was calculated by one way ANOVA. *, $p < 0.05$; ***, $p < 0.0001$ between 5 mM+S1P and 5 mM groups. #, $p < 0.05$; ### $p < 0.0001$ between 5 mM + S1P+SB431542 and 5 mM+S1P groups. n=3. Scale bar represents 50μm.

4.B.8 ACE2 upregulation results in improved cardiac remodelling in hyperglycemic stressed cardiomyocyte

Finally, as ACE2 upregulation in our study has been observed to be associated with lowering of fibrotic markers and reduced EMT phenotypes; to further assess the beneficial function of ACE2, we have externally induced ACE2 expression in hyperglycemic H9c2 cells with its activator resorcinolnapthlein (Res) following standardization (Fig. 31A). The standardized dose of Res i.e 20 μM for 24 h resulted in (6.55 ± 0.99-fold) increase in *ace2* expression in real time PCR analysis; and (80.13 ± 1.58%, Fig. 31B' vs. 27.3 ± 3.32%, Fig. 31B) increase in the IF staining images. The cells treated with Res were further subjected to immunostaining analyses for the EMT and fibrosis markers. The immunostaining images with E–cad antibody showed significantly stabilized expression in the ACE2 upregulated group (86.04 ± 1.42%, Fig. 31F') compared to the HG group without ACE2 activation (22.41 ± 1.09%, Fig. 31F). This simultaneously showed significantly reduced N- cadherin expression in the Res treated group (24.36 ± 1.41%, Fig. 31G') to the control group (53.59 ± 1.36%, Fig. 31G). ACE2 activation was followed by significant reduction in the expression of COL1 (25.42 ± 1.75%, Fig. 31C' vs. 62.53 ± 1.53%, Fig. 31C) and FN (0.32 ± 0.06-fold, Fig. 31D', 31D) in the Res treated hyperglycemic H9c2 cells compared to the HG cells without res. In the immunofluorescence data with TGF-β1 antibody staining we have observed significantly reduced expression (18.05 ± 1.82%, Fig. 31E') in the res treated HG H9c2 cells over HG acclimatized cells with Res treatment (70.93 ± 2.36%, Fig. 31E). The expression of p-SMAD2/3 was significantly reduced (Fig. 31H) following Res treatment in cardiomyocyte cells compared to cells without Res treatment. Altogether these results indicate Res mediated ACE2 upregulation significantly alleviates EMT mediated fibrotic remodelling in the cardiac cells. Thus, the study demonstrates that in hyperglycemic stress, YAP1 promotes β-catenin/ACE/ACE2/TGF-β signaling in the induction of fibrosis through EMT like process and ACE2 upregulation can significantly protect heart from hyperglycemic stress induced cardiac remodelling.
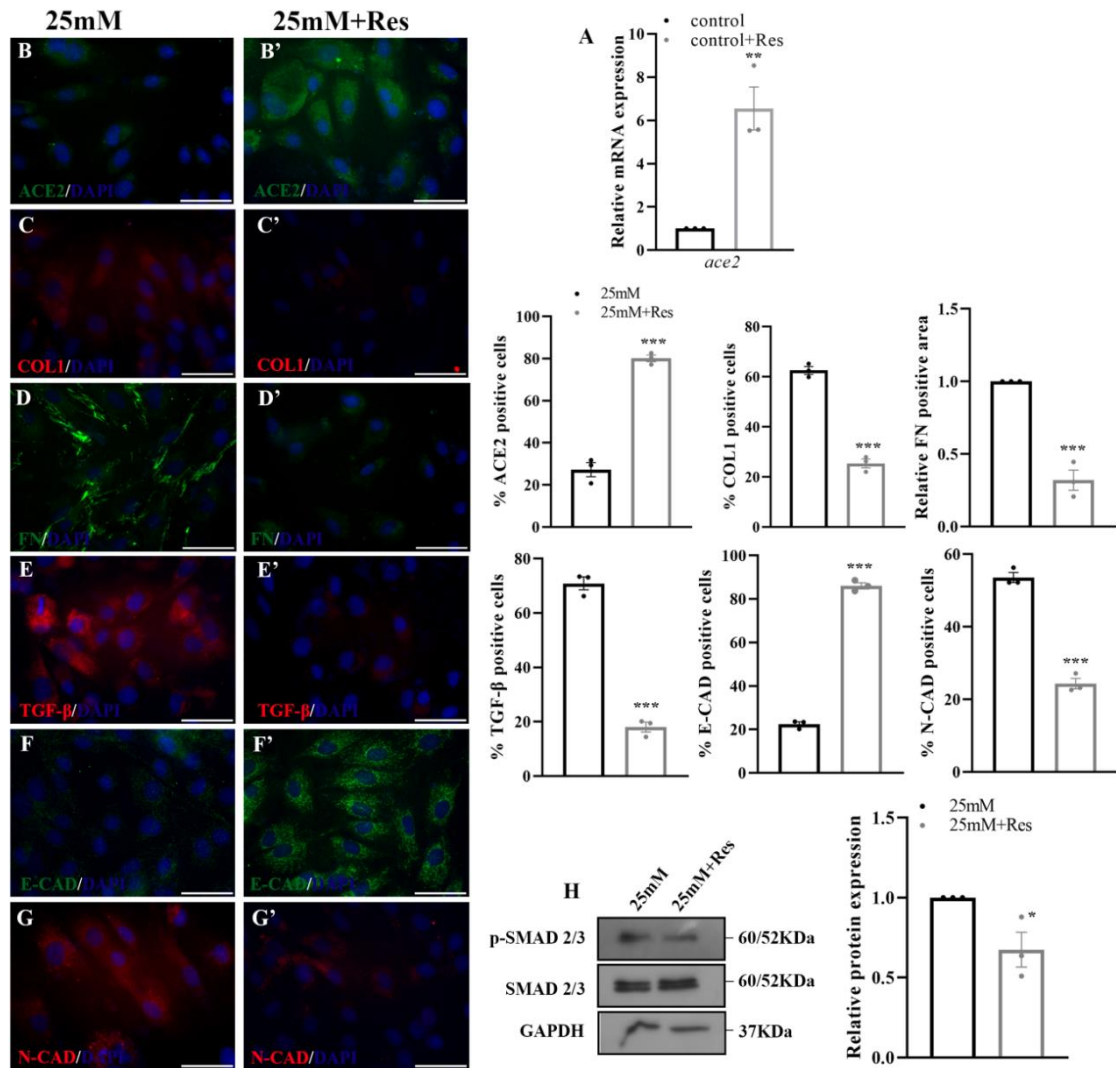
Figure 31. ACE2 upregulation results in improved cardiac remodelling in hyperglycemic stressed cardiomyocyte. A. Relative m-RNA expression of ace2 following Resorcinol treatment at 20μM for 24 hrs. **B-B'.** Immunofluorescence images of ACE2 antibody show significantly upregulated expression in the Res treated H9c2 cells compared to the HG cells without Res. **C-C'.** COL1 immunostaining results showing significantly reduced expression in the Res treated HG cells compared to the HG cells without Res. **D-D'.** IF data of FN staining reveals reduced expression in the Res treated group compared to HG group. **E-E'.** TGF-β1 antibody staining images showing the Res treated group have significantly downregulated expression in the Res treated HG cells compared to HG cells without Res. **F-F'.** Immunostaining images of E cad antibody show significant increase in the E-cad expression in the HG+Res groups compared to the HG cells. **G-G'.** IF staining images of N-cad antibody showing reduced expression in the Res pre-treated HG cells to that of HG cells without Res treatment. **H.** Western blot data showing reduced p-SMAD2/3 expression in the Res treatment group compared to the HG group without Res treatment. Corresponding graph shows relative p-SMAD2/3 expression in the experimental groups. Statistical significance was calculated by Students' t-test. *, p< 0.05; **, p<0.01; ***, p<0.0001 between 25 mM and 25 mM+Res groups. n=3. Scale bar represents 50μm.

4. B.9 Chapter Discussion:

Diabetes is currently considered as the most common metabolic disorder posing increasing health issues globally. High glucose stress often results in chronic disorders of heart, lungs and kidney among others(Dillmann 2019; Boudina and Abel 2010). Often cardiac diseases like hypertrophy and fibrosis in diabetic patients lead to an increasing rate of heart failure(Jia et al. 2019; Frustaci et al. 2000). Even with advancement in the clinical treatment, control of diabetic cardiomyopathy still requires an extensive understanding at the molecular level. Our study focuses on identifying the molecular players underlying hyperglycemia stressed cardiac tissue leading to disease pathogenesis. Previously, we have reported hyperglycemia to promote reactivation of fetal genes like YAP1 and FOXM1 in cardiomyocytes to promote hypertrophy(Mondal et al. 2022). In this study we aim to understand more on the role of YAP1 in cardiac pathogenesis especially in the induction of cardiac fibrotic remodelling.

The hippo pathway plays a crucial role in early cardiac development, but in the adult organ it wanes off to a basal level(Jun Wang et al. 2018). Various reports have so far suggested that tissue injury or stress condition results in aberrant activation of YAP1, the main regulatory molecule of the pathway that causes worsening of the structural and functional integrity of the cell (Liu et al. 2015; Xu et al. 2020). However, the detailed role of YAP1 in cardiac fibrosis induction in diabetic organs still remains unknown. In our study we have observed high blood glucose level induces YAP1 expression in the CF cells along with increased collagen-I and fibronectin expression in the ECM. High glucose also resulted in increased epithelial to mesenchymal transition (EMT) in cardiac cells (Fig. 22).

EMT is the process in which epithelial cells lose their basal polarity to transform into the more plastic mesenchymal cells. This is a process that acts in embryogenesis, wound healing and sometimes in pathological remodelling of organ fibrosis and cancer metastasis(Lamouille, Xu, and Derynck 2014; Kalluri and Weinberg 2009). In cardiac cells, one study reported the occurrence of EMT process, however it did not elucidate the detailed molecular mechanism involved in the process(Ouyang et al. 2016). Here, we have reported YAP1 to have some role in EMT induction.

In our study, we observed YAP1 overexpression, either in HG treated cells or in NG cells with S1P mediated YAP1 activation, have significantly upregulated the EMT process with increased fibrotic response compared to the control groups (Fig. 23, 24 and 29). On the

contrary, YAP1 inhibition with verteporfin in the HG cells resulted in reduced EMT activity and fibrosis in the cells (Fig. 25). This led us to believe that YAP1 may promote EMT like process in fibrosis induction in hyperglycemic fibroblast and cardiomyocyte.

We have also reported that in hyperglycemic CF and H9c2 cells, activated YAP1 leads to β-catenin upregulation (Fig. 22 and 24). The interplay of hippo signalling and Wnt signalling has been well established in regulating cardiac development(Jun Wang et al. 2018). In the hyperglycemic cells VP treatment resulted in significantly reduced expression of β-catenin (Fig. 26). Now, in a follow up experiment, with β-catenin inhibitor XAV-939 treatment, we found that β-catenin inhibition is sufficient to inhibit the fibrotic activity of YAP1. In the HG treated cells, we have observed that following XAV-939 pre-treatment, there is reduction in the expression of COL1 and FN in the ECM and simultaneously reduced TGF-β and p-SMAD2/3 levels (Fig. 28). Also, β-catenin depletion in YAP1 overexpressing cells significantly normalizes EMT like activity in cardiomyocytes (Fig. 28). This confirms the fact that YAP1 and β-catenin interaction regulates EMT mediated fibrosis in cardiac cells. However as XAV-939 had little effect on the expression of YAP1, we concluded that β-catenin may work downstream to YAP1 in this signalling cascade. Moreover, the inhibition of β-catenin in H9c2 cells resulted in reduced ACE level while significantly upregulating ACE2 expression (Fig. 27).

Finally, our experimental analyses regarding TGFβ inhibition transpired a probable pathway of interaction between the molecules in cardiac cells. While we have treated NG cells with YAP1 activator S1P, it almost always resulted in upregulated β-catenin and ACE expression with declining ACE2 level (Fig. 29). There was increased fibrotic response in the cells seen in increased COL1 and FN expression level, and increased EMT process leading to pathogenesis. But, on treating S1P activated cells with TGFβ inhibitor SB431542, this resulted in improved pathological state in both CF and H9c2 cells (Fig. 30). However, the expression of YAP1, β-catenin and ACE-ACE2 remained unchanged following SB431542 treatment (Fig. 29). Hence, this was enough to conclude the fact that under hyperglycemic stress YAP1 promotes β-catenin-RAS signaling mediated upregulation of TGFβ to induce cardiac fibrotic remodelling possibly through exaggerated EMT activity.

Importantly, as part of our main objective, we further have reported here that modulating a key RAS molecule ACE2 could be beneficial in the disease outcome. Following externally

upregulating ACE2 with its activator resorcinolnapthalein, we have observed significantly reduced fibrotic activity in the cardiac cells even under hyperglycemic stress. Resorcinolnapthalein treatment resulted in increased E-cad expression in the cell whereas reduced N-cad expression indicating ACE2 elevation also hindered the excessive EMT activity in hyperglycemic stress (Fig. 31). Importantly, in recent clinical practices ACE inhibitors are frequently used as anti-hypertensive drugs that help with controlling cardiac hypertrophy in diabetic patients(Strauss, Hall, and Narkiewicz 2021; "ACE Inhibitors vs. Beta Blockers: What Do They Do? - GoodRx" n.d.). ACE blockers are preferred to β-blockers in diabetic patients as β-blockers are known to lower heartbeats in diabetic patients masking the symptoms of glycemic fluctuations(Strauss, Hall, and Narkiewicz 2021; "ACE Inhibitors vs. Beta Blockers: What Do They Do? - GoodRx" n.d.). However, even ACE inhibitors can cause significant side effects thus requiring more insight into alternative approaches("ACE Inhibitors vs. Beta Blockers: What Do They Do? - GoodRx" n.d.). Our study not only demonstrated use of ACE2 as a counteractive therapeutic option to increased ACE activity, but also reported ACE2 to specifically address diabetic cardiac remodelling.

In conclusion, our study has reported that under hyperglycemic stress, activated YAP1-β catenin exert opposing effects on RAS signalling molecule ACE and ACE2. While ACE is upregulated, prominent downregulation of ACE2 leads to activation of the pro-fibrotic TGF-β pathway and EMT induction. This molecular event in the hyperglycemic stress plays a critical role in promoting fibrotic remodelling of cardiac cells. This study will not only help in understanding the basic molecular interplay in the pathogenesis of hyperglycemia mediated cardiac hypertrophy and fibrosis, but will also help in better therapeutics in future.
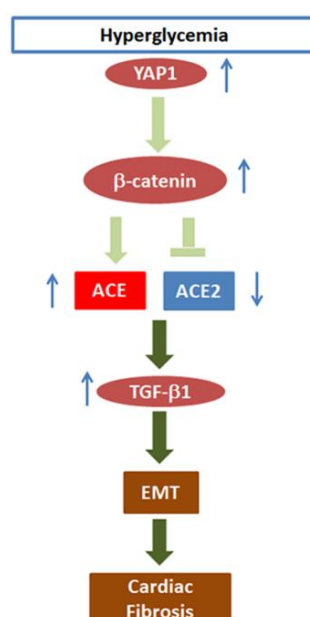
Figure 32. Schematic representation of signaling network of YAP1 regulated cardiac fibrosis induction in hyperglycemic stress. Hyperglycemia induced overexpression of cardiac YAP1 upregulates β-catenin expression that further increases the RAS mediator ACE expression while significantly reducing the ACE2 level in cardiac cells. The collective effect of increased ACE activity and reduction in beneficial molecule ACE2 leads to increased TGF-β/SMAD2-3 signaling thereby leading to exacerbated EMT-like process and fibrotic response.

CHAPTER 4.C

YAP1 promotes hyperglycemia induced β-catenin/TGF-β Signaling mediated dysregulation in cardiac EMT and fibrosis

4. C.1 Chapter Overview:

Cardiac fibrosis very commonly affects people suffering from diabetes leading to increased mortality rate globally. In the cardiac tissue fibrosis is initiated as a reparative response to increased cell death under pathological stress such as high blood sugar, coronary artery disease among others. Cardiac fibrosis is indicated by excessive collagen and other extracellular matrix deposition in the myocardial interstitium following cardiac injury or stress resulting in stiffening of cardiac muscle and loss of pumping capability eventually leading to heart failure. There are two main type of cardiac fibrosis namely, 1. Reactive Interstitial fibrosis (RIF) and 2. Replacement fibrosis (RF) (Tian, An, and Niu 2017). RIF occurs in response to increased pressure-volume loads in the cases of hypertension, ischemia, hyperglycemia, or ageing. It is characterized by increased collagen deposition without cardiomyocyte loss and an increased interstitial compartment volume without any associated changes in myocyte volume(Tian, An, and Niu 2017; Weber et al. 1989). Whereas, RF occurs as a result of signals released from dying cardiomyocyte that activates cardiac fibroblasts and elicits fibrotic tissue remodelling(Psarras et al. 2019; Biernacka, Dobaczewski, and Frangogiannis 2011). Emerging studies also reported other cell type such as cardiac macrophage and lymphocyte to also release mediators of cardiac fibroblast activation under pathological stress conditions(Biernacka, Dobaczewski, and Frangogiannis 2011). Therefore, in cardiac biology, the interaction of different cell population and their signaling interaction in regulating structural homeostasis and tissue remodelling have drawn significant attention over the recent years.

In our study, we have observed hyperglycemic stress results in significant fibrotic remodelling in diabetic cardiac tissue along with cardiac hypertrophy. Further, we have observed hyperglycemia to induce EMT-like process and activation of TGF-β pro fibrotic signaling in the cardiomyocyte H9c2 cells subjected to hyperglycemic condition. This alteration was found to be associated with increased fibrotic response in the H9c2 cells evident from significantly upregulated expression of fibrotic markers like COL1 and Fibronectin. Further, to assess the effect of hyperglycemia on cardiac fibroblast activation we have subjected adult rat primary cardiac fibroblast cells to varying glycemic conditions and observed a similar upregulation of EMT-like process and associated fibrotic remodelling. A similar alteration in the molecular signature of YAP1, β-catenin and ACE-ACE2 was evident in the CF cells also. Therefore, it can be speculated that there may be a signaling crosstalk or some form of association between the two major subpopulations of cardiac cells, that is cardiac fibroblast and cardiomyocyte contributing to the overall degenerative structural

changes in cardiac tissues. **In the following chapter we have investigated the effect of hyperglycemia stress on CF to have a preliminary observation on EMT associated fibrotic response under hyperglycemic stress and the role of YAP1-β-catenin activation in mediating fibrotic remodelling.**

4.C.2 High Glucose induced overexpression of YAP1-β-catenin in cardiac fibroblast cells results in aberrant RAS signaling and EMT mediated fibrotic remodelling

To observe the effect of fibrosis induction under hyperglycemic stress, we have treated adult rat primary cardiac fibroblast (CF) cells with high glucose (25mM) containing DMEM media for 48 hours. In the cells treated with high glucose (HG) we have observed significantly upregulated expression of fibrotic marker COL1 and FN. Immunofluorescence staining with collagen 1 (COL1) antibody showed increased expression in the HG treated cells (51.41 ± 1.87%, Fig. 33A') compared to that of normal glucose (NG) treated cells (14.49 ± 1.52%, Fig. 33A). FN expression in the immunofluorescence study also revealed increased staining (2.16 ± 0.16-fold, Fig. 33B') in the hyperglycemic CF cells to that of normoglycemic CF cells (Fig. 33B). At the molecular level, pro-fibrotic pathway mediator TGF-β1 expression was observed to be significantly increased in the HG treated fibroblast cells (51.35 ± 3.82%, Supplemental Figure 33E') compared to control cells (16.48 ± 3.77%, Fig. 33E) indicating increased fibrotic response in the cardiac cells following high glucose treatment. In addition, protein expression of TGF-β1 and its downstream target p-SMAD2/3 activity were observed to be significantly increased (3.7±0.59-fold, Fig. 33F) in the HG treated cells compared to control cells.

Furthermore, cardiac fibroblast cells under hyperglycemic condition showed epithelial to mesenchymal transition (EMT) which was found to be significantly upregulated compared to that of cells maintained in normal glucose condition. EMT, known to play an important role in wound healing and fibrosis induction, was hence speculated to play some role in the hyperglycmia mediated fibrosis induction in the cardiac cells. Cardiac fibroblast exposed to high glucose showed significantly lower expression of E-cadherin (23.05 ± 0.96%, Fig. 33C') to that of NG treated cells (63.22 ± 2.4%, Fig. 33C) with a concomitant increased expression of N-cadherin in hyperglycemic cells (53.32 ± 3.73%, Fig. 33D') compared to normal cells (20.19 ± 3.12%, Fig. 33D) indicating the induction of the EMT process. Altogether these scenarios point to an EMT associated fibrotic remodelling in cardiac cells upon induction of hyperglycemis stress.
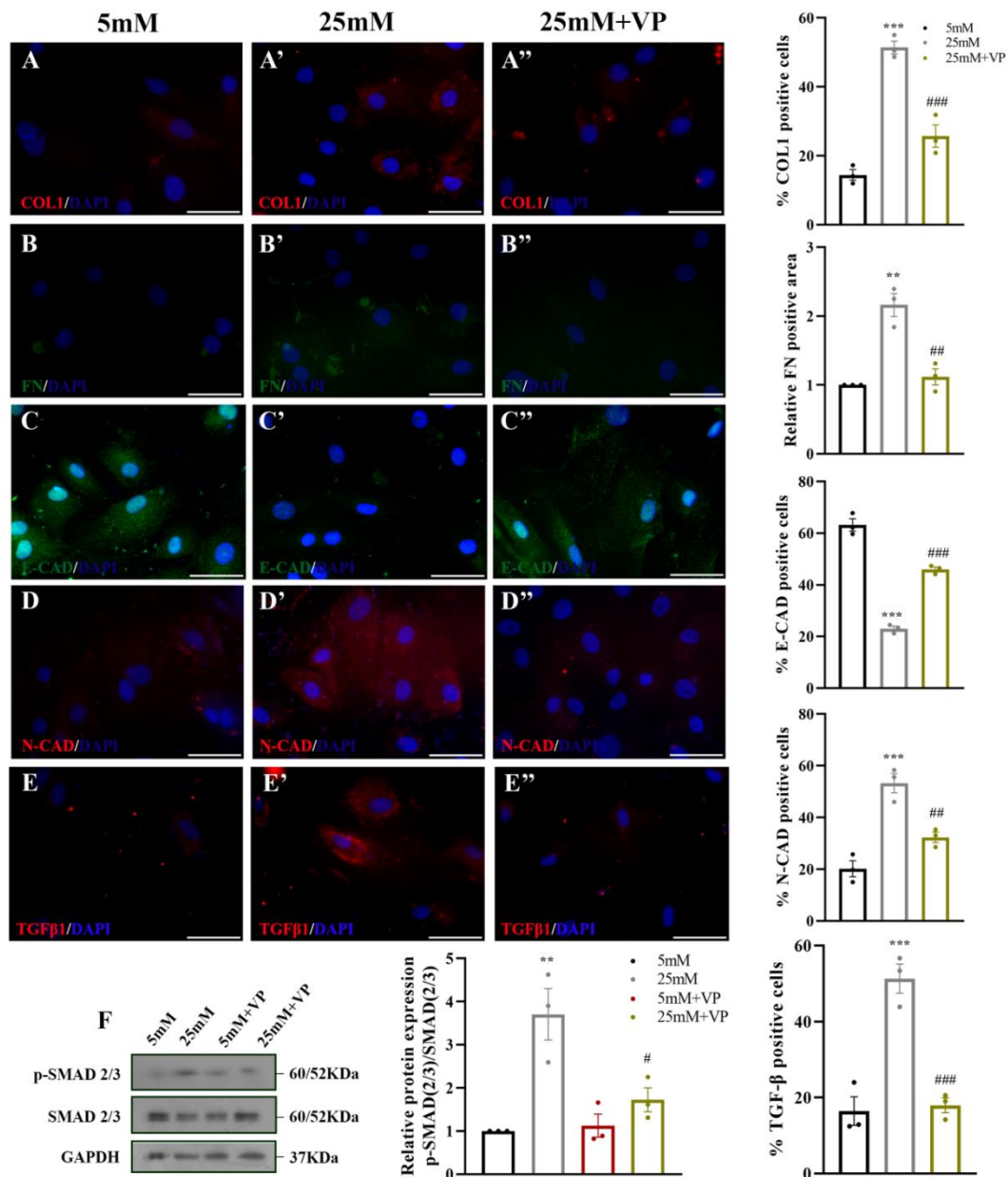
Figure 33. High Glucose induces EMT mediated fibrotic remodelling in primary adult rat cardiac fibroblast cells. A-A''. Immunostaining for fibrosis marker COL1 shows increased COL1 deposition in the HG treated CF cells compared to NG cells which is further reduced in the verteporfin (VP) treated group. **B-B''.** Fibronectin (FN) immunostaining images showing increased FN deposition in the ECM in cells treated with HG compared to cells maintained in NG. In the VP treated CF cells ECM was observed to have reduced expression of FN. **C-C''.** IF images of E-cad show significantly reduced expression in the HG treated cells, which is increased in the VP treated groups. **D-D''.** Immunostaining images of N-cad antibody showing significantly upregulated expression in the HG groups compared to the NG group. In the VP treated groups significantly reduced expression in the treated cells was observed compared to the untreated HG cells indicating EMT induction in the CF cells under HG condition. **E-E''.** TGF-β1 immunostaining images shows increased expression in the HG groups which is reduced in the VP treated group. **F.** Western blot data shows enhanced SMAD2/3 activity in the HG treated VP cells compared to CF cells maintained in NG. p-SMAD2/3 expression was again observed to be lower in the VP treated groups compared to the untreated cells. Statistical significance was calculated by one way ANOVA. **, $p<0.01$; ***, $p<0.0001$ between 25 mM and 5 mM groups. #, $p<0.05$; ##, $p<0.01$; ### $p<0.0001$ between 25 mM + VP and 25 mM groups. n=3. Scale bar in E-F represents 50μm.

In the hyperglycemic cardiomyocyte, upregulated YAP1 expression has previously been reported to play a crucial role in hypertrophy induction(Mondal et al. 2022). Importantly, in the cardiac tissue, recent researches have indicated cardiomyocyte and cardiac fibroblast among other cell types, to interact in mediating postnatal cardiac development(Uscategui Calderon, Gonzalez, and Yutzey 2023), therefore necessitating to look further into the activity of YAP1 also in the cardiac fibroblast cells. Similarly, in the cardiac fibroblast cells treated with HG, YAP1 was observed to have a significantly increased expression ($54.04 \pm 1.89\%$, Fig. 34A') compared to the normal glucose treated cells ($15.78 \pm 0.69\%$, Fig. 34A).

Our previous study showed that YAP1 inhibition in cardiomyocyte cells resulted in significantly improved hypertrophic phenotype under pathological stress(Mondal et al. 2022), we have performed similar YAP1 inhibition in the cardiac fibroblast cells with verteporfin (VP) to examine the effect of YAP1 in cardiac fibrotic remodeling. YAP1 inhibition resulted in rescue of the EMT process as evident from reduced N-cadherin expression ($32.33 \pm 2\%$ vs. $53.32 \pm 3.73\%$, Fig. 33D'', 33D') with improved E-cadherin expression ($46 \pm 0.95\%$ vs. $23.05 \pm 0.96\%$, Fig. 33C'', 33C') in the hyperglycemic cells as opposed to hyperglycemic cells without inhibitor. Along with this, VP pre-treatment significantly resulted in the reduced expression of fibrotic marker COL1 ($25.72 \pm 3.23\%$ vs. $51.41 \pm 1.87\%$, Fig. 33A'', 33A') and FN (1.11 ± 0.11-fold vs. 2.16 ± 0.16-fold, Fig. 33B'', 33B') in the extracellular matrix (ECM) compared to the HG treated cells without VP treatment.

In the developing heart, hippo signaling has been earlier reported to crosstalk with Wnt signaling through YAP-βcatenin interaction in restricting cardiomyocyte proliferation(Heallen et al. 2011). However, the impact of β-catenin activation in adult tissue especially in the context of cardiac pathogenesis following hyperglycemic stress is not well known. In the preliminary study, we observed a significantly upregulated expression of β-catenin in HG treated CF cells ($60.19 \pm 2.58\%$, Fig. 34B') compared to NG treated cells ($10.92 \pm 0.8\%$, Fig. 34B) from the immunofluorescence staining result. β-catenin expression was reduced following YAP1 inhibition ($25.58 \pm 2.02\%$, Fig. 34B'') compared to HG treated CF cells without VP inhibitor ($60.19 \pm 2.58\%$, Fig. 34B'). This indicates YAP1 activates β-catenin in CF cells. Moreover, immunofluorescence data for ACE and ACE2 antibody revealed increased ACE expression in the HG conditioned cells ($59.06 \pm 1.65\%$, Fig. 34C') over NG conditioned cells ($13.52 \pm 1.17\%$, Fig. 34C) while reduced expression of ACE2 was observed in the hyperglycemic cells ($23.43 \pm 0.88\%$, Fig. 34D') to that of normal cells (50.66

± 2.78%, Fig. 34D). YAP1 inhibition with VP results in significant inhibition of ACE expression in the HG treated CF cells (26.83 ± 2.3%, Fig. 34C'') compared to HG cells without VP (59.06 ± 1.65%, Fig. 34C'), while, significantly upregulating ACE2 expression (45.47 ± 2.27%, Fig. 34D'') compared to the untreated cells (23.43 ± 0.88%, fig, 34D'). This suggests a regulatory role of YAP1 on the expression of β-catenin, ACE and ACE2. Downregulating YAP1 expression can reduce ACE activity and simultaneously increase ACE2 activity to reduce EMT and fibrosis under pathological stress in cardiac cells.
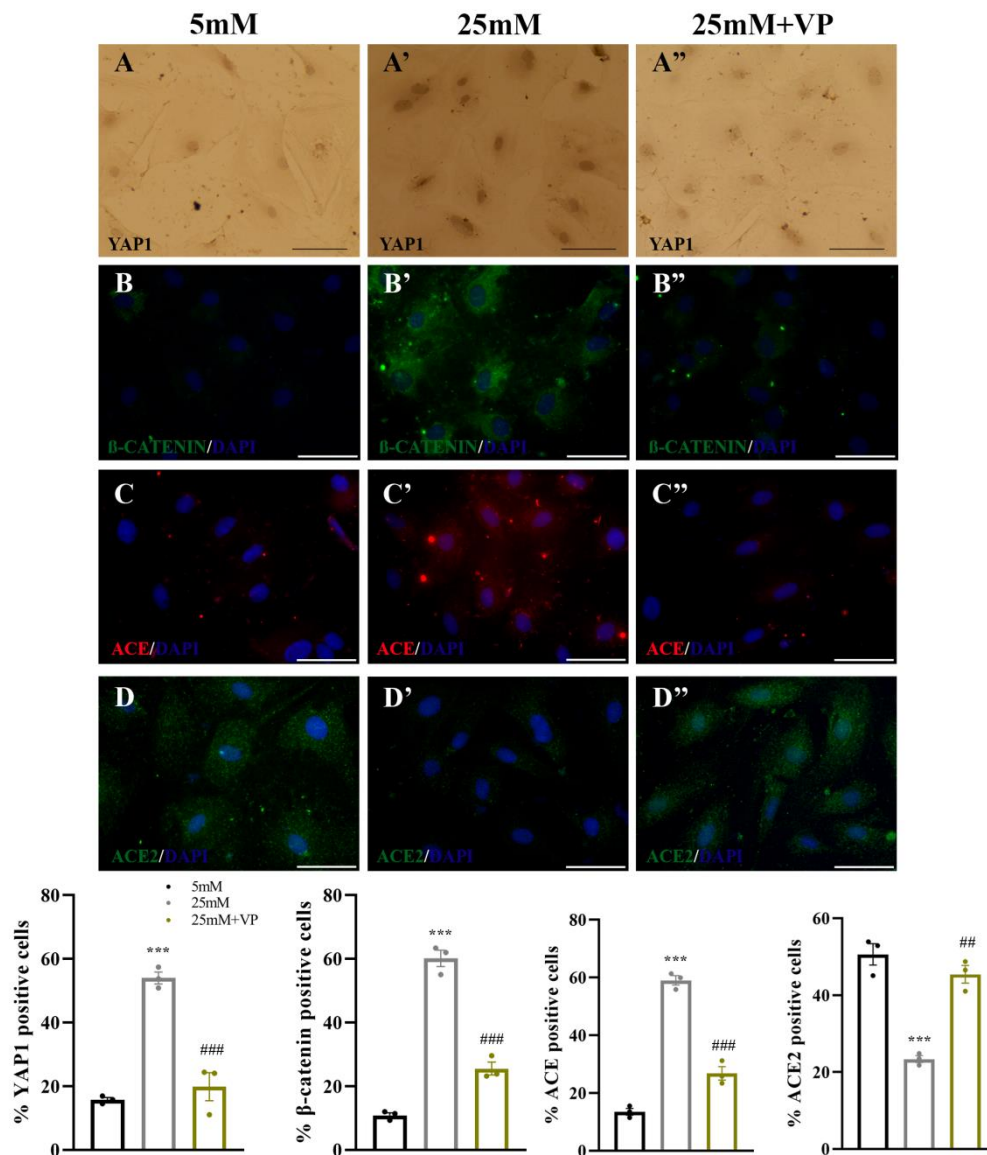
Figure 34. Hyperglycemia mediated overexpression of YAP1-βcatenin in cardiac fibroblast cells results in aberrant RAS signaling in EMT mediated fibrotic remodelling. A-A''. Immunofluorescence images of YAP1 antibody showing significantly increased expression of YAP1 in the HG treated cells compared to the NG treated cells. VP treatment in the HG cells resulted in significant downregulation of YAP1. Scale bar represents 20μM. **B-B''.** β-catenin IF images showing significant increased expression under HG treatment compared to NG cells. VP treatment resulted in significant reduction of β-catenin compared to HG cells without VP . **C-C''.** IF images of ACE antibody staining

revealed significantly increased expression in HG CF cells to that of NG cells. Significantly lower expression was observed in the VP pre-treated HG cells compared to HG cells. **D-D''.** ACE2 IF staining images showing increased ACE2 expression under HG compared to the NG group which was reduced in the VP treated HG cells. Statistical significance was calculated by one way ANOVA. ***, $p < 0.0001$ between 25 mM and 5 mM groups. ### $p < 0.0001$ between 25 mM + VP and 25 mM groups. n=3. Scale bar in C-E represents 50μm.

4.C.3 YAP1/ACE-ACE2 signaling mediated fibrosis induction in cardiac cell is dependent on TGF-β1 activity

In order to determine the effect of constitutive activation of YAP1 on hyperglycemia induced EMT mediated fibrosis in CF cells, we have incubated the cells under NG condition in presence of YAP activator, S1P (Mondal et al. 2022). In this study, we have observed that there is an increased β-catenin expression in the S1P treated normoglycemic cells (78.01 ± 1.5%, Fig. 35B') as opposed to NG treated cells without YAP1 activator (19.94 ± 2.26 %, Fig. 35B). YAP1 activation also, resulted in significant upregulation of ACE expression in CF cells (73.16 ± 2.48%, Fig. 35C') compared to NG cells without activator (20.94 ± 2.25%, Fig. 35C). ACE2 on the other hand was found to have significantly downregulated expression following YAP1 activation even under normoglycemic condition (30.21 ± 2.6%, Fig. 35D') compared to NG cells without YAP1 activation (70.81 ± 1.57%, Fig. 35D). Furthermore, immunostaining was performed against TGF-β1 to determine the effect of YAP1 activation on the fibrotic responses in S1P treated NG CF cells. We have observed the high level of TGF-β1 expression in the S1P treated NG CF cells (59.9 ± 1.44%, Fig. 36E') compared to NG cells without YAP1 activation (18.63 ± 1.24%, Fig. 36E). TGF-β1 upregulation in the S1P treated cells significantly increased the phosphorylation of its downstream signalling molecule, SMAD2/3 activity to lead to an increased fibrotic response in the CF cells (2.91 ± 0.31-fold, Fig. 36F). As a result, the expression of COL1 (64.78 ± 1.81% vs. 18.93 ± 1.89%, Fig. 36A', 36A) and FN (4.95 ± 0.86-fold, Fig. 36B', 36B), two important ECM proteins, were found to be significantly higher in the S1P treated cells compared to the untreated cells. In the S1P treated cells, EMT activation was evident from the immunostaining expression data of the marker molecules E-cad and N-cad. While the epithelial marker E-cad had significantly lower expression observed in the S1P+5mM group (29.17 ± 5.79%, Fig. 36C') compared to 5mM without S1P (70.42 ± 1.78%, Fig. 36C), N-cad had markedly increased expression following S1P treatment (66.13 ± 2.7%, Fig. 36D) compared to control cells (24.06 ± 2.48%, Fig. 36D) confirming YAP1 to be instrumental in the induction of EMT mediated fibrosis in the cardiac cells.
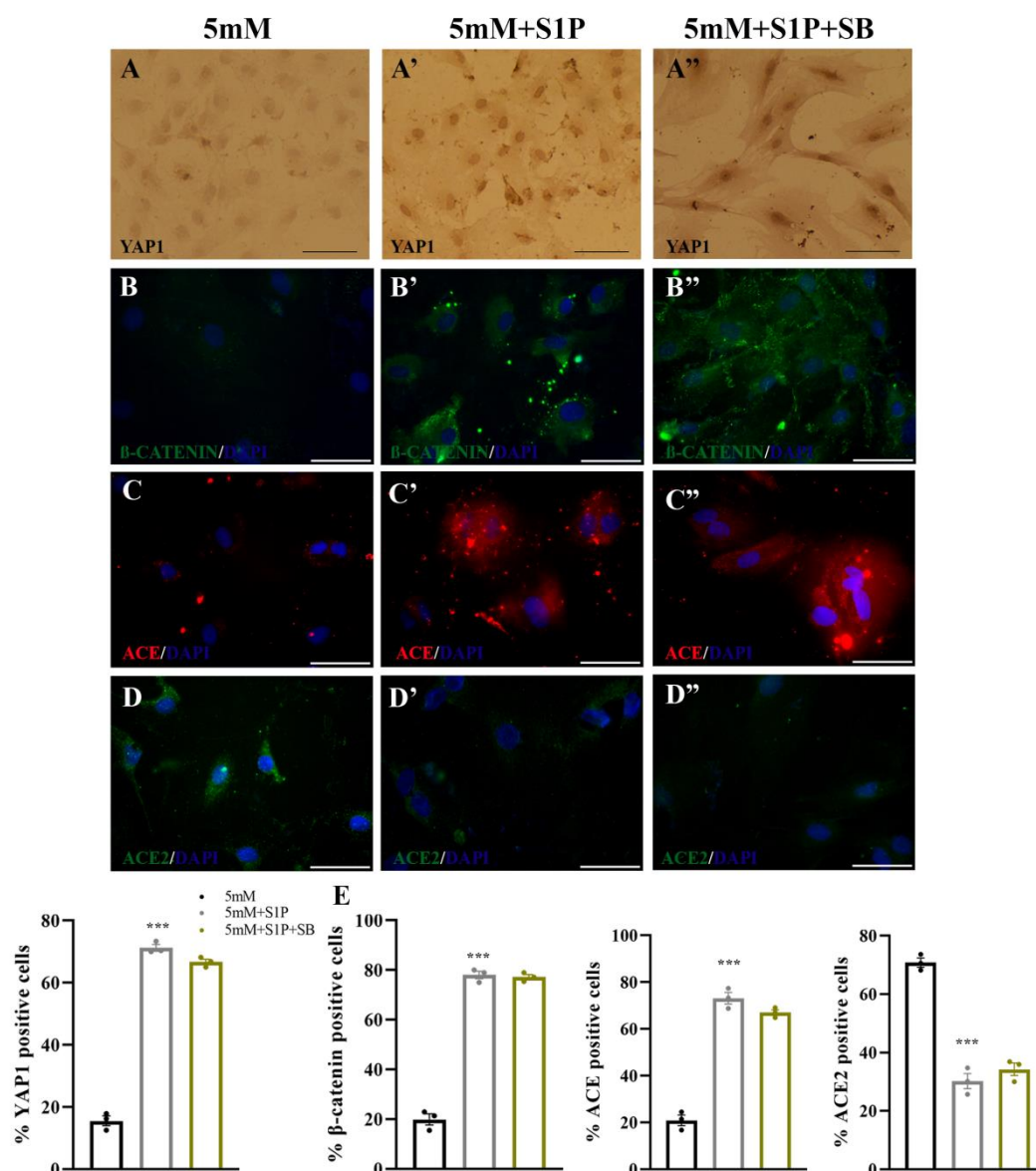
Figure 35. YAP1 regulated ACE-ACE2 expression leads to cardiac fibrosis in the TGF-β pathway. A-A''. Immunostaining images of YAP1 antibody staining in the experimental groups, showing increased expression in the HG treated groups (A') compared to NG treated cells (A) which is reduced following VP treatment (A''). Scale bar represents 20μM. **B-B''.** Immunofluorescence staining data of β-catenin antibody shows upregulated expression in the HG treatment group (B') over NG treated cells (B). The expression of β-catenin is ameliorated in the HG treated cells with VP pre-treatment (B''). **C-C''.** S1P treatment in the 5mM cells (C') resulted in significantly upregulated expression of ACE in the IF staining data with respect to the 5mM without S1P treated cells (C). SB431542 treatment in the S1P+5mM cells (C'') is observed to have significantly reduced ACE expression to that of cells without SB (C'). **D-D''.** ACE2 IF images showing significantly reduced expression in the S1P+5mM cells (D') to that of 5mM cells without S1P (D). In the SB treated cells (D'') ACE2 expression was again observed to be significantly upregulated compared to that of S1P+5mM cells (D'). Statistical significance was calculated by one way ANOVA. **, p<0.01; ***, p<0.0001 between 5 mM+S1P and 5 mM groups. #, p< 0.05; ##, p<0.01; ### p<0.0001 between 5 mM + S1P+SB431542 and 5 mM+S1P groups. n=3. Scale bar in E-F represents 50μm.

Next, to understand the role of YAP1 and β-catenin to regulate the EMT mediated fibrosis induction in cardiac cell is dependent on TGF-β1 activity; we have subjected S1P treated cells with TGF-β1 inhibitor SB431542. SB431542 pre-treatment in the HG treated cells resulted in significant inhibition of TGF-β1 expression seen in the immunofluorescence data (14.99 ± 1.86% vs. 59.9 ± 1.44%, Fig. 36E'', 36E'), along with reduced SMAD2/3 activity (0.93 ± 0.09-fold vs. 2.91 ± 0.31-fold, Fig. 36F) compared to HG treated cells without SB431542. Interestingly, no significant changes were observed in the expression of either YAP1 (66.67 ± 0.91% vs. 71.25 ± 1.06%, Fig. 35A'', 35A') or β-catenin (77.2 ± 1.02% vs. 78.01 ± 1.5%, Fig. 35B'', 35B') following TGF-β inhibition compared to the S1P treated cells without TGF-β inhibitor. No significant changes in the ACE (67.03 ± 1.21% vs. 73.16 ± 2.48%, Fig. 35C'', 35C') and ACE2 (34.32 ± 2.14% vs. 30.21 ± 2.6%, Fig. 35D'', 35D') expression was observed following TGF-β1 inhibition compared to the S1P treated cells without TGF-β inhibition. These data suggests that the regulation of YAP 1 and β-catenin on ACE- ACE2 molecule in CF cells to be upstream of TGF-β-SMAD 2/3 activity.

Very interestingly, TGFβ inhibition had a profound effect on the EMT activity in the cardiac fibroblast cells under hyperglycemia. SB431542 treatment significantly resulted in E-cad expression recovery (54.19 ± 2.67%, Fig. 35C'') which was earlier observed to have significantly reduced in S1P treated condition (29.17 ± 5.79%, Fig. 35C'). Similarly, N-cad expression was observed to be reduced in the S1P+SB431542 treated cells (32.76 ± 1.33%, Fig. 36D'') compared to S1P group without SB431542 (66.13 ± 2.7%, Fig. 36D'). Moreover, overexpression of YAP1 results in excessive collagen (33.52 ±1.45% vs. 64.78 ± 1.87%, Fig. 36A'', 36A') and fibronectin (2.27 ± 0.47-fold vs. 4.95 ± 0.86-fold, Fig 36B'', 36B') accumulation and had significant reversal following TGF-β inhibition compared to the control groups. Therefore, TGF-β can be confirmed to mediate EMT induced fibrosis in the hyperglycemia stress subjected cardiac cells.
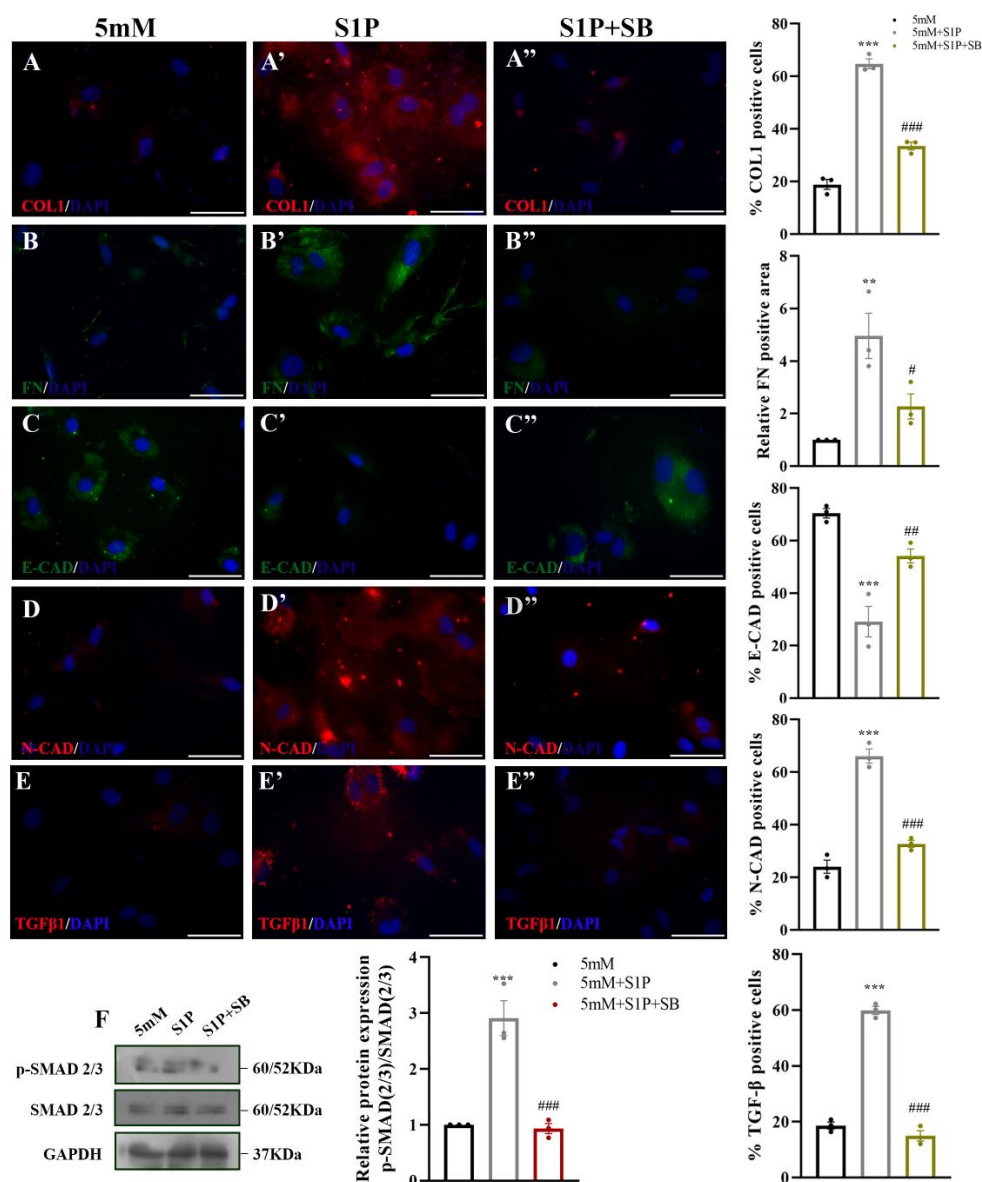
Figure 36. YAP1 regulated ACE-ACE2 expression leads to cardiac EMT mediated fibrosis in TGF-β-SMAD pathway. A-A''. Immunofluorescence images of COL1 shows significantly increased expression in the S1P treated cells (A') to that of untreated 5mM cells (A). Reduced COL1 expression was observed in the 5mM+S1P+SB431542 group (A'') compared to the S1P+5mM cells (A'). **B-B''.** Fibronectin immunostaining showing increased FN expression in the S1P treated NG cells (B') to that of NG cells (B) indicating YAP1 overexpression induced fibrosis in the CF cells. SB treatment in the S1P+5mM groups (B'') resulted in significant reduction of FN staining compared to that of NG+S1P cells (B') **C-C''.** IF data of E-cad revealed reduced expression in the S1P+5mM group (C') compared to 5mM cells (C). E-cad expression was further observed to be higher following SB treatment (C'') to that of 5mM+S1P treated cells (C'). **D-D''.** N-cad immunostaining shows S1P treatment (D') resulted in increased N-cad expression compared to the NG group (D), which was significantly reduced in the SB treated cells (D'') compared to 5mM+S1P group (D'). **E-E''.** TGF-β1 immunostaining images show increased expression in the HG CF cells (E') to NG treated cells (E) which is reduced in SB treated group (E''). **F.** western blot data of p-SMAD2/3 shows increased expression in the S1P treated 5mM CF cells over 5mM cells without S1P. The expression of p-SMAD2/3 was observed to be reduced following SB treatment. ***, p<0.0001 between 5 mM and 5 mM+S1P groups. ### p<0.0001 between 5 mM + S1P+SB431542 and 5 mM+S1P groups. n=3. Scale bar in E-F represents 50μm.

4. C.4 Chapter Discussion:

High glycemic stress in the cardiac cells, results in activation of cardiac fibroblast cells resulting in aberrant ECM remodeling and scar formation within the tissue. Cardiac fibrosis in diabetic patients is a rather common occurence contributing to high rates of heart failure incidents. However, how the hyperglycemic stress is perceived at the cellular level leading to such a pathological effect is rather not clearly understood. In our study, we have observed a high level of developmental regulatory molecules like, YAP1, β-catenin activation in the hyperglycemic CF cells (Fig. 34 and 35). This was observed to be accompanied with increased EMT induction in CF cells (Fig. 33 and 36). As we observed in H9c2 cells, TGF-β/SMAD2/3 signaling was significantly upregulated in the hyperglycemic CF cells. As, CF cells are the main mediator of cardiac fibrosis, activated fibroblast have recently been speculated to interact with cardiomyocyte directly or through paracrine mediators, ECM interactions, electrical modulators, mechanical junctions, and membrane nanotubes generating pathological response within myocytes, in the diseased heart(Pellman, Zhang, and Sheikh 2016). In the fibrotic heart, similar upregulation of YAP1, β-catenin alongwith pro fibrotic TGF-β signaling hints a probable interaction between the two cell populations in conjuring a fibrotic response in the myocyte cell population. The differential expression of ACE-ACE2 by YAP1-βcatenin brings about the pathological EMT-like process in both the cell population leading to structural and functional damage of myocardium. Suppression of the high level of YAP1 or β-catenin in CF or H9c2 cells in high glucose condition ameliorates fibrotic remodeling of cardiac cells indicating YAP1 plays a critical role in mediating cardiac fibrosis in hyperglycemia stressed cardiac tissue (Fig. 33 and 35). ACE, acting downstream to YAP1-β-catenin pathway, mediates the patholgical EMT and and fibrosis while its counterpart ACE2 negates the activity YAP1, β-catenin to stop TGFβ-SMAD signaling, thereby alleviating EMT and associated fibrosis (Fig. 34 and 36). In our study, ACE2 has been proved to be exceedingly beneficial in cardiac pathophysiology, esp in diabetic cardiomyopathy (Fig. 34 and 36). Further, our study highlights a probable interaction between cardiac fibroblast cells and cardiomyocytes in disease induction, which can further be extended in co culture study to specifically understand the mode of interaction. This may help in better understanding of the disease and development of better therapeutics in future.

CONCLUSION

Cardiac disease is one of the most common complications associated with diabetes. Cardiac hypertrophy and fibrosis often lead to structural and functional abnormalities leading to risks of heart failure. Several regulatory molecules related to major signaling pathways have been found to overexpress in different tissues during diabetes which show a very low level of expression in non-diabetic condition. YAP1 and FOXM1 are recently being reported to play an important role in various hypertrophic and fibrotic disorders. But, very limited information is still known regarding their roles in cardiomyopathies especially in the context of diabetes and hyperglycemic stress. YAP1 is known to be associated with AKT- GSK3β signaling that is one of the important regulatory pathways in glucose and lipid metabolism. On the other hand, the expression of FOXM1 has been found to be significantly upregulated in adult lung tissue with induction of fibrosis but little is known about their role in cardiac diseases. In our study, YAP1 and FOXM1 have been found to overexpress in cardiac tissue under hyperglycemic condition leading to cardiomyocyte hypertrophy and increased fibrotic response. Further YAP1 inhibition has resulted in a reduced expression of FOXM1 pointing to a possible association of YAP1 and FOXM1 in high glucose-stressed cardiomyocytes. As a mechanism we have found that YAP1 undergoes reduced ser127 phosphorylation as well as extensive O-GlcNAcylation mediated activation under hyperglycemia. Upregulated YAP1 further acts through increased AKT phosphorylation causing inhibition of GSK3β that in turn results in increased FOXM1 expression, leading to cardiomyocyte hypertrophy and fibrosis.

Further, diabetes induced activated renin angiotensin system has been reported to play a critical role in mediating cardiac hypertrophy and fibrosis. While Angiotensin-II promotes cardiomyocyte hypertrophy and fibrotic damage, various blockers of angiotensin converting enzyme (ACE) that help in production of Ang-II are used clinically to reduce the progression of myopathy. Recently discovered analogue of ACE, ACE2, has been reported to be beneficial in reducing the effect of RAS driven pathologies. In the first phase of our study, we have reported YAP1 to play a crucial role in the pathogenesis of diabetes induced cardiac remodelling. Further, in this study, we have reported YAP1 modulates the RAS signalling pathway by inducing ACE and inhibiting ACE2 activity to augment cardiomyocyte hypertrophy and fibrosis in hyperglycemic condition. Furthermore, we have also reported that hyperglycemic stress results in EMT induction in the cardiac cells promoting cardiac fibrosis. Moreover, we have observed YAP1 regulates ACE-ACE2 activity through a β-catenin and further it acts through TGF-β pro fibrotic pathway in cardiac cells. This study also suggests that there could be interactions among the different cell populations of cardiac tissue mainly,

cardiac fibroblast and cardiomyocyte in cardiac pathophysiology. This can further be extensively studied in future, with co-culturing of the cell populations to identify the precise interplay between the cellular groups.

Moreover, the primary goal of this study was to identify the key molecular players in disease induction, which can be modulated or targeted to improve cardiac function clinically with minimum side effects. In our study we have reported FOXM1 and ACE2 as two molecules that can be used in future as drug targets in controlling diabetic cardiomyopathy.

BIBLIOGRAPHY

"19.1 Heart Anatomy - Anatomy and Physiology | OpenStax." n.d. Accessed January 8, 2023. https://openstax.org/books/anatomy-and-physiology/pages/19-1-heart-anatomy.

Abe, Taiki, Ryota Shizu, Takamitsu Sasaki, Yuki Shimizu, Takuomi Hosaka, Susumu Kodama, Atsushi Matsuzawa, and Kouichi YOSHINARI. 2019. "Functional Interaction between PXR and YAP in Xenobiotic-Dependent Liver Hypertrophy and Drug Metabolism." *Journal of Pharmacology and Experimental Therapeutics* 371 (3): 590–601. https://doi.org/10.1124/JPET.119.258632.

Abylkassov, Ramazan, and Yingqiu Xie. 2016. "Role of Yes-Associated Protein in Cancer : An Update (Review)," no. 7: 2277–82. https://doi.org/10.3892/ol.2016.4955.

"ACE Inhibitors vs. Beta Blockers: What Do They Do? - GoodRx." n.d. Accessed September 19, 2023. https://www.goodrx.com/conditions/hypertension/ace-inhibitors-vs-beta-blockers-how-do-they-work.

Acevedo, J. 2014. "Multimodal Image Registration for the Characterization of the Hypertrophic Cardiomyopathy and the Cardiac Asynchronism. (Intégration d'images Multimodales Pour La Caractérisation de Cardiomyopathies Hypertrophiques et d'asynchronismes Cardiaques)."

AL, Gartel. 2008. "FoxM1 Inhibitors as Potential Anticancer Drugs." *Expert Opinion on Therapeutic Targets* 12 (6): 663–65. https://doi.org/10.1517/14728222.12.6.663.

"Arterial Hypertension: Benefits and Limitations of Treatment." n.d. Accessed September 1, 2023. https://www.escardio.org/Journals/E-Journal-of-Cardiology-Practice/Volume-13/arterial-hypertension-benefits-and-limitations-of-treatment.

Balli, David, Vladimir Ustiyan, Yufang Zhang, I. Ching Wang, Alex J. Masino, Xiaomeng Ren, Jeffrey A. Whitsett, Vladimir V. Kalinichenko, and Tanya V. Kalin. 2013. "Foxm1 Transcription Factor Is Required for Lung Fibrosis and Epithelial-to-Mesenchymal Transition." *The EMBO Journal* 32 (2): 231–44. https://doi.org/10.1038/EMBOJ.2012.336.

"Beta Blockers and Diabetes | Orlando | UCF Health." n.d. Accessed September 1, 2023. https://ucfhealth.com/our-services/endocrinology/beta-blockers-and-diabetes/.

Biernacka, Anna, Marcin Dobaczewski, and Nikolaos G. Frangogiannis. 2011. "TGF-β Signaling in Fibrosis." *Growth Factors (Chur, Switzerland)* 29 (5): 196. https://doi.org/10.3109/08977194.2011.595714.

Bolte, Craig, Yufang Zhang, I. Ching Wang, Tanya V. Kalin, Jeffrey D. Molkentin, and

Vladimir V. Kalinichenko. 2011. "Expression of Foxm1 Transcription Factor in Cardiomyocytes Is Required for Myocardial Development." *PLoS ONE* 6 (7). https://doi.org/10.1371/journal.pone.0022217.

Boudina, Sihem, and Evan Dale Abel. 2010. "Diabetic Cardiomyopathy, Causes and Effects." *Reviews in Endocrine & Metabolic Disorders* 11 (1): 31. https://doi.org/10.1007/S11154-010-9131-7.

"Cardiomyopathy | Cdc.Gov." n.d. Accessed January 8, 2023. https://www.cdc.gov/heartdisease/cardiomyopathy.htm.

"Cardiovascular Disease - Ventricular Dysfunction, Heart Failure, Treatment | Britannica." n.d. Accessed October 4, 2023. https://www.britannica.com/science/cardiovascular-disease/Ventricular-dysfunction-in-heart-failure.

Chakraborty, Santanu, Arunima Sengupta, and Katherine E Yutzey. 2013a. "Journal of Molecular and Cellular Cardiology Tbx20 Promotes Cardiomyocyte Proliferation and Persistence of Fetal Characteristics in Adult Mouse Hearts" 62: 203–13.

———. 2013b. "Tbx20 Promotes Cardiomyocyte Proliferation and Persistence of Fetal Characteristics in Adult Mouse Hearts Journal of Molecular and Cellular Cardiology Tbx20 Promotes Cardiomyocyte Proliferation and Persistence of Fetal Characteristics in Adult Mouse Heart." *Journal of Molecular and Cellular Cardiology* 62 (May 2014): 203–13. https://doi.org/10.1016/j.yjmcc.2013.05.018.

Chen, Yaohui, Yu Li, Jianfei Xue, Aihua Gong, Guanzhen Yu, Aidong Zhou, Kangyu Lin, et al. 2016. "Wnt-induced Deubiquitination FoxM1 Ensures Nucleus B-catenin Transactivation." *The EMBO Journal* 35 (6): 668–84. https://doi.org/10.15252/embj.201592810.

Dillmann, Wolfgang H. 2019. "Diabetic Cardiomyopathy." *Circulation Research* 124 (8): 1160–62. https://doi.org/10.1161/CIRCRESAHA.118.314665.

Du, Linna, Chungang Liu, Meiyu Teng, Qingfan Meng, Jiahui Lu, Yulin Zhou, Yan Liu, Yingkun Cheng, Di Wang, and Lesheng Teng. 2016. "Anti-Diabetic Activities of Paecilomyces Tenuipes N45 Extract in Alloxan-Induced Diabetic Mice." *Molecular Medicine Reports* 13 (2): 1701–8. https://doi.org/10.3892/mmr.2015.4736.

Fan, Qipeng, Qingchun Cai, and Yan Xu. 2015. "FOXM1 Is a Downstream Target of LPA and YAP Oncogenic Signaling Pathways in High Grade Serous Ovarian Cancer" 6 (29).

Fresno Vara, Juan Ángel, Enrique Casado, Javier de Castro, Paloma Cejas, Cristóbal Belda-

Iniesta, and Manuel González-Barón. 2004. "P13K/Akt Signalling Pathway and Cancer." *Cancer Treatment Reviews* 30 (2): 193–204. https://doi.org/10.1016/j.ctrv.2003.07.007.

Frustaci, Andrea, Jan Kajstura, Cristina Chimenti, Igor Jakoniuk, Annarosa Leri, Attilio Maseri, Bernardo Nadal-ginard, and Piero Anversa. 2000. "Clinical Research."

Gartel, Andrei L. 2017. "FOXM1 in Cancer : Interactions and Vulnerabilities," 8–13. https://doi.org/10.1158/0008-5472.CAN-16-3566.

Goyal, Amandeep, Austin S. Cusick, and Blair Thielemier. 2023. "ACE Inhibitors." *StatPearls*, June. https://www.ncbi.nlm.nih.gov/books/NBK430896/.

Hall, J E, and M E Hall. 2020. "Guyton and Hall Textbook of Medical Physiology E-Book," Guyton Physiology, . https://books.google.co.id/books?id=H1rrDwAAQBAJ.

Heallen, Todd, Min Zhang, Jun Wang, Margarita Bonilla-Claudio, Ela Klysik, Randy L. Johnson, and James F. Martin. 2011. "Hippo Pathway Inhibits Wnt Signaling to Restrain Cardiomyocyte Proliferation and Heart Size." *Science (New York, N.Y.)* 332 (6028): 458. https://doi.org/10.1126/SCIENCE.1199010.

Hinderer, Svenja, and Katja Schenke-Layland. 2019. "Cardiac Fibrosis – A Short Review of Causes and Therapeutic Strategies." *Advanced Drug Delivery Reviews* 146 (June): 77–82. https://doi.org/10.1016/J.ADDR.2019.05.011.

Imai, Yumiko, Keiji Kuba, Takayo Ohto-Nakanishi, and Josef M. Penninger. 2010. "Angiotensin-Converting Enzyme 2 (ACE2) in Disease Pathogenesis." *Circulation Journal* 74 (3): 405–10. https://doi.org/10.1253/CIRCJ.CJ-10-0045.

Jackman, Herbert L., Malek G. Massad, Marin Sekosan, Fulong Tan, Viktor Brovkovych, Branislav M. Marcic, and Ervin G. Erdös. 2002. "Angiotensin 1-9 and 1-7 Release in Human Heart." *Hypertension* 39 (5): 976–81. https://doi.org/10.1161/01.HYP.0000017283.67962.02.

Jia, Guanghong, Michael A. Hill, and James R. Sowers. 2018. "Diabetic Cardiomyopathy." *Circulation Research* 122 (4): 624–38. https://doi.org/10.1161/CIRCRESAHA.117.311586.

Jia, Guanghong, Michael A Hill, James R Sowers, Truman Memorial, and Veterans Hospital. 2019. "To This Clinical Entity" 122 (4): 624–38. https://doi.org/10.1161/CIRCRESAHA.117.311586.Diabetic.

Juan, Wen Chun, and Wanjin Hong. 2016. "Targeting the Hippo Signaling Pathway for Tissue Regeneration and Cancer Therapy." *Genes* 7 (9): 1–25. https://doi.org/10.3390/genes7090055.

Kalin, Tanya V., Vladimir Ustiyan, and Vladimir V. Kalinichenko. 2011. "Multiple Faces of FoxM1 Transcription Factor: Lessons from Transgenic Mouse Models." *Cell Cycle*. Taylor and Francis Inc. https://doi.org/10.4161/cc.10.3.14709.

Kalluri, Raghu, and Robert A. Weinberg. 2009. "The Basics of Epithelial-Mesenchymal Transition." *The Journal of Clinical Investigation* 119 (6): 1420. https://doi.org/10.1172/JCI39104.

Khalil, Hadi, Onur Kanisicak, Vikram Prasad, Robert N. Correll, Xing Fu, Tobias Schips, Ronald J. Vagnozzi, et al. 2017. "Fibroblast-Specific TGF-β–Smad2/3 Signaling Underlies Cardiac Fibrosis." *The Journal of Clinical Investigation* 127 (10): 3770. https://doi.org/10.1172/JCI94753.

Kohli, Shrey, Aastha Chhabra, Astha Jaiswal, Yashika Rustagi, Manish Sharma, and Vibha Rani. 2013. "Curcumin Suppresses Gelatinase B Mediated Norepinephrine Induced Stress in H9c2 Cardiomyocytes." *PLoS ONE* 8 (10): 1–12. https://doi.org/10.1371/journal.pone.0076519.

Krishnan, Anirudh, Harman Sharma, Daniel Yuan, Alexandra F. Trollope, and Lisa Chilton. 2022. "The Role of Epicardial Adipose Tissue in the Development of Atrial Fibrillation, Coronary Artery Disease and Chronic Heart Failure in the Context of Obesity and Type 2 Diabetes Mellitus: A Narrative Review." *Journal of Cardiovascular Development and Disease 2022, Vol. 9, Page 217* 9 (7): 217. https://doi.org/10.3390/JCDD9070217.

Kumar N , Abbas V, Fausto A. 2005. "Patología Estructural y Funcional." *Pediatrics* 130: 1193 – 1208. https://doi.org/10.1542/peds.2011-3808.

Kumric, Marko, Tina Ticinovic Kurir, Josip A Borovac, and Josko Bozic. 2021. "Role of Novel Biomarkers in Diabetic Cardiomyopathy." *World Journal of Diabetes* 12 (6): 685–705. https://doi.org/10.4239/wjd.v12.i6.685.

Lamouille, Samy, Jian Xu, and Rik Derynck. 2014. "Molecular Mechanisms of Epithelial–Mesenchymal Transition." *Nature Reviews. Molecular Cell Biology* 15 (3): 178. https://doi.org/10.1038/NRM3758.

Laoukili, Jamila, Matthijs R.H. Kooistra, Alexandra Brás, Jos Kauw, Ron M. Kerkhoven, Ashby Morrison, Hans Clevers, and René H. Medema. 2005. "FoxM1 Is Required for

Execution of the Mitotic Programme and Chromosome Stability." *Nature Cell Biology 2005 7:2* 7 (2): 126–36. https://doi.org/10.1038/ncb1217.

Li, Chenguang, Jie Zhang, Mei Xue, Xiaoyu Li, Fei Han, Xiangyang Liu, Linxin Xu, Yunhong Lu, and Ying Cheng. 2019. "SGLT2 Inhibition with Empagliflozin Attenuates Myocardial Oxidative Stress and Fibrosis in Diabetic Mice Heart." *Cardiovascular Diabetology*, 1–13. https://doi.org/10.1186/s12933-019-0816-2.

Li, Dongliang, Jianjian Sun, and Tao P. Zhong. 2022. "Wnt Signaling in Heart Development and Regeneration." *Current Cardiology Reports* 24 (10): 1425–38. https://doi.org/10.1007/S11886-022-01756-8/TABLES/1.

Li, Yumei, Feng Wu, Qi Tan, Mengfei Guo, Pei Ma, Xuan Wang, Shuai Zhang, Juanjuan Xu, Ping Luo, and Yang Jin. 2019. "The Multifaceted Roles of FOXM1 in Pulmonary Disease." *Cell Communication and Signaling 2019 17:1* 17 (1): 1–16. https://doi.org/10.1186/S12964-019-0347-1.

Liao, Guo-bin, Xin-zhe Li, Shuo Zeng, Cheng Liu, Shi-ming Yang, Li Yang, Chang-jiang Hu, and Jian-ying Bai. 2018. "Regulation of the Master Regulator FOXM1 in Cancer," 1–15.

Lin, Zhiqiang, Pingzhu Zhou, Alexander Von Gise, Fei Gu, Qing Ma, Jinghai Chen, Haidong Guo, Pim R.R. Van Gorp, Da Zhi Wang, and William T. Pu. 2015. "Pi3kcb Links Hippo-YAP and PI3K-AKT Signaling Pathways to Promote Cardiomyocyte Proliferation and Survival." *Circulation Research* 116 (1): 35–45. https://doi.org/10.1161/CIRCRESAHA.115.304457.

Litviňuková, Monika, Carlos Talavera-López, Henrike Maatz, Daniel Reichart, Catherine L. Worth, Eric L. Lindberg, Masatoshi Kanda, et al. 2020. "Cells of the Adult Human Heart." *Nature* 588 (7838): 466–72. https://doi.org/10.1038/s41586-020-2797-4.

Liu, Fei, David Lagares, Kyoung Moo Choi, Lauren Stopfer, Aleksandar Marinković, Vladimir Vrbanac, Clemens K. Probst, et al. 2015. "Mechanosignaling through YAP and TAZ Drives Fibroblast Activation and Fibrosis." *American Journal of Physiology - Lung Cellular and Molecular Physiology* 308 (4): L344–57. https://doi.org/10.1152/AJPLUNG.00300.2014/ASSET/IMAGES/LARGE/ZH50051566870008.JPEG.

Maruyama, Kazuaki, and Kyoko Imanaka-Yoshida. 2022. "The Pathogenesis of Cardiac Fibrosis: A Review of Recent Progress." *International Journal of Molecular Sciences*

2022, Vol. 23, Page 2617 23 (5): 2617. https://doi.org/10.3390/IJMS23052617.

Meng, Xiao Ming, David J. Nikolic-Paterson, and Hui Yao Lan. 2016. "TGF-β: The Master Regulator of Fibrosis." *Nature Reviews Nephrology 2016 12:6* 12 (6): 325–38. https://doi.org/10.1038/nrneph.2016.48.

Mia, Masum M., and Manvendra K. Singh. 2022. "New Insights into Hippo/YAP Signaling in Fibrotic Diseases." *Cells* 11 (13): 1–22. https://doi.org/10.3390/cells11132065.

Mondal, Arunima, Shreya Das, Jayeeta Samanta, Santanu Chakraborty, and Arunima sengupta. 2022. "YAP1 Induces Hyperglycemic Stress-Mediated Cardiac Hypertrophy and Fibrosis in an AKT-FOXM1 Dependent Signaling Pathway." *Archives of Biochemistry and Biophysics* 722 (June): 109198. https://doi.org/10.1016/J.ABB.2022.109198.

Mori, Jun, Liyan Zhang, Gavin Y. Oudit, and Gary D. Lopaschuk. 2013. "Impact of the Renin-Angiotensin System on Cardiac Energy Metabolism in Heart Failure." *Journal of Molecular and Cellular Cardiology* 63 (October): 98–106. https://doi.org/10.1016/J.YJMCC.2013.07.010.

Myatt, Stephen S., and Eric W.F. Lam. 2007. "The Emerging Roles of Forkhead Box (Fox) Proteins in Cancer." *Nature Reviews Cancer 2007 7:11* 7 (11): 847–59. https://doi.org/10.1038/nrc2223.

Najjar, Rami S., Arielle M. Schwartz, Brett J. Wong, Puja K. Mehta, and Rafaela G. Feresin. 2021. "Berries and Their Polyphenols as a Potential Therapy for Coronary Microvascular Dysfunction: A Mini-Review." *International Journal of Molecular Sciences* 22 (7). https://doi.org/10.3390/IJMS22073373.

Nandi, Shyam Sundar, and Paras Kumar Mishra. 2015. "Harnessing Fetal and Adult Genetic Reprograming for Therapy of Heart Disease." *Journal of Nature and Science* 1 (4). /pmc/articles/PMC4394627/.

Noguchi, Satoshi, Akira Saito, and Takahide Nagase. 2018. "YAP/TAZ Signaling as a Molecular Link between Fibrosis and Cancer." *International Journal of Molecular Sciences*. MDPI AG. https://doi.org/10.3390/ijms19113674.

Ouyang, Fan, He Huang, Mingyu Zhang, Mingxian Chen, Haobo Huang, Fang Huang, and Shenghua Zhou. 2016. "HMGB1 Induces Apoptosis and EMT in Association with Increased Autophagy Following H/R Injury in Cardiomyocytes." *International Journal of Molecular Medicine* 37 (3): 679–89.

https://doi.org/10.3892/IJMM.2016.2474/HTML.

Ozhan, Gunes, and Gilbert Weidinger. 2015. "Wnt/β-Catenin Signaling in Heart Regeneration." *Cell Regeneration* 4 (1): 4:3. https://doi.org/10.1186/s13619-015-0017-8.

Patel, Seema, Abdur Rauf, Haroon Khan, and Tareq Abu-Izneid. 2017. "Renin-Angiotensin-Aldosterone (RAAS): The Ubiquitous System for Homeostasis and Pathologies." *Biomedicine & Pharmacotherapy* 94 (October): 317–25. https://doi.org/10.1016/J.BIOPHA.2017.07.091.

Pellman, Jason, Jing Zhang, and Farah Sheikh. 2016. "Myocyte-Fibroblast Communication in Cardiac Fibrosis and Arrhythmias: Mechanisms and Model Systems." *Journal of Molecular and Cellular Cardiology* 94 (May): 22. https://doi.org/10.1016/J.YJMCC.2016.03.005.

Peltier, Joseph, Analeah O'Neill, and David V. Schaffer. 2007. "PI3K/Akt and CREB Regulate Adult Neural Hippocampal Progenitor Proliferation and Differentiation." *Developmental Neurobiology* 67 (10): 1348–61. https://doi.org/10.1002/DNEU.20506.

Penke, Loka R., Jennifer M. Speth, Vijaya L. Dommeti, Eric S. White, Ingrid L. Bergin, and Marc Peters-Golden. 2018. "FOXM1 Is a Critical Driver of Lung Fibroblast Activation and Fibrogenesis." *Journal of Clinical Investigation* 128 (6): 2389–2405. https://doi.org/10.1172/JCI87631.

Phang, Ren Jie, Rebecca H. Ritchie, Derek J. Hausenloy, Jarmon G. Lees, and Shiang Y. Lim. 2023. "Cellular Interplay between Cardiomyocytes and Non-Myocytes in Diabetic Cardiomyopathy." *Cardiovascular Research* 119 (3). https://doi.org/10.1093/CVR/CVAC049.

Porta, Camillo, Chiara Paglino, and Alessandra Mosca. 2014. "Targeting PI3K/Akt/MTOR Signaling in Cancer." *Frontiers in Oncology* 4 APR (April): 67531. https://doi.org/10.3389/FONC.2014.00064/BIBTEX.

Psarras, Stelios, Dimitris Beis, Sofia Nikouli, Mary Tsikitis, and Yassemi Capetanaki. 2019. "Three in a Box: Understanding Cardiomyocyte, Fibroblast, and Innate Immune Cell Interactions to Orchestrate Cardiac Repair Processes." *Frontiers in Cardiovascular Medicine* 6 (April): 32. https://doi.org/10.3389/FCVM.2019.00032.

Ribeiro-Oliveira, Antônio, Anelise Impeliziere Nogueira, Regina Maria Pereira, Walkiria Wingester Vilas Boas, Robson Augusta Souza dos Santos, and Ana Cristina Simões e

Silva. 2008. "The Renin–Angiotensin System and Diabetes: An Update." *Vascular Health and Risk Management* 4 (4): 787. https://doi.org/10.2147/vhrm.s1905.

Saadat, Somayeh, Mahdi Noureddini, Maryam Mahjoubin-Tehran, Sina Nazemi, Layla Shojaie, Michael Aschner, Behnaz Maleki, et al. 2021. "Pivotal Role of TGF-β/Smad Signaling in Cardiac Fibrosis: Non-Coding RNAs as Effectual Players." *Frontiers in Cardiovascular Medicine* 7 (January): 588347. https://doi.org/10.3389/FCVM.2020.588347/BIBTEX.

Samanta, Jayeeta, Arunima Mondal, Srimoyee Saha, Santanu Chakraborty, and Arunima Sengupta. 2019. "Oleic Acid Protects from Arsenic - Induced Cardiac Hypertrophy via AMPK / FoxO / NFATc3 Pathway Fetal Bovine Serum." *Cardiovascular Toxicology*. https://doi.org/10.1007/s12012-019-09550-9.

Schultze, Simon M., Brian A. Hemmings, Markus Niessen, and Oliver Tschopp. 2012. "PI3K/AKT, MAPK and AMPK Signalling: Protein Kinases in Glucose Homeostasis." *Schultze, S M; Hemmings, B A; Niessen, M; Tschopp, O (2012). PI3K/AKT, MAPK and AMPK Signalling: Protein Kinases in Glucose Homeostasis. Expert Reviews in Molecular Medicine, 14:E1.* 14 (January): e1. https://doi.org/10.1017/S1462399411002109.

Sengupta, Arunima, Vladimir V Kalinichenko, Katherine E Yutzey, and Circ Res. 2012. "FoxO and FoxM1 Transcription Factors Have Antagonistic Functions in Neonatal Cardiomyocyte Cell Cycle Withdrawal and IGF1 Gene Regulation The Online Version of This Article , along with Updated Information and Services , Is Located on the World Wide Web A." https://doi.org/10.1161/CIRCRESAHA.112.277442.

Sinha, Sonali, Nidhi Dwivedi, James Woodgett, Shixin Tao, Christianna Howard, Timothy A. Fields, Abeda Jamadar, and Reena Rao. 2020. "Glycogen Synthase Kinase-3β Inhibits Tubular Regeneration in Acute Kidney Injury by a FoxM1-Dependent Mechanism." *FASEB Journal* 34 (10): 13597–608. https://doi.org/10.1096/fj.202000526RR.

Strauss, Martin H., Alistair S. Hall, and Krzysztof Narkiewicz. 2021. "The Combination of Beta-Blockers and ACE Inhibitors Across the Spectrum of Cardiovascular Diseases." *Cardiovascular Drugs and Therapy* 37 (4): 757–70. https://doi.org/10.1007/S10557-021-07248-1/FIGURES/2.

Tang, Patrick Ming Kuen, Ying Ying Zhang, Thomas Shiu Kwong Mak, Philip Chiu Tsun Tang, Xiao Ru Huang, and Hui Yao Lan. 2018. "Transforming Growth Factor-β Signalling in Renal Fibrosis: From Smads to Non-Coding RNAs." *The Journal of*

Physiology 596 (16): 3493–3503. https://doi.org/10.1113/JP274492.

Tarbit, Emiri, Indu Singh, Jason Nigel Peart, Svetlana Bivol, and Roselyn Barbara Rose'Meyer. 2021. "Increased Release of Serotonin from Rat Primary Isolated Adult Cardiac Myofibroblasts." *Scientific Reports* 11 (1): 20376. https://doi.org/10.1038/S41598-021-99632-Y.

Tian, Jing, Xinjiang An, and Ling Niu. 2017. "Myocardial Fibrosis in Congenital and Pediatric Heart Disease." *Experimental and Therapeutic Medicine* 13 (5): 1660. https://doi.org/10.3892/ETM.2017.4224.

Trackman, Philip C., Debashree Saxena, and Manish V. Bais. 2017. "TGF-B1- and CCN2-Stimulated Sirius Red Assay for Collagen Accumulation in Cultured Cells." *Methods in Molecular Biology* 1489: 481–85. https://doi.org/10.1007/978-1-4939-6430-7_39.

Uscategui Calderon, Maria, Brittany A. Gonzalez, and Katherine E. Yutzey. 2023. "Cardiomyocyte-Fibroblast Crosstalk in the Postnatal Heart." *Frontiers in Cell and Developmental Biology* 11. https://doi.org/10.3389/FCELL.2023.1163331.

Vučković, Sofija, Rafeeh Dinani, Edgar E. Nollet, Diederik W.D. Kuster, Jan Willem Buikema, Riekelt H. Houtkooper, Miranda Nabben, Jolanda van der Velden, and Birgit Goversen. 2022. "Characterization of Cardiac Metabolism in IPSC-Derived Cardiomyocytes: Lessons from Maturation and Disease Modeling." *Stem Cell Research & Therapy* 13 (1). https://doi.org/10.1186/S13287-022-03021-9.

Wang, Jincheng, Kaili Hu, Xuanyan Cai, Bo Yang, Qiaojun He, Jiajia Wang, and Qinjie Weng. 2022. "Targeting PI3K/AKT Signaling for Treatment of Idiopathic Pulmonary Fibrosis." *Acta Pharmaceutica Sinica B* 12 (1): 18–32. https://doi.org/10.1016/J.APSB.2021.07.023.

Wang, Jun, Shijie Liu, Todd Heallen, and James F Martin. 2018. "The Hippo Pathway in the Heart :" *Nature Reviews Cardiology*. https://doi.org/10.1038/s41569-018-0063-3.

Wang, Pei, Beibei Mao, Wen Luo, Bin Wei, Wenjian Jiang, Dong Liu, Lei Song, et al. n.d. "The Alteration of Hippo/YAP Signaling in the Development of Hypertrophic Cardiomyopathy." https://doi.org/10.1007/s00395-014-0435-8.

———. 2014. "The Alteration of Hippo/YAP Signaling in the Development of Hypertrophic Cardiomyopathy." *Basic Research in Cardiology* 109 (5): 1–11. https://doi.org/10.1007/s00395-014-0435-8.

Wang, Yanhui, Qiaoling Zhou, Rong Tang, Yuyu Huang, and Ting He. 2020. "FoxM1

Inhibition Ameliorates Renal Interstitial Fibrosis by Decreasing Extracellular Matrix and Epithelial–Mesenchymal Transition." *Journal of Pharmacological Sciences* 143 (4): 281–89. https://doi.org/10.1016/J.JPHS.2020.05.007.

Weber, Karl T., Ruth Pick, Jorge E. Jalil, Joseph S. Janicki, and Eugenia P. Carroll. 1989. "Patterns of Myocardial Fibrosis." *Journal of Molecular and Cellular Cardiology* 21 Suppl 5 (SUPPL. 5): 121–31. https://doi.org/10.1016/0022-2828(89)90778-5.

Weiler, Sofia M.E., Federico Pinna, Thomas Wolf, Teresa Lutz, Aman Geldiyev, Carsten Sticht, Maria Knaub, et al. 2017. "Induction of Chromosome Instability by Activation of Yes-Associated Protein and Forkhead Box M1 in Liver Cancer." *Gastroenterology* 152 (8): 2037-2051.e22. https://doi.org/10.1053/j.gastro.2017.02.018.

Wong, Jenny S., Kristin Meliambro, Justina Ray, and Kirk N. Campbell. 2016. "Hippo Signaling in the Kidney: The Good and the Bad." *American Journal of Physiology - Renal Physiology* 311 (2): F241–48. https://doi.org/10.1152/AJPRENAL.00500.2015.

World Health Organization. 2016. "DISEASE (CVD) CRISIS Cardiovascular Disease Increasing." *World Health Organization*, no. Cvd: 2030. http://www.who.int/cardiovascular_diseases/en/.

wu, Anbiao, Lihong Zhang, Jingyang Chen, Hekai Li, Pingzhen Yang, Minsheng Chen, and Qicai Liu. 2021. "Limb-Bud and Heart (LBH) Mediates Proliferation, Fibroblast-to-Myofibroblast Transition and EMT-like Processes in Cardiac Fibroblasts." *Molecular and Cellular Biochemistry* 476 (7): 2685–2701. https://doi.org/10.1007/s11010-021-04111-7.

X, Zhang, Qiao Y, Wu Q, Chen Y, Zou S, Liu X, Zhu G, et al. 2017. "The Essential Role of YAP O-GlcNAcylation in High-Glucose-Stimulated Liver Tumorigenesis." *Nature Communications* 8 (May). https://doi.org/10.1038/NCOMMS15280.

Xie, Jiahong, Yuxin Wang, Ding Ai, Liu Yao, and Hongfeng Jiang. 2022. "The Role of the Hippo Pathway in Heart Disease." *The FEBS Journal* 289 (19): 5819–33. https://doi.org/10.1111/FEBS.16092.

Xie, Youbang, Xuefeng Shi, Kuo Sheng, Guoxiong Han, Wenqian Li, Qiangqiang Zhao, Baili Jiang, Jianming Feng, Jianping Li, and Yuhai Gu. 2019. "PI3K/Akt Signaling Transduction Pathway, Erythropoiesis and Glycolysis in Hypoxia (Review)." *Molecular Medicine Reports* 19 (2): 783–91. https://doi.org/10.3892/MMR.2018.9713/HTML.

Xin, Mei, Eric N. Olson, and Rhonda Bassel-Duby. 2013. "Mending Broken Hearts: Cardiac

Development as a Basis for Adult Heart Regeneration and Repair." *Nature Reviews Molecular Cell Biology 2013 14:8* 14 (8): 529–41. https://doi.org/10.1038/nrm3619.

Xu, Dan, Pan pan Chen, Pei qing Zheng, Fan Yin, Qian Cheng, Zhuan li Zhou, Hong yan Xie, et al. 2020. "KLF4 Initiates Sustained YAP Activation to Promote Renal Fibrosis in Mice after Ischemia-Reperfusion Kidney Injury." *Acta Pharmacologica Sinica 2020 42:3* 42 (3): 436–50. https://doi.org/10.1038/s41401-020-0463-x.

Yoshida, Tadashi, and Patrice Delafontaine. 2020. "Mechanisms of IGF-1-Mediated Regulation of Skeletal Muscle Hypertrophy and Atrophy." *Cells 2020, Vol. 9, Page 1970* 9 (9): 1970. https://doi.org/10.3390/CELLS9091970.

Zanconato, Francesca, Michelangelo Cordenonsi, and Stefano Piccolo. 2016. "Review YAP / TAZ at the Roots of Cancer."

Zhang, Nailing, Haibo Bai, Karen K David, Jixin Dong, Yonggang Zheng, Jing Cai, Marco Giovannini, Pentao Liu, Robert A Anders, and Duojia Pan. 2010. "Article The Merlin / NF2 Tumor Suppressor Functions through the YAP Oncoprotein to Regulate Tissue Homeostasis in Mammals." *Developmental Cell* 19 (1): 27–38. https://doi.org/10.1016/j.devcel.2010.06.015.

Zhang, Yuqing, De Jin, Xiaomin Kang, Rongrong Zhou, Yuting Sun, Fengmei Lian, and Xiaolin Tong. 2021. "Signaling Pathways Involved in Diabetic Renal Fibrosis." *Frontiers in Cell and Developmental Biology* 9 (July): 696542. https://doi.org/10.3389/FCELL.2021.696542/BIBTEX.

Zhao, Yue, Cong Wang, Xue Hong, Jinhua Miao, Yulin Liao, Fan Fan Hou, Lili Zhou, and Youhua Liu. 2019. "Wnt/β-Catenin Signaling Mediates Both Heart and Kidney Injury in Type 2 Cardiorenal Syndrome." *Kidney International* 95 (4): 815–29. https://doi.org/10.1016/j.kint.2018.11.021.

Zheng, Ancheng, Qishan Chen, and Li Zhang. 2022. "The Hippo-YAP Pathway in Various Cardiovascular Diseases: Focusing on the Inflammatory Response." *Frontiers in Immunology* 13 (August): 1–18. https://doi.org/10.3389/fimmu.2022.971416.

Zhou, Qi, Li Li, Bin Zhao, and Kun-liang Guan. 2015. "The Hippo Pathway in Heart Development, Regeneration, and Diseases," 1431–47. https://doi.org/10.1161/CIRCRESAHA.116.303311.

PRESENTATIONS

grf
Conferences

2019 NGBT

9th International Meeting

NextGen Genomics, Biology, BioInformatics and Technologies (NGBT) Conference

30th Sep - 2nd Oct 2019, Mumbai, India

Participation Certificate

Miss. Arunima Mondal

Participated at the 2019 NGBT Meeting

Dr. Sekar Seshagri
2019 NGBT Chair

Dr. Krishnaraj Rajalingam
2019 NGBT Co-chair

Sgrf
Conferences

2019 NGBT

9th International Meeting

NextGen Genomics, Biology, BioInformatics and Technologies (NGBT) Conference

30th Sep - 2nd Oct 2019, Mumbai, India

Poster Presentation Certificate

Miss. Arunima Mondal

Participated and presented a poster at the 2019 NGBT meeting

Dr. Sekar Seshagri
2019 NGBT Chair

Dr. Krishnaraj Rajalingam
2019 NGBT Co-chair

UGC-SAP (DRS II) Sponsored National Conference on Stress Responses and Diseases (SR&D)

06TH & 07TH MARCH, 2020

ORGANIZED BY

DEPARTMENT OF BIOCHEMISTRY AND BIOPHYSICS, UNIVERSITY OF KALYANI

This is to certify that Prof./Dr./Mr./Mrs./Ms. Arunima Mondal participated in the UGC-SAP (DRS II) sponsored National Conference on SR&D, as Invited Speaker/Presenter of an Abstract (Oral/Speed Talk/Poster) /Organiser/Participant held on 06th and 7th March, 2020 at the Department of Biochemistry and Biophysics, University of Kalyani, West Bengal.

Dr. Angshuman Bagchi
Joint Convener

Prof. Tapati Chakraborti
HOD, Dept. of Biochem. & Biophys.

Dr. Jishu Naskar
Joint Convener

Department of Biochemistry, University of Kashmir
NAAC Accredited A⁺

and

Indian Society Of Cell Biology

44ᵗʰ All India Cell Biology Conference and International Symposium on Molecular & Cellular Insights of Human Diseases

CERTIFICATE OF PARTICIPATION

This is to certify that Dr/Mr/Ms _Arunima Mondal_ participated/presented from _Jadavpur University_ a poster/delivered a talk in the **44ᵗʰ All India Cell Biology Conference** held at the University of Kashmir, Srinagar from September 2-3, 2022.

Dr. Shajrul Amin
Convenor

Dr. Shaida Andrabi
Organizing Secretary

Prof. Bhupendra N Singh
Secretary ISCB

CERTIFICATE

— OF PARTICIPATION —

Cardiovascular Research Convergence 2022

This is to certify that Dr./Mr./Ms.

Arunima Mondal .... has participated

in Poster Presentation in the Cardiovascular Research Convergence 2022, held on 25th June

2022 at CSIR-IICB, Kolkata.

Dr. Arun Bandyopadhyay
Chairman, CRC 2022

Dr. Partha Chakrabarti and Sanjay K Banerjee
Convenors, CRC-2022

Prof. Sandeep Seth
Chief Editor, JPCS

INTERNATIONAL SEMINAR ON

"EMERGING FIELDS OF RESEARCH IN BIOTECHNOLOGY & BIOMEDICINE"
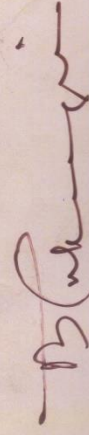
CERTIFICATE OF APPRECIATION

THIS CERTIFICATE RECOGNIZES THE CONTRIBUTION OF
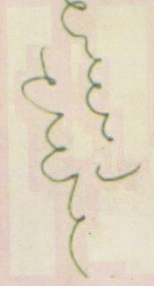
Prof/Dr./Mr./Ms./Miss _Arunima Mondal_

as Invited Speaker/Chair Person/Co-Chair Person/Evaluator/Delegate/Presenter(Oral/Poster)

In the International Seminar Jointly Organized by Dr. V. Ravi Chandran Centre for Advanced Research in Pharmaceutical Sciences, Jadavpur University, Kolkata, India & Indian Association of Pharmaceutical Scientists and Technologists (IAPST), Kolkata, India. held at Jadavpur University, Kolkata, India on 16 November 2022.

Prof.Dr.Biswajit Mukherjee
Coordinator,
Dr. V. Ravi Chandran Centre for
Advanced Research in
Pharmaceutical Sciences, Jadavpur
University, Kolkata, India.

Dr.N.Udupa
President,
Indian Association of
Pharmaceutical Scientists
and Technologists (IAPST),
Kolkata, India.

Department of Zoology, University of Calcutta

INTZOOCON 2018

an International Conference to celebrate 100 years of excellence from 1919-2019

at the

**Ramakrishna Mission Institute of Culture
& University of Calcutta (Ballygunge Campus)**

February 1-3, 2018

Certificate of appreciation

This to certify that Prof./Dr./Mr./Mrs./Ms. *Arunima Mondal*

....

participated in the International Conference as a Delegate/ Presenter of a Paper entitled ....

....

Parthiba Basu & Sagartirtha Sarkar
Jt. Secretaries

Urmi Chatterji
President

PUBLICATIONS

YAP1 induces hyperglycemic stress-mediated cardiac hypertrophy and fibrosis in an AKT-FOXM1 dependent signaling pathway

Arunima Mondal [a], Shreya Das [a], Jayeeta Samanta [a], Santanu Chakraborty [b], Arunima sengupta [a,*]

[a] *Department of Life Science and Biotechnology, Jadavpur University, Kolkata, India*
[b] *Department of Life Sciences, Presidency University, Kolkata, India*

A R T I C L E   I N F O

A B S T R A C T

Cardiac disease is one of the most common complications associated with diabetes. Cardiac hypertrophy and fibrosis often lead to structural and functional abnormalities leading to risks of heart failure. Several regulatory molecules related to major signaling pathways have been found to overexpress in different tissues during diabetes which show very low level of expression in non-diabetic condition. YAP1 and FOXM1 are recently being reported to play important role in various hypertrophic and fibrotic disorders. But, very limited information is still known regarding their roles in cardiomyopathies especially in the context of diabetes and hyperglycemic stress. YAP1 is known to be associated with AKT- GSK3β signaling that is one of the important regulatory pathways in glucose and lipid metabolism. On the other hand, the expression of FOXM1 has been found to be significantly upregulated in adult lung tissue with induction of fibrosis but little is known about their role in cardiac diseases. In our study, YAP1 and FOXM1 have been found to overexpress in cardiac tissue under hyperglycemic condition leading to cardiomyocyte hypertrophy and increased fibrotic response. Further YAP1 inhibition has resulted in a reduced expression of FOXM1 pointing to a possible association of YAP1 and FOXM1 in high glucose-stressed cardiomyocyte. As mechanism we have found that YAP1 undergoes reduced ser127 phosphorylation as well as extensive O-GlcNAcylation mediated activation under hyperglycemia. Upregulated YAP1 further acts through increased AKT phosphorylation causing inhibition of GSK3β that in turn results in increased FOXM1 expression, leading to cardiomyocyte hypertrophy and fibrosis.

1. Introduction

Cardiac diseases are currently one of the major health issues especially in urban areas with modern lifestyle and food habits [11]. Currently, diabetes is considered as one of the leading causes of cardiac disease across the globe. This metabolic disease leads to inefficient uptake of glucose by the cells resulting in persistent high glucose content in the blood, which often leads to cardiac hypertrophy and associated fibrotic damages [7,16]. During diabetes, the continuous hyperglycemic stress to the primary contractile cells of heart, the cardiomyocyte results in increased cellular apoptosis, which in turn leads to cardiomyocyte hypertrophy and fibrosis [10,16]. Within the cells an extensive reactivation of fetal genes causes significant alteration in transcriptional activity of different important genes responsible for the pathogenesis [23,27,36].

YAP1 is an important regulatory molecule which is known to be

expressed largely during the developmental stages of various organs and subsequently its expression declines with postnatal growth. Interestingly, increased expression of YAP1 has been found in some pathologically stressed adult organs including fibrotic lung and kidney [21,30, 36]. In both human hypertrophic cardiomyopathy (HCM) patient and experimental mice, YAP1 overexpression has been shown to be associated with pathological cardiac hypertrophy [32]. Several studies have recently reported an important glucose mediated activation of YAP1, however, very little information has been known regarding the role of YAP1 in the induction of cardiac hypertrophy especially in the context of diabetic cardiomyopathy [34]. In our study we have reported that hyperglycemia increases O-GlcNAcylation of YAP1 as well as inhibits phosphorylation at ser127 thereby dramatically increasing the YAP1 level within the cardiomyocyte. Along with this we observed a high level of FOXM1 that correlated with cardiomyocyte hypertrophy and fibrosis induction.

---

* Corresponding author.
  E-mail address: arunima.sengupta@jadavpuruniversity.in (A. sengupta).

FOXM1 transcription factor has been reported in several studies to play an important role in early heart development [4,18]. But, FOXM1 expression has been shown to get reduced with progression to adult stages of heart development [3]. In adult lung and liver, FOXM1 upregulation has been shown to be associated with injury response and tissue repair [17]. Recent studies have reported that overexpression of FOXM1, causes lung fibrosis [22]. *In vitro,* hyperglycemia upregulates FOXM1 expression in adult pancreatic islet cells [13]. But, no studies so far have been carried out on the role of FOXM1 in diabetes mediated pathogenesis in adult heart. Our study focuses on the role of FOXM1 in specific disease model of diabetic cardiomyopathy. Some recent studies have shown, YAP1 regulates the expression of FOXM1 [9,33]. Therefore we can speculate an interaction between these two molecules that may play a role in the cardiac disease induction under hyperglycemic stress. But, nothing has been shown regarding the mechanistic regulation of FOXM1 in the cardiomyocyte and pathogenesis.

YAP1 is also known to be functionally associated with protein kinase B/AKT which plays an important regulatory role in glucose metabolism along with its downstream regulatory molecule GSK3β [12,14,29,35]. AKT-GSK3β signaling is activated in the cardiomyocyte following cardiac stress condition and has been known to regulate several key downstream regulatory molecules that eventually lead to the exacerbated stress response [5,25]. AKT is known to positively regulate FOXM1 expression and studies have also shown that GSK3β degrades FOXM1 protein whereas inhibition of GSK3β activity leads to FOXM1 stabilization in brain cancer cells but nothing is known regarding the role of AKT/GSK3β signaling in regulation of FOXM1 in cardiomyocyte [15,25,28].

Based on these individual reports, in the present study we have focused to observe that how the high glucose stress in diabetic cardiomyopathy condition acts at the transcriptional level to promote the prevailing pathogenic condition of cardiac hypertrophy and fibrosis through YAP1/FOXM1 signaling pathway. We have hypothesized that increased hyperglycemia-mediated YAP1 activity may induce AKT that in turn inhibits GSK3β activity to stabilize the expression of FOXM1 in the cardiomyocyte. Upon stabilization, elevated level of FOXM1 leads to increased cardiomyocyte hypertrophy and fibrosis.

2. Materials and methods

2.1. Generation of diabetic animal model

Diabetes was induced *in vivo* by injecting adult male Swiss Albino mice (8 weeks old) with alloxan at a dose of 150 mg/kg body weight intra-peritoneally [8]. The animals were starved overnight prior to injection. The control animals were injected with equal volume of 0.9% saline solution as vehicle. Mice with blood glucose >200 mg/dl maintained up to 2 weeks were taken for experimental analysis [20]. Blood glucose was periodically measured using Accu-chekR glucometer (Roche). All animals were maintained at the animal facility as per the CPCSEA guidelines. Animals were provided with standard chow feed and water ad libitum. All the experimental procedures were approved by the Institutional Ethical Committee, Presidency University (Registration PU/IAEC/SC/39), registered under "Committee for the purpose of Control and Supervision of Experiments on Laboratory Animals (CPCSEA), Ministry of Environment and forests, Govt. of India.

2.2. Heart weight body weight ratio

Heart weight to Body weight ratio was calculated in mg/g (milligram/gram) unit after successfully harvesting heart tissue after sacrificing the animals.

2.3. Immunohistological analyses

Heart tissues from different animal groups were washed in PBS and fixed in 4% paraformaldehyde overnight. Tissues were embedded in paraffin and sectioned at 5 μm. For histological staining, sections were deparaffinized, rehydrated and subjected to subsequent staining procedures [24].

2.3.1. Cardiomyocyte size determination

Animal tissue sections were stained with FITC conjugated wheat germ agglutinin (WGA, #L4895, SIGMA) and nuclei were counterstained with DAPI (#D9542, SIGMA). Images were taken by Leica DFC7000T at 40x magnification across different field.Cell size were measured using ImageJ (NIH) software.

2.3.2. Fibrosis detection

Tissue samples were stained with Masson's Trichrome reagent for collagen deposition. The amount of collagen was quantified as percent fibrotic tissue area with respect to the total tissue area using ImageJ (NIH) software. The data has been represented as fold change with respect to the control group.

2.4. Immunostaining

Tissue sections were processed similarly as described previously and blocking was done with 2% BSA for 1 h at room temperature, then incubated with following primary antibodies as per experimental studies: YAP1 (1:200; #14074 Cell Signaling), FOXM1(1:100; #sc-502 Santa Cruz Biotechnology), α-SMA(1:640, #19245 Cell signaling), periostin (1:500; #ab14041, Abcam). For *in vitro* studies cells cultured on coverslips were washed with PBS and fixed using 4%PFA, blocked in 2% BSA and subsequently incubated with antibodies and DAPI nuclear staining as mentioned earlier.

2.5. Cell culture and treatments

To establish the hyperglycemic model *in vitro*, H9c2 cells were incubated in serum free and glucose free media for 24 h prior to treatment. For hyperglycemia experiment, cells were supplemented with 25 mM glucose and 5 mM glucose containing media as hyperglycemic condition and normal glycemic condition respectively. Cells were treated with activators and inhibitors for manipulation of signaling molecules as follows: YAP1 inhibitor verteporfin (1 μM, #SML0534 Sigma), FOXM1 inhibitor thiostrepton (1 μM, 24 h; #), YAP1 activator S1P (1 μM, 2 h; #S9666 SIGMA), AKT inhibitor LY294002 (10 μM, 2 h; #L9908 SIGMA). For FOXM1 activation FOXM1 recombinant protein (0.1 ng protein per ml DMEM, overnight, #H00002305–P0 Abnova) was used. The cells were maintained in DMEM media containing 10% fetal bovine serum and 1% penstrep at 37 °C incubator and 5% CO2 condition [24].

2.6. Cell size determination by phalloidin staining

Cells from different experimental groups were washed with PBS and fixed in 4% PFA. The cells were permeabilized in 2% Triton-X followed by incubation with Alexa fluor-488 tagged phalloidin (A12379, Thermo Fisher). The cells were counterstained with DAPI. Cell size was measured using ImgaeJ (NIH) software and shown as fold change with respect to the control group.

2.7. Real time PCR

RNA from cell and tissue was isolated using TRIzol reagent (Invitrogen, #15596026), quantified using Qubit 4 machine and cDNA was prepared using iScript cDNA synthesis kit (170889, BIORAD) using 1 μg of RNA from each sample. Real time PCR was performed from the cDNA samples using SsoFast EvaGreen for hypertrophy marker gene *bnp* (Brain natriuretic peptide), *β-mhc* (Beta myosin heavy chain), and fibrosis marker genes: *col1* (colagen1), *col3* (colagen3) and analysis of our target

Table 1

Primer sequence used in the PCR analyses.

Primer Gene/Accession No.		Sequence	Amplicon size (bp)	Annealing temperature (°C)
yap1(M) [NM_001171147.1]	Forward	5′-ACCCTCGTTTTGCCATGAAC-3′	172	56.5
	Reverse	5′-TTCAACCGCAGTCTCTCCTT-3′		
foxm1 (M) [NM_008021.4]	Forward	5′-AAGGCAAAGACAGGAGAGCT-3′	188	55.7
	Reverse	5′- AGGGCTCCTCAACCTTAACC-3′		
bnp (M) [NM_008726.6]	Forward	5′-AAGTCCTAGCCAGTCTCCAGA-3′	91	56.2
	Reverse	5′-GAGCTGTCTCTGGGCCATTTC-3′		
beta-mhc (M) [NM_080728.3]	Forward	5′-ACGGATGCCATACAGAGGAC-3′	340	56.1
	Reverse	5′-CCTCATAGGCGTTCTTGAGC-3′		
col1 (M) [NM_007742.4]	Forward	5′-CACCCTCAAGAGCCTGAGTC-3′	269	58
	Reverse	5′-GCTTCTTTTCCTTGGGGTTC-3′		
col3(M) NM_009930.2]	Forward	5′-ACGTGGTAGTCCTGGTGGTC-3′	287	60
	Reverse	5′-GACCTCGTGCTCCAGTTAGC-3′		
serca2 (M) [NM_001110140.3]	Forward	5′-GGGCGAGCCATCTACAACAA-3′	150	60
	Reverse	5′-TGTCACCAGATTGACCCAGAGT-3′		
beta-actin (M) [NM_007393.5]	Forward	5′-CCTCTATGCCAACACAGTGC-3′	206	56
	Reverse	5′-CCTGCTTGCTGATCCACATC-3′		
yap1(R) [NM_001394328.1]	Forward	5′-CGCTGAGTTCCGAAATCCTG-3′	234	56.1
	Reverse	5′-AGAGCAGAGCAACAGTGGAT-3′		
foxm1 (R) [NM_031633.3]	Forward	5′-ACCAATATCCAGTGGCTTGG-3′	210	54
	Reverse	5′-GCTGTTGATCGCGAACTGTA-3′		
bnp(R) [NM_031545.1]	Forward	5′- AGTCCTAGCCAGTCTCCAGA -3′	172	60
	Reverse	5′-GTCTCTCCTGGATCCGGAAG-3′		
beta-mhc(R) [NM_017240.2]	Forward	5′-CCAGTCCCGAGGTGTACTTT-3′	195	60
	Reverse	5′-TCCTCCTTCATGTTGGCCAT-3′		
col1(R) [NM_053304.1]	Forward	5′- ATCCTGCCGATGTCGCTAT-3′	207	60
	Reverse	5′- CCACAAGCGTGCTGTAGGT-3′		
col3(R) [NM_032085.1]	Forward	5′- CTGGTCCTGTTGGTCCATCT-3′	131	60
	Reverse	5′- ACCTTTGTCACCTCGTGGAC-3′		
beta-actin (R) [NM_031144.3]	Forward	5′-TCTTCCAGCCTTCCTTCCTG-3′	238	58
	Reverse	5′-CACACAGAGTACTTGCGCTC-3′		

genes: *yap1*, *foxm1* and marker gene for cardiac function: *serca2*. All the primers have been obtained from IDT and mentioned in Table 1. (M-mouse, R-rat). All the Gene expression has been normalized against *beta actin* gene expression.

2.8. Western Blot (WB) and Immunoprecipitation (IP) assay

Total protein lysates from H9c2 cells or mouse cardiac tissue were isolated using RIPA protein extraction buffer containing protease inhibitor cocktail (Puregene, GX-2811AR) and phosphatase inhibitor cocktail (Puregene, GX-1211AR). Protein was quantified by BCA protein assay kit (Puregene, GX-6410AR). The immunoblots with specific primary antibodies were incubated with HRP tagged secondary antibody (Abcam, ab97051) and developed using ClarityTM Western ECL substrate (Luminol/enhancer solution and peroxide solution, 1610182, BIORAD).

For immunoprecipitation assay, the protein lysates from tissues and cells were precleared with agarose beads (Protein A Plus agarose, #BB-PA001P, BioBharati Life Science Pvt.Ltd.) as per the supplier's protocol. The lysates were then incubated with the specified antibody overnight at 4 °C followed by incubation with agarose beads for 4 h. The proteins were finally eluted from the beads with elution buffer followed by western blotting [19].

The following primary antibodies were used in the experiment:, p-YAP (1:1000; #13008 Cell Signaling), YAP (1:1000 WB; 1:50 IP; #14074 Cell Signaling), Anti-O-Linked N-Acetylglucosamine antibody [RL2] (1:1000; ab2739, Abcam), FOXM1(1:500 #sc-502, Santa Cruz), *p*-AKT (1:1000; #9271 Cell Signaling), AKT (1:1000; #9272 Cell Signaling), *p*-GSK3β (1:1000; #9322 Cell Signaling) GSK3β (1:1000; #9315 Cell Signaling). GAPDH antibody (1:2000; #BB-AB0060 Bio-BharatiLifeScience Pvt.Ltd.) was used as loading control. The original uncropped immunoblots of the representative images have been shown in the supplemental figure (Figs. S9, S10, S11).

2.9. Statistical analysis

All the results were calculated as ±S.E.M of three independent experiments. Statistical significance were determined by Students' t-test for two groups and by one way analysis of variance (ANOVA) for multiple groups using Graphpad Prism software. Results with p value < 0.05 were considered as significant.

3. Results

3.1. Hyperglycemia induces cardiac hypertrophy and fibrosis in adult mice

To analyze the effect of hyperglycemia on cardiomyocyte, mice under experiment were injected with alloxan to mimic type II diabetic condition. From initial time-point experiment (Fig. 1A, Supplementary Figs. 1A and S1A), we observed a significant increase of blood glucose level in day1 (382 ± 17.58 mg/dl) after injecting the mice with alloxan at a dose of 150 mg/kg body weight compared to the day 0 (126 ± 9.04 mg/dl) group. The data also suggests the blood glucose level stays at significantly higher level up to 2 weeks (1 week: 340 ± 19.53 mg/dl; 2 week: 208.5 ± 12.93 mg/dl) compared to the day 0 group. The mice with high glucose level kept for 2 weeks were used as diabetic cardiomyopathy (DCM) group. The DCM group showed significant increase in heart weight to body weight ratio (5.78 ± 0.21 mg/g) compared to the control group (4.66 ± 0.06 mg/g) (Figs. 1B and S1B). The fixed tissue sections stained with WGA antibody showed significant enlargement of the cardiac cells in the DCM group (2.6 ± 0.22-fold) compared to the control group (Figs. 1C and S1C), indicating cardiac hypertrophy occurrence in hyperglycemic stress condition. Massons' trichrome staining showed significantly increased collagen deposition in the DCM group (4.37 ± 0.24 fold) compared to the control heart sections (Figs. 1D and S1D) which confirmed increased fibrotic activity in cardiac environment stressed due to hyperglycemic response.
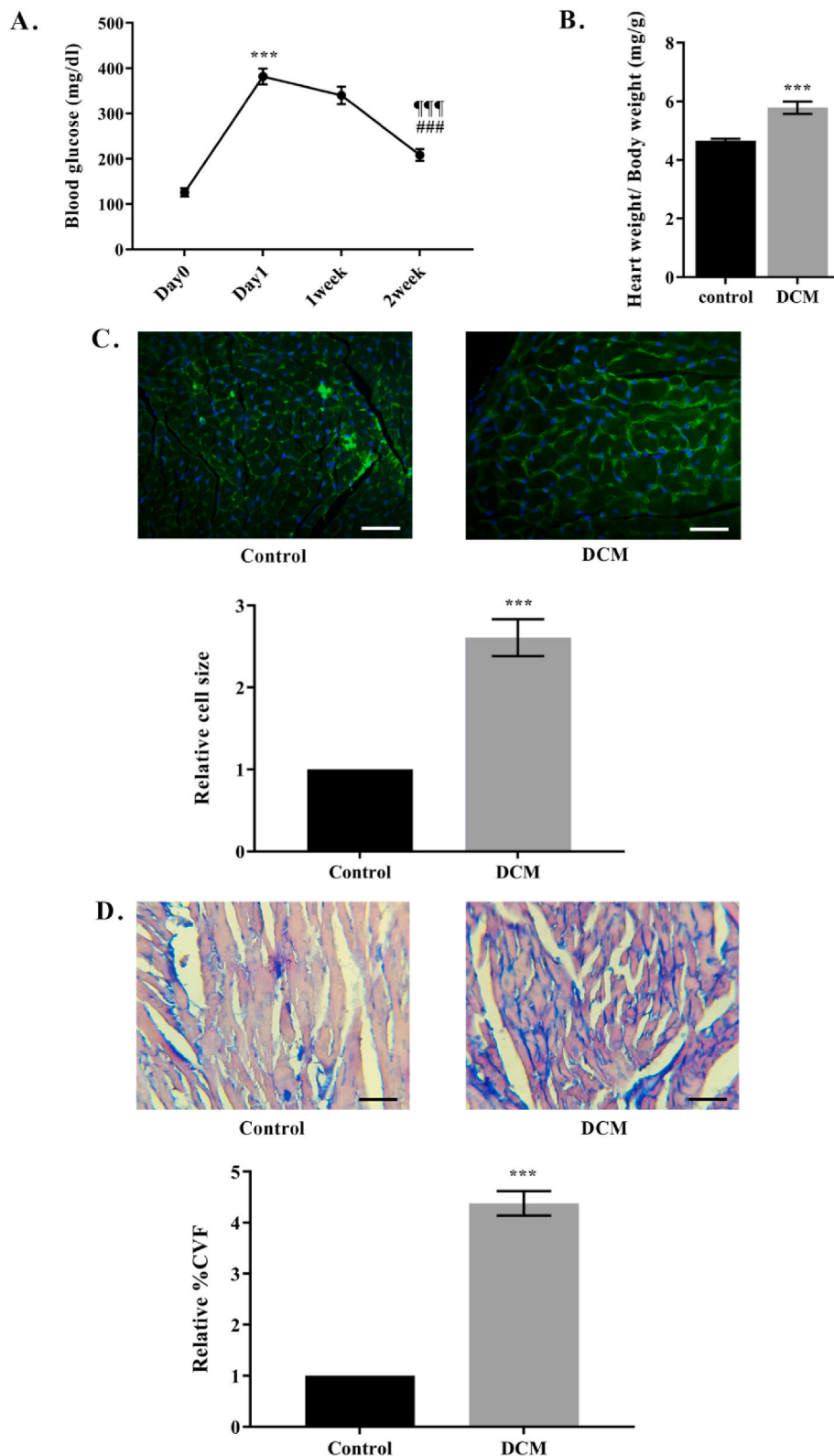
Fig. 1. High glucose stress induces cardiac hypertrophy and fibrosis in adult heart.

A. The fasting blood glucose level of adult mice after alloxan injection at a dose of 150 mg/kg body weight (i.p). Control animals were simultaneously injected with vehicle (0.9% normal saline). Animals with blood glucose level >200 mg/dl for 4 weeks were taken for further experiments as diabetic. Blood glucose parameters were measured from 6 adult animals. Statistical significance was calculated by one way ANOVA. ***, $p < 0.0001$ with respect to day 0; ###, $p < 0.0001$ with respect to 1 week;, $p < 0.0001$ with respect to day1. B. Graphical representation of the heart weight to body weight ratio (mg/g). Increased HW/BW ratio indicates cardiac hypertrophy in DCM animals. C. Diabetic heart tissue has an overall increased cell size compared to control tissue indicated by WGA staining shows cellular hypertrophy in high glucose stress. The graph represents mean cell size of control and DCM tissue quantified using ImageJ software (NIH). D. Masson's trichrome staining shows an increased collagen deposition in the DCM mice heart indicating cardiac fibrosis in the diabetic animal. The corresponding graph represents relative collagen deposition as par cent collagen volume fraction (CVF) quantified using ImageJ (NIH) software. Statistical significance of B-D was performed using Student's t-test. . ***, $p < 0.0001$ ($n = 6$). Scale bar represents 20 μm.

3.2. High blood sugar stress induces overexpression of YAP1, FOXM1 and AKT along with reduced activity of GSK3β in adult mice concomitant with increased expression of hypertrophy and fibrosis markers

To further confirm the occurrence of cardiac hypertrophy and fibrosis due to hyperglycemic stress, we looked into the mRNA expression of the marker gene. We observed a significant increase in hypertrophy marker *bnp* (3.51 ± 0.5-fold) and *β-mhc* (2.39 ± 0.24-fold) expression and an increased expression of fibrosis marker *col1* (3.52 ± 0.55-fold) and *col3* (2.47 ± 0.12-fold) in the DCM group compared to the control animals (Figs. 2B and S2B). Moreover, periostin expression is markedly increased in the diabetic cardiac tissue (6.63 ± 0.71-fold) as
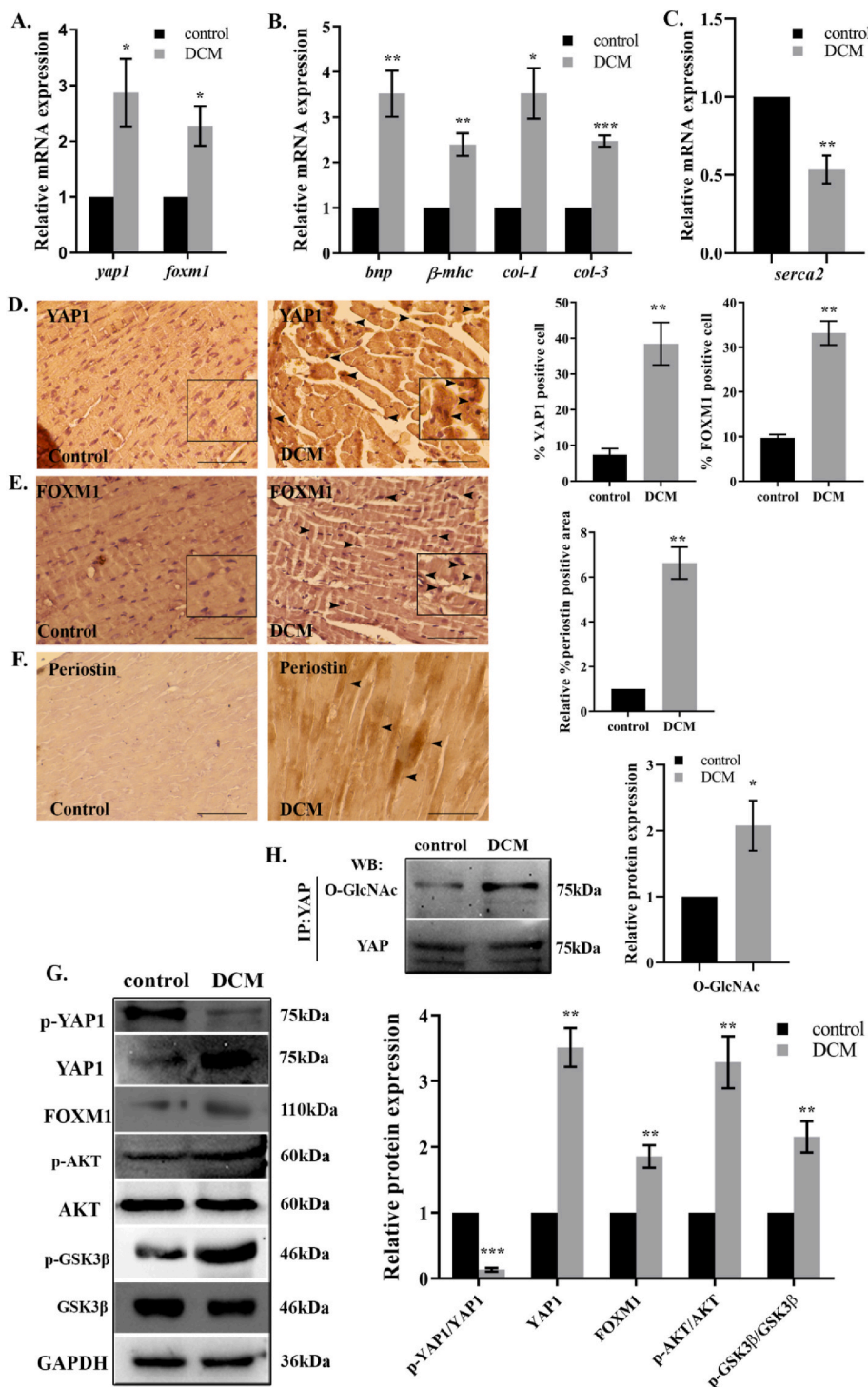
Fig. 2. High glucose induces YAP1, FOXM1 over-expression along with increased expression of hypertrophy and fibrosis marker.

A. *m*-RNA expression of *yap1* and *foxm1* genes by real time PCR shows up regulated expression in the DCM group compared to the control group. The Cq value of target genes were normalized against β-actin gene. B. *m*-RNA expression level of hypertrophy marker *bnp, β-mhc* and fibrosis marker *col-1, col-3* done by real time PCR can be seen to be significantly up regulated in the DCM group compared to the control group. The Cq value of target genes were normalized against β-actin gene. C. *serca2* expression in heart showing cardiac functions in the experimental model animal group. A significant decrease in the *serca2* expression in the DCM animal groups indicates impaired cardiac function in the diabetic animals. The Cq value of target genes were normalized against β-actin gene. D. Immunostaining with YAP1 antibody shows over-expression of YAP1 in the diabetic heart tissues compared to the control heart tissue, corresponding graph shows the quantitative value of the experiment within the specified groups. E. FOXM1 antibody staining shows increased FOXM1 expression in the DCM group compared to the control tissue. Corresponding graph shows the quantitative values of FOXM1 expression within the experimental groups. Inset in C, D shows images of immuno positive cells in magnified view. F. Periostin immunostaining showing increased expression in the DCM than in the control group. representative graph shows the quantitative value of the periostin expression in the experimental groups. G. Western blots images show increased YAP1, FOXM1 expression in the HG group. ser473 p-AKT/AKT was significantly higher in the DCM group compared to the control group with increased ser9 p-GSK3β/GSK3β in the DCM group was observed compared to the control group. H. Expression of O-GlcNAc of YAP in IP experiments. Immunprecipitation was performed with YAP antibody and expression of O-GlcNAc was observed by western blotting with O-GlcNAc antibody. Corresponding graph shows relative expression of O-GlcNAc in the experimental groups. Statistical significance was calculated by students' t *t*-test. ***, $p < 0.0001$; **, $p < 0.01$; *, $p < 0.05$; between DCM and control group, n = 3. Scale bar represents 20 μm.

compared to the control tissue (Figs. 2F and S2F) suggesting an increased fibrosis in the tissue. These results correlate with our previous findings as shown in Fig. 1 indicating hyperglycemia mediated hypertrophy and fibrosis induction in our diabetic cardiomyopathy animal model. In the DCM animal model reduced expression of *serca2* gene (0.53 ± 0.08-fold) (Figs. 2C and S2C) was observed that along with elevated *bnp* levels further indicated impaired contractile function in the DCM animals [26]. Since altered glycemic condition in different tissues lead to activation of YAP1 and its target genes we wanted to further investigate the effect of high glucose in regulating YAP1 and its downstream effectors in our hyperglycemic model. In the cardiac tissue YAP1

is known to be associated with AKT-GSK3β signaling that is an important signaling pathway in glucose metabolism. On the other hand, as AKT-GSK3β has recently been reported to regulate FOXM1 expression, we further attempted to investigate the expression of FOXM1 along with AKT and GSK3β to identify the molecular hierarchy of the YAP1/FOXM1 mediated signaling pathway in inducing hypertrophy and fibrosis in diabetic cardiomyopathy.

In the DCM tissue *yap1* showed an increased mRNA expression (2.86 ± 0.6 fold) compared to the control tissue (Figs. 2A and S2A). In the immunohistochemistry data of YAP1 antibody in mice tissue sections, an overall increased number of YAP1 positive cells was seen in the
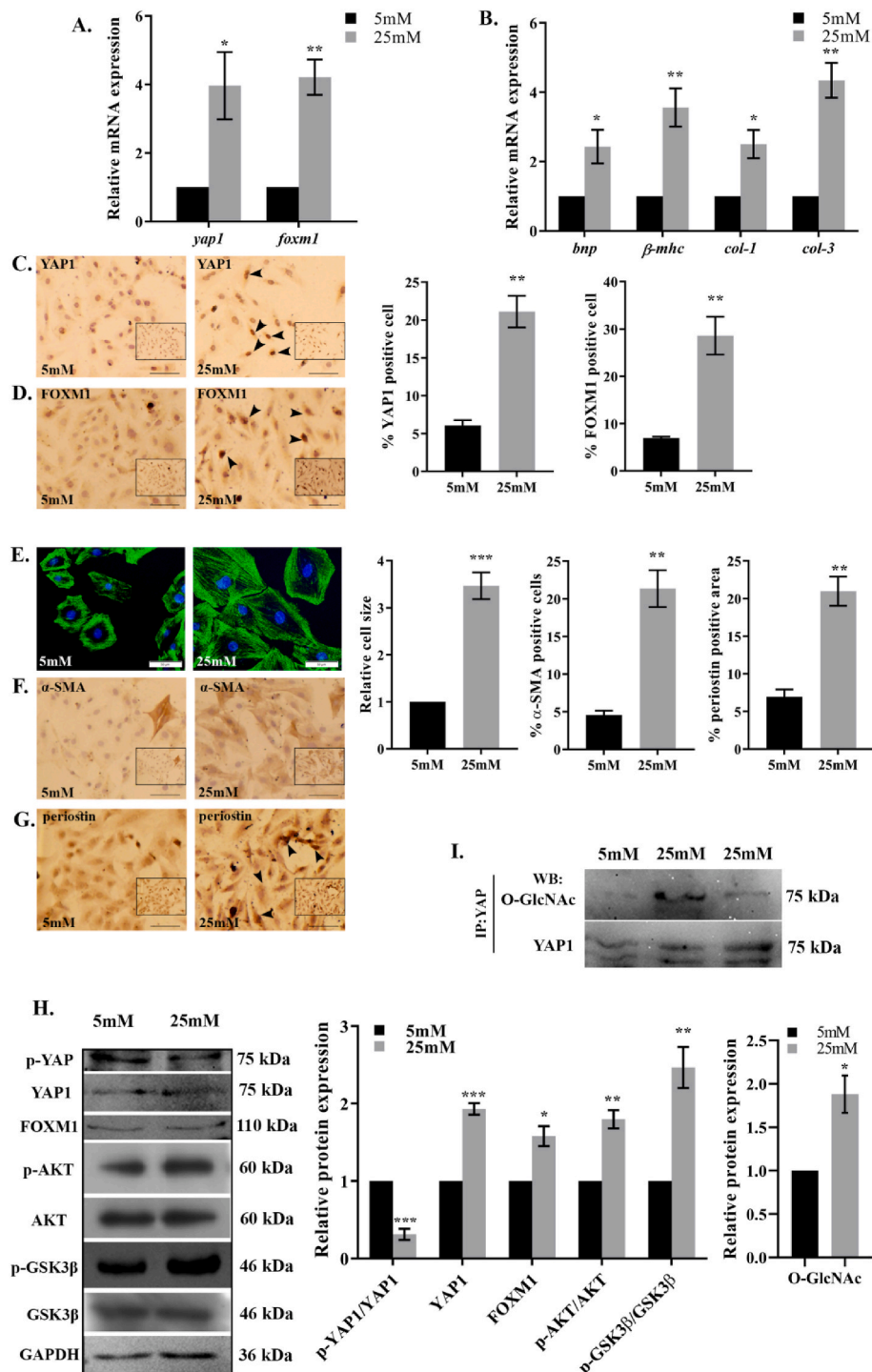
Fig. 3. Hyperglycemia induces hypertrophy and fibrosis along with YAP1, FOXM1 in H9c2 cells.
A. Real time PCR data of *yap1* and *foxm1* shows upregulated expression in the H9c2 cells treated with high glucose (HG) (25 mM) media compared to the normal glucose (NG) (5 mM) treated cells. B. Real time PCR data showing increased expression of hypertrophy marker *bnp, β-mhc* and fibrosis marker *col-1, col-3* in the HG treated H9c2 cells compared to the NG treated cells. C. H9c2 cells with YAP1 antibody staining shows increased YAP1 positive cells in the high glucose treated cells compared to normal glucose. Graph shows the percent YAP1 positive cells in HG and NG group. The corresponding graph represents quantitative values as percent YAP1 positive cells to total cells between the groups. D. Immunostaining images of FOXM1 antibody showing overexpression of FOXM1 in HG treated H9c2 cells compared to NG treated cells. The corresponding graph represents quantitative values as percent FOXM1 positive cells to total cells between the experimental groups. E. Phalloidin staining images showing enlarged cell size in the high glucose treated cells compared to the normal glucose treated cells. Corresponding graph shows relative cell size increase between the groups as fold change. F. Immunostaining with α-SMA antibody showing higher number positive cells in cells treated with HG to that of NG treated cells. Representative graph shows the quantified values of the data between the groups as percent α-SMA positive cells to total cells. G. Periostin immunostaining images showing increased expression indicative of fibrosis in the HG treated cells compared to the NG treated cells. Graph shows the corresponding quantitative values as percent positive staining cells between the groups. Scale bar represents 50 μm. Insets in C, D, F, and G shows lower magnification images of the representative image. H. Western blot data showing increased expression of YAP1, FOXM1 in the 25 mM group compared to the 5 mM group. Increased ser473 p-AKT/AKT and ser9 p-GSK3β/GSK3β expression showing increased activity of AKT and reduced GSK3β activity in the 25 mM group compared to 5 mM group. Corresponding graph shows the densitometric analyses of the Western blot data within the groups. I. Western Blot images of O-GlcNAc in IP experiments. Immunoprecipitation was performed by YAP antibody followed by western blotting with O-GlcNAc antibody. HG was observed to significantly increase the O-GlcNAcylation of YAP compared to the NG treated cells. Representative images show one more replicate image of HG treated condition. Graph shows relative O-GlcNAc expression in the groups. Statistical significance was calculated by students' *t*-test. ns, p: non-significant, *, p < 0.05, **, p < 0.01***, p < 0.0001 between the high glucose and the normal glucose group. n = 3.

hyperglycemic tissue (38.42 ± 5.96%) compared to the control tissue (7.41 ± 1.68%) (Figs. 2D and S2D). Western blot shows in diabetic cardiac tissue, significantly increased expression of YAP1 (3.51 ± 0.29-fold) to the control group at total protein level along with increased activity evident from the reduced expression of inhibitory p-YAP1/YAP1 (0.13 ± 0.02-fold) compared to the control group (Figs. 2G and S2G). Moreover, immunoprecipitation experiment showed high level of O-GlcNAcylation of YAP1 in the DCM animals (2.07 ± 0.38-fold) compared to the control animal (Figs. 2H and S2H). As YAP1 is known to be majorly activated following O-GlcNAcylation, therefore, our data confirms the initial observation that high glucose induces YAP1

overexpression and activity in the cardiac tissue and its downstream transcriptional effectors resulting in increased hypertrophic and fibrotic response.

Likewise we have also observed that the expression level of FOXM1 was significantly increased in diabetic cardiac tissue as compared to control tissue both at the mRNA level (2.27 ± 0.35 fold) (Figs. 2A and S2A) and protein level (1.85 ± 0.17 fold) (Figs. 2G and S2G) as detected by real time RT-PCR assay and Western blot analyses respectively. Immunostaining with FOXM1 antibody shows an overall increased number of FOXM1 positive cells (33.17 ± 2.7%) in the diabetic tissue over the control tissue (9.75 ± 0.7%) (Figs. 2E and S2E). Thus, like YAP1 we also
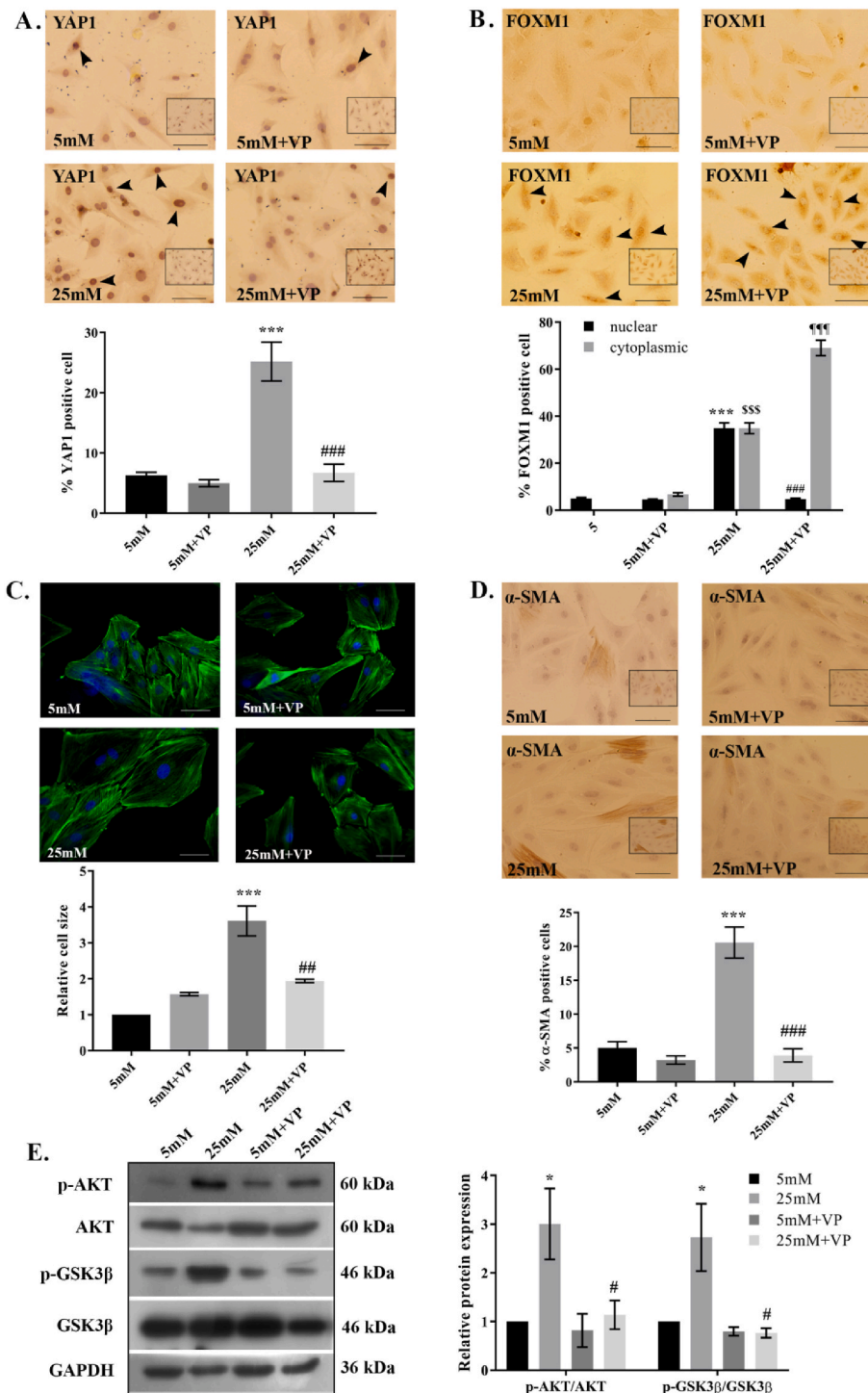
Fig. 4. YAP1 inhibition in H9c2 cells reduces the hypertrophy and fibrosis in the H9c2 cells with increased cytoplasmic localization of FOXM1 and increased AKT activity.

A. Verteporfin (VP) inhibits the expression of YAP1 in the H9c2 cells. Graph shows the corresponding quantitative values between the groups. B. FOXM1 immunostaining images showing increased cytoplasmic localization of FOXM1 in the verteporfin treated high glucose cells to that of high glucose treated cells without YAP1 inhibitor. Corresponding graph shows the quantitative representation as percent FOXM1 cells as nuclear vs. cytoplasmic expression. ***, $p < 0.0001$ between 25 mM nuclear and 5 mM nuclear groups; $\$\$\$$, $p < 0.0001$ between 25 mM cytoplasmic and 5 mM cytoplasmic groups. ###, $p < 0.0001$ between 25 mM nuclear and 25 mM without verteporfin group; $p < 0.0001$ between 25 mM cytoplasmic and 25 mM without verteporfin cytoplasmic group. n = 3. C. Phalloidin staining images showing YAP1 inhibition significantly reduces H9c2 cell size in the HG condition compared to the HG conditioned cells without inhibitor. Corresponding graph shows the quantitative value as fold change in cell size between the groups. D. α-SMA staining images showing reduced expression in the HG treated cells with verteporfin compared to the HG cells without verteporfin. Corresponding graph represents the quantified values as percent α-SMA positive cells to total cells between the groups. Scale bar represents 50 μm. Insets in A, B, D shows lower magnification images of the representative image. E. Western blot data shows reduced ser473 p-AKT/AKT and reduced inhibitory ser9 p-GSK/GSK3β expression in the HG treated cells with verteporfin compared to the HG cells without verteporfin. Statistical significance was calculated by one way ANOVA. *, $p < 0.05$; ***, $p < 0.0001$ between 25 mM and 5 mM group. #, $p < 0.05$; ##, $p < 0.01$; ###$p < 0.0001$ between 25 mM + verteporfin and 25 mM group. n = 3.

observed an increase expression of FOXM1 transcription factor in the diabetic animals compared to the control animals which may suggest that the increased level of expression of FOXM1 in adult cardiac cells may play a crucial pathological role in the adult cardiac cells.

We further observed a significantly increased in *p*-AKT level (3.28 ± 0.39-fold) over total AKT in the diabetic condition along with simultaneous decrease in the activity of GSK3β as evident from the increased expression of inhibitory phosphorylated form of GSK3β (2.15 ± 0.23-fold) over total GSK3β (Figs. 2G and S2G). This data suggests that high glucose promotes AKT activity and reduces GSK3β activity in the cardiomyocyte. In the adult heart under high glucose stress this abnormally

higher expression of YAP1, FOXM1 protein and altered AKT/GSK signaling pathway over the basal level indicates the pathological status of diabetic cardiomyopathy. Next we have used H9c2 cardiomyocyte cells to dissect out the molecular hierarchy of the YAP1/FOXM1 mediated signaling pathway in inducing hypertrophy and fibrosis in diabetic cardiomyopathy.
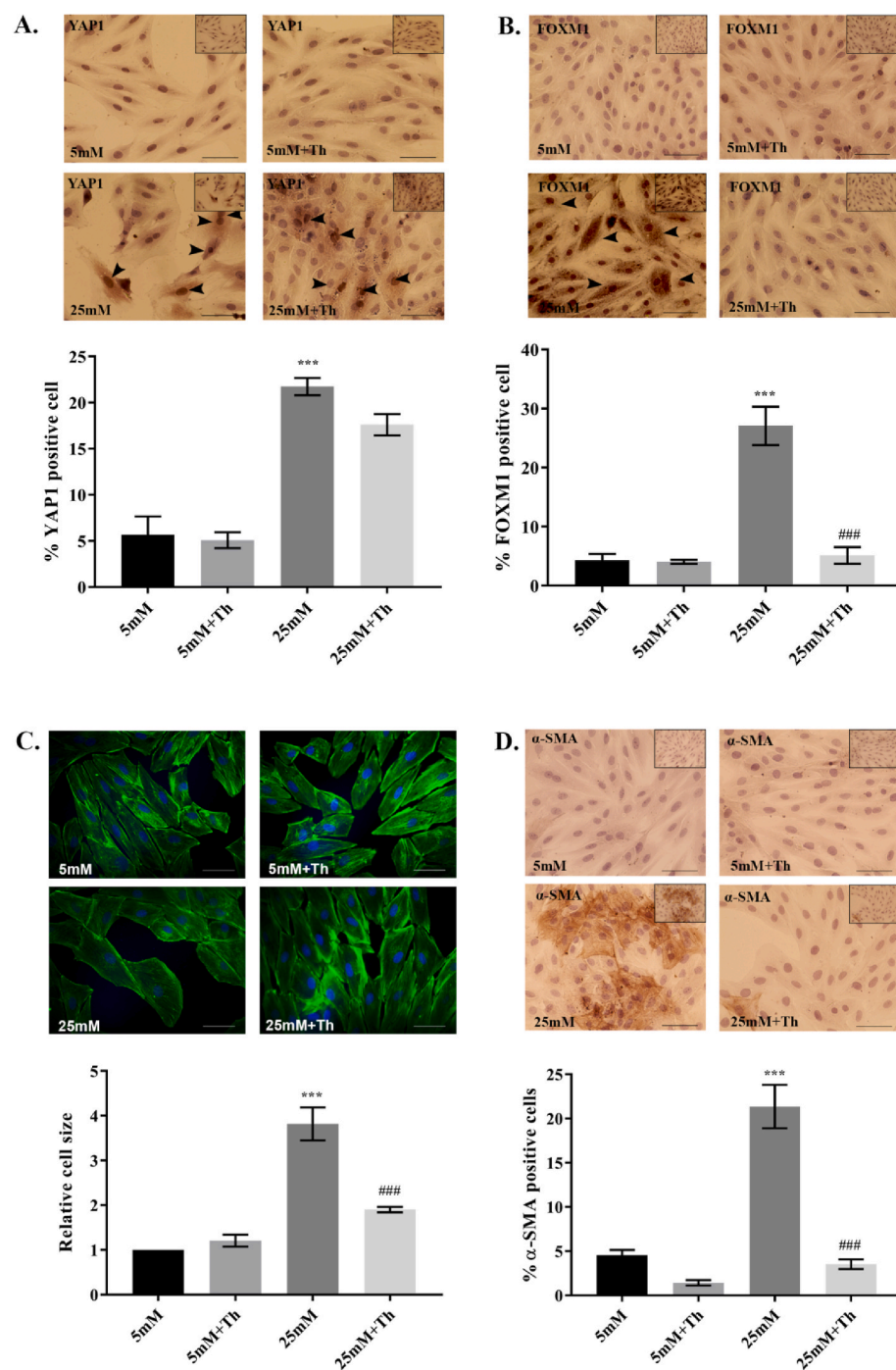
Fig. 5. FOXM1 inhibition in H9c2 cells reverse cardiomyocyte hypertrophy and fibrosis.

A. Immunostaining images of YAP1 in H9c2 cells treated with FOXM1 inhibitor thiostrepton (Th) shows no changes in YAP1 expression in the 25 mM with thiostrepton treated group compared to the 25 mM group without inhibitor. YAP1 shows high expression in both groups. The graph represents the overall quantitative analyses of YAP1 expression in different groups. B. FOXM1 immunostaining images showing reduced FOXM1 expression in H9c2 cells treated with thiostrepton. Graph shows the quantified vales of overall FOXM1 expression in different groups. C. Phalloidin staining images of H9c2 cells treated with thiostrepton shows reduction in cell size in thiostrepton treated cells. The corresponding graph shows overall quantitative cell size of H9c2 among different groups. D. α-SMA immunostainng images shows reduced number of cell positive staining in HG treated cells with thiostrepton group compared to only HG conditioned cells. Graph represents corresponding quantitative values across various fields in the experimental groups. Scale bar represents 50 μm. Insets in A, B, D shows lower magnification images of the representative image. Statistical significance was calculated by one way ANOVA. ***, $p < 0.0001$ between 25 mM and 5 mM group; ###, $p < 0.0001$ between 25 mM + thiostrepton and 25 mM group. n = 3.

3.3. Induction of hyperglycemic condition in H9c2 cells in vitro similarly results in increased expression of YAP1, AKT and FOXM1 with simultaneous inhibition of GSK3β activity along with the high expression of hypertrophy and fibrotic markers

Next to investigate the molecular mechanism of induction of cardiac hypertrophy and fibrosis in hyperglycemic condition by YAP1 and FOXM1 signaling we further investigated the findings in the *in vitro* model of hyperglycemia. In this experiment when H9c2 cells were infused with high glucose medium (25 mM glucose) for 48 h we observed high expression of *bnp* (2.43 ± 0.48-fold) *β-mhc* (3.56 ± 0.55-fold) along with *col1* (2.5 ± 0.40-fold), *col3* (4.34 ± 0.5-fold) over control cells (Figs. 3B and S3B) that indicated cardiomyocyte hypertrophy and fibrosis induction as it was observed in the diabetic cardiomyopathy model *in vivo*. We also confirmed cellular hypertrophy under high glucose condition from phalloidin stained cells (Figs. 3E and S3E) where an increase in cell size (3.46 ± 0.28-fold) was seen in the cells treated with high glucose media compared to the cells treated with normal glucose. In the immunostaining experiment we also observed an increase in the myofibroblast marker α-SMA expression in high glucose group (21.36 ± 2.44%) compared to the control group (4.56 ± 0.57%) and increased fibrosis marker periostin expression in the high glucose group (20.97 ± 1.93%) to the control group (6.94 ± 0.97%) that further validates the observation that high glucose induces fibrotic responses in the cardiac cells (Figs. 3F, G, S3F, S3G).

In the high glucose treated cells we observed significant upregulation of *yap1* mRNA expression (3.96 ± 0.98 fold), along with higher expression of *foxm1* m-RNA (4.21 ± 0.51 fold) over normal glucose treated cells (Figs. 3A and S3A). We observed significantly increased expression of YAP1 in the high glucose condition (1.93 ± 0.07-fold) compared to control group (Figs. 3H and S3H). We have also found significantly reduced activity of YAP1 from p-YAP1/YAP1 expression (0.31 ± 0.07-fold) compared to control as seen in western blot experiments (Figs. 3H and S3H). Increased activity of YAP1 was also evident from the higher YAP- O-GlcNacylation (1.88 ± 0.21-fold) observed in the high glucose treated H9c2 cells as compared to the NG treated cells (Figs. 3I and S3I). Significantly increased expression of cellular FOXM1 protein in the hyperglycemic cells (1.58 ± 0.12-fold) compared to control cells was also seen in the hyperglycemic condition over normal glucose condition (Figs. 3H and S3H). These data correlate with the higher YAP1 and FOXM1 expression seen in diabetic cardiomyopathy *in vivo*. Western blot results from high glucose and normal glucose treated cells also showed a significant upregulated expression of ser473 p-AKT (1.79 ± 0.11 fold) to total AKT and increased ser9 inhibitory phosphorylation of GSK3β (2.46 ± 0.26-fold) compared to total GSK3β (Figs. 3H and S3H) in the cells under hyperglycemic environment indicating an increased activity of AKT along with decreased activity of GSK3β in the hyperglycemic cells. Immunostaining data performed on high glucose treated and fixed H9c2 cells with YAP1 antibody clearly showed a significantly increased number of positive cells (21.1 ± 2.09%) in the hyperglycemic condition over the normoglycemic cells (6.04 ± 0.73%) (Figs. 3C and S3C). A higher number of FOXM1 immunopositive cells can also be seen in 25 mM glucose condition (28.6 ± 4.0%) over normal glucose treated cells (6.95 ± 0.29%) (Figs. 3D and S3D), which further confirmed the fact that YAP1, FOXM1 show upregulated expression in the high glucose treated H9c2 cells. These results correlate with our *in vivo* data where YAP1, FOXM1 and AKT showed a significantly upregulated expression in the diabetic cardiomyopathy animal group.

3.4. YAP1 down regulation in H9c2 cells resulted in reduced expression of AKT/GSK3β signaling with reduced FOXM1 expression and recovery from pathogenic condition

To determine whether YAP1 is necessary to induce cardiac hypertrophy and fibrosis, H9C2 cells maintained in presence of high glucose

containing media were treated with either in presence or absence of YAP inhibitor, verteporfin (VP) at a concentration of 10 μM for 48 h. Inhibition of YAP1 activity by verteporfin in H9C2 cells with 25 mM glucose resulted in reduced expression of YAP1 (6.72 ± 1.43%) compared to 25 mM glucose treated cells without inhibitor (25.19 ± 3.23%) (Figs. 4A and S4A). If YAP1 activity is necessary to induce cardiac hypertrophy and fibrosis then pre-treatment with verteporfin would fail to induce cardiac hypertrophy and fibrosis even in presence of high glucose as compared to cells maintained in absence of verteporfin. Interestingly, a significant reduction in the H9c2 size or hypertrophic condition was observed as seen by phalloidin staining in the cells treated with high glucose with verteporfin (1.93 ± 0.04-fold) compared to high glucose condition without the inhibitor (3.61 ± 0.41-fold) (Figs. 4C and S4C). Furthermore, the data also showed a significant decrease in expression of myofibroblast marker α-SMA (3.91 ± 0.96%) compared to high glucose treated cells without verteporfin (20.57 ± 2.29%) (Figs. 4D and S4D). Therefore, the data confirmed an obvious role of YAP1 overexpression in the induction of cardiomyocyte hypertrophy and fibrosis under hyperglycemic stress and would suggest that active YAP1 is necessary to induce cardiac hypertrophy and fibrosis in hyperglycemic condition.

To Further look into the association between YAP1, FOXM1 and AKT we have next observed the status of these molecules under verteporfin treated condition in the high glucose group. Interestingly, verteporfin treatment in H9c2 cells under hyperglycemic condition in turn resulted in an increased cytoplasmic localization of FOXM1 (69.06 ± 3.32% cytoplasmic to 4.77 ± 0.30% nuclear) compared to hyperglycemic cells without inhibitor (34.87 ± 2.28% overall cellular expression) (Figs. 4B and S4B). This result indicates that during hyperglycemic stress YAP1 overexpression in the cardiomyocyte promotes FOXM1 expression. YAP1 inhibition with its specific inhibitor causes the cytoplasmic retention of FOXM1 protein in the cardiomyocyte. This data further confirms the proposed association between YAP1 and FOXM1 molecule in the cardiomyocyte.

From Western blot analysis, we have also observed a downregulated expression of ser473 p-AKT/AKT (1.13 ± 0.29 fold) in the 25 mM glucose with verteporfin group compared to 25 mM glucose treated cells without inhibitor (3.0 ± 0.72 fold) which confirmed reduced activity of AKT in verteporfin treated cells in high glucose condition. Reduced activity of AKT in turn significantly downregulated the inhibitory phosphorylation on GSK3β (0.76 ± 0.09 fold) in the verteporfin treated high glucose group over high glucose group without inhibitor (2.73 ± 0.69 fold) (Figs. 4E and S4E). The results conferred that in the high glucose treated H9c2 cells YAP1 promotes the activity of AKT and reduces GSK3β activity. Overall, all these data indicate that YAP1 regulates the expression of FOXM1 and AKT/GSK3β signaling and under high glucose condition promotes cardiomyocyte hypertrophy and fibrosis.

3.5. FOXM1 inhibition resulted in decreased hypertrophy and fibrogenic condition of H9c2 cardiomyocyte cells

Like in the observations found with verteporfin treated cells, we next attempted to observe the effect of FOXM1 inhibition on the cells using its specific inhibitor thiostrepton (Th). In this experimental group, we observed a significant inhibition of the FOXM1 expression in the thiostrepton treated hyperglycemic cells (5.12 ± 1.4%) compared to hyperglycemic cells without the inhibitor (27.07 ± 3.24%) (Figs. 5B and S5B). This observation was followed by a significant reduction in hypertrophy and fibrotic response in H9c2 cells under hyperglycemic condition that was pre-treated with thiostrepton, as was observed from phalloidin and α-SMA staining. In the phalloidin staining, we have observed a significant reduction in cell size (1.9 ± 0.06-fold) in the high glucose with thiostrepton group compared to control group (3.81 ± 0.37-fold) (Figs. 5C and S5C) and significantly decreased number of α-SMA positive cells (3.52 ± 0.54%) in the hyperglycemic cells treated with thiostrepton over hyperglycemic cells without FOXM1 inhibitor
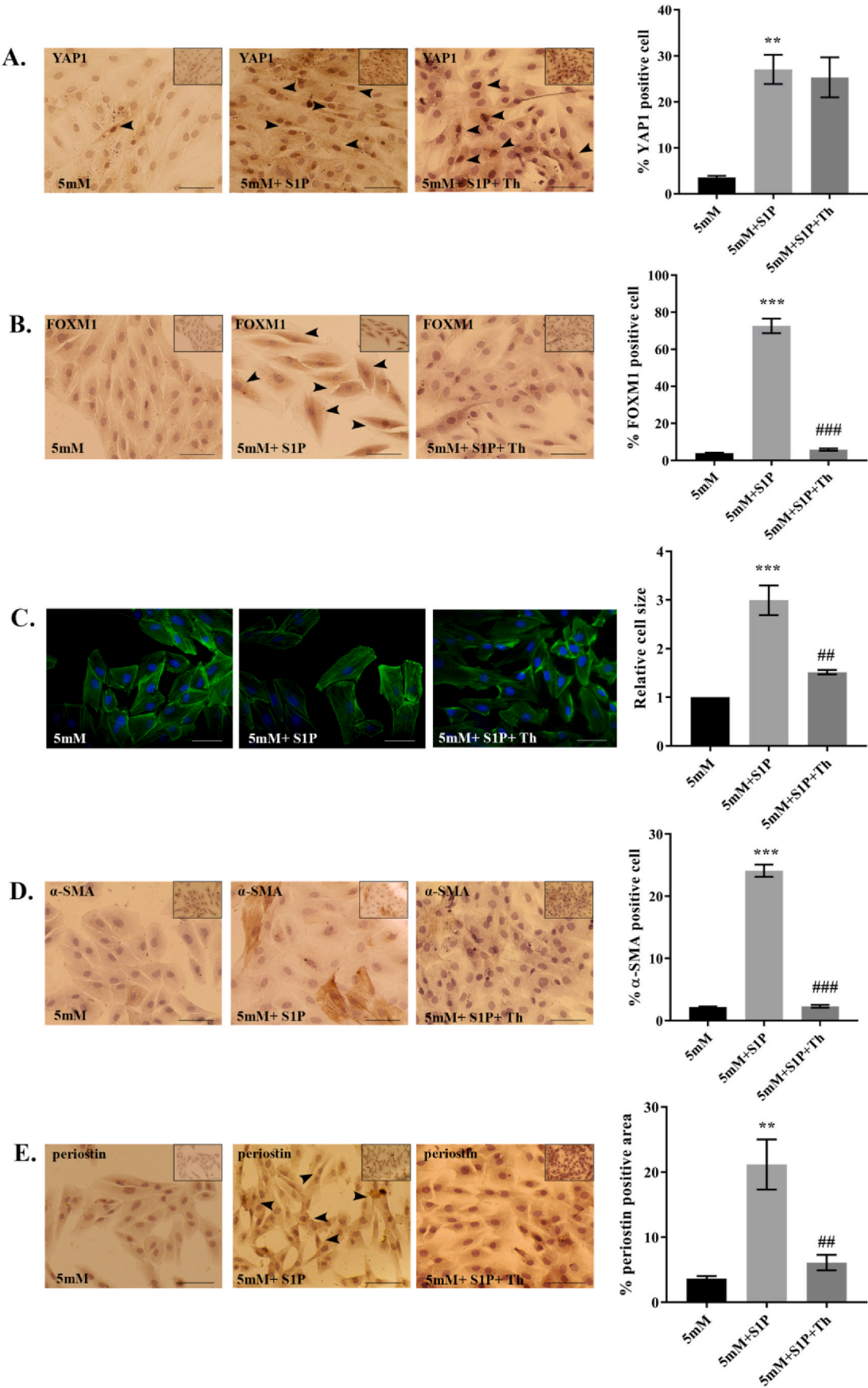
Fig. 6. Upregulation of YAP1 with S1P followed by inhibition of FOXM1 with thiostrepton determines FOXM1 is a downstream effector of YAP1 in H9c2 cells A. Immunostaining images of YAP1 shows increased expression of YAP1 in S1P treated cells. Thiostrepton mediated FOXM1 inhibition in the S1P treated group has no effect on YAP1 expression. Graph represents quantitative values of overall YAP1 expression in different groups. B. Immunostaining images of FOXM1 show upon YAP1 activation there is an increased FOXM1 expression in normoglycemic H9c2 cells. However, this increase is ameliorated when the cells are treated with S1P along with thiostrepton. Corresponding graph shows overall FOXM1 expression in the experimental groups. C. Phalloidin staining images show there is an increase in cell size in the S1P mediated YAP1 activated H9c2 cells. Upon thiostrepton treatment in the S1P group, this phenotype was reversed to normoglycemic condition. Graphical image shows overall quantitative values of cell size in the experimental groups. D. α-SMA immunostaining images show upon S1P treatment there is an increase in number of α-SMA positive cells which is again reduced to normoglycemic condition when cells are treated with S1P along with thiostrepton. Graph represents the overall percent positive staining over in different groups. E. Periostin marker immunostaining images also show an increased positive staining in the S1P group compared to normoglycemic group that was also reduced upon thiostrepton treatment. Graph represents the corresponding quantitative values of periostin expression in the experimental groups. Scale bar represents 50 μm. Insets in A, B, D, E shows lower magnification images of the representative image. Statistical significance was calculated by one way ANOVA. ***, $p < 0.0001$; **, $p < 0.01$ between 5 mM + S1P group and 5 mM group. ###, $p < 0.0001$; ##, $p < 0.01$ between 5 mM + S1P + thiostrepton and 5 mM + S1P group. n = 3.

(21.35 ± 2.44%) (Figs. 5D and S5D). These data so far proved that FOXM1 overexpression in the cardiomyocyte resulted in increased pathogenesis of hypertrophy and fibrosis which is one of the potential pathways through which hyperglycemia acts to induce cardiac hypertrophy and fibrosis.

However, the thiostrepton mediated FOXM1 inhibition interestingly had almost an insignificant effect on the YAP1 expression (21.74 ± 0.93%) in the high glucose condition to that of high glucose cells treated with thiostrepton group (17.61 ± 1.15%) (Figs. 5A and S5A). These data indicate that either YAP1 acts upstream to FOXM1 in cardiomyocyte to induce hypertrophy and fibrosis or, YAP1 and FOXM1 act independently to induce hypertrophy and fibrosis in cardiomyocyte treated with high glucose which eventually leads to pathogenesis.

3.6. YAP1 up regulation followed by FOXM1 inhibition indicates regulation of FOXM1 activity by YAP1 in the H9c2 cells as their possible pathway of action

In order to investigate whether YAP1 mediated induction of cardiomyocyte hypertrophy and fibrosis is dependent on FOXM1 activity, H9C2 cells under normoglycemic condition were pre-treated with YAP activator, S1P (1 μM) for 2 h followed by FOXM1-specific inhibitor, thiostrepton for overnight. If YAP1 mediated induction of cardiomyocyte hypertrophy is FOXM1 dependent then H9C2 cells pre-treated with FOXM1-specific inhibitor thiostrepton would fail to induce cardiac hypertrophy and fibrosis even in presence of YAP activator, S1P. Conversely, if H9c2 cells without the FOXM1 inhibitor but in presence of S1P in normoglycemic condition would still induce cardiac hypertrophy and fibrosis suggesting that YAP1 mediated induction of cardiomyocyte hypertrophy is FOXM1 dependent. Here, our experiment found significant increase of the cell size in the S1P treated H9c2 cells in normal glucose (5 mM) condition (2.99 ± 0.3 fold) (Figs. 6C and S6C) compared to cells under normal glucose condition without S1P. We also observed significantly higher expression of α-SMA in S1P treated cells in normal glucose condition (24.09 ± 0.96%) compared to normal glucose treated cells without YAP1 activator (2.20 ± 0.09%) (Figs. 6D and S6D). Significantly increased periostin expression (21.2 ± 3.85%) was found even in the normoglycemic treated cells with S1P compared to the cells that were maintained without YAP1 activator (3.67 ± 0.38%) (Figs. 6E and S6E). FOXM1 expression in the S1P treated group was significantly higher (72.61 ± 3.89%) in contrast to the cells maintained in normal glucose media (3.97 ± 0.25%) (Figs. 6B and S6B).

Interestingly, we observed a reversal in cell size to almost normoglycemic condition in the S1P treated cells that were simultaneously treated with thiostrepton (1.51 ± 0.04-fold) compared to S1P treated cells without thiostrepton (2.99 ± 0.3-fold) (Figs. 6C and S6C). A significant decrease in the number of α-SMA positive cells was observed in the S1P and thiostrepton treated group (2.32 ± 0.22%) compared to S1P

treated group without thiostrepton (24.09 ± 0.96%) (Figs. 6D and S6D). Immunostaining revealed significantly reduced expression of periostin (6.12 ± 1.18%) in S1P and thiostrepton treated cells in comparison to S1P treated cells without thiostrepton (21.2 ± 3.85%) (Figs. 6E and S6E).

As for the target gene expression, we have observed a diminished FOXM1 in the S1P group treated with thiostrepton group expression (5.84 ± 0.62%) compared to S1P treated group without thiostrepton (72.61 ± 3.89%) (Figs. 6B and S6B); while FOXM1 inhibition with thiostrepton had no significant effect on YAP1 expression (25.33 ± 4.33% vs. 27.08 ± 3.1%) seen in S1P + thiostrepton group compared to S1P treated group without thiostrepton (Figs. 6A and S6A). This data confirmed that YAP1 activation followed by FOXM1 inhibition resulted in reduced cardiomyocyte size and fibrosis *in vitro* suggesting a FOXM1 mediated activity of YAP1 in induction of cardiomyocyte hypertrophy and fibrosis. The data also suggests that FOXM1 acts downstream of YAP1.

3.7. Simultaneous activation of YAP1 and inhibition of AKT shows increased GSK3β activity and inhibition of FOXM1 expression in H9c2 cells

In order to further confirm that YAP1 induced FOXM1 activity in the cardiomyocyte is mediated through AKT-GSK3β signaling, we attempted to modulate the expression of AKT in H9c2 cells with LY294002 (LY). We have observed LY294002 treatment in the hyperglycemic H9c2 cells significantly reduced the expression of FOXM1 (5.4 ± 0.37%) compared to the high glucose cells without inhibitor (28.20 ± 3.29%) (data not shown). But LY294002 had no significant effect on the expression of YAP1 (24.96 ± 0.9%) in the high glucose with LY294002 group to the high glucose without inhibitor group (22.20 ± 0.97%) (data not shown). These results indicate that AKT-GSK3β may be a downstream effector of YAP1 that furthers regulates FOXM1 expression in a signaling pathway.

However, to confirm our observations earlier we have performed a simultaneous upregulation of YAP1 with S1P alongwith inhibition of AKT with LY294002 in the normal glucose condition. Firstly in the S1P treated cells with LY294002 treatment under normal glucose condition there was a significantly reduced FOXM1 expression (6.55 ± 0.22%) compared to the S1P treated cells without LY294002 (62.32 ± 4.01%) (Figs. 7B and S7B) Now, at par with our previous report of S1P mediated YAP1 activation (Fig. 6A), a reduction in the cell size was observed in the S1P with LY294002 treated normoglycemic cells (1.06 ± 0.06-fold) compared to S1P group without inhibitor (2.23 ± 0.06-fold) (Figs. 7C and S7C). In the α-SMA immunostaining data we have also observed a reduced number of positively stained cells in the S1P with AKT inhibitor group (3.18 ± 0.7%) compared to S1P treated group without AKT inhibitor (17.78 ± 3.42%) (Figs. 7D and S7D). But, as was observed earlier no significant change was observed in the expression of YAP1 in the S1P
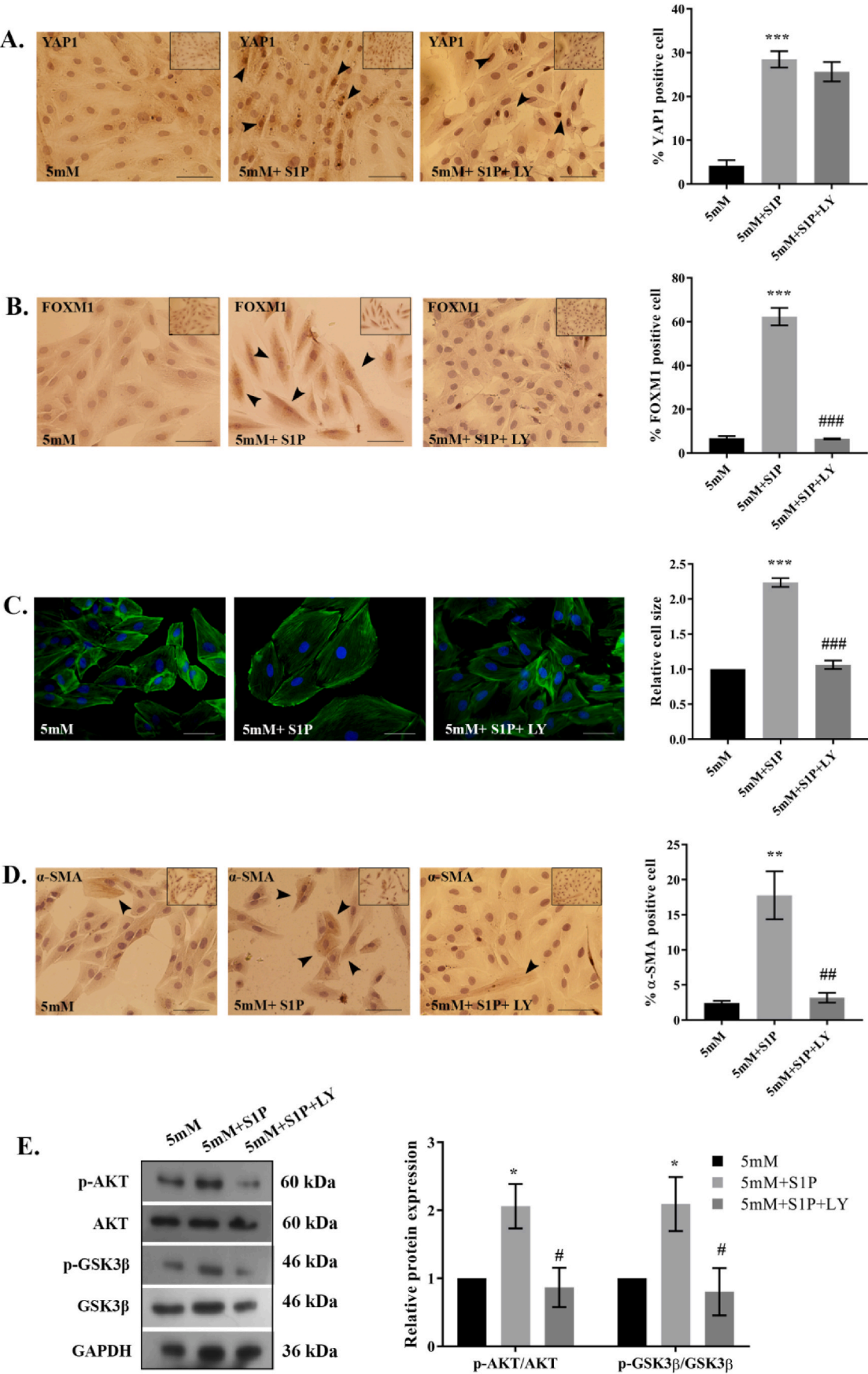
(caption on next page)

Fig. 7. YAP1 upregulation along with AKT inhibition determines YAP1 regulates FOXM1 via AKT-GSK3β signalling pathway
A. YAP1 immunostaining images show increased expression of YAP1 in S1P treated group. In the S1P with AKT inhibitor LY294002 (LY) group YAP1 had an insignificant change in expression compared to the only S1P group. Corresponding graph represents quantitative values of YAP1 expression in different groups. B. FOXM1 immunostaining images showing increased FOXM1 positive cells in the S1P group compared to the control group. However, FOXM1 expression was significantly reduced upon LY294002 treatment even under S1P treated condition. Corresponding graph shows the quantitative values across different fields in the experimental groups. C. Phalloidin staining images shows increase in the H9c2 size when treated with S1P. However, LY294002 treatment attenuated the increase in cell size even when cells were treated with S1P. Corresponding graph shows the quantitative values of overall cell size in different experimental groups. D. α-SMA immunostaining images showing increased number of positive cells in H9c2 cells treated with S1P. But, when cells were treated with S1P along with LY294002, the α-SMA staining was significantly reduced. Graph represents quantified value of α-SMA expression across different field in the experimental groups. Scale bar represents 50 μm. Insets in A, B, D shows lower magnification images of the representative image. E. Western blot images showing increased p-AKT/AKT and inhibitory Ser9 p-GSK3β/GSK3β in the S1P treated H9c2 cell group compared to the control group. This was again seen to be downregulated when cells were treated with S1P along with LY294002. Corresponding graph shows densitometry analyses of the Western blot data. Statistical significance was calculated by one way ANOVA. ***, $p < 0.0001$; **, $p < 0.01$; *, $p < 0.05$ between 5 mM + S1P and 5 mM group. ###, $p < 0.0001$; ##, $p < 0.01$; #, $p < 0.05$ between 5 mM + S1P + LY294002 and 5 mM + S1P group. n = 3.

treated cells that was simultaneously treated with AKT inhibitor LY294002 ($25.65 \pm 2.21\%$) to that of H9c2 cells treated with only S1P ($28.49 \pm 1.85\%$) (Figs. 7A and S7A). This indicates that YAP1 acts upstream of AKT-GSK in the regulatory pathway.

To, follow up with our findings in the Western blot data, we observed increased p-AKT/AKT in the S1P treated group (2.07 ± 0.32 fold) compared to H9c2 cells without the YAP activator S1P (Figs. 7E and S7E). Also a simultaneous increased Ser9-p-GSK3β/GSK3β was observed in the S1P treated H9c2 cells (2.22 ± 0.31 fold) (Figs. 7E and S7E) compared to the H9c2 cells without S1P that confirms our hypothesis that YAP1 expression increases AKT activity in the cardiomyocyte cells that in turn inhibits GSK3β activity with increased inhibitory Ser9 phosphorylation of GSK3β. With GSK3β inhibition, FOXM1 is stabilized in the cardiomyocyte (Figs. 7B and S7B) and thus, YAP1 confers its regulatory effect on FOXM1 via AKT/GSK3β signaling. Further, we observed a reduced pAKT activity in the S1P mediated YAP1 activated group that has been treated with LY294002 (0.90 ± 0.28 fold) compared to the only S1P treated cells without LY294002, alongwith reduced inhibitory p-GSK3β in the S1P treated cells with LY294002 (0.82 ± 0.36 fold) compared to only S1P treated cells (Figs. 7E and S7E). This correlates with our findings that although FOXM1 expression is high in S1P treated cells, with AKT inhibition the FOXM1 expression has been downregulated (Figs. 7B and S7B), confirmed now by the regulatory effect of GSK3β.

In the normal glucose treated cells with activated YAP1 expression, on application of AKT inhibitor we observed an improved pathological state of the H9c2 cells similar to verteporfin mediated YAP1 inhibited condition which may suggest YAP1 have some association with AKT/GSK signaling in the exertion of its regulatory effect on FOXM1 as well as hypertrophy and fibrosis induction. But in this experimental group as we have observed that while AKT inhibition reduced FOXM1 expression but had an insignificant effect on YAP1. From this observation we can conclude that AKT acts downstream to YAP1 rather than a co-regulation or upstream regulation. This also indicates that in hyperglycemia, YAP1 mediated AKT expression inhibits GSK3β activity that leads to an increased FOXM1 expression in the H9c2 cells.

3.8. Overexpression of FOXM1 in normoglycemic condition results in cardiomyocyte hypertrophy and high α-SMA expression indicating a definite role of FOXM1 in the hyperglycemia mediated pathogenesis of cardiac cells

Finally, as very little work has been reported on the role of FOXM1 in the cardiomyopathy induction in the adult heart, to confirm the effect of FOXM1 overexpression on cardiomyocyte we have treated H9c2 cells with FOXM1 recombinant protein and observed overexpression of

hypertrophic and fibrotic markers with cell size enlargement and increased number of α-SMA positive cells even under normal glucose condition. Phalloidin staining showed a significant enlargement of overall cell size in the FOXM1 recombinant protein (FOXM1 RP) group (2.33 ± 0.11-folds) was seen over control cells (Figs. 8B and S8B). In immunostaining experiment, we observed that the cells treated with FOXM1 recombinant protein showed significant increase in the number of α-SMA positive cells ($40.54 \pm 3.77\%$) compared to control cells ($3.65 \pm 0.08\%$) (Figs. 8C and S8C). In the periostin immunostaining data we have also observed significantly increased periostin expression in FOXM1 RP group ($28.49 \pm 2.81\%$) compared to the control group ($6.26 \pm 1.39\%$) (Figs. 8D and S8D).

Also, to further support our proposed hypothesis, we have performed a YAP1 inhibition followed by exogenous administration of FOXM1 protein in the H9c2 cells, where it was observed that even if we inhibit YAP1 activity, addition of FOXM1 protein to the medium resulted in an increased hypertrophic and fibrotic response in the H9c2 cells. In the phalloidin staining we observed an ($2.4 \pm 0.31\%$) increase in cell size in the VP with FOXM1 recombinant protein as compared to control cells (Figs. 8B and S8B). in the VP with FOXM1 RP group an increased number of α-SMA positive staining ($45.52 \pm 1.94\%$) was observed compared to control cells ($3.65 \pm 0.08\%$) (Figs. 8C and S8C). Also, in the VP with FOXM1 RP treated cells a significantly increased periostin immunostaining ($31.51 \pm 1.8\%$) was observed compared to control cells ($6.26 \pm 1.3\%$) These observations suggest that in cardiomyocyte cells, FOXM1 overexpression (Figs. 8A and S8A) induces cardiomyocyte hypertrophy and fibrosis leading to cardiac pathogenicity. Therefore, in conclusion, our study has inferred that in the adult diabetic heart increased YAP1-FOXM1 expression via AKT-GSK3β signaling is responsible for the induction of cardiomyocyte hypertrophy and fibrosis.

4. Discussion

Diabetic cardiomyopathy is currently one of the leading health issues worldwide that prompts to look into the understanding of the disease mechanism at the molecular level. YAP1 and FOXM1 are important cardiac development regulatory molecules that have recently been investigated for their role in pathogenesis [21,22,32]. In our study we aim to see how the hyperglycemic stress is perceived at the transcriptional level in cardiomyopathy induction and their specific mechanism of action. We have reported that hyperglycemic stress in both *in vivo* and *in vitro* conditions largely induces the expression of YAP1 as seen from total YAP1 expression compared to control group. We have also found that hyperglycemia causes increased YAP1 activity as confirmed by reduced p-YAP1/total YAP1 expression compared to normoglycemia group. Moreover, increased O-GlcNAcylation of YAP1 was also observed
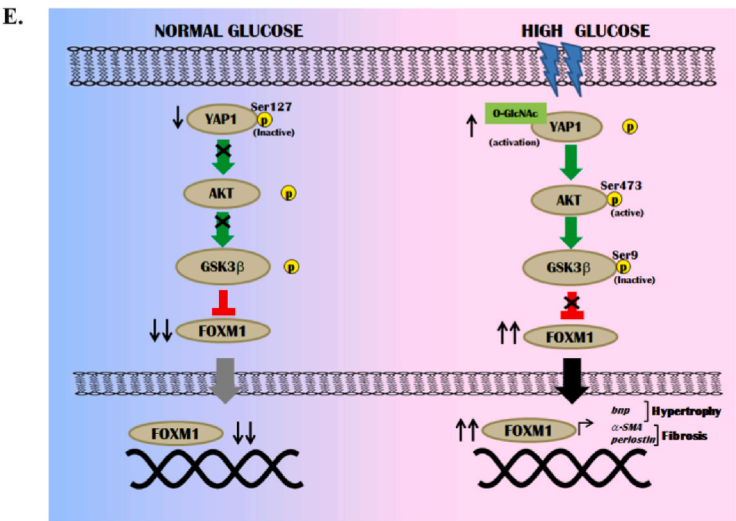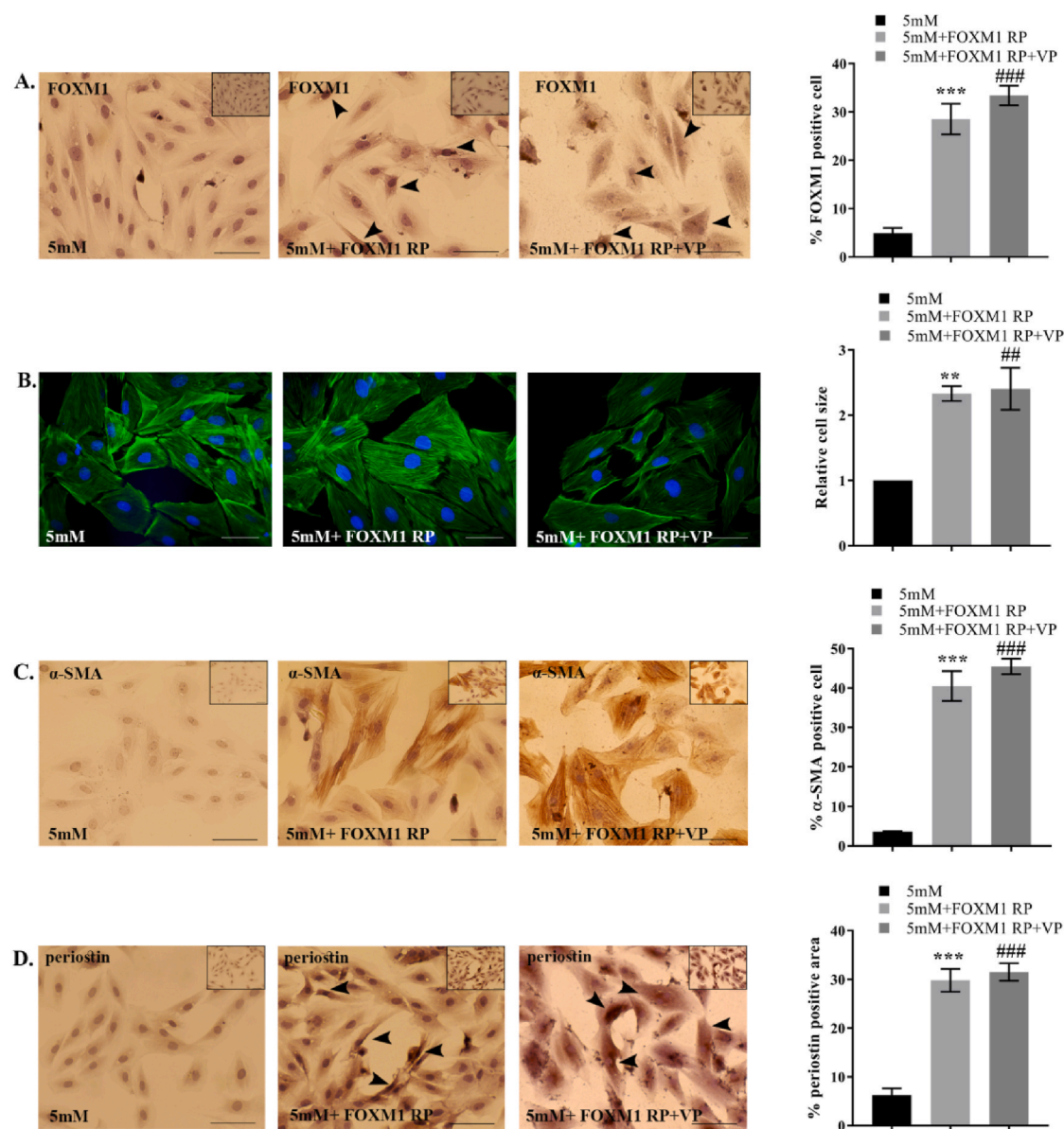
Fig. 8. FOXM1 overexpression with recombinant protein in promotes cardiomyocyte hypertrophy and fibrosis even in the normoglycemic condition.
A. FOXM1 immunostaining images shows increased expression of FOXM1 in the recombinant FOXM1 protein treated group compared to the control group, even when YAP1 is downregulated with verteporfin treatment. Graphical image represents the corresponding quantitative values in different groups. B. Phalloidin images show enlargement in the H9c2 cell size upon recombinant protein treatment. The enlarged cell size was also observed in the verteporfin treated cells followed by FOXM1 RP treatment. Corresponding graph shows overall quantitative analyses of cell size in different groups. C. α-SMA immunostaining images shows increased number of positive staining in both the FOXM1 RP and verteporfin with FOXM1 RP treated group compared to the control groups. Corresponding graph represents the quantified values of α-SMA staining in the experimental groups. D. Periostin immunostaining images show FOXM1 RP treatment leads to increased periostin staining compared to the control group. This was also observed in the verteporfin treated group that were simultaneously treated with FOXM1 recombinant protein. Corresponding graphical image represents overall periostin staining in the experimental groups. Scale bar represents 50 μm. Insets in A, C, D shows lower magnification images of the representative image. Statistical significance was calculated by one way ANOVA. ***, $p < 0.0001$; **, $p < 0.01$ between 5 mM + FOXM1 RP and 5 mM group. ###, $p < 0.0001$; ##, $p < 0.01$ between 5 mM + FOXM1 RP + VP and 5 mM + S1P group. n = 3. E. Schematic diagram representing the signalling pathway of YAP-FOXM1 activity in the induction cardiomyocyte hypertrophy and fibrosis. Under hyperglycemia stress YAP1 is activated in the cardiomyocyte following reduced inactivating phosphorylation on YAP1. High Glucose also increased activating O-GlcNAcylation of YAP1. Elevated YAP1 level further leads to increased AKT phosphorylation thus promoting AKT activity. Increased AKT mediated inactivation of GSK3β under hyperglycemic stress results in removal of the inhibitory regulation of GSK3β over FOXM1. Upregulated YAP1 therefore leads to aberrant FOXM1 accumulation within the cardiomyocyte. This elevated FOXM1 eventually promotes pathological remodelling of cardiomyocyte leading to cardiomyocyte hypertrophy and fibrosis.

in the high glucose treated condition indicating increased YAP1 activation in hyperglycemic condition.

YAP1 is an important effector molecule in the hippo pathway that regulates organ size and growth during development [30,37]. In recent years several studies reported overexpression of YAP1 to be associated with hypertrophic disorders [1,31]. Also some studies reported high glucose condition like diabetes stimulates YAP1 expression leading to pathogenesis [34]. However, little work has been done on the role of YAP1 in cardiomyocyte hypertrophy and fibrosis induction especially under hyperglycemic stress condition. In our study we have observed enlargement of H9c2 cell size and increased expression of fibrotic markers like periostin and α-SMA in the high glucose treated H9c2 cells that confirmed the observation that high glucose induces cardiomyocyte hypertrophy and fibrosis. Interestingly we observed that inhibition of YAP1 in H9c2 cells with its specific inhibitor verteporfin, there is a significant reduction in the H9c2 size and reduced fibrotic responses in the hyperglycemia stressed cardiomyocyte. Also, in cells under normoglycemic condition when treated with YAP1 activator S1P, this resulted in increased cellular hypertrophy and fibrosis in the H9c2 cells.

FOXM1, an important cardiac development regulatory molecule has been shown in several studies to be associated with hippo-pathway molecule YAP1 [3,9,33]. Reports suggests FOXM1 is downregulated in different adult organs and have been shown to express during injury in some organs like liver and lung to facilitate tissue repair and regeneration [17]. However, recent reports have shown FOXM1 overexpression in adult lung tissue to cause fibrosis [22]. But, no studies so far addressed the role of FOXM1 in cardiac pathogenesis in the diabetic condition. In this study we have observed high expression of FOXM1 in the diabetic tissue as well as hyperglycemia treated cardiomyocyte cells that are consistent with the increased hypertrophy and fibrotic condition observed in the experimental groups. In a separate study of treating H9c2 cells externally with FOXM1 recombinant protein to overexpress under normal glucose condition we observed increase in H9c2 cell size and increased fibrosis. On the contrary, in the high glucose treated H9c2 cells thiostrepton mediated FOXM1 inhibition reduced the hypertrophic and fibrotic condition. This observation for the first time reported that FOXM1 plays a crucial role in the induction of hyperglycemic stress mediated cardiomyocyte hypertrophy and fibrosis. Also, we have shown YAP1 inhibition in H9c2 cells in high glucose condition decreased FOXM1 expression and reversed the pathological phenotype. Interestingly, YAP1 activation in H9c2 cells in normal glucose condition upregulated FOXM1 expression and aggravated hypertrophy and fibrotic condition in cardiomyocyte. Also, while thiostrepton mediated FOXM1

downregulation resulted in amelioration of cardiomyocyte hypertrophy and fibrosis, inhibition of FOXM1 had little effect on the expression of YAP1. This observation shows that there might be an association between YAP1 and FOXM1 in the cardiomyocyte and the effect of overexpression of YAP1 might be mediated through FOXM1 at the transcriptional level. However, to further confirm the molecular hierarchy in this signalling pathway; in a follow up experiment, we demonstrated that activation of YAP1 with simultaneous inhibition of FOXM1 did not result in cardiomyocyte hypertrophy and fibrosis as compared to only YAP1 activated cells where visible cardiomyocyte enlargement and fibrosis were seen. If FOXM1 have acted independently of YAP1 then inhibition of FOXM1 would not have any effect on YAP1 activation and hence, reduction of hypertrophy and fibrosis of cardiomyocyte. Thus, it confirms the hypothesis in our study that FOXM1 is a downstream effector of YAP1 in the hyperglycemic cardiomyocyte cells.

In our previous experiments we have observed that hyperglycemia resulted in an increased expression of AKT and p-GSKβ expression along with YAP1 and FOXM1. AKT-GSK3β is a well-known signaling mediator in glucose metabolism pathway and reports have previously shown that this pathway is activated in cardiac cells in response to injury [5]. In recent studies GSK3β has been reported to regulate the expression of FOXM1 [6]. Therefore to understand the detailed regulatory mechanism of FOXM1 under hyperglycemic stress we have further looked into the association of YAP1, AKT and GSK3β. We have found that increased p-AKT activity with increased inhibitory p-GSK3β that was observed in the high glucose conditioned cells were in sync with the expression of YAP1 in the cardiomyocyte. In Fig. 4 we have observed that verteporfin treatment in the high glucose incubated H9c2 cells reduced the p-AKT and inhibitory p-GSK3β protein levels. With reduced GSK3β inhibition the active GSK3β may lead to reduced FOXM1 expression. Furthermore, YAP1 activation with S1P in Fig. 7 clearly showed upregulated AKT activity which in turn increased the inhibitory effect of p-GSK3β, thus aggravating the FOXM1 activity. To confirm the proposed mechanism of AKT mediated FOXM1 activation by YAP1 we have performed a similar experiment of simultaneous overexpression of YAP1 with its activator S1P followed by inhibition of AKT by LY294002. Here we have observed in Fig. 8 that in spite of high YAP1 expression in the S1P treated groups, on LY294002 treatment there is an increased cytoplasmic retention of FOXM1 along with reduced H9c2 cell size and reduced expression of fibrosis markers α-SMA and periostin as compared to the S1P only treated cells. This data indicates that YAP1 mediated FOXM1 activity is regulated via AKT-GSK3β signaling pathway in the cardiomyocyte cells

under hyperglycemic stress condition which ultimately leads to cardiac hypertrophy and fibrosis.

With diabetes being the most serious metabolic disorder that largely affects cardiac function; it is necessary to look into the molecular disturbances in the cardiac cells caused by the hyperglycemic stress. Our data altogether shows that YAP1 and FOXM1 in the cardiac myocyte, in diabetic or hyperglycemic stress is upregulated to a pathological level and works via AKT/GSK3β signaling to induce cardiomyocyte hypertrophy and fibrosis. As currently both FOXM1 and AKT remains one of the widely looked out molecules as drug therapy option in various disease models there remains a need to understand the detailed regulation of these molecules for development of better targeted therapy [2,22]. Therefore our reports on the detailed pathway of action of YAP1 and FOXM1 in diabetic cardiomyopathy will help in better combating the disease outcome in future.

5. Conclusion

- Overexpression of YAP1 and FOXM1 growth regulatory molecules during diabetic or hyperglycemic stress in the adult heart over basal expression level seen in the normal condition leads to cardiomyopathy like cardiomyocyte hypertrophy and fibrosis.
- YAP1 acts through AKT-FOXM1 signaling path in the cardiomyocyte to exert its pathogenic functions.
- Reversing the unbalanced expression of YAP1, FOXM1 even in hyperglycemic condition results in rescue of pathological phenotype up to some extent in the *in vitro* cultured cell model.

Credit authorship contribution statement

Arunima Mondal: Investigation, methodology, Writing - original draft; Writing - review & editing. Shreya Das: Investigation, Methodology. Jayeeta Samanta: Investigation, Methodology. Santanu Chakraborty: Data curation, Methodology. Arunima Sengupta: Supervision, Conceptualization, analysis; Funding acquisition, Resources, Formal analysis, Writing - original draft, Writing - review & editing.

Funding source

Declaration of competing interest

The authors declare no conflict of interests.

Acknowledgement

Appendix A. Supplementary data

Supplementary data to this article can be found online at https://doi.org/10.1016/j.abb.2022.109198.

References

[1] T. Abe, R. Shizu, T. Sasaki, Y. Shimizu, T. Hosaka, S. Kodama, A. Matsuzawa, K. Yoshinari, Functional interaction between PXR and YAP in xenobiotic-dependent liver hypertrophy and drug metabolism, J. Pharmacol. Exp. Therapeut. 371 (2019) 590–601.

[2] G. AL, FoxM1 inhibitors as potential anticancer drugs, Expert Opin. Ther. Targets 12 (2008) 663–665.

[3] C. Bolte, Y. Zhang, I.C. Wang, T.V. Kalin, J.D. Molkentin, V.V. Kalinichenko, Expression of Foxm1 transcription factor in cardiomyocytes is required for myocardial development, PLoS One 6 (2011).

[4] C. Bolte, Y. Zhang, A. York, T. V Kalin, J.E.J. Schultz, J.D. Molkentin, V. V Kalinichenko, Postnatal Ablation of Foxm1 from Cardiomyocytes Causes Late Onset Cardiac Hypertrophy and Fibrosis without Exacerbating Pressure Overload-Induced Cardiac Remodeling, vol. 7, 2012, pp. 1–10.

[5] S. Chakraborty, A. Sengupta, K.E. Yutzey, Tbx20 promotes cardiomyocyte proliferation and persistence in fetal characteristics in adult mouse hearts Journal of Molecular and Cellular Cardiology Tbx20 promotes cardiomyocyte proliferation and persistence of fetal characteristics in adult mouse heart, J. Mol. Cell. Cardiol. 62 (2013) 203–213.

[6] Y. Chen, Y. Li, J. Xue, A. Gong, G. Yu, A. Zhou, K. Lin, S. Zhang, N. Zhang, C. J. Gottardi, S. Huang, Wnt-induced deubiquitination FoxM1 ensures nucleus β-catenin transactivation, EMBO J. 35 (2016) 668–684.

[7] B.B. Dokken, The pathophysiology of cardiovascular disease and diabetes: beyond blood pressure and lipids, Diabetes Spectr. 21 (2008) 160–165.

[8] L. Du, C. Liu, M. Teng, Q. Meng, J. Lu, Y. Zhou, Y. Liu, Y. Cheng, D. Wang, L. Teng, Anti-diabetic activities of Paecilomyces tenuipes N45 extract in alloxan-induced diabetic mice, Mol. Med. Rep. 13 (2016) 1701–1708.

[9] Q. Fan, Q. Cai, Y. Xu, FOXM1 Is a Downstream Target of LPA and YAP Oncogenic Signaling Pathways in High Grade Serous Ovarian Cancer, 2015, p. 6.

[10] A. Frustaci, J. Kajstura, C. Chimenti, I. Jakoniuk, A. Leri, A. Maseri, B. Nadal-ginard, P. Anversa, Clinical Research, 2000.

[11] A.V. Haas, M.E. McDonnell, Pathogenesis of cardiovascular disease in diabetes, Endocrinol Metab. Clin. N. Am. 47 (2018) 51–63.

[12] M.A. Hermida, J. Dinesh Kumar, N.R. Leslie, GSK3 and its interactions with the PI3K/AKT/mTOR signalling network, Adv. Biol. Regul. 65 (2017) 5–15.

[13] S. Hsu, S.H. Fu, S.T. Chen, B.R.S. Hsu, Hyperglycemia in vitro up-regulates growth-related cell cycle proteins of adult mouse pancreatic islets, Transplant. Proc. 41 (2009) 339–342.

[14] X. Huang, G. Liu, J. Guo, Z.Q. Su, The PI3K/AKT pathway in obesity and type 2 diabetes, Int. J. Biol. Sci. 14 (2018) 1483–1496.

[15] Y. Inoue, M. Moriwaki, Y. Ueda, T. Takeuchi, M. Asahi, K. Moriwaki, Y. Ueda, T. Takeuchi, K. Higuchi, M. Asahi, Accepted Manuscript, (2017).

[16] G. Jia, M.A. Hill, J.R. Sowers, T. Memorial, V. Hospital, To This Clinical Entity 122 (2019) 624–638.

[17] T.V. Kalin, V. Ustiyan, V.V. Kalinichenko, Multiple faces of FoxM1 transcription factor: lessons from transgenic mouse models, Cell Cycle 10 (2011) 396–405.

[18] S. Ksmiakrishna, I.M. Kim, V. Petrovic, D. Malin, I.C. Wang, T.V. Kalin, L. Meliton, Y.Y. Zhao, T. Ackerson, Y. Qin, A.B. Malik, R.H. Costa, V.V. Kalinichenko, Myocardium defects and ventricular hypoplasia in mice homozygous null for the Forkhead Box M1 transcription factor, Dev. Dynam. 236 (2007) 1000–1013.

[19] K.K. Lee, S. Yonehara, Identification of mechanism that couples multisite phosphorylation of Yes-associated Protein (YAP) with transcriptional coactivation and regulation of apoptosis, J. Biol. Chem. 287 (2012) 9568–9578.

[20] C. Li, J. Zhang, M. Xue, X. Li, F. Han, X. Liu, L. Xu, Y. Lu, Y. Cheng, SGLT2 inhibition with empagliflozin attenuates myocardial oxidative stress and fibrosis in diabetic mice heart, Cardiovasc. Diabetol. (2019) 1–13.

[21] S. Noguchi, A. Saito, T. Nagase, YAP/TAZ signaling as a molecular link between fibrosis and cancer, Int. J. Mol. Sci. 19 (2018).

[22] L.R. Penke, J.M. Speth, V.L. Dommeti, E.S. White, I.L. Bergin, M. Peters-Golden, FOXM1 is a critical driver of lung fibroblast activation and fibrogenesis, J. Clin. Invest. 128 (2018) 2389–2405.

[23] M. Samak, J. Fatullayev, A. Sabashnikov, M. Zeriouh, B. Schmack, M. Farag, A. F. Popov, P.M. Dohmen, Y.H. Choi, T. Wahlers, A. Weymann, Cardiac hypertrophy: an introduction to molecular and cellular basis, Med. Sci. Monit. Basic Res. 22 (2016) 75–79.

[24] J. Samanta, A. Mondal, S. Saha, S. Chakraborty, A. Sengupta, Oleic acid protects from arsenic - induced cardiac hypertrophy via AMPK/FoxO/NFATc3 pathway fetal bovine serum, Cardiovasc. Toxicol. 20 (3) (2020) 261–280.

[25] A. Sengupta, V. V Kalinichenko, K.E. Yutzey, C. Res, FoxO and FoxM1 Transcription Factors Have Antagonistic Functions in Neonatal Cardiomyocyte Cell Cycle Withdrawal and IGF1 Gene Regulation the Online Version of This Article , along with Updated Information and Services , Is Located on the World Wide Web a, 2012.

[26] M.A. Shareef, L.A. Anwer, C. Poizat, Cardiac SERCA2A/B: therapeutic targets for heart failure, Eur. J. Pharmacol. 724 (2014) 1–8.

[27] I. Shimizu, T. Minamino, Journal of Molecular and Cellular Cardiology Physiological and pathological cardiac hypertrophy 97 (2016) 245–262.

[28] S. Sinha, N. Dwivedi, J. Woodgett, S. Tao, C. Howard, T.A. Fields, A. Jamadar, R. Rao, Glycogen synthase kinase-3β inhibits tubular regeneration in acute kidney injury by a FoxM1-dependent mechanism, Faseb. J. 34 (2020) 13597–13608.

[29] K. Tumaneng, K. Schlegelmilch, R.C. Russell, D. Yimlamai, H. Basnet, N. Mahadevan, J. Fitamant, N. Bardeesy, F.D. Camargo, K.L. Guan, YAP mediates crosstalk between the Hippo and PI(3)K-TOR pathways by suppressing PTEN via miR-29, Nat. Cell Biol. 14 (2012) 1322–1329.

[30] J. Wang, S. Liu, T. Heallen, J.F. Martin, The Hippo pathway in the heart, Nat. Rev. Cardiol. 15 (11) (2018) 672–684.

[31] P. Wang, B. Mao, W. Luo, B. Wei, W. Jiang, D. Liu, L. Song, G. Ji, Z. Yang, Y.-Q. Lai, Z. Yuan,The Alteration of Hippo/YAP Signaling in the Development of Hypertrophic Cardiomyopathy, (n.d.).

[32] P. Wang, B. Mao, W. Luo, B. Wei, W. Jiang, D. Liu, L. Song, G. Ji, Z. Yang, Y.Q. Lai, Z. Yuan, The alteration of Hippo/YAP signaling in the development of hypertrophic cardiomyopathy, Basic Res. Cardiol. 109 (2014) 1–11.

[33] S.M.E. Weiler, F. Pinna, T. Wolf, T. Lutz, A. Geldiyev, C. Sticht, M. Knaub, S. Thomann, M. Bissinger, S. Wan, S. Rössler, D. Becker, N. Gretz, H. Lang, F. Bergmann, V. Ustiyan, T.V. Kalin, S. Singer, J.S. Lee, J.U. Marquardt, P. Schirmacher, V.V. Kalinichenko, K. Breuhahn, Induction of chromosome instability by activation of yes-associated protein and forkhead box M1 in liver cancer, Gastroenterology 152 (2017) 2037–2051, e22.

[34] X. Zhang, Y. Qiao, Q. Wu, Y. Chen, S. Zou, X. Liu, G. Zhu, Y. Zhao, Y. Chen, Y. Yu, Q. Pan, J. W, F. Sun, The essential role of YAP O-GlcNAcylation in high-glucose-stimulated liver tumorigenesis, Nat. Commun. 8 (2017).

[35] F. Xiao, W. Kimura, H.A. Sadek, A Hippo "AKT" regulates cardiomyocyte proliferation, Circ. Res. 116 (2015) 3–5.

[36] K.E. Yutzey,Teaching an Old Dogma New Tricks, (n.d.) 627–630.

[37] Q. Zhou, L. Li, B. Zhao, K. Guan, The Hippo Pathway in Heart Development, Regeneration, and Diseases, 2015, pp. 1431–1447.

Oleic Acid Protects from Arsenic-Induced Cardiac Hypertrophy via AMPK/FoxO/NFATc3 Pathway

Jayeeta Samanta[1] · Arunima Mondal[1] · Srimoyee Saha[2] · Santanu Chakraborty[3] · Arunima Sengupta[1]

Abstract

Arsenic toxicity is one of the major environmental problems causing various diseases, cardiovascular disorders is one of them. Several epidemiological studies have shown that arsenic causes cardiac hypertrophy but the detailed molecular mechanism is to be studied yet. This study is designed to determine the molecules involved in the augmentation of arsenic-induced cardiac hypertrophy. Furthermore, the effects of oleic acid on arsenic-induced hypertrophy and cardiac injury have also been investigated. Our results show that arsenic induces cardiac hypertrophy both in vivo in mice and in vitro in rat H9c2 cardiomyocytes. Moreover, arsenic results in decreased activity of AMPK and FoxO1 along with increased NFATc3 expression, a known cardiac hypertrophy inducer. In addition, activation of AMPK and FoxO1 results in reduced NFATc3 expression causing attenuation of arsenic-induced cardiac hypertrophy in H9c2 cells. Interestingly, we have observed that oleic acid helps in ameliorating cardiac hypertrophy in arsenic-exposed mice. Our studies on protection from arsenic-induced cardiac hypertrophy by oleic acid in H9c2 cells shows that oleic acid activates AMPK along with increased nuclear FoxO1 localization, thereby reducing NFATc3 expression and attenuating cardiomyocyte hypertrophy. This study will help in finding out new avenues in treating arsenic-induced cardiac hypertrophy.

Keywords Arsenic toxicity · Cardiac hypertrophy · AMPK · FoxO1 · NFATc3 · Oleic acid

Abbreviations

AMPK	Adenosine monophosphate-activated protein kinase
FoxO	Forkhead box transcription factor
CVDs	Cardiovascular-associated diseases
ROS	Reactive oxygen species
OA	Oleic acid
i.p.	Intraperitoneal
ppm	Parts per million
IAEC	Institutional Animal Ethics Committee
DMEM	Dulbecco's modified Eagle's medium
FBS	Fetal Bovine serum
PBS	Phosphate-buffered saline
PCR	Polymerase chain reaction
PFA	Paraformaldehyde
WGA	Wheat germ agglutinin
BSA	Bovine serum albumin
ANP	Atrial natriuretic peptide
BNP	Brain natriuretic peptide
S.E.	Standard error

✉ Arunima Sengupta
arunimasengupta2013@gmail.com

1 Department of Life science and Biotechnology, Jadavpur University, 188, Raja S. C. Mallick Road, Kolkata, West Bengal 700032, India

2 Department of Physics, Jadavpur University, Kolkata, India

3 Department of Life sciences, Presidency University, Kolkata, India

Introduction

Arsenic pollution is one of the major recent environmental threats out of the various toxic substances which induce pollution. Chronic exposure to arsenic leads to the damage of various organs of the body and several diseases of skin, lungs, liver, urinary bladder, heart, out of which cardiovascular problems mediated by arsenic pollution are a huge threat nowadays worldwide [22, 33]. The exposure to arsenic mainly occurs via groundwater pollution and

ER stress induces upregulation of transcription factor Tbx20 and downstream Bmp2 signaling to promote cardiomyocyte survival

Shreya Das[1], Arunima Mondal[1], Chandrani Dey[1], Santanu Chakraborty[2], Rudranil Bhowmik[3], Sanmoy Karmakar[3], and Arunima Sengupta[1,*]

From the [1]Department of Life Science and Biotechnology, Jadavpur University, Kolkata, India; [2]Department of Life Sciences, Presidency University, Kolkata, India; [3]Bioequivalence Study Centre, Department of Pharmaceutical Technology, Jadavpur University, Kolkata, India

Reviewed by members of the JBC Editorial Board. Edited by Ronald Wek

In the mammalian heart, fetal cardiomyocytes proliferate prior to birth; however, they exit the cell cycle shortly after birth. Recent studies show that adult cardiomyocytes re-enters the cell cycle postinjury to promote cardiac regeneration. The endoplasmic reticulum (ER) orchestrates the production and assembly of different types of proteins, and a disruption in this machinery leads to the generation of ER stress, which activates the unfolded protein response. There is a very fine balance between ER stress–mediated protective and proapoptotic responses. T-box transcription factor 20 (Tbx20) promotes embryonic and adult cardiomyocyte proliferation postinjury to restore cardiac homeostasis. However, the function and regulatory interactions of Tbx20 in ER stress–induced cardiomyopathy have not yet been reported. We show here that ER stress upregulates Tbx20, which activates downstream bone morphogenetic protein 2 (Bmp2)-pSmad1/5/8 signaling to induce cardiomyocyte proliferation and limit apoptosis. However, augmenting ER stress reverses this protective response. We also show that increased expression of *tbx20* during ER stress is mediated by the activating transcription factor 6 arm of the unfolded protein response. Cardiomyocyte-specific loss of Tbx20 results in decreased cardiomyocyte proliferation and increased apoptosis. Administration of recombinant Bmp2 protein during ER stress upregulates Tbx20 leading to augmented proliferation, indicating a feed-forward loop mechanism. In *in vivo* ER stress, as well as in diabetic cardiomyopathy, the activity of Tbx20 is increased with concomitant increased cardiomyocyte proliferation and decreased apoptosis. These data support a critical role of Tbx20-Bmp2 signaling in promoting cardiomyocyte survival during ER stress–induced cardiomyopathies.

In mammals, the developing heart is highly proliferative prior to birth, and it involves the interplay of multiple signaling pathways. However, after birth, the cardiomyocytes lose its plasticity, exit the cell cycle, its proliferative capacity dissipates, and the cells grow in size primarily by hypertrophy (1). In the neonates, post 1 week after birth, the cardiomyocytes become binucleated, express adult contractile protein isoforms, and lose its ability to regenerate (2–4). The notion that adult cardiomyocytes lose their capacity to proliferate because of cell cycle arrest was revoked by growing studies showing that resident adult myocardial cardiomyocyte re-enters cell cycle following myocardial injury by regulating key regulatory pathways (5).

T-box transcription factor 20 (Tbx20) is a member of the Tbx1 subfamily of T-box–containing genes and plays pivotal roles in development and maintenance of heart by driving cardiomyocyte proliferation (6). Loss of function of Tbx20 leads to unlooped and severely hypoplastic heart with embryonic lethality (7–9). Ablation of Tbx20 in adult cardiomyocytes leads to severe cardiomyopathy with arrhythmias and death (10). Gain of function of Tbx20 leads to increased cardiomyocyte proliferation in fetal heart development (11).

Endoplasmic reticulum (ER) is an organelle that mediates production and folding of different secretory and membrane proteins (12). Any sort of dysregulation in the machinery of the ER because of external factors or internal stimulus leads to accumulation of misfolded protein leading to generation of ER stress. ER stress activates the adaptive cellular response signaling cascade known as unfolded protein response (UPR), which consists of three pathways, activating transcription factor 6 (ATF6), inositol-requiring enzyme 1 alpha (IRE1α), and protein kinase RNA-activated-like ER kinase (PERK). The protective UPR is initially beneficial as it works for restoration of homeostasis; however, a severe ER stress leads to cell death *via* apoptosis. There is a very delicate balance between ER stress–induced prosurvival and proapoptosis (13). Tbx20 overexpression was previously shown to induce proliferation of cardiomyocytes during oxidative stress and hypoxia (14); however, its mechanistic role during ER stress–mediated cardiomyopathy is still elusive.

Our study for the first time identified the novel unknown function of Tbx20 that is able to directly enhance the protective responses of the UPR for restoration of ER homeostasis in the milieu of cardiac injury. Since ER stress have been

* For correspondence: Arunima Sengupta, arunimasengupta2013@gmail.com.

Induction of cardiomyocyte calcification is dependent on FoxO1/NFATc3/Runx2 signaling

Jayeeta Samanta[1] · Arunima Mondal[1] · Shreya Das[1] · Santanu Chakraborty[2] · Arunima Sengupta[1] ID

Abstract

Cardiovascular disorders (CAVDs) being a major concern over the past several years due to the huge number of morbidity and mortality worldwide, a number of studies have been done on the various aspects of cardiac problems. One of the various CAVDs is cardiovascular calcification. A number of investigations and research work have been done previously on the molecular mechanism of vascular and heart valve calcification but the mechanism of myocardial and cardiomyocyte calcification has remained uninvestigated. A number of case studies have shown the presence of calcific deposits in the myocardial/ventricular region of the heart in fetal condition as well as in individuals of different ages but no detailed studies have been done yet. In this study, we have mainly investigated the role of Forkhead box transcription factor FoxO1 and nuclear factor of activated T-cells NFATc3 in cardiomyocyte calcification. Our studies in H9c2 cardiomyocytes show that calcific deposition in cardiomyocytes does not occur in 15 d but upon osteogenic induction for 1 mo where FoxO1 expression gets reduced thereby increasing the expression of its downstream target NFATc3, thus increasing the expression of the osteogenic marker Runx2. Detailed studies on the molecular mechanism of cardiomyocyte calcification will help in finding out therapeutic strategies in the treatment of cardiac calcification.

Keywords Cardiovascular · Cardiomyocyte · Calcification · FoxO1 · NFATc3

Introduction

Cardiovascular disorders (CAVDs) are a very common pathological condition that leads to mortality of a number of people worldwide. Various studies are being done extensively on the various types of CAVDs like cardiac hypertrophy,

✉ Arunima Sengupta
arunimasengupta2013@gmail.com

Jayeeta Samanta
jayeeta1993@gmail.com

Arunima Mondal
mondal.arunima18@gmail.com

Shreya Das
shreyadas1991@gmail.com

Santanu Chakraborty
santanu.dbs@presiuniv.ac.in

[1] Department of Life Science and Biotechnology, Jadavpur University, 188, Raja S. C. Mallick Road, Kolkata 700032, West Bengal, India

[2] Department of Life Sciences, Presidency University, 86/1, College Street, Kolkata 700073, India

fibrosis and myocardial infarction, cardiomyocyte apoptosis, and arterial and valvular calcification. Another known CAVD that has been detected in a number of cases not only in adult hearts but also in fetal condition is cardiac/myocardial calcification. Many case studies have been done so far on the aspect of cardiac calcification but very few detailed studies have been done on the molecular mechanism that leads to the calcific deposition in the cardiomyocytes/myocardium/ventricular region of the heart (Ivandic *et al.* 1996; Korff *et al.* 2006; Elsherif *et al.* 2008). A number of case studies have shown that calcific deposition occurs in the ventricular region in the case of renal disorder patients. Cardiac calcification has also been detected in heart failure and in other pathological condition (Lasser 1983; Catellier *et al.* 1990; Olbrich *et al.* 1990; Aras *et al.* 2006; Lee *et al.* 2007; Kruijsdijk *et al.* 2011; Rios *et al.* 2014). Myocardial/cardiomyocyte calcification is a delayed process and is often detected in patients with sepsis and other complications as observed in a number of case studies like postoperative complications and kidney disorders. For example, a patient with acute myeloid leukemia (AML) developed myocardial calcification after several weeks of suffering from sepsis.

Unfolded protein response during cardiovascular disorders: a tilt towards pro-survival and cellular homeostasis

Shreya Das[1] · Arunima Mondal[1] · Jayeeta Samanta[1] · Santanu Chakraborty[2] · Arunima Sengupta[1]

Abstract

The endoplasmic reticulum (ER) is an organelle that orchestrates the production and proper assembly of an extensive types of secretory and membrane proteins. Endoplasmic reticulum stress is conventionally related to prolonged disruption in the protein folding machinery resulting in the accumulation of unfolded proteins in the ER. This disruption is often manifested due to oxidative stress, Ca^{2+} leakage, iron imbalance, disease conditions which in turn hampers the cellular homeostasis and induces cellular apoptosis. A mild ER stress is often reverted back to normal. However, cells retaliate to acute ER stress by activating the unfolded protein response (UPR) which comprises three signaling pathways, Activating transcription factor 6 (ATF6), inositol requiring enzyme 1 alpha (IRE1α), and protein kinase RNA-activated-like ER kinase (PERK). The UPR response participates in both protective and pro-apoptotic responses and not much is known about the mechanistic aspects of the switch from pro-survival to pro-apoptosis. When ER stress outpaces UPR response then cell apoptosis prevails which often leads to the development of various diseases including cardiomyopathies. Therefore, it is important to identify molecules that modulate the UPR that may serve as promising tools towards effective treatment of cardiovascular diseases. In this review, we elucidated the latest advances in construing the contribution imparted by the three arms of UPR to combat the adverse environment in the ER to restore cellular homeostasis during cardiomyopathies. We also summarized the various therapeutic agents that plays crucial role in tilting the UPR response towards pro-survival.

Keywords ER stress · Unfolded protein response · Cardiovascular diseases · Cardioprotective · Chemical · Natural products

Introduction

The endoplasmic reticulum (ER) serves as the primary gateway for protein synthesis [1]. It is involved in a multitudinal array of cellular processes including protein folding, serving as a site for synthesis of both secretory and membrane proteins as well as many steroids, cholesterol and lipids [1, 2]. The endoplasmic reticulum is an organelle that houses escalating demand for protein folding. However, any kind of dysregulation in proper protein folding due to any extracellular stimuli or intracellular loss of equilibrium often leads to the accumulation of misfolded proteins in the ER [3].

✉ Arunima Sengupta
arunimasengupta2013@gmail.com

1 Department of Life Science and Biotechnology, Jadavpur University, 188, Raja S. C. Mallick Road, Kolkata, West Bengal 700032, India

2 Department of Life Sciences, Presidency University, Kolkata, India

Glucose-regulated protein 78 (GRP78), an ER chaperone plays a critical role in gauging the intensity of insult done to ER due to accumulation of misfolded proteins. It acts as a protein quality control agent of the ER. A mild insult to the ER is often reverted by the chaperone function of GRP78. However, an intense disruption of the ER homeostasis causes GRP78 to activate ER transmembrane signaling molecules. The stress caused due to the accumulation of misfolded proteins is perceived by three ER resident proteins namely PERK, IRE1α and ATF6α which in turn triggers the activation of an adaptive cellular response signaling cascade known as the unfolded protein response (UPR) [4]. All the three resident proteins initially remains bound to GRP78. The UPR recruits various molecules to revert back the damaged caused and restore the cellular homeostasis. However, prolonged ER stress often leads to cell death [5]. There is a delicate balance between adaptation and apoptosis due to the upregulation of UPR during ER stress.

Cardiovascular diseases are one of the leading causes of death worldwide [6, 7]. Compelling evidences suggests that

Cetuximab-conjugated PLGA nanoparticles as a prospective targeting therapeutics for non-small cell lung cancer

Leena Kumari, Iman Ehsan, Arunima Mondal, Ashique Al Hoque, Biswajit Mukherjee, Pritha Choudhury, Arunima Sengupta, Ramkrishna Sen & Prasanta Ghosh

View supplementary material ⧉

Submit your article to this journal ⧉

View related articles ⧉

Published online: 14 Apr 2023.

Article views: 58

View Crossmark data ⧉